

Experiments in Modern Physics P451: Earth's Field NMR Apparatus

David V. Baxter
Indiana University, Bloomington, IN 47405
(Dated: September 25, 2014)

This experiment introduces a number of the concepts underlying modern NMR and MRI techniques using very small magnetic fields (and audio frequencies) rather than the more common high-field and RF applications common in analytical NMR and clinical MRI. In the lab you can explore the effects of field gradients on the signal, understand the difference between instrumental and intrinsic effects in limiting the lifetime of the observed oscillation signal coming from precessing spins. You can also explore the spin-lattice relaxation time (T_1), Curie's law, and spin-echo techniques. The connection between the time and frequency domains can also be investigated by exploring magnetic resonance imaging through Fourier analysis.

A. Introduction

The techniques exploited in Nuclear Magnetic Resonance are of fundamental importance to Materials Research, Biochemistry, and a variety of precision measurements (ranging from atomic clocks to neutron spin-echo). In this lab you will study a number of the phenomena that may be explored by carefully manipulating and detecting signals from ensembles of magnetic moments as they precess in a magnetic field. This experiment makes use of the apparatus built by "Teach Spin" and most of your information should be obtained from reading the student manuals provided by that company [1–3]. Here we will simply provide some guidelines to make your reading of that manual more efficient.

Equipment

The Teach Spin apparatus consists of two electronic modules (the lower one controls the detector settings and the application of a polarization field; the upper one controls the gradient coils used to "shim" the local field and/or produce the gradient needed for MRI mode) and the sample environment (cylindrical space for samples surrounded by many different coils for providing suitable fields and detecting the signal from the precessing spins).

In addition to the Teach Spin apparatus itself, you will need a digital oscilloscope, a compass (also provided by Teach Spin, and housed in the lovely wooden box on the desk top), and a power supply capable of delivering ~ 3 amps at ≤ 36 V. For some of the initial alignment a four-channel scope may be useful, but for some later tasks it is more important to have a scope with a large memory (more than 8000 points) in order to avoid aliasing on signals recorded with durations on the order of 2 sec. (e.g. the Rigol DS1102E scope should provide adequate resolution). Check with your instructor if you cannot find a suitable scope.

Detecting NMR signals typically requires extraordinarily uniform magnetic fields so that all the nuclear spins in the sample precess at the same rate. Any variation

in the magnetic field over the volume of the sample will result in the signal decaying more rapidly than would be produced by processes intrinsic to the sample itself as the spins in different field regions get out of phase with each other. Indeed for this experiment these extrinsic effects will dominate the decay time for most of the signals you will observe. The sample position has been established in order to get as uniform a field as we have been able to find in this lab, so please do not shift the position of the table away from the tape marks on the floor without checking with your instructor (in particular, do not follow the instructions regarding the east-west positioning of the coils in the section entitled "Positioning the Coils" on page 16 of the Student Manual #2 (SM2)[2], except to check the area near the coils to make sure that there are no steel carts or other magnetic materials in the vicinity). You should adjust the tilt of the coil set so that the main coils are perpendicular to the local ambient field (use the Teach Spin compass and perform this alignment with NO CURRENT in the gradient coils).

Alignment and Tuning

Start your adjustment of the equipment, and your efforts to familiarize yourself with its operation with step 2 of the section titled "Tuning the Instrument to Obtain Maximum Signal" on page 16 of SM2. The gradient coils should have no current flowing through them during this initial procedure (i.e. the X, Y, and Z ten-turn potentiometers should all be set to their midpoint 5.00, which corresponds to zero current in each). Complete the steps outlined in SM2 from the bottom of page 16 through to page 24 (it may also be useful to look at the discussion on the triggering signals for the scope on page 14). This will tune the amplifier to the resonant frequency in the ambient field of our lab, and will introduce you to the phenomenon of "aliasing" (if you have not previously encountered this term, you should study appendix B of SM2[2] to familiarize yourself with the phenomenon). Your observations may be confused by it if you monitor the oscillating signal on a scope with too slow a sampling rate; this is likely for the TDS series scopes if you are using a time base with more than 50

ms/div). Within my experience, despite what the Teach Spin manuals suggest, there does not appear to be a lot of difference with the room lights on or off, so you may find it convenient to work with the lights on. The manual defines success in this operation as achieving a signal with a decay time on the order of 50 ms. In our location, with the gradient coils off, we have achieved as long as 150 ms until the signal disappears into the ambient background even without using the gradient coils to shim the field (but keep in mind that this depends on the details of the magnetic environment and therefore can change from day to day; 50 ms is fine).

After completing your alignment of the amplifier tuning, you should spend some time “shimming” the field with the gradient coils (note, this terminology is left over from the early days of NMR when researchers would adjust the homogeneity of the magnetic field by adding thin pieces of magnetic material [i.e. shim stock] on and around the pole pieces of the main magnet; nowadays this is done with more conveniently and systematically using currents applied to suitably designed coils). To do this, follow the steps in section I.C of the “EFNMR Gradient/Field Coil System Operating Manual student

version (condensed)” (GFCS) [3]. This will guide you through adjustments to the orientation of the coils about a horizontal axis, and lowest-order cancelation of the residual gradients in the ambient field. After this process is complete, you should see decay times on the order of a second or longer in the free precession signal.

Experiments

Once you have achieved a free precession signal lasting a second or longer, you are in a position to conduct a variety of experiments, and the choice of which to pursue is largely up to you. It is recommended, however, that you complete any experiments you want to conduct with proton NMR (including MRI as described in GFCS section II.F, if you would like) before attempting to find a signal from any of the other isotopes mentioned in the manuals. It is probably a good idea to start with the T_1 and “Curie Law” measurements discussed starting on page 34 of SM2.

- [1] (SM1) “Earth’s-Field NMR apparatus Student Manual #1”, rev. 1.3, Teach Spin, Buffalo, NY (2010)
- [2] (SM2) “Earth’s-Field NMR apparatus Student Manual #2”, rev. 1.2, Teach Spin, Buffalo, NY (2009)

- [3] (GFCS) “Earth’s-Field NMR Gradient/Field Coil System Operating Manual, student version (condensed), Teach Spin, Buffalo, NY (2010)



Instruments Designed for Teaching

EFNMR1-B

Student Manual #1

**A Product of TeachSpin, Inc.
Written by Bill Melton, UNC Charlotte**

www.teachspin.com

4. Student Instruction Manual #1

NUCLEAR MAGNETIC RESONANCE IN THE EARTH'S MAGNETIC FIELD

Careful reading of this manual and the completion of the pre-lab written assignment will prepare you for making your first magnetic resonance measurements. It is essential that you come to the lab prepared, having reviewed the basic physics ideas of the pre-lab, learned some new definitions, and understood the basic workings of the apparatus.

4.1. Introduction

a) The People

On a snowy December 15, in 1945, a group of three young Harvard physicists, fresh from working on a secret radar system at the MIT Radiation Laboratory that greatly helped the allies win World War II, adjusted the controls on a crude electromagnet borrowed from Professor Curry Street's comic ray experiments. They became excited when they observed a repeatable deflection on the detector output meter. It was the first measurement of nuclear magnetic resonance in condensed matter. The material used for these first experiments was paraffin wax. The experimenters were Edward Purcell, Robert Pound and Henry Torrey.ⁱ

Ed Purcell, who led the group and received the Nobel Prize for this discovery, was born and raised in Taylorville Illinois, population 11,133. His father ran a local telephone office and Edward went off to Purdue University to study electrical engineering. How he ended up at Harvard and become one of the great scientist and teachers of the twentieth century is a fascinating story.

Simultaneously on the west coast, at Stanford University, a group headed by a European Jew who had fled Nazi oppression, had their quite different apparatus almost assembled. Their intent was also to observe signals from magnetic nuclei in condensed matter. Felix Bloch, already a world-renowned solid-state theoretical physicist, born and educated in Zurich, Switzerland, had devised an apparatus to observe "nuclear induction". His work with W.W. Hansen and M. Packard, published shortly after Purcell's, is in many ways close to the experiments you will be doing in this laboratory.ⁱⁱ

Neither of these two giants of twentieth century physics had any idea that their discoveries would change physics, chemistry, biology, and medicine in truly profound ways. Physicists seem to be very good at making fundamental breakthroughs in science but rather poor at predicting the impact of their discoveries. Mattson and Simon have written a very readable account of history of NMR and the major players in this drama.ⁱⁱⁱ

b) The Phenomenon

What kind of atomic size particles in condensed matter exhibit magnetic resonance? Magnetic resonance signals can only be observed from condensed matter whose atomic constituents have two properties: **magnetic moment** and **angular momentum**.

Both are required. Both are absolutely essential. And both act along a common axis, either parallel or anti-parallel. Nature has provided us with many examples, such as a single electron, certain collections of electrons, protons, neutrons, the nuclei of He³, Li⁷, Be⁹, C¹³, N¹⁴, O¹⁷, F¹⁹, Na²³, Al²⁷, P³¹, and many, many more. Magnetic resonance refers to the characteristic precession of these particles in the presence of an external magnetic field.

There is a fundamental relationship between the magnetic moment of a nucleus and its angular momentum. This is written as:

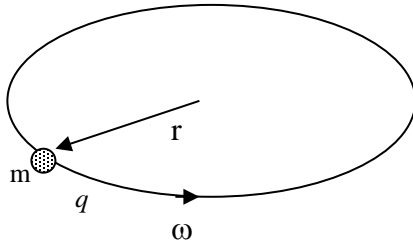
$$\vec{\mu} = \gamma \hbar \vec{I}$$

where \mathbf{I} is the nuclear spin, $\boldsymbol{\mu}$ is the magnetic moment, \hbar is Planck's constant divided by 2π , and γ is the gyromagnetic ratio. The product $\hbar \vec{I}$ is the angular momentum of the nucleus.

In these experiments we will concern ourselves with only two nuclei, the proton which is hydrogen's nucleus and possibly with the fluorine nucleus, which is in special samples of fluorinated oils. Mostly, these experiments will examine the signals from the hydrogen nuclei, the protons, in ordinary water.

4.2 Pre-Lab Written Assignment

- a) The diagram below shows a point charge q executing uniform circular motion.



1. Derive the relationship between the magnetic moment $\boldsymbol{\mu}$ and the angular momentum \mathbf{L} for this point charge q with mass m which is rotating at a constant angular velocity ω around a circle of radius r . This is a non-relativistic classical physics calculation.
 2. How does this relationship depend on the speed of the rotation?
- b) Show that the same relationship holds for a solid sphere of charge spinning about a fixed axis. Assume a total charge, Q , is uniformly distributed throughout the sphere of mass M .
- c) The ratio of the magnitude of the magnetic moment $\boldsymbol{\mu}$ to the magnitude of the angular momentum \mathbf{L} is defined as the gyromagnetic ratio, gamma, γ :

$$\frac{|\vec{\mu}|}{|\vec{L}|} \equiv \gamma$$

Calculate the numerical value of the ratio for an electron and for a proton.

- d) All of your calculations assume that both the electron and proton are classical particles. They are not! In fact, calculating gyromagnetic ratios for these particles is one of the important theoretical physics problems. Our interest is in the hydrogen nucleus (the proton) and the fluorine nucleus. Your answer for the proton should be off by a factor of 2(2.79). The experimentally measured values are:

$$\gamma_{\text{proton}} = 2.675 \times 10^8 \text{ rad/(s}\cdot\text{Tesla)}$$

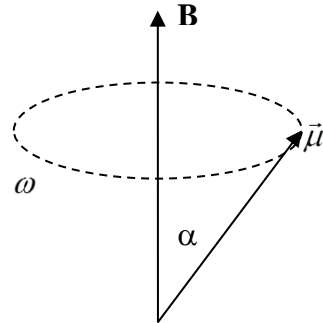
$$\gamma_{\text{fluorine}} = 2.517 \times 10^8 \text{ rad/(s}\cdot\text{Tesla)}$$

These are the numbers you should use in any future calculations.

- e) The diagram to the right shows the orientations of the axis and the magnetic moment μ of a spinning sphere of charge with respect to a uniform magnetic field \mathbf{B} .

Start with the following two fundamental relationships:

$$\vec{\tau} = \frac{d\vec{L}}{dt} \quad \text{and} \quad \vec{\tau} = \vec{\mu} \times \vec{B}$$



1. Show that a spinning sphere of charge will execute precessional motion when placed in a uniform magnetic field \mathbf{B} with its axis of rotation at an angle α with respect to that field.
2. Show that the angular frequency of precession (in radians/s), called the Larmor precession frequency, is independent of angle α and is given by the relationship:

$$\omega_{\text{precession}} = \gamma B$$

- f) Review Faraday's Law of electromagnetic induction. Be sure you understand it!

4.3. Magnetic Resonance

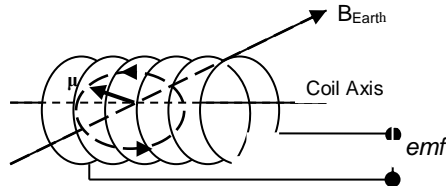
It would perhaps be more accurate to call these experiments "Studies of Free Precession of Nuclear Moments in the Earth's Magnetic Field." This instrument detects the collective precession of the nuclear magnetic moments in the sample. How do we create this "collective" precession? How do we detect this precession once it is created?

- a) Detecting the precession

1. Generating emf

Let's start with the question of how to detect the precession of a magnetic moment. Suppose we place our sample in a coil of wire whose axis is perpendicular to the axis of precession of the nuclear moments. This is shown on the diagram. As the magnetic moments precess in the magnetic field \mathbf{B} , the nuclear moments produce a time varying flux of their magnetic field through a plane defined by a turn on the coil. This time varying flux produces an emf in the coil. The collective nuclei produce a collective emf through all the turns in this coil, which

results in a time-varying voltage at the coil's terminals. It is this voltage which is amplified and measured in these experiments.



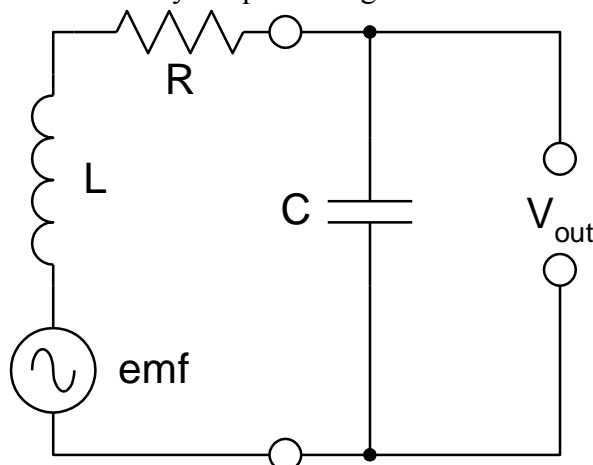
The frequency of the time-varying signal indicates the magnetic field in which the nuclei are precessing. The amplitude of the signal is proportional to net number of nuclei that are collectively precessing. This net number of collectively precessing nuclei is called the magnetization, or, in different terms, the polarization.

2. Tuning the Coil - What does tuning mean and how does it affect our signal detection?

Nuclear magnetism is generally a rather weak form of magnetism. You cannot attach your water sample to your refrigerator using its nuclear magnetism. It is so weak that special coils and amplifier electronics are required to detect this signal. Even with this, it is essential to “tune” the receiver coil, which in our instrument is called the sample coil.

The emf generated in the coil depends on the number of nuclei, the rate of precession, the number of turns of the coil, and the coil's geometry. But the actual voltage at the terminals of the coil can be significantly increased by tuning. (Note that the emf and the voltage are not the same for a tuned coil. They are the same for a simple coil which has no appreciable capacitance or inductance.)

Let us consider our sample coil to be an inductor which has a capacitor across its terminals. The equivalent circuit is shown in the diagram below, where C is the added capacitance, L the coil's inductance, R the coil's resistance, and the emf shown is the one described by Faraday's Law, generated in the coil by the precessing nuclear moments.



To ‘tune the coil’ is to choose our capacitance so that its capacitive reactance is equal to the coil’s inductive reactance (but 180° out of phase) at the Larmor precession frequency. As you may recall, capacitive reactance is $1/\omega C$, and inductive reactance is ωL .

In this case, the signal current flowing in the LCR circuit loop is given by

$$I_s = \text{emf} /(\text{net reactance}) = \text{emf} /R \quad [\text{provided } \omega L = 1/\omega C] \quad (\text{a})$$

The potential difference appearing at the output terminals is given by

$$V_{\text{out}} = I_s \cdot (\text{capacitor's reactance}) = I_s \cdot \omega L \quad [\text{as } \omega L = 1/\omega C] \quad (\text{b})$$

So, by substitution of (b) into (a),

$$V_{\text{out}} = \frac{\text{emf}}{R} \omega L \quad (\text{c})$$

The quality factor, or Q , of a coil is defined as 2π times the energy stored divided by the energy dissipated per cycle. For a parallel, tuned, resonant, circuit it can be shown that:

$$Q = \frac{\omega L}{R} \quad (\text{d})$$

Substituting into (c), we get

$$V_{\text{out}} = (\text{emf}) \cdot Q \quad (\text{e})$$

The output voltage of the parallel tuned circuit is a factor of Q times the emf generated by the precessing spins. The special sample coil designed by TeachSpin has a Q of about 70. This tuned coil gives a giant enhancement of almost two orders of magnitude when the capacitor is adjusted so that its reactance is equal in magnitude to the inductive reactance, at the Larmor precession frequency. If the capacitance is not properly tuned, then the voltage output is not thus enhanced and the signal is just the emf.

This tuning has another advantage. It partially reduces random noise signals. The voltage at the terminals of the coil depends not only on the magnitude of the time-varying flux from the precessing spins, but also on the frequency of that precession. Only noise signals at or near the Larmor frequency are enhanced by the tuning, and therefore noise signals outside this range are significantly reduced relative to the precession signals. In effect, the tuned coil acts like a band-pass filter for the system.

b) Creating the collective precession – Magnetization

Now we turn to the question of how to create a “collective” precession which can induce a measurable emf. With this apparatus, or indeed most NMR instruments, it is not possible to observe a single proton’s free precession. The proton’s magnetic moment is far too small to detect the voltage at the coil’s terminal. Both externally induced pickup noise, and internally created thermal noise from the coil itself, make such detection impossible.

Suppose, however, that we use 125 ml of water as a sample. This contains about 10^{25}

hydrogen nuclei (protons). If all those protons were aligned with their magnetic moments pointing in the same direction and they were all to precess and remain aligned, then our signal would be 10^{25} times as large as from a single proton!

The degree of alignment in a sample is formally referred to as the polarization or as the magnetization, M . Quantum physics tells us that there are only two possible magnetic states for the proton to reside in, spin along \mathbf{B} , and spin opposed to \mathbf{B} . The magnitude of proton magnetization is given by the difference between spin along \mathbf{B} and against \mathbf{B} as

$$M = n_{\uparrow}\mu_{\uparrow} - n_{\downarrow}\mu_{\downarrow}$$

where n_{\uparrow} and n_{\downarrow} refer to the number/unit volume of magnetic moments along and against the magnetic field \mathbf{B} .

In this apparatus, the initial signal amplitude is proportional to the magnetization of the sample. You can use this to amplitude to explore two parameters that might control the magnitude of the magnetization, the strength and the duration of the polarizing magnetic field. Both the polarizing field and the polarizing time are under your control!

Does the strength of the polarizing field matter? If so, what is the mathematical form of that dependence? Does the magnetization occur instantaneously when the magnetic field is turned on? If not, your job is to discover the mathematical relationship for the magnetization as a function of the time you leave the polarizing field on.

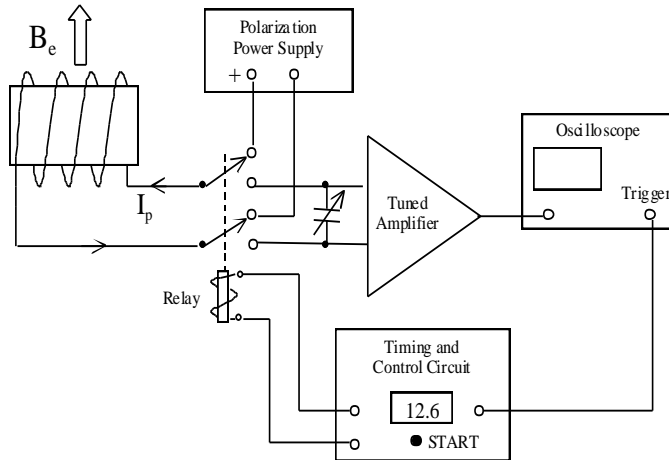
d) Summary of Objectives for the First Set of Experiments

1. Measure the magnitude of your local Earth's magnetic field by determining the frequency of precession of the protons in a water sample.
2. Does the degree of polarization (or the magnetization) of the protons depend on the strength of the magnetic field they are placed in? If so, what is the mathematical relationship between the polarizing magnetic field and the polarization?
3. Does the polarization occur instantaneously? If not, how long does it take to polarize (or magnetize) the water sample? What is the mathematical description of the time dependence of the polarization?
4. Are the degree of polarization and the rate of polarization interrelated? In other words, does the rate of polarization depend upon the polarizing magnetic field?
5. Does the frequency of the precession signal depend on the polarizing field you choose? On the polarizing time you use?

e) Overview of the Apparatus

Perhaps the best way to explain the apparatus is to examine the simplified block diagram shown at the right.

The high- Q sample coil surrounds a 125 ml plastic bottle filled with distilled water, or another liquid to be investigated. The sample is placed in a uniform part of the local Earth's magnetic field with the **axis of the coil perpendicular to the Earth's field.**



At the beginning of the experiment, the electronic timers and relays connect the sample coil to the external dc power supply. The current from this external supply produces the so-called “Polarizing Magnetic Field.” This polarizing field is perpendicular to the Earth’s magnetic field and **much** larger in magnitude. The time the sample coil remains connected to this supply is set by the thumbwheel switches on the electronic controls.

After the predetermined time of “soaking” the nuclei in this large polarizing magnetic field, the polarizing current is disconnected from the coil, the stored magnetic energy in the coil is quickly dissipated, and the coil is connected to the tuning capacitors and the low-noise amplifiers. The polarizing magnetic field is removed so quickly that the nuclei remain polarized along the direction of the polarizing field. With the polarizing magnetic field turned off, the nuclear magnetization precesses in the Earth’s magnetic field, producing a time varying flux through the sample coil. The time varying flux creates an emf, which creates a time varying voltage at the terminals of the tuned circuit. This voltage is amplified by the preamplifier and tuned amplifier in the electronics.

The precession signal is directed both to the oscilloscope and to the audio amplifier and speaker. You can not only see the signal from the precessing nuclear moments, you can hear it!

f) Investigating the Six Distinct Pieces of the Apparatus

A quick list – You should examine each piece carefully.

1. Coils with special low-loss cable.
2. Support stand for coils.
3. Electronic controller
4. Brick-on-a-rope (power supply for electronics)
5. External dc high-current power supply.
6. Oscilloscope (or computer with interface)

1. Coils – Note that the instrument has two coils.

The larger outer (halo, or ‘bucking’) coil is essential for dramatically reducing the pickup from external electromagnetic noise fields. Although an important part of the instrument, making it possible to observe the magnetic resonance signal in the presence of extraneous noise, this coil can be ignored by beginning students. They can simply assume that electromagnetic noise is not present in their laboratory. (Turn off all fluorescent lights and incandescent lights that are on dimmer switches. Dimmers usually produce significant noise fields which are only partly cancelled by this outer coil.)

The inner coil is the sample coil. It has two functions (please refer to the simplified circuit diagram): First, it provides a large (and variable) magnetic field to polarize (magnetize) the nuclear spins. Then, because of its high Q and multiple turns, it generates an optimum signal voltage from the precessing nuclear spins.

2. Support stand for coils.

This nonmagnetic stand allows the student to conveniently place the coils in a region of the best uniform Earth’s magnetic field in the laboratory. It is important to place the sample in the most uniform part of the Earth’s magnetic field. If the nuclear moments in the sample find themselves in different magnetic fields they will precess at different rates. In fact, for pure water, the rate at which the signal decays to zero tells the experimenter the field gradient across the sample.

It is usually best to place the coils away from walls, tables with steel parts, off the floor where iron drain pipes may be buried and away from steel support columns. Your equipment might not include this stand, but you must make sure that the sample is placed away from all ferromagnetic materials. Small spatial adjustments, even just a few inches, can often make a significant difference in the observed decay time of the precession signal.

3. Electronic Controls

a. Timing Circuits. These circuits provide the various timing functions

- The length of polarizing time, which is set by the thumbwheel switches on the panel. This is variable in steps of 0.1s, from 0.1 to 99.9 seconds.
- Various delay times, such as a 5-second delay after every experimental cycle, an 80 millisecond delay after switching off polarizing current to allow voltage transients of die out, and a delay time equal to polarization time to keep duty cycle to under 50%.
- Synchronizing pulses for oscilloscope triggering. For NMR signals, the scope should be set to trigger on a negative pulse, negative slope, at minus one volt.
- Manual Start. A push-button switch that starts the entire sequence.
- External Start. A contact closure to ground or a negative TTL pulse performs the same function as pressing the manual start button. Use this only if you need to start the experiment with an external electronic signal.
- Wait light. Tells the experimenter that the instrument is still going through its cycle and the operator needs to wait before pushing the start button again.

b. Amplifier

As we discussed earlier, it is essential to tune the sample coil to the frequency of the precessing magnetic moments. Since this precession frequency is uniquely determined by the local Earth's magnetic field in your laboratory, the student must experiment with the controls to determine the proper tuning. There are both COARSE and FINE controls. Note that the tuning frequency increases with counterclockwise rotation. If you find your instrument adjusted to the wrong frequency, you may not be able to detect any signal from the precessing moments.

There are two outputs on the amplifier, one marked preamplifier and the other NMR signal. First adjust the tuning capacitors to maximize the output of the preamplifier. (Note: Use a.c. coupling on the oscilloscope since the preamplifier has a d.c. offset imposed on the signal from the electronics). The NMR output comes from the second-stage amplifier. This is a tunable bandpass amplifier. It must also be adjusted so that the center of the bandpass is at the Larmor frequency. This adjustment is made by the 10-turn counter dial. All these adjustments can be made on a signal from the distilled water sample.

c. Amplitude Detector

The signal available at the NMR SIGNAL OUTPUT is also connected internally to an Amplitude Detector, which consists of a precision Full-Wave Rectifier followed by a Low-Pass Filter. The output of the filter is the average value of the full-wave rectified free precession signal. For a full-wave rectified sinusoidal signal, the average value is $2/\pi$ of the peak value. Thus, the output of the NMR AMPLITUDE DETECTOR has the same shape as the envelope of the free-precession signal, but the amplitude is about $2/3$ as large. This signal is particularly useful for signal averaging of repetitive experiments. Signal averaging is a common feature on digital oscilloscopes. It can enhance the signal-to-noise ratio for weak signals.

d. Audio Amplifier and Speaker.

The precession frequency for both protons and fluorine nuclei in a typical local Earth's magnetic field is about two thousand cycles per second. This is in the audible frequency range. This instrument has a volume-controlled audio amplifier connected to an internal speaker. You can hear the signal generated by the precessing nuclear moments in the sample. If you are lucky to have a particularly uniform field in your lab enough (or you take the instrument outside and away from the building), then you might hear the sound last for several seconds.

4. Brick-on-a-Rope (wall-transformer power supply for electronics)

This is the dc regulated power supply that provides ± 15 volts and $+ 5$ volts to operate the electronics. The supply (brick) plugs directly into the ac power line and the dc outputs are connected by cable (rope) to the rear panel of the control box. It is best to leave the d.c. line plugged into the rear panel and remove the supply from the power line when you have completed the experiments. There is no on-off power switch.

5. External Power Supply

This power supply provides the direct current for the polarizing magnetic field. This supply should be CURRENT REGULATED with a current range between 0.5 and 3 amperes and with a maximum voltage of about 38 volts. Ask your instructor to explain how you adjust the supply for current regulation. Do not run the experiment with less than 0.5 amperes or more than 3.5 amperes.

DO NOT GROUND EITHER SIDE OF THE EXTERNAL POWER SUPPLY. This supply must be floating!

The polarizing field is changed by adjusting the output current. If the supply is not current-regulated, the voltage must be adjusted during the experimental run to keep the current and thus the polarizing field, constant. With repeated measurements, the copper wire heats up, the coil resistance increases and, if the supply is only voltage-regulated, the current and magnetic field decrease.

DO NOT TURN THE POLARIZING CURRENT ON UNTIL THE INSTRUMENT ITSELF HAS BEEN POWERED BY THE BRICK-ON-A-ROPE.

6. Oscilloscope

A digital scope is highly recommended, but it need not have great bandwidth. A 20 MHz scope is more than sufficient for these measurements. However, “aliasing” can be a major problem for beginning students. Some digital scopes are particularly bad and the signals they present can be extremely confusing. If you are not familiar with this inherent problem with digitizing data, you should carefully read Appendix A6. One simple test for incorrect data presentation due to aliasing is to change the sweep time to a faster sweep by one unit and observe the same signal. If the signal changes appropriately, it is not aliasing, but if the scope presents significantly different data, then the first data should be ignored.

g) Basic Experiments

The first set of experiments will be done on distilled water sample in the 125-ml plastic bottles. This will provide you with a large signal that should be relatively easy to find. Here are a few helpful hints:

1. The preamplifier output maximum signal amplitude should be about 200-300 mV peak-to-peak.
2. The Larmor frequency should be about 2 kHz, ie. it should have a period of about half a millisecond. Set the oscilloscope so that you can observe the oscillations. After you have observed them, change the time scale so you can observe the decay of the envelope of these oscillations. What causes this decay?
3. The NMR output from the bandpass amplifier should be about 6 volts peak-to-peak.
4. Use the NMR detector output to measure relative signal amplitude if you want to signal average or avoid aliasing problems on your digital scope.

Play with the apparatus until you feel comfortable with it. Get some ideas on how you will go about designing experiments to answer all the questions in the summary section. Take your data in a systematic way and find an appropriate way to plot it.

It is absolutely essential THAT YOU PLOT THE DATA AS YOU RECORD IT. That means you may want to manipulate this data. Always record the raw data in your data table, for example, 4.5 divisions, with sensitivity of 5 mV/div. Do not do the multiplication in your head and record 22.5 mV. You are likely to make a mistake. But suppose this magnetization depends on T^2 , what do you plot? If you plot M vs. T^2 you should get a straight line. If this data fits a straight line in such a plot, you have very strong evidence that $M \propto T^2$. But a plot of M vs. T cannot yield such a conclusion.

Why must you plot the manipulated data as you do the experiments? Suppose you make a mistake. You read the scope incorrectly, you set the time wrong, the polarization field current drifted, the amplifiers became unstable, or some other problem. You will immediately see that you have a problem from your plot. You can now check everything and attempt to find the problem. This gives you the chance to correct it. If you take the data home and plot it on your computer, you will not be able to understand the one or two “crazy” data points. On the other hand, they may not be crazy – you may have made a discovery.

Once again, PLOT your manipulated or raw data as you do the experiment. This is the best advice you'll ever get!

h) Additional Experiments

Once you have determined the basic relationships between magnetization, polarizing current and polarization time for distilled water, you can explore the effect of adding solutes on proton magnetization, or you can do experiments on fluorine-containing samples.

1. Does the effect of doping the water with NaCl (table salt), or sugar, differ from the effect of doping with compounds such as copper sulfate and ferric chloride?
2. How does the concentration of the solute change the way the magnetization behaves?
3. Try using a fluorine compound. You will have to retune the amplifier because the Larmor frequency for your fluorine nucleus will be different from that of the proton.
 - a. Use the Larmor frequencies you have determined for fluorine and water to determine the ratio of the gyromagnetic ratios of these nuclei. Does this ratio depend on the local magnetic field?
 - b. How does the viscosity of the fluorine sample affect the NMR parameters?
4. If your instructor is willing to have you work with volatile, flammable liquids, try studying the proton resonance in a sample such as fluorobenzene which contains both protons and fluorine.

i "Resonance absorption by Nuclear Magnetic Moments in a solid", E. Purcell, R. Pound, and H. Torrey, Phys. Rev. 69, 37-38 (1946)

ii "The Nuclear Induction Experiments", F. Bloch, W.W. Hansen, and M. Puckard, Phys. Rev. 70, 474 (1946)

iii "The Pioneers of NMR and Magnetic Resonance in Medicine", James Mattson and Merrill Simon. Deana Books Co. ISBN 09619243-1-4



Instruments Designed for Teaching

EFNMR1-B

Student Manual #2

**A Product of TeachSpin, Inc.
Written by Bill Melton, UNC Charlotte**

www.teachspin.com

5. Student Instruction Manual #2

TABLE OF CONTENTS

INTRODUCTION TO NMR IN THE EARTH'S MAGNETIC FIELD	5-2
Gyromagnetic Ratio	
The Curie Law	
Spin-Lattice Relaxation Time	
Larmor Precession	
The Earth's-Field Free Precession Technique	
THE EARTH'S-FIELD NMR INSTRUMENT	5-10
Block Diagram and General Description	
Controls and Connectors	
Front Panel	
Back Panel	
INITIAL SETUP	5-17
Positioning the Coils	
Tuning the Instrument to Obtain Maximum Signal	
Adjusting the Center (Resonant) Frequency of the Bandpass Amplifier	
NMR AMPLITUDE DETECTOR	5-22
APPENDIX A: Larmor Precession	5-24
APPENDIX B: Aliasing	5-26
EXPERIMENTS	5-33
1. Measurement of the Proton Spin-Lattice Relaxation Time in Water	
2. The Curie Law	

INTRODUCTION TO NMR IN THE EARTH'S MAGNETIC FIELD

Gyromagnetic Ratio

Consider a particle of mass m and charge $+q$ rotating at constant angular velocity ω in a circular orbit of radius r . The angular momentum of the particle is

$$L = I\omega = mr^2(2\pi f).$$

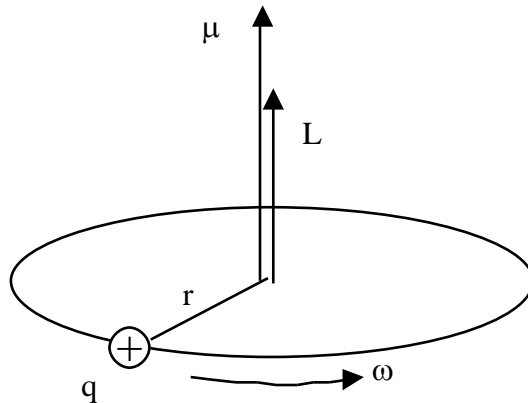


Fig. 5.1: Magnetic moment and angular momentum vectors for a charged particle rotating at constant angular velocity in a circle of radius r .

Associated with the moving charge is an average current $I = qf$ in the loop, and a magnetic moment

$$\mu = IA = qf(\pi r^2).$$

Eliminating r^2 from the last two equations yields

$$\vec{\mu} = \gamma \vec{L}, \quad (1a)$$

where

$$\gamma = \frac{q}{2m}. \quad (1b)$$

Vector symbols have been included in Eq. (1a) to indicate that the magnetic moment and angular momentum vectors point in the same direction, as shown in Fig. 1. The constant γ is known as the *gyromagnetic ratio*. (Perhaps "magnetogyric" ratio would have been a better name.) Although derived here for just one very special case, Eqs. (1a) and (1b) can be shown to hold equally well for other cases, like spinning charged rings, balls, and spherical shells.

Equation (1a)—but not (1b)—even holds for atomic nuclei and orbital electrons, as has been verified by both experiment and application of the quantum theory. For protons, for example, calculating the gyromagnetic ratio using Eq. (1b) gives

$$\gamma = q/2m = (1.602 \times 10^{-19} \text{ C})/(2 \times 1.672 \times 10^{-27} \text{ kg}) = 4.79 \times 10^7 \text{ C/kg.}$$

The measured value is $\gamma = \vec{\mu}/\vec{L} = 2.675 \times 10^8 \text{ C/kg}$, which is larger than the classically computed value by a factor of 5.58. Still, considering the simplicity of the classical model, the agreement between the measured and classically computed gyromagnetic ratios for protons is surprisingly good.

The Curie Law

Figure 2 shows an idealized model of a proton, which we imagine classically to be a ball of spinning positive charge. It has spin angular momentum \vec{L} and magnetic moment $\vec{\mu}$, both of which point in the same direction along the axis of rotation.

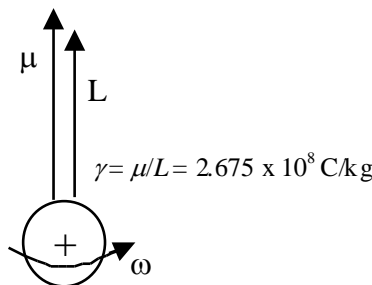


Fig. 5.2: Classical model of a proton. The magnetic moment and spin angular momentum vectors point in the same direction along the axis of rotation.

Consider the water sample shown schematically in Fig 3. Each water molecule contains two hydrogen atoms, and each hydrogen atom has a nucleus consisting of a single proton. In the absence of a magnetic field, the proton magnetic moments in water are, according to the classical model, randomly oriented in space. If, however, the water sample is placed in an external field \vec{B} , the proton magnetic moments will tend to align themselves with the field. At absolute zero the alignment would be perfect, and the net nuclear magnetization of the sample, defined as the magnetic moment per unit volume, would be $M = n\mu$, where μ is the magnetic moment of a single proton, and n is the number of

magnetic moments (hydrogen nuclei) per unit volume. (For water, n is just twice the number of water molecules per unit volume.) At temperatures above

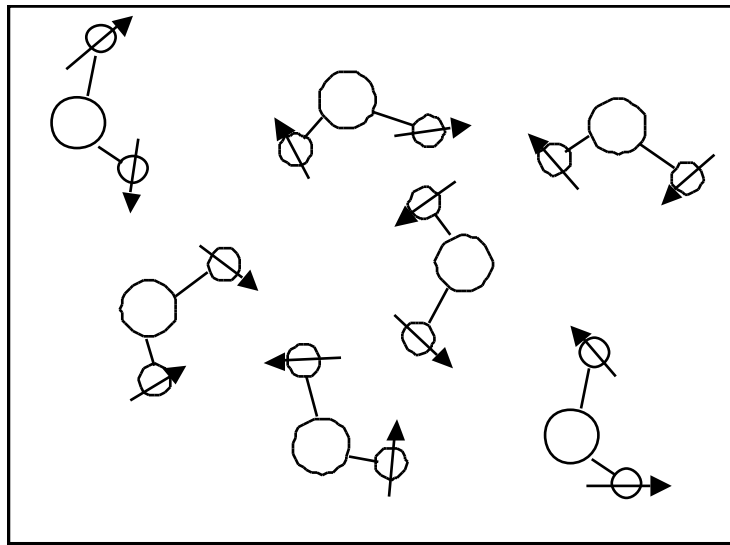


Fig. 5.3: Schematic representation of molecules of water, H_2O . In the absence of an external magnetic field, the magnetic moment of each proton (hydrogen nucleus) is randomly oriented in space.

absolute zero, thermal motions disturb the alignment, so that a typical magnetic moment makes some angle θ with the external field. The magnetization of the sample is

$M = n \mu \overline{\cos \theta}$, where $\overline{\cos \theta}$ represents the average value of $\cos \theta$ for all magnetic moments in the sample. Calculation of $\overline{\cos \theta}$ using classical thermodynamics gives the familiar result known as the Curie law:

$$M_o = \frac{n\mu^2 B}{3kT}, \quad (2)$$

where M_o is the equilibrium magnetization in the field B , k is Boltzmann's constant, and T is the temperature on the Kelvin scale. The derivation of the Curie law can also be done using quantum mechanics. The end result can be written in exactly the same form as Eq. (2) if one makes the substitution

$$\mu = \gamma \hbar \sqrt{I(I+1)}, \quad (3)$$

where γ is the gyromagnetic ratio and I is the nuclear spin quantum number, equal to $1/2$ for protons.

The Curie law predicts a magnetization proportional to the field B and inversely proportional to the temperature in kelvins. It is valid so long as $\mu B/kT \ll 1$. Because of the small size of nuclear magnetic moments, the Curie law holds at virtually all obtainable temperatures.

Spin-Lattice Relaxation Time

When an external field B is applied to a sample, the magnetization M does not assume the value predicted by the Curie law instantaneously, but approaches the equilibrium magnetization in a manner that is, in most cases, exponential. Representative graphs of B and M versus time are shown in Fig. 4.

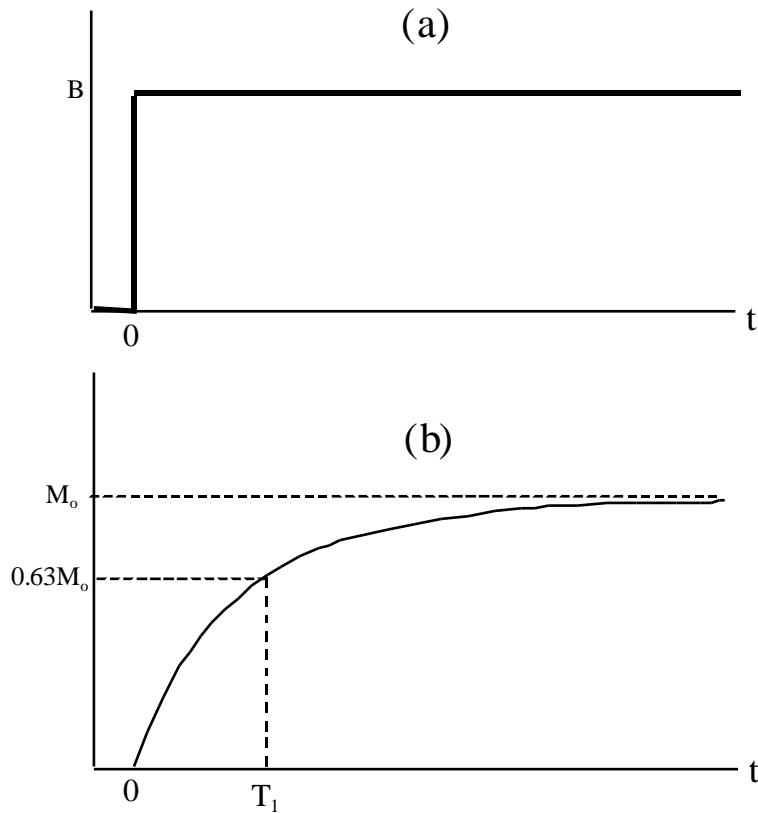


Fig. 5.4: (a) A constant magnetic field B is switched on at time $t = 0$. (b) The magnetization grows exponentially with time constant T_1 toward the equilibrium Curie value M_∞ .

The graph of M versus time in Fig. 4(b) is described by the equation

$$M(t) = M_\infty (1 - e^{-t/T_1}), \quad (4)$$

where M_∞ represents the equilibrium magnetization given by Eq. (3). The time constant T_1 , known as the spin-lattice relaxation time, is the time it takes for the magnetization to rise to $(1 - e^{-1})$, or about 63%, of the equilibrium Curie magnetization M_∞ . After two time constants $M(2T_1) = 0.86 M_\infty$. After five time constants $M(5T_1) = 0.99 M_\infty$. In water, for example, for which the relaxation time is about 2.5 s at room temperature, the magnetization will have reached slightly more than 99% of its equilibrium value within 12.5 s after the field is turned on.

Larmor Precession

When a proton is placed in an external magnetic field \vec{B} , it experiences a magnetic torque $\vec{\tau} = \vec{\mu} \times \vec{B}$ that tends to align the proton magnetic moment with the field. However, because of its spin angular momentum \vec{L} , the proton's motion is a precession about the field \vec{B} at angular frequency $\omega = \gamma B$. (See Appendix A for a derivation of this expression.) In an earth's field of approximately 0.5 Gauss = 50 μT , the precession frequency is

$$f = \omega/2\pi = \gamma B_e/2\pi = (2.675 \times 10^8 \text{ s}^{-1}\text{T}^{-1})(50. \times 10^{-6}\text{T})/2\pi = 2.1 \text{ kHz} .$$

It is interesting to note that, in a uniform field, all protons within a sample precess at the same frequency independent of cone angle θ . Furthermore, since f is independent of θ , the magnetization \vec{M} precesses at the same frequency f also.

The Earth's-Field Free Precession Technique

In the earth's-field free precession technique of studying magnetic moments and relaxation times, the sample is placed inside a coil oriented with its axis perpendicular to the earth's field \vec{B}_e as in Fig. 5. A current I_p in the coil produces a polarizing field \vec{B}_p perpendicular to \vec{B}_e , and nuclear magnetization \vec{M} builds up with time constant T_1 toward the equilibrium Curie value in the resultant field \vec{B} , the vector sum of \vec{B}_p and \vec{B}_e . We designate the angle between \vec{B} and the earth's field as α . Since the polarizing field is normally several hundred times the earth's field, the initial value of this angle (α_0) is usually very close to 90° .

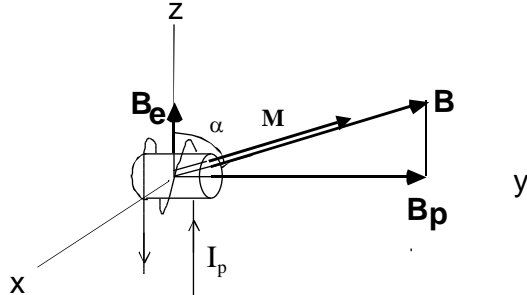


Fig. 5.5: A schematic representation of the geometry for the earth's-field free precession technique.

When the coil current is reduced to zero, the resultant field \vec{B} shrinks in magnitude and rotates through angle α_0 . If the polarizing field is reduced *quickly* (sudden passage), the magnetization is "left behind" and ends up precessing about \vec{B}_e at frequency $\omega = \gamma B_e$ in a cone of angle $\theta_f \approx \alpha_0 \approx 90^\circ$. The precessing magnetization produces a changing magnetic field in the coil, which induces a signal in the coil, with signal amplitude proportional to $M \sin \theta_f$, the component of \vec{M} perpendicular to \vec{B}_e . For maximum signal, the polarizing field must be reduced to zero quickly in order to achieve the desired sudden-passage condition $\theta_f \approx \alpha_0 \approx 90^\circ$.

A simplified block diagram of the apparatus required for detecting the free precession signal is shown in Fig. 6. A switching circuit (represented by a relay in Fig. 6) connects the coil to a dc power supply for polarizing the sample, or to a high-gain, narrow-bandwidth, tuned amplifier for detecting the free precession signal. When the user presses the START button, the switching circuit connects the coil to the power supply, and turns the polarizing current on in the coil. Magnetization M grows exponentially with time constant T_1 toward the equilibrium Curie value in the polarizing field. Graphs of B_p and M versus time are shown in Fig. 5.7. When the polarizing field is switched off suddenly at the end of the polarizing time t_p , the magnetization is left behind, and begins precessing about the earth's magnetic field at frequency $f = \omega/2\pi = (\gamma/2\pi)B_e$. The precession frequency is typically in the range 2.0 - 2.5 kHz.

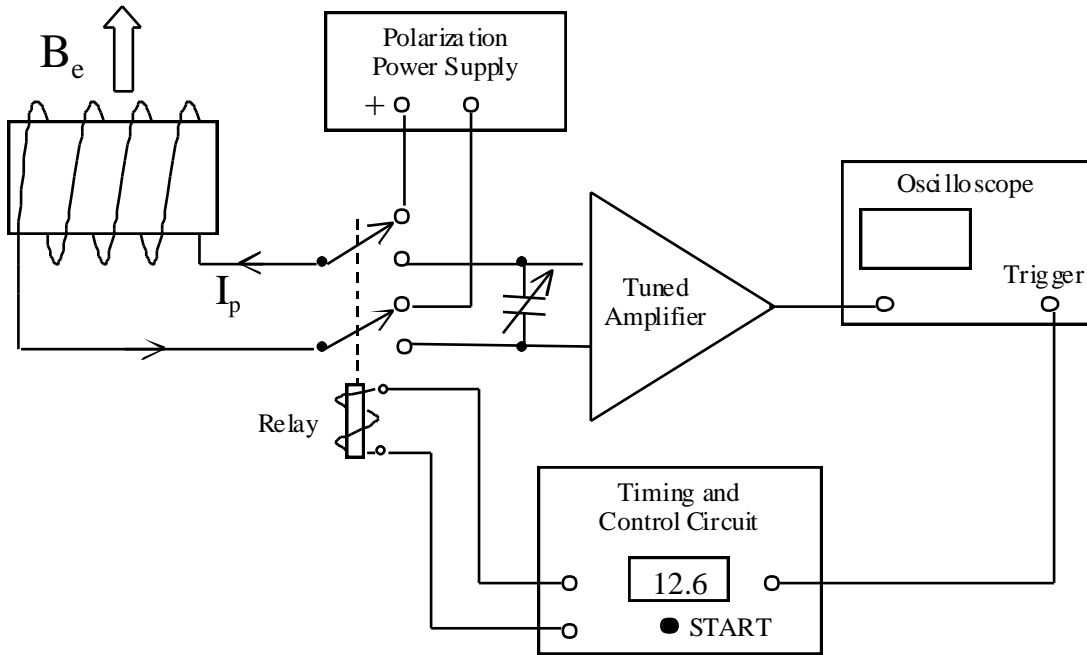


Fig. 5.6: Simplified block diagram of the apparatus required for the earth's-field free precession technique.

The precessing magnetization induces a sinusoidal signal in the coil at the precession frequency (see Fig. 5.7b) whose amplitude is proportional to the magnetization $M(t_p)$. The switching circuit quickly disconnects the coil from the power supply, and connects the coil to the tuned amplifier, which allows the user to view the free precession signal on an oscilloscope screen. The signal does not persist indefinitely. Magnetization \vec{M} relaxes toward its new, and much smaller, equilibrium value along the direction of the earth's magnetic field. The free precession signal decays toward zero with time constant T_2 , the spin-spin relaxation time in the earth's field B_e . By measuring the initial amplitude of the free precession signal as a function of polarizing time t_p , the user can trace out the magnetization curve in Fig. 5.7b and determine the spin-lattice relaxation time T_1 in the field B_p . One of the most attractive features of the technique is that the earth provides—for free—a stable uniform magnetic field in which to detect the free precession.

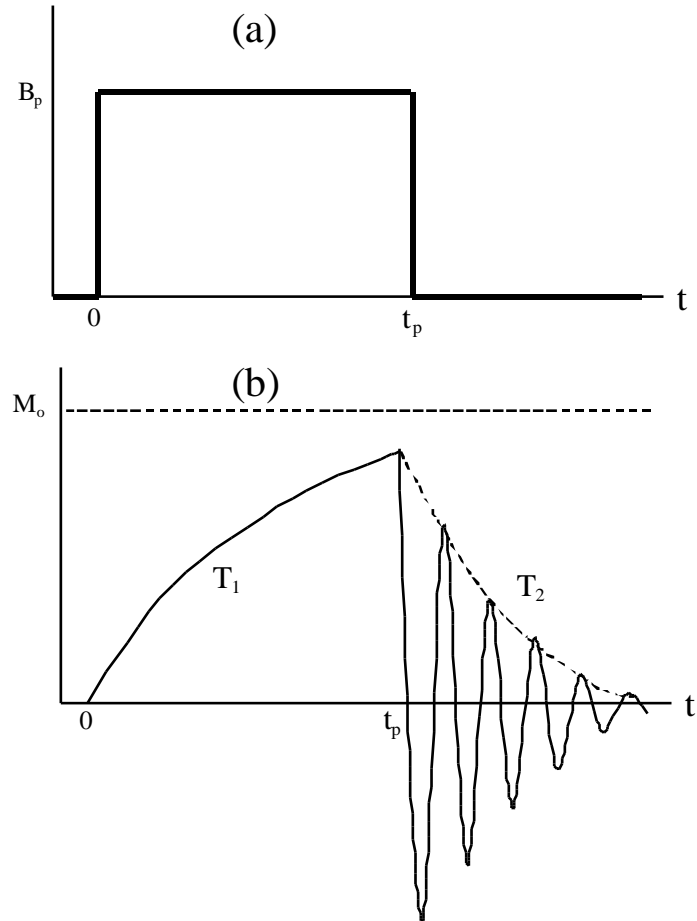


Fig. 5.7: Variation of polarizing field B_p and magnetization M with time in the earth's-field free precession technique. (a) The polarizing field B_p is switched on at time $t = 0$, and switched off at the end of the polarizing time t_p . (b) When the field is first turned on, magnetization rises exponentially toward the equilibrium value with time constant T_1 . When the polarizing field is reduced suddenly to zero at time t_p , the magnetization precesses about the earth's field and induces a signal in the Sample Coil having initial amplitude proportional to $M(t_p)$. The magnetization and signal decay toward zero with time constant T_2 .

THE EARTH'S-FIELD NMR INSTRUMENT

Block Diagram and General Description

A more detailed block diagram of the apparatus required for the earth's-field free precession technique is shown in Fig. 5.8. It consists of 4 major elements:

- 1) Sample and Bucking Coils,
- 2) Digital Timing and Control Circuit,
- 3) Current-Switching and Relay Circuits,
- 4) Preamplifier, Bandpass Amplifier, and Amplitude Detector.

The two Bucking Coils are included to compensate for any stray signals that may be picked up by the Sample Coil due to fluorescent lights and other sources of electrical noise. During signal detection, the Sample and Bucking Coils are connected in series. The Bucking Coils together have the same total number of area-turns as the Sample Coil (number of turns times the average surface area of one turn), but the turns on the Bucking Coils are wound in the opposite direction. Therefore, the majority of the pickup noise in the Sample Coil is cancelled by an equal and opposite emf induced in the Bucking Coils.

The Signal and Current Relays in Fig. 5.8 are both double-pole. They are shown in Fig. 5.8 in their quiescent (un-energized) states, with the Current Relay open, which disconnects the coils from the Polarization Power Supply and Current-Switching Circuit. In the quiescent state, the Signal Relay connects the Sample and Bucking Coils to the Preamplifier for signal detection. Pressing the MANUAL START switch initiates the following ordered sequence of events:

- 1) The Signal Relay is energized, which disconnects the coils from the Preamplifier and grounds the Preamplifier input.
- 2) The Current Relay is energized, which connects the Sample Coil to the Current-Switching Circuit and Polarization Power Supply.
- 3) The Digital Timing and Control Circuit sends a pulse to the Current-Switching Circuit, which turns current on in the coil. A counter begins counting from the preset polarizing time down to zero.

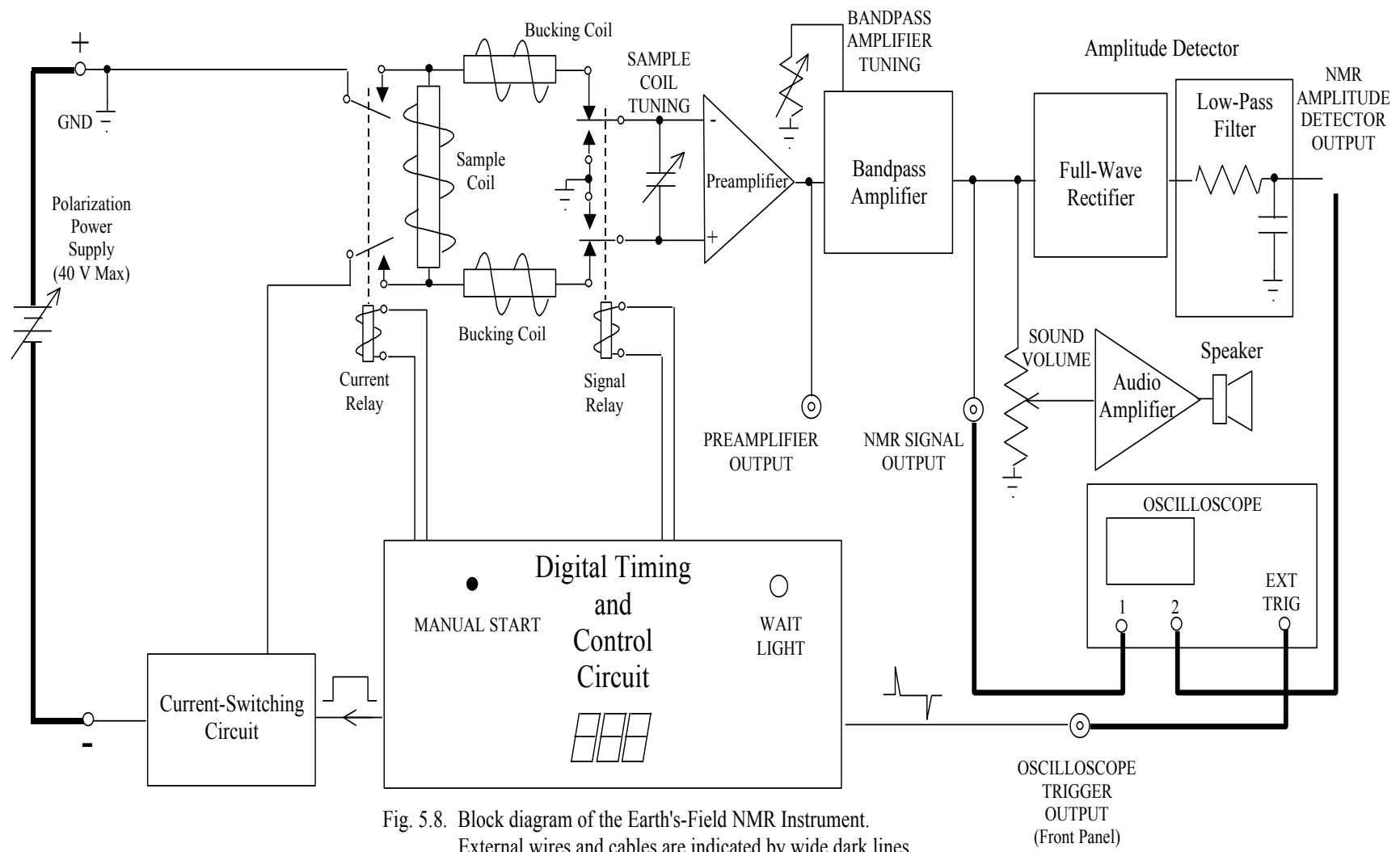


Fig. 5.8. Block diagram of the Earth's-Field NMR Instrument.
External wires and cables are indicated by wide dark lines.

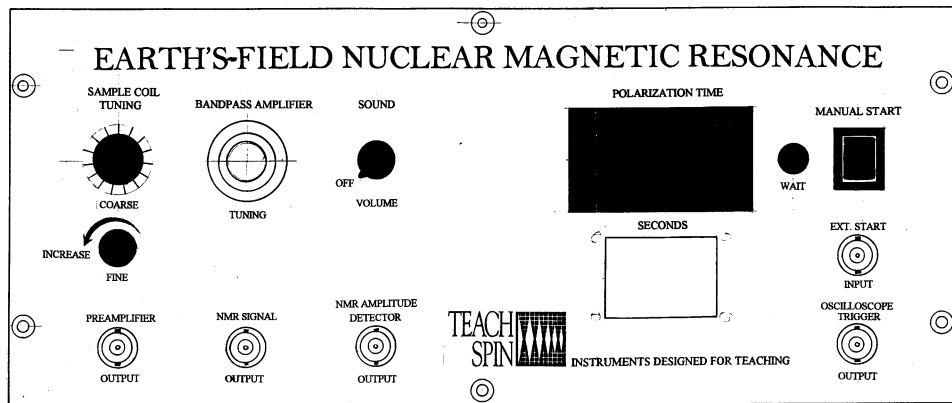
On the count of zero, counting stops, and the Current-Switching Circuit turns off the current in the Sample Coil within a few milliseconds, which is sufficiently fast to meet the condition for sudden passage.

- 4) After a short delay, to insure that the current has been reduced to zero, the Current Relay is de-energized, which opens the relay and disconnects the Sample Coil from the Current-Switching Circuit and Polarization Power Supply.
- 5) After another short delay, to insure that the Current Relay has opened, the Signal Relay is de-energized, which connects the Sample and Bucking Coils to the Preamplifier. At the same time, the control circuit provides a pulse to trigger the oscilloscope sweep for signal detection. On the count of zero, the WAIT light comes on. The digital counter remains on the count of zero for 5.0 s, and then counts back up to the original polarizing time. These two time delays are included to prevent rapid cycling of the instrument that might cause overheating of the Sample Coil and Current-Switching Circuit.

The free precession signal is normally viewed by connecting an oscilloscope to the NMR SIGNAL OUTPUT. The PREAMPLIFIER OUTPUT is provided as an aid in adjusting the input capacitors to tune the series LC resonant circuit to the precession frequency. The NMR AMPLITUDE DETECTOR OUTPUT is useful for samples for which the signal is small; multiple signals can be collected and averaged to improve signal-to-noise.

Controls and Connectors

Front Panel



THUMBWHEEL SWITCHES and DIGITAL DISPLAY

Users set the polarizing time in the range 0.1 to 99.9 seconds by means of thumbwheel switches on the front panel. Switch settings are automatically loaded into the count register of an internal presettable down counter. Contents of the count register are continuously displayed on the seven-segment digital displays during both loading and counting operations.

MANUAL START

Pressing the MANUAL START button initiates the automatic sequence necessary for acquiring a free precession signal. The polarization time t_p is the time set via the thumbwheel switches and displayed on the seven-segment displays.

EXTernal START INPUT

A contact closure to ground on this input (or a negative TTL pulse) performs the same function as pressing the MANUAL START button.

WAIT light

To prevent rapid cycling of the apparatus that would lead to overheating the Sample Coil and Current-Switching Circuit, the apparatus automatically delays 5.0 s on the count of zero. There is an additional delay (equal to the polarization time) as the counter counts from zero back up to the time that was set on the thumbwheel switches when the MANUAL START button was pressed. The WAIT light is turned on during both of these delays.

SAMPLE COIL TUNING (COARSE and FINE)

The input to the Preamplifier (see Fig. 8) is the voltage across a capacitor that is connected in series with the Sample and Bucking Coils. The resonant frequency of this series circuit, $\omega_0 = (LC)^{-1/2}$, can be adjusted to coincide with the Larmor precession frequency by rotating the COARSE and FINE switches to vary the capacitance. Rotating either switch counterclockwise decreases the capacitance and increases the resonant frequency

PREAMPLIFIER OUTPUT

This output is provided for monitoring the output of the Preamplifier while adjusting the COARSE and FINE controls to tune the resonant frequency of the input circuit to the Larmor precession frequency. When the input circuit is properly tuned to the frequency of the free precession signal, the amplitude of the signal at the output of the Preamplifier will be a maximum.

BANDPASS AMPLIFIER TUNING

The Preamplifier is followed by a Bandpass Amplifier that is included to block high and low frequency noise from the Preamplifier. The center frequency of the Bandpass Amplifier can be adjusted by means of this ten-turn potentiometer.

NMR SIGNAL OUTPUT

The output of the Bandpass Amplifier is connected to the NMR SIGNAL OUTPUT, which is normally connected to an oscilloscope for observing the free precession signal.

SOUND VOLUME

The NMR SIGNAL OUTPUT is connected internally to an audio power amplifier that drives an internal speaker. This allows users to hear the free precession signal, as well as view it on an oscilloscope.

NMR AMPLITUDE DETECTOR OUTPUT

The signal available at the NMR SIGNAL OUTPUT is also connected internally to an Amplitude Detector, which consists of a Full-Wave Rectifier followed by a Low-Pass Filter. The output of

the filter is the average value of the full-wave rectified free precession signal. For a full-wave rectified sinusoidal signal, the average value is $2/\pi$ of the peak value. Thus, the output of the NMR AMPLITUDE DETECTOR has essentially the same shape as the envelope of the free-precession signal, but the amplitude is about $2/3$ as large

OSCILLOSCOPE TRIGGER OUTPUT

When using an oscilloscope to view the free precession signal at any one of the three outputs on the front panel (PREAMPLIFIER OUTPUT, NMR SIGNAL OUTPUT, or NMR AMPLITUDE DETECTOR OUTPUT), connect the OSCILLOSCOPE TRIGGER OUTPUT on the front panel to the EXTernal TRIGger input on the oscilloscope. The signal at the OSCILLOSCOPE TRIGGER OUTPUT is two narrow pulses similar to those shown in Fig. 9. The leading (positive) pulse occurs at the instant the Signal Relay is deactivated, which connects the amplifier to the Sample and Bucking Coils. The trailing (negative) pulse occurs after a fixed delay of 80 ms, which is sufficient time to allow switching transients to die away before triggering the scope to view the precession signal.

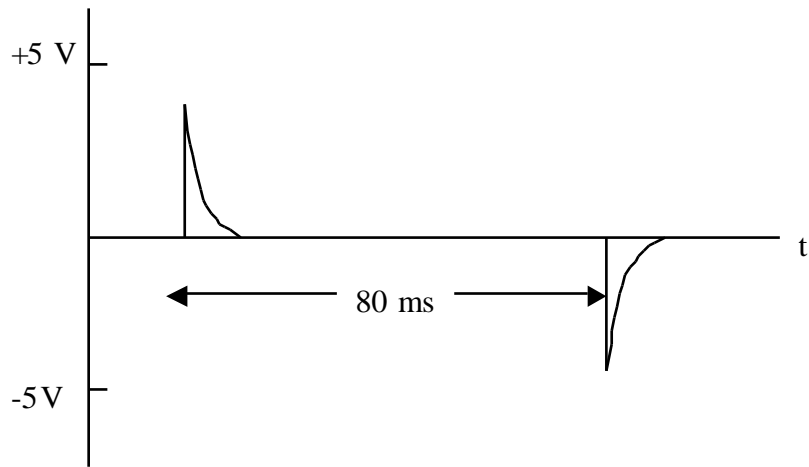
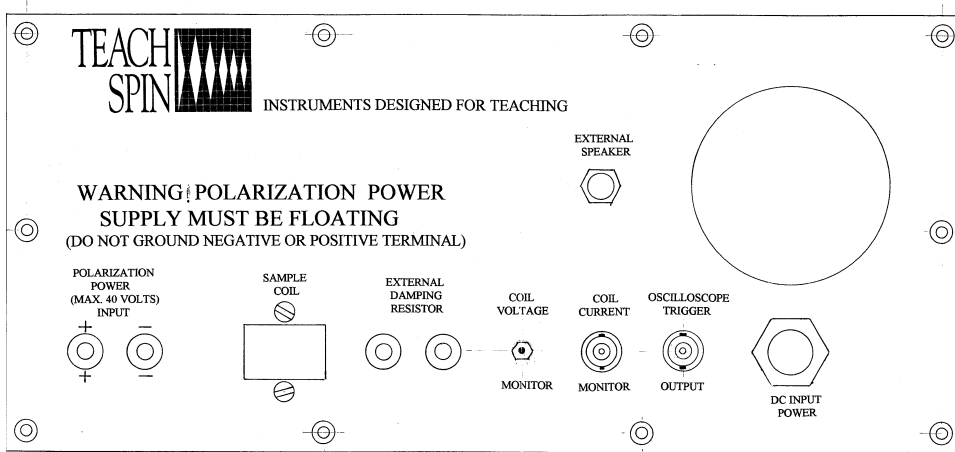


Fig. 5.9: Pulse sequence at the front-panel OSCILLOSCOPE TRIGGER OUTPUT.

Back Panel



POLARIZATION POWER INPUT (MAX 40 VOLTS)

The external power supply for providing polarizing current is connected to these two banana plug sockets. In order to obtain maximum signal, the power supply should be capable of providing 3.0 A at 36 volts. Both terminals of the power supply should be **floating**, i.e., neither terminal should be connected to ground. The positive terminal is connected to ground inside the Earth's-Field NMR instrument.

SAMPLE COIL

The four-wire shielded cable that connects to the Sample and Bucking Coils plugs into this socket.

EXTERNAL SPEAKER

The speaker converts to live and audible sound the output of the band-pass amplifier.

EXTERNAL DAMPING RESISTOR

COIL VOLTAGE MONITOR

COIL CURRENT MONITOR

OSCILLOSCOPE TRIGGER OUTPUT

These connections are provided for testing and for special applications. Their use is covered in Appendix A9 of the full Manual.

Detailed Description of the EF-NMR Field Coils Controller

The smaller of the two Controller units is devoted to the Field/Gradient Coil system. Its operation is markedly simpler than the complicated timing/sequencing involved in the main Controller unit. Note that this Field Coils Controller has separate modules for the Gradient Coils and the Helmholtz Coils.

There are three ten-turn knobs which are used to hand-adjust the constant currents that are sent to the Gradient Coils; their main function is to create steady field gradients which cancel out pre-existing gradients in the ambient magnetic field at your location.

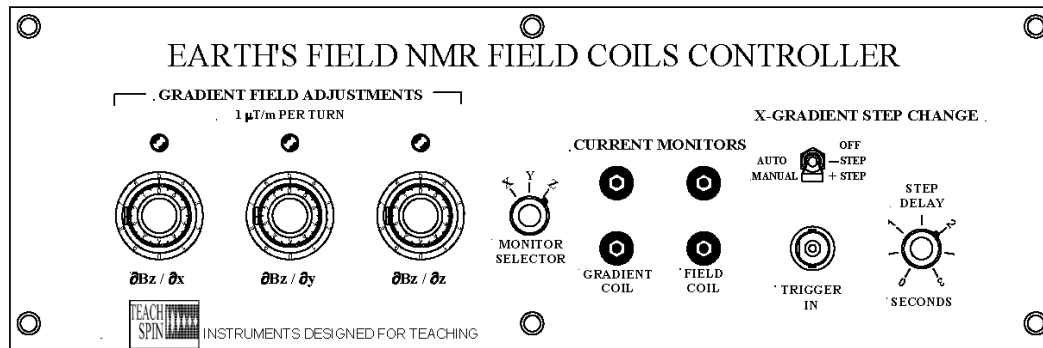
There are two Monitor points, where tip-jacks can be used to measure a *voltage* drop proportional to one of the three gradient-coil currents. A selector switch controls which of the three gradient-coil currents will be monitored. Another pair of tip-jacks permit the measurement of a *voltage* drop proportional to the Helmholtz-coil current. The Helmholtz coils, in turn, allow the addition of a spatially-uniform user-chosen increment of magnetic field to the local field.

Note that while this Controller *does* include the power supplies which run the gradient coils, it does *not* include the power supply which runs the Helmholtz coils.

Finally, there is one module in the Field Coils Controller labeled Step Gradient. You should put its toggle switch in the uppermost, OFF, position for all your initial experiments. This subsystem is used only in forming a certain kind of ‘spin echo’ (described in Chapter 9), which it achieves by creating some step-changes-in-time in the current sent to the $\partial B_z / \partial x$ gradient coil. Those step changes are described below, and form time-dependent additions to the steady, or d.c., current sent to this gradient coil by the leftmost of the 10-turn knobs.

Controls and Connectors

Front Panel



GRADIENT ADJUSTMENTS

Three 10-turn knobs permit the user to set the current sent through the three gradient coils built into the Field/Gradient Coil assembly. Each knob can change the current over the range -20 mA to +20 mA, so each delivers current with a 4 mA/turn sensitivity. The gradient coils have been

designed so that each turn of the dial, ie. each change by 4 mA in current, creates a change of very nearly 1 $\mu\text{T}/\text{m}$ in the relevant gradient. Note that for these controls to leave the ambient gradients as they are, they need to be dialed to **mid-scale**, and set to the 5.00-turn position.

GRADIENT-ADJUSTMENT LEDs

Above each of the three 10-turn dials is a red LED. Though all three ± 20 -mA gradient-coil current supplies are active whenever this Controller is turned on, only one of the three LEDs will be lit. Which one is lit is set by the Selector Switch in the Current Monitor module. This lit-up LED serves as another indication of which (of the three) gradient-coil currents you might be monitoring with a multimeter.

CURRENT MONITORS

For user convenience, we have installed series resistors into the three gradient-coil systems and into the Helmholtz-coil system, so as to make available front-panel connections to a potential difference which is a surrogate for the current in each of coil systems. Attach a **voltmeter** (*not* an ammeter) to the tip-jacks to read these voltages.

MONITOR SELECTOR

Each of the three gradient-coil systems has a series $100\text{-}\Omega$ 1% resistor permanently in place in its current path. Depending on the setting of this three-position selector switch, *one* of those three voltage drops is brought out to the tip-jacks where it may be monitored. Each turn of the relevant 10-turn control will change the current by 4 mA, the gradient by $1 \mu\text{T}/\text{m}$, and the monitor voltage by 0.4 Volts. When the monitor voltage reads zero, you can be sure the relevant gradient-coil current is zero.

GRADIENT

This labels the tip-jacks at which the voltage drop across the selected $100\text{-}\Omega$ resistor will be connected to a meter. The full range of gradient-coil current adjustment will create a voltage drop in the -2-V to +2-V range at these monitor points.

FIELD

This labels the tip-jack at which the voltage drop across a $0.1\text{-}\Omega$, 1%, 5-W resistor in series with the Helmholtz Coils may be monitored at any time. The Helmholtz coils are designed for use in the ± 3 -A range, so the monitor voltage expected here will be in the ± 0.3 -V range. Note that no current will flow, and no voltage drop will arise, unless a separate Helmholtz-Coil power supply is attached at the Controller's back panel.

X-GRADIENT STEP CHANGE

This section of the Controller allows the step-wise change in time of the current in the $\partial B_z/\partial x$ gradient coil. This module is used to make possible the formation of a 'pulsed-gradient spin echo', described in Chapter 9.2 of this manual.

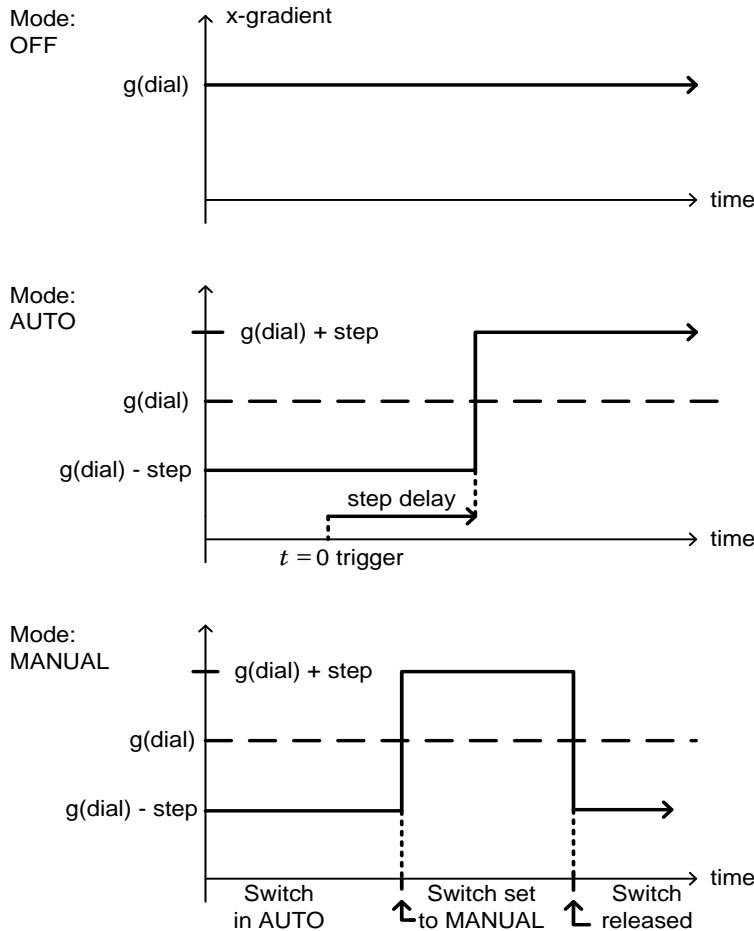


Fig. 2.3: A timing diagram, in each case showing the size of the gradient $\partial B_z / \partial x$ as a function of time, illustrating the three modes of the STEP GRADIENT function.

SELECTOR SWITCH

This is a three-position toggle switch which controls this step-change module of the Controller. Any experiments *not* involving pulsed-gradient spin echoes should be conducted with this switch in the uppermost, OFF, position. In this position, the current in the $\partial B_z / \partial x$ gradient coil is steady in time, and controlled only by the leftmost of the three 10-turn dials.

AUTO

The middle position of this toggle switch puts the current in the $\partial B_z / \partial x$ coil into a different mode, in which its value is fixed by the sum of two terms. The first of these is set by the leftmost 10-turn dial, and the second is an offset of fixed magnitude and negative sign. That's the meaning of the '- STEP' indication next to the switch. (The size of that offset is set by a user-adjustable control on the back panel.)

MANUAL

The bottom position of the three-position toggle switch is spring-loaded, and reverts to the AUTO position when released. Deflecting the switch from AUTO to MANUAL will cause a change in the

current in the $\partial B_z/\partial x$ coil from the previous (10-turn dial setting *minus* offset) to a temporary value of (10-turn dial setting *plus* offset). That's the meaning of the '+ STEP' indication next to the switch. The '+ STEP' condition will persist as long as the toggle switch is held in the lowest position.

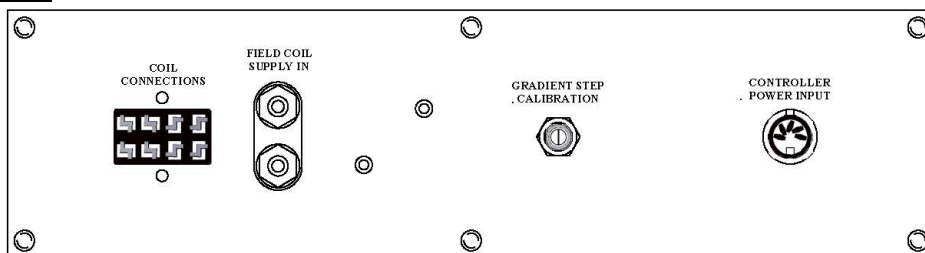
TRIGGER IN

As an alternative to the MANUAL mode, of hand-initiating a gradient step, this input, together with the AUTO setting of the selector switch, permits an externally-initiated reversal of the step-gradient from the '- STEP' to the '+ STEP' condition. The input is designed to accept a negative-level, negative-going pulse, such as the second of the pulse pair which emerges from the TRIGGER OUTput of the (main) EF-NMR Controller. If this triggering pulse is present at the beginning of the free-induction-decay interval, and the selector toggle switch is in the AUTO position, then the gradient will have the value given by (10-turn dial setting *minus* offset) for part of the free-induction-decay interval, and will automatically change to the value given by (10-turn dial setting *plus* offset) after a selected time delay.

STEP DELAY

This one-turn dial control applies only in the AUTO mode of the selector toggle switch. It controls how much time is spent in the (10-turn dial setting *minus* offset) mode, before the current in the $\partial B_z/\partial x$ coil changes to the (10-turn dial setting *plus* offset) mode. That time delay is variable in the range 0-3 seconds.

Back Panel



COIL CONNECTIONS

The eight-wire cable that connects to the Gradient and Helmholtz Coils plugs into this socket.

FIELD COIL SUPPLY IN

These terminals are the place to connect an external power supply to energize the Helmholtz coils. They are designed for a 0-36 Volt, 0-3 Ampere current-controlled d.c. power supply. The coil current passes through the power supply, the Helmholtz Coils, and the $0.1\text{-}\Omega$ monitor resistor. The Helmholtz-coil system is 'floating', not connected to ground at any point in the Controller. So the external power supply used for it may be floating, negative-grounded, or positive-grounded.

If the Helmholtz Coils are not being used, then a ground connection to the black terminal of these connections will ground the windings of the Helmholtz coil, to serve as partial electrostatic shielding of the EF-NMR head.

GRADIENT STEP CALIBRATION

This one-turn locked dial controls the size of the ‘step’ which is applied, in the AUTO or MANUAL gradient step-change mode, alternatively subtracted from and added to, the current in the $\partial B_z / \partial x$ gradient coil. If you wish to change the size of this offset, you will need first to loosen the hex nut on the shaft-lock of the potentiometer involved. You can re-tighten that locking nut once you have made a new setting in the size of the gradient-step current.

CONTROLLER POWER INPUT

The special connector from the wall-transformer power unit plugs into the Controller at this point. As there is no separate on-off switch in the Controller, power will be present when this connection is made, and the wall-transformer unit is active.

Note that the wall transformers for the (main) Controller, and for the Field/Gradient Coil Controller, are identical and compatible, so either may be used to power either Controller.

INITIAL SETUP

Positioning the Coils

If the sample is located in a region where the earth's magnetic field B_e is perfectly homogeneous, the free precession signal decays with time constant T_2 , the spin-spin relaxation time that is characteristic of the sample. For water, T_2 is equal to T_1 in the range of magnetic fields accessible to the earth's-field free precession technique; both are about 2.5 seconds at room temperature. In practice, however, one finds that the earth's magnetic field is not perfectly homogeneous, even outdoors, and even over relatively small sample volumes of 100 ml. Because of the earth's-field inhomogeneity, spins in different parts of the sample precess at slightly different frequencies $\omega_e = \gamma B_e$. As the spins precess they gradually lose phase coherence with each other, which causes the signal to decay toward zero with time constant T_{2*} that is less than T_2 . If there are magnets or magnetic materials nearby that significantly distort the earth's magnetic field, T_{2*} can be so short that the signal dies away before the switching transient, which persists for times on the order of 50 ms. It is, therefore, desirable to position the coils in an area where the earth's magnetic field is as homogeneous as possible. That usually means near the open center of a room, about four or five feet above the floor.

Ideally, the coils should also be placed in an area as far away as possible from sources of radiated electrical noise. Fluorescent lights in the same room as the coils should be turned off.

Once you have positioned the coils, orient the coils with their axes pointing east-west, perpendicular to magnetic north. Now you are ready to tune the instrument in order to detect a free precession signal.

Tuning the Instrument to Obtain Maximum Signal

- 1) To avoid distorting the earth's magnetic field, and to minimize possible pickup noise, position the Earth's-Field NMR instrument as far as practical away from the coils. About 3 meters (10 feet) is usually sufficient. Connect the coils to the instrument by inserting the plug on the coil cable into the socket on the back panel
- 2) Fill a 125-ml plastic bottle with tap water, and place it in the center of the Sample Coil.

- 3) Make sure the power supply you intend to use for providing the polarizing current does not exceed 40 volts. Also, make certain that both outputs are floating, i.e., neither terminal is connected to ground. With the power supply turned off, connect the + and - terminals on the power supply to the corresponding terminals on the back panel. The + terminal of the power supply is connected to ground inside the instrument. DO NOT TURN THE POLARIZING POWER SUPPLY ON JUST YET. WAIT UNTIL INSTRUCTED TO DO SO IN STEP 7.
- 4) Connect the low-voltage "brick on a rope" power supply to the DC INPUT POWER connector on the back panel. The instrument should now be on, and the seven-segment displays on the front panel should display whatever polarizing time happens to be set on the thumbwheel switches.
- 5) In order to detect a free precession signal, connect the PREAMPLIFIER OUTPUT to one of the input channels of an oscilloscope. Superimposed on the signal is a d.c. offset of up to ± 500 mV. To eliminate the offset, set the oscilloscope COUPLING to AC. Set the vertical sensitivity to 50 mV/div, and the sweep speed to 2 ms/div.
- 6) Connect the OSCILLOSCOPE TRIGGER OUTPUT on the front panel to the EXternal TRIGger input on the oscilloscope. Set the oscilloscope to trigger on EXternal, DC COUPLING with HF (High Frequency) REJECT, -SLOPE, and LEVEL ≈ -1 V). This will insert an 80-ms delay between the time the Signal Relay is de-energized (which connects the coils to the Preamplifier) and the time the oscilloscope begins its sweep. Thus, the switching transient will not be visible since it will have died away before the oscilloscope sweep begins.
- 7) Set the COARSE and FINE SAMPLE COIL TUNING switches to the middle of their ranges. Turn on the Polarization Power Supply; set the voltage at about 34 volts. If it is a current-limiting supply, set the current limit at maximum. Set the polarizing time to about two times T_1 (about 5.0 s for water); then press the MANUAL START button. If the precession frequency is near the resonant frequency of the tuned circuit, you will see a free precession signal.
- 8) Turn the COARSE SAMPLE COIL TUNING switch clockwise one position, and try again.
If the signal is larger than before, you are searching in the right direction. Turn the COARSE switch clockwise one additional position, and repeat the process.
If the signal is smaller than before, you have gone in the wrong direction. Rotate the COARSE switch counterclockwise two positions, and try again.

If you still haven't seen any signal at all it may be because the resonant frequency of the tuned circuit is still too far away from the precession frequency. Turn the COARSE switch clockwise one additional notch, and try again. Keep rotating the switch clockwise until you detect the signal or come to the end of the range. If you come to the end of the range and still haven't detected the signal, set the COARSE switch back to the center of its range, and begin searching for the signal as you rotate the COARSE switch counterclockwise one step a time.

- 9) Once you have found the setting of the COARSE switch that gives maximum signal, begin adjusting the FINE switch to obtain the largest signal possible. When you have finished, the resonant frequency of the tuned circuit coincides with the free precession frequency.

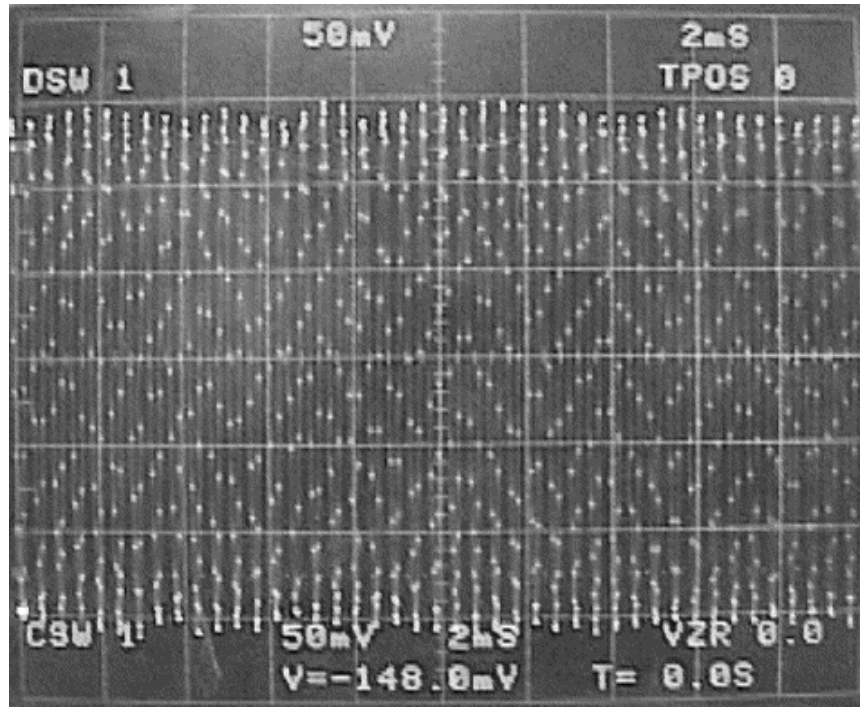


Fig. 5.10: Free precession signal at the PREAMPLIFIER OUTPUT. The oscilloscope is set at 50 mV/div and 2 ms/div. The sample frequency is 100 samples/div for all oscilloscope waveforms shown in this Student Manual.

Adjusting the Center (Resonant) Frequency of the Bandpass Amplifier

In addition to supplying more signal amplification, the Bandpass Amplifier prevents electrical noise at frequencies far above and below the free precession frequency from reaching the NMR SIGNAL OUTPUT. By adjusting the ten-turn BANDPASS AMPLIFIER TUNING potentiometer, it is possible to adjust the center frequency of the Bandpass Amplifier to coincide with the frequency

of the free precession signal. When that occurs, the amplitude of the free precession signal at the NMR SIGNAL OUTPUT will be a maximum. You will accomplish that in the steps that follow:

- 10) Leaving the PREAMPLIFIER OUTPUT connected to the oscilloscope, connect the NMR SIGNAL OUTPUT to the unused oscilloscope input channel. Adjust the controls on the oscilloscope to view *only* the channel connected to the NMR SIGNAL OUTPUT. (Since the NMR SIGNAL OUTPUT has no d.c. offset, you may set the oscilloscope COUPLING to either AC or DC.) Set the vertical sensitivity to 1 Volt/div. As a first approximation, set the ten-turn BANDPASS AMPLIFIER TUNING potentiometer to the center of its range. Without changing the settings of the COARSE and FINE SAMPLE COIL TUNING switches, cycle the instrument; as you do so, adjust the potentiometer to obtain a signal of maximum amplitude at the NMR SIGNAL OUTPUT. (Adjusting the potentiometer should have little or no effect on the amplitude of the signal at the PREAMPLIFIER OUTPUT.) As you adjust the potentiometer you can start by making relatively coarse adjustments in one- or one-half-turn increments. As the center bandpass frequency gets nearer the free precession frequency, you will need to make finer adjustments.

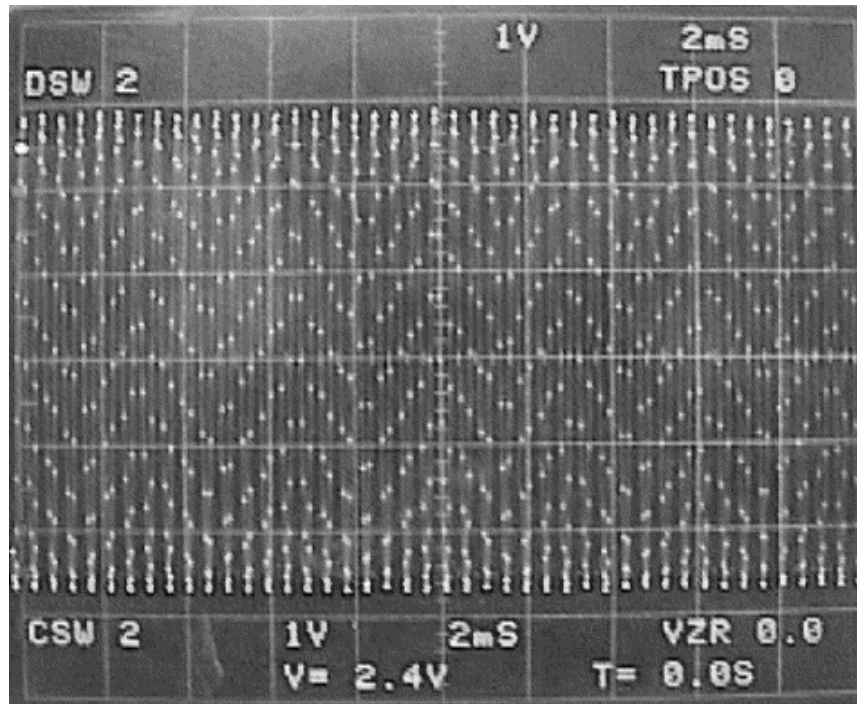


Fig. 5.11: Free precession signal at the NMR SIGNAL OUTPUT. The oscilloscope is set at 1 Volt/div and 2 ms/div.

Figure 12 shows a free precession signal at the NMR SIGNAL OUTPUT obtained with the oscilloscope sweep speed reduced to 50 ms/div. (The free precession frequency was 2088 Hz; yet the digitized waveform appears to have a much lower frequency of only 88 Hz. A discussion of the source of this problem – called aliasing – and what to do about it may be found in *Appendix B* and in the section on the *NMR Amplitude Detector*.)

The signal in Fig. 12 exhibits the Gaussian-shaped decay that is commonly observed where the earth's field indoors is relatively inhomogeneous. Refer to Fig. 5.13 on page 5-23 for an example of the longer decays that are observed in more homogeneous earth's magnetic fields.

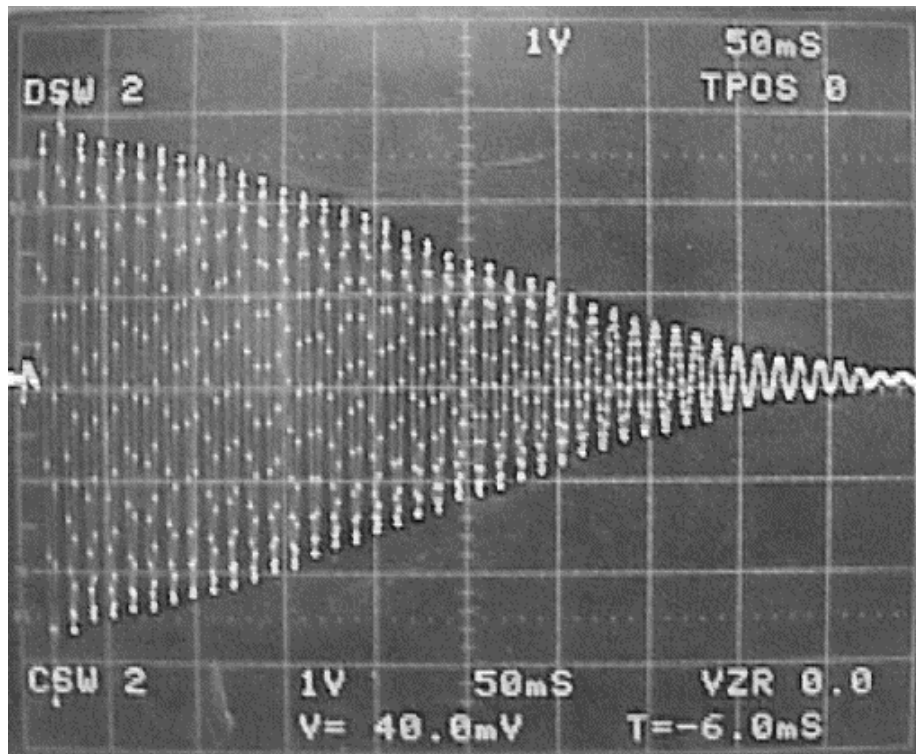


Fig. 5.12: Water free precession signal at the NMR SIGNAL OUTPUT. Note the Gaussian-shaped decay caused by a relatively inhomogeneous earth's magnetic field. The oscilloscope is set at 1 V/div and 50 ms/div.

NMR AMPLITUDE DETECTOR

Figure 13 shows the NMR SIGNAL from a water sample viewed simultaneously with the signal at the NMR AMPLITUDE DETECTOR OUTPUT. As discussed in the section on *Front Panel Controls and Connectors*, the output of the Amplitude Detector has essentially the same shape as the envelope of the free precession signal, but an amplitude that is $2/\pi$, or about $2/3$, as large. The signals in Fig. 5-13 were obtained with the 80-ms oscilloscope sweep delay disabled. Therefore, we can see the switching transient and initial growth of the signal, followed by the exponential decay. The same signals as in Fig. 5-13 are shown in Fig. 5-14, but there the sweep speed has been increased from 50 ms/div to 20 ms/div. Note in Fig. 5-14 the apparent ‘beats’ in the amplitude of the free precession signal at the NMR SIGNAL OUTPUT. These beats are not real; they are artifacts caused by the fact that the digital storage oscilloscope samples and digitizes the input waveforms at a frequency that depends on the oscilloscope sweep speed. Significant distortions can occur when the sample frequency is less than, or on the order of, the frequency of the input signal. Since the output of the NMR AMPLITUDE DETECTOR is a relatively slowly-varying signal, it is relatively immune to problems associated with reducing the oscilloscope sample rate. Refer to *Appendix B* for a more complete discussion.

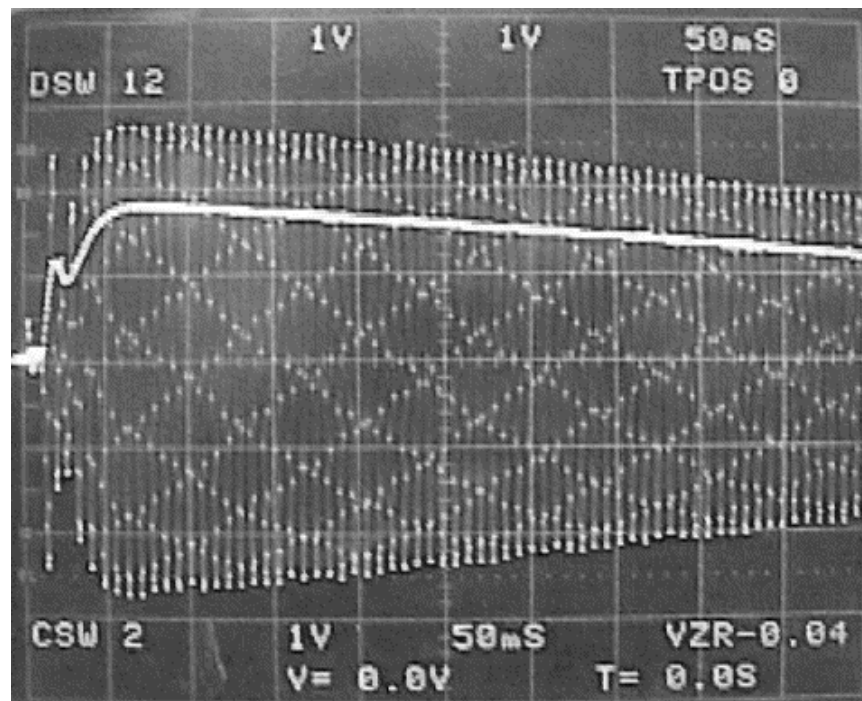


Fig. 5.13: Water NMR SIGNAL shown along with the output of the NMR AMPLITUDE DETECTOR. Both oscilloscope channels are set at 1 V/div and 50 ms/div.

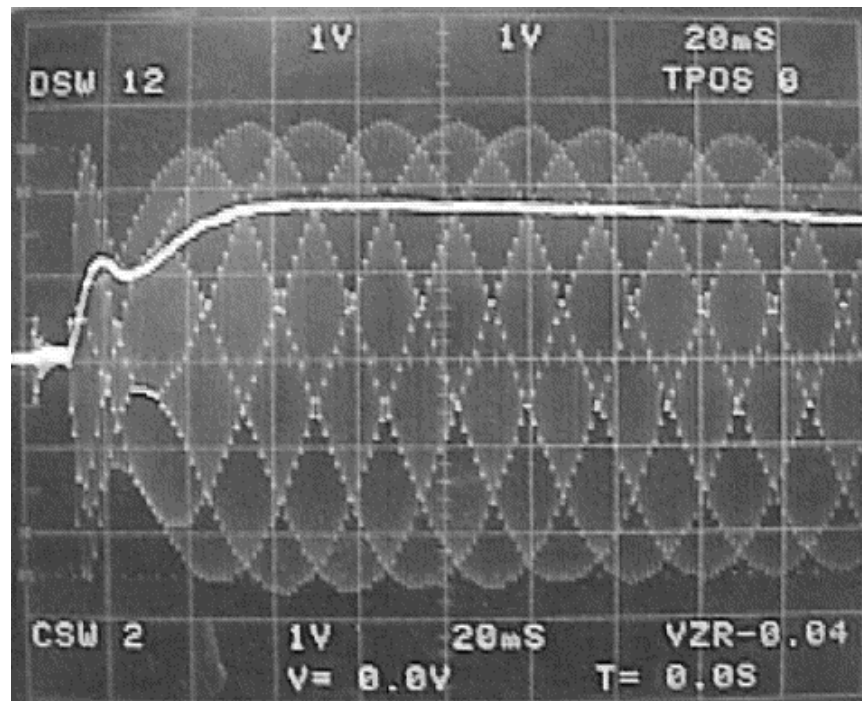


Fig. 5.14: Same signals as in Fig. 13, but with the oscilloscope sweep speed increased to 20 ms/div. Note the appearance of "beats" in the NMR SIGNAL OUTPUT caused by problems associated with aliasing.

APPENDIX A: Larmor Precession

Figure A1 shows a positively charged nucleus with its magnetic moment oriented at angle θ with respect to a magnetic field \vec{B} pointing along the $+z$ -axis. The spin angular momentum vector \vec{L} is not shown in the figure, but it points in the same direction as $\vec{\mu}$. We wish to prove that at the magnetic moment $\vec{\mu}$ will precess about \vec{B} at constant angular velocity $\omega = \gamma B$. That is, the tip of $\vec{\mu}$ will follow the circular dotted path shown in the figure.

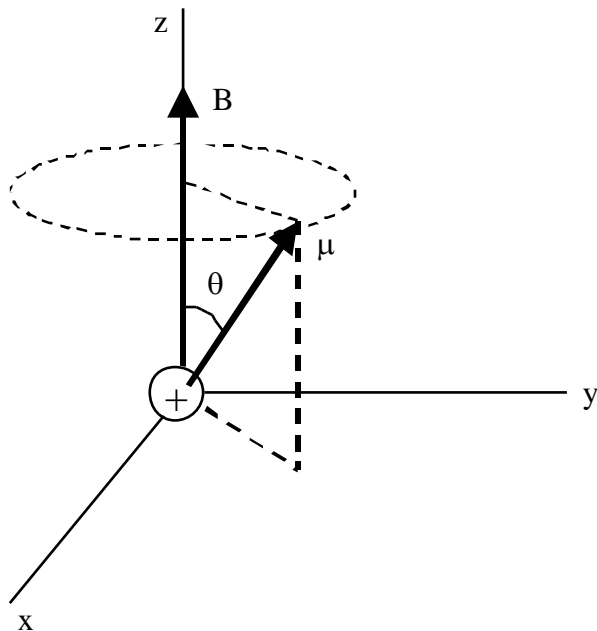


Fig. 5.A1: A positively charged nucleus with its magnetic moment $\vec{\mu}$ oriented at angle θ with respect to a magnetic field \vec{B} pointing along the $+z$ -axis. The angular momentum vector \vec{L} , not shown, points in the same direction as $\vec{\mu}$.

We begin by writing Newton's 2nd law in the form

$$\vec{\tau} = \frac{d\vec{L}}{dt} . \quad (\text{A1})$$

The magnetic torque tending to align $\vec{\mu}$ with \vec{B} is given by

$$\vec{\tau} = \vec{\mu} \times \vec{B} . \quad (\text{A2})$$

By combining Eqs. (A1) and (A2), and making the substitution $\vec{\mu} = \gamma \vec{L}$, we obtain

$$\frac{d\vec{\mu}}{dt} = \gamma \vec{\mu} \times \vec{B} . \quad (\text{A3})$$

By making the substitutions $\vec{B} = \hat{k} B$ and $\vec{\mu} = \hat{i} \mu_x + \hat{j} \mu_y + \hat{k} \mu_z$ the vector equation (A3) can be written as three separate scalar equations, one for each of the components:

$$\frac{d\mu_x}{dt} = \gamma B \mu_y, \quad (\text{A4})$$

$$\frac{d\mu_y}{dt} = -\gamma B \mu_x, \quad (\text{A5})$$

and

$$\frac{d\mu_z}{dt} = 0. \quad (\text{A6})$$

Solving Eq. (A6) yields $\mu_z(t) = \mu_z(0) = \text{constant}$. By multiplying Eq. (A5) by $i = \sqrt{-1}$ and adding the result to Eq. (A4) we obtain

$$\frac{d}{dt} (\mu_x + i\mu_y) = -i\gamma B (\mu_x + i\mu_y).$$

By making the substitution $\mu_+ = \mu_x + i\mu_y$ this equation may be simplified to

$$\frac{d\mu_+}{dt} = -i\gamma B \mu_+,$$

which has as its solution

$$\mu_+(t) = \mu_+(0)e^{-i\gamma B t}.$$

Expanding by using Euler's identity, and substituting $\mu_+ = \mu_x + i\mu_y$, yields

$$\mu_x(t) + i\mu_y(t) = (\mu_x(0) + i\mu_y(0))(\cos \gamma B t - i \sin \gamma B t).$$

By choice of axes let $\mu_x(0) = 0$. Then, by equating the real and imaginary parts of both sides of the previous equation, we obtain

$$\mu_x(t) = \mu_y(0) \sin \gamma B t$$

and

$$\mu_y(t) = \mu_y(0) \cos \gamma B t,$$

which shows that the angular velocity of precession is $\omega = \gamma B$. It is interesting, perhaps surprising, to note that the angular frequency of precession is independent of cone angle θ .

APPENDIX B: Aliasing

A typical digital oscilloscope samples the input waveform at fixed time intervals, and then displays the digitized samples on the oscilloscope screen. These samples are normally connected by straight-line segments in order to give, at least roughly, the appearance of a smooth waveform. Figure B1 shows a 2200 Hz sinusoidal waveform and, for comparison, the sampled approximation.

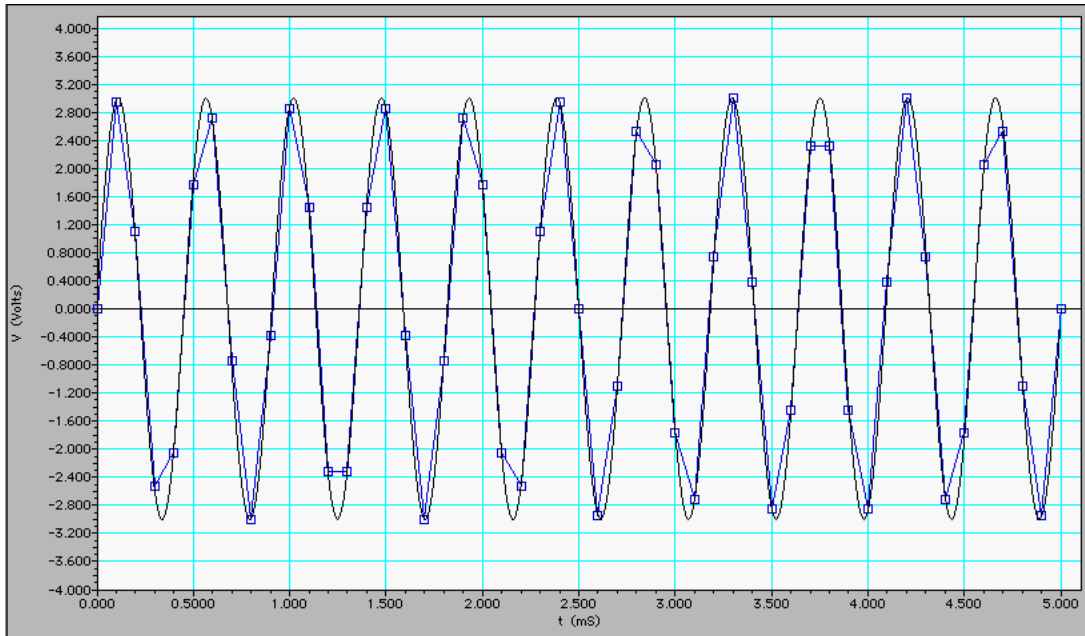


Fig. 5.B1: The rough approximation that results when a 2.2 kHz sinusoidal waveform is sampled at 10 kHz.

The samples are shown as squares, and the squares are shown connected by straight-line segments. In constructing Fig. 5.B1 the time between samples was assumed to be 0.1 ms, which corresponds to a sampling frequency of 10 kHz, which is only 4.5 times the frequency of the input signal. Thus, on average, each cycle of the input signal is approximated by only about 5 points. Furthermore, the points are joined by straight-line segments rather than a smooth curve. The distortion is obvious. Some of the cycles appear to have "missing peaks" since the oscilloscope digitizer did not happen to sample the input waveform when it was at a maximum.

A similar graph is shown in Fig. 5.B2, but in this case the sampling frequency has been increased to 20 kHz, which is almost ten times the frequency of the input waveform. The digitized

approximation now appears to have about the same shape as the input waveform. Now each cycle is approximated by ten straight-line segments, rather than just five as before. However, there are still some obvious distortions. Note, for example, the 4th peak from the left, which occurs near time $t = 1.5$ ms.

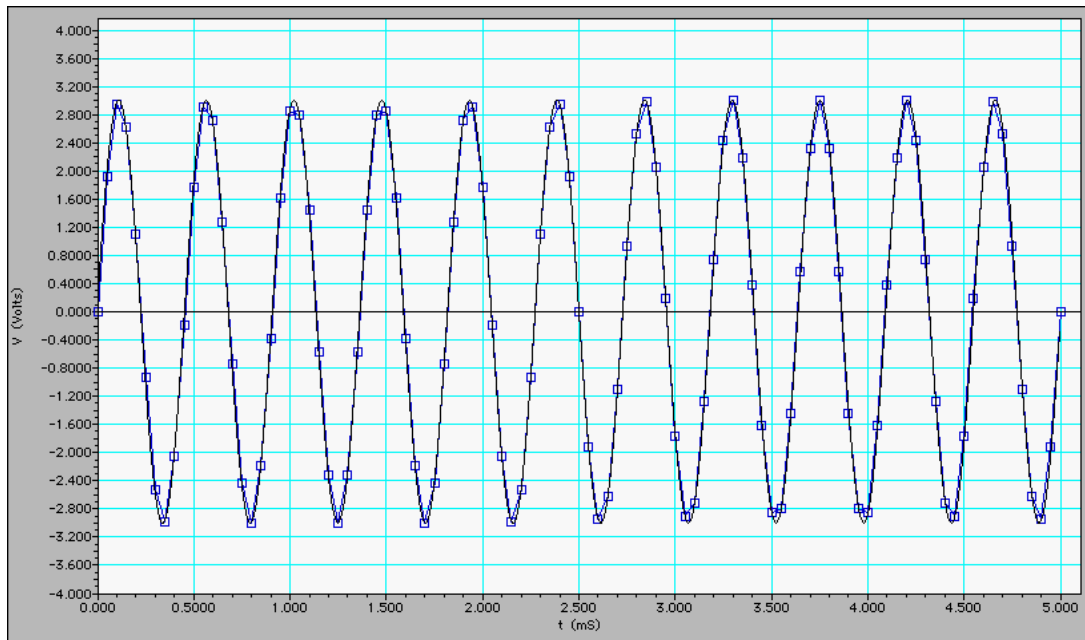


Fig. 5.B2: The relatively smooth waveform that results when a 2.2 kHz sinusoidal waveform sampled at 20 kHz.

The oscilloscope happened to sample the waveform on either side of the peak, but not at the peak itself. Therefore, when viewed on the oscilloscope screen, the peak will appear to be "flattened off" and slightly reduced in size relative to other peaks of the waveform. Thus, in order to obtain a waveform that is displayed smoothly on the screen, it is necessary to have an oscilloscope sampling frequency that is *more* than ten times the frequency of the signal.

At low sampling frequencies it is easy to be completely misled by the digitized waveform displayed on the oscilloscope screen. Figure 5.B3 shows the same 2200 Hz signal as before, but the sampling frequency has been reduced to 2 kHz. Note that the input waveform is sampled only about once each cycle, and the digitized waveform

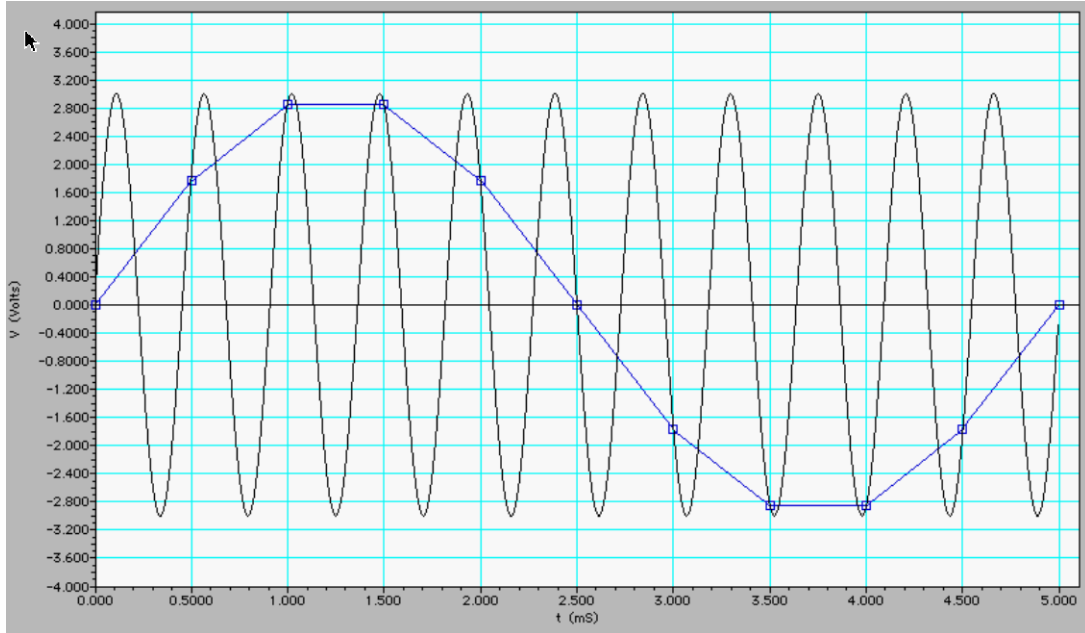


Fig. 5.B3: Missing cycles that result when a 2.2 kHz sinusoidal waveform is sampled at 2 kHz, which does not meet the Nyquist criterion.

appears to be, at least approximately, a sinusoidal signal of much lower frequency than the input waveform! To avoid these kinds of errors, the sampling frequency must meet the requirement of the Nyquist theorem, which states that the sampling frequency must be at least twice the signal frequency. For comparison, Fig. 5.B4 shows the 2200 Hz input waveform sampled at 5 kHz (time between samples is 0.2 ms). This sampling frequency meets the Nyquist criterion, which effectively means that the sampled waveform has no "missing cycles." However, it still looks greatly distorted. Based on the appearance of the sampled waveform in Fig. 5.B4 one might be tempted to conclude, quite incorrectly, that the input waveform exhibits beats. (For an example of apparent beats in a free precession signal, refer to Fig. 5.14 on p. 5-23.)

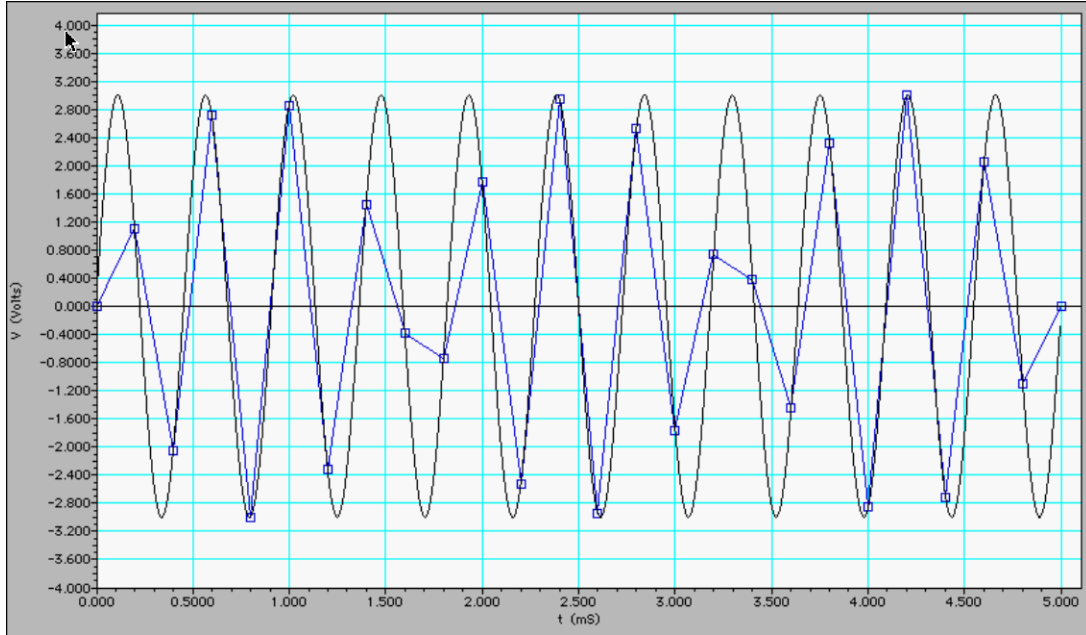


Fig. 5.B4: A 2.2 kHz sinusoidal waveform sampled at 5.0 kHz. There is significant distortion, even though the sampling frequency meets the Nyquist criterion.

So, what does all this mean with regard to using digital storage oscilloscopes for capturing free precession signals? First of all, it is obviously desirable to have a sampling frequency that is at least ten times the frequency of the free precession signal. For signals at 2.1 kHz, corresponding to an earth's field of 0.05 mT, the sample frequency should be of the order of 20 kHz or more. Specifications for digital oscilloscopes may claim maximum sampling frequencies of hundreds of thousands, or even millions, of samples per second. But those specifications may be misleading. Digital oscilloscopes vary, but, for most commonly used oscilloscopes, the oscilloscope takes only 500 or 1000 samples during one horizontal sweep. Assuming the screen is 10 divisions wide, that corresponds to as few as 50 samples per division. At a sweep speed of 0.2 ms/div, 50 samples per division corresponds to a time interval of 0.004 ms between each sample, which is equivalent to a sample frequency of only 25 kHz, barely sufficient to produce a smooth digitized waveform. At 50 samples per division and a sweep speed of 20 ms/div, the time between samples is 0.4 ms. The corresponding sample frequency is only 2.5 kHz, which does not even meet the Nyquist criterion. Therefore, severe sampling errors like that shown in Fig. 5.B3 can be expected when the oscilloscope sweep speed is 20 ms/div or slower. The following examples will illustrate this principle.

Figure 5.B5 shows a photograph of an oscilloscope waveform obtained from a 125-ml sample of water. The frequency of the free precession signal was 2.088 kHz. The oscilloscope sweep speed was 50 ms/div. The waveform appears to be relatively

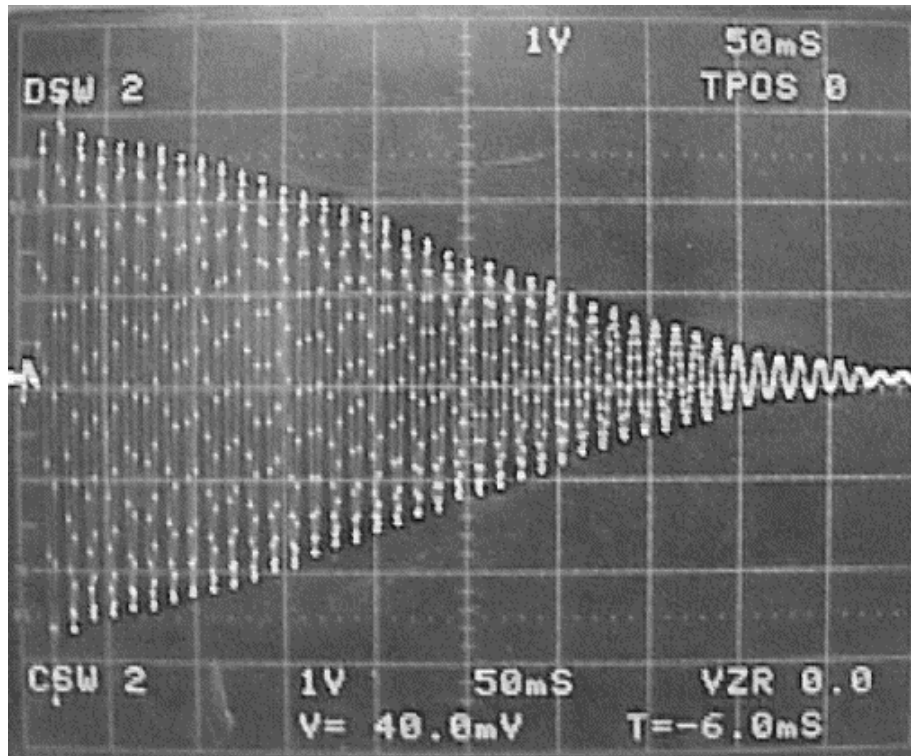


Fig. 5.B5: Apparently smooth free precession signal at a frequency of 2.088 kHz. The sample frequency was 2 kHz.

smooth, with multiple samples per cycle. However, that is not the case. The oscilloscope was sampling at 100 samples/division, which corresponds to a time interval between samples of 0.5 ms and a sample frequency of 2 kHz. Thus, the sample frequency is just slightly less than the frequency of the signal. The situation is similar to that in Fig. 5.B3. What appears in Fig. 5.B5 to be many closely spaced samples on the same cycle are actually single samples taken on many successive cycles. For a signal frequency of 2.088 kHz and a sample frequency of 2.000 kHz, the difference in frequencies (or beat frequency) is 88 Hz, which is the apparent or ‘aliased’ frequency of the digitized waveform in Fig. 5.B5.

The waveform in Fig. 5.B6 shows an even more extreme example of aliasing. The 2.007 kHz signal was obtained from fluorine nuclei in a 25-gram sample of

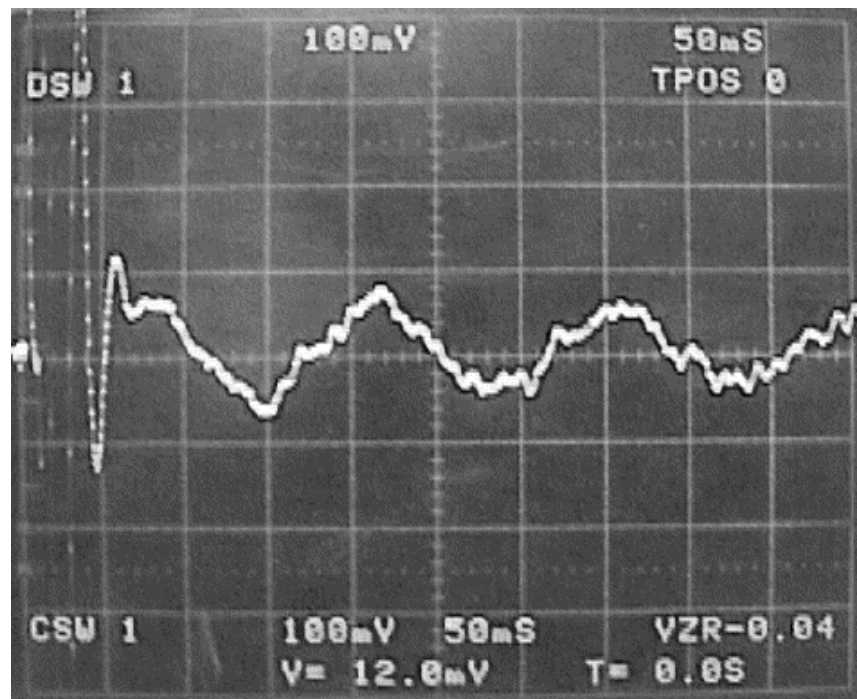


Fig. 5.B6: 2.007 kHz fluorine signal from a 25-gram sample of C_6F_6 . The oscilloscope sample frequency was 2.000 kHz. The digitized waveform appears to have a frequency equal to the difference, 7 Hz.

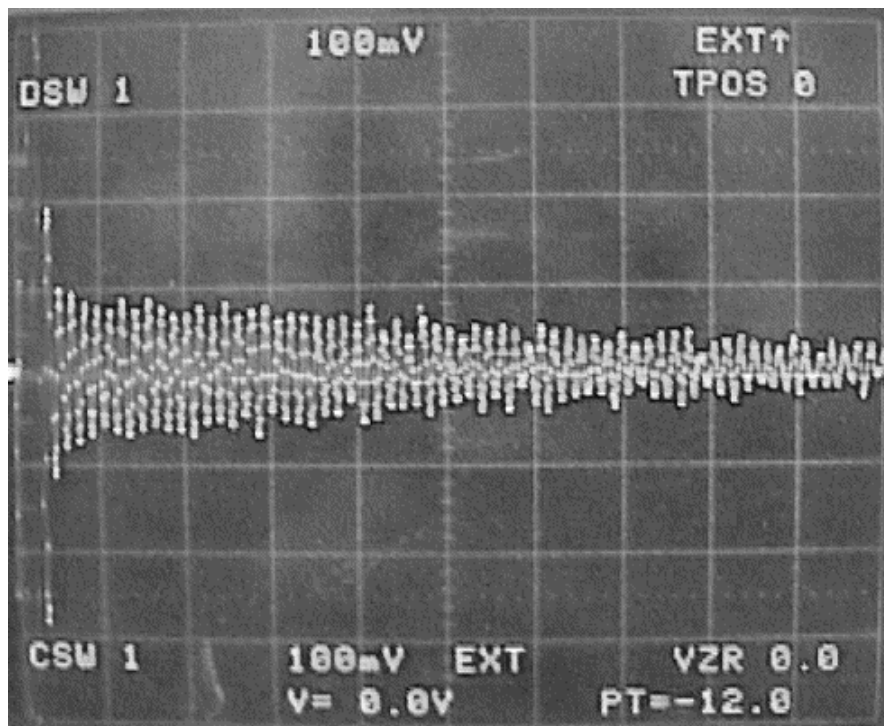


Fig. 5.B7: Same as Fig. 5.B6, except the oscilloscope sample frequency was reduced to 1.040 kHz. Since the oscilloscope displays 100 samples per division, the equivalent sweep speed is 96 ms/div.

hexafluorobenzene, C₆F₆. The oscilloscope sweep speed was 50 ms/div, and the oscilloscope sample frequency was 2 kHz. Here, the signal and sample frequencies differ by only 7 Hz, which is identical to the apparent frequency of the sampled waveform observed on the oscilloscope screen. The same fluorine signal is shown in Fig. B7, but there the sample frequency was reduced to 1.040 kHz. The time between samples was 0.96 ms, which is almost twice the period. The situation is similar to that shown in Fig. 5.B3, except the sample frequency was so low that the sampling process skipped whole cycles. Yet, the sampled waveform appears surprisingly smooth.

EXPERIMENTS

PRIOR TO PERFORMING ANY OF THESE EXPERIMENTS, THE APPARATUS MUST BE POSITIONED AND TUNED AS DESCRIBED IN THE SECTION ON **INITIAL SETUP**.

EXPERIMENT 1: Measurement of the Proton Spin-Lattice Relaxation Time in Water

Objectives

The objective of this experiment is to measure the proton spin-lattice relaxation time T_1 in water at room temperature.

Equipment

Earth's-Field NMR instrument

Polarization power supply (floating outputs, 40 volts maximum)

Oscilloscope

125-ml sample bottle

Theory

According to the Curie law, the equilibrium magnetization of a sample containing magnetic moments μ is

$$M_\infty = \frac{n\mu^2}{3kT} B , \quad (1)$$

where μ is the magnetic moment of each spin, n is the number of magnetic moments per unit volume, B is the magnetic field, k is Boltzmann's constant, and T is the temperature on the Kelvin scale. The magnetization of the sample does not assume the equilibrium value instantaneously, but, rather, rises exponentially toward the Curie value with time constant T_1 , the spin-lattice relaxation time. The growth of $M(t)$ toward M_∞ is described by the equation

$$M(t) = M_\infty (1 - e^{-t/T_1}) , \quad (2)$$

where M_∞ is the equilibrium Curie magnetization, and $M(t)$ is the magnetization at time t . By rearranging Eq. (2) we obtain

$$M_\infty - M(t) = M_\infty e^{-t/T_1} . \quad (3)$$

By taking the natural logarithm of both sides, Eq. (3) can be rewritten

$$\ln(M_\infty - M(t)) = \ln(M_\infty) - \frac{1}{T_1} t . \quad (4)$$

From Eq. (4) we see that a plot of $\ln(M_\infty - M(t))$ versus t should be a straight line having intercept $\ln(M_\infty)$ and slope equal to $-1/T_1$. This provides a straightforward graphical method of determining the spin-lattice relaxation time.

Procedure

1. Fill a 125-ml sample bottle with tap water, and place it in the center of the Sample Coil.
2. Connect the NMR SIGNAL OUTPUT and NMR AMPLITUDE DETECTOR OUTPUT to oscilloscope channels 1 and 2 (or A and B), respectively. Adjust the oscilloscope controls so you can view both channels simultaneously. Set the vertical sensitivities of both channels to 1 V/div and the COUPLING to DC. Set the horizontal sweep speed to 2 ms/div.
3. Connect the OSCILLOSCOPE TRIGGER OUTPUT on the front panel of the instrument to the EXTERNAL TRIGger input on the oscilloscope. Set the oscilloscope to trigger on EXTERNAL, DC COUPLING with HF REJECT, -SLOPE, and LEVEL \approx -1 V. These settings will cause the oscilloscope to delay its sweep 80 ms, which is sufficiently long to allow switching transients to die away before start of the sweep.
4. If the power supply is a variable voltage supply, set it at about 36 volts. If the power supply has variable voltage and current limiting, set the voltage on 36 volts, and set the current limit knob at maximum.
5. Set the polarizing time to 13.0 s.
6. Press the MANUAL START button. When the current switches on, make the following adjustments depending on your type of power supply:

Variable Voltage but No Current Limiting

If the polarization power supply has variable voltage, but not current limiting, reduce the power supply voltage to give a polarizing current of 3.0 A. Note the voltage that is required. At 3.0 A the power dissipated in the Sample Coil is roughly 100 watts. As time goes by, the Sample Coil will get warm; its resistance will increase, and it will be necessary to increase the voltage slightly in order to maintain the polarizing current constant.

Variable Voltage With Current Limiting

If the polarization power supply has both variable voltage and current limiting, wait until the current switches on. Then turn the current limit knob counterclockwise until the polarizing current drops to 3.0 A. Note the power supply voltage. You will find that the current-limiting power supply has automatically reduced the output voltage in order to provide the desired current of 3.0 A. At 3.0 A the power dissipated in the Sample Coil is roughly 100 watts. As time goes by, the Sample Coil will get warm; its resistance will increase. But the power supply will automatically increase the voltage as necessary in order to maintain the current fixed at 3.0 A. Ideally, the initial power supply voltage, which was set before the current was switched on, should be about 2 to 3 volts greater than the voltage actually required to provide the desired current. A difference of 2 to 3 volts is sufficient to allow the power supply to compensate for the coil's rise in temperature. If the voltage difference is too large, there may be problems associated with voltage transients that are invariably produced when the power supply current is suddenly switched from zero to 3.0 A.

7. Once the power supply has been properly adjusted to deliver 3.0 A, you are ready to measure the relaxation time by measuring the amplitude of the free precession signal as a function of polarizing time. The amplified free precession signal is available on the NMR SIGNAL OUTPUT. The output of the NMR AMPLITUDE DETECTOR is the NMR SIGNAL after it has been full-wave rectified and filtered. It has the same shape as the envelope of the free precession signal, but its amplitude is $2/\pi$, or about $2/3$, as large.

Pick a convenient reference point on the oscilloscope screen, say 1.0 division (which corresponds to 2.0 ms) after start of the sweep. Measure the zero-to-peak amplitude of the free-precession signal. Also measure the amplitude of the signal at the NMR AMPLITUDE DETECTOR OUTPUT. Do this for polarizing times of 13.0, 5.0, 4.0, 3.0, 2.0, 1.0, and 0.5 seconds. As a general rule, for maximum accuracy in measuring signal amplitudes, the oscilloscope vertical sensitivity should always be adjusted so that waveforms fill as much of the screen as possible. For low-level signals, you will need to increase the vertical sensitivity of both channels to 500 or 200 mV/div.

8. Trace out the magnetization curve by plotting the amplitude of the free precession signal versus polarizing time. On the same sheet, graph the output of the NMR AMPLITUDE DETECTOR versus polarizing time. Both curves should have the same shape.
9. The relaxation time T_1 can be determined, at least in principle, by fitting Eq. (2), with M_∞ and T_1 as adjustable parameters, to either of the data sets plotted in Procedure 8. Alternatively, one can assume that M_∞ is approximately equal to the amplitude of the signal at the longest polarizing time (13.0 s in this case), and plot $M_\infty - M(t)$ versus t on semi-log graph paper. Equation (4) shows that the slope of this graph is $-1/T_1$. A third alternative is to use a spreadsheet, or similar program, to graph $\ln(M_\infty - M(t))$ versus t . A least-squares fit of a line to the data obtained will give the slope, which can then be used to calculate T_1 . Whichever method you choose, determine two values for T_1 , one for each data set. These values of T_1 should agree to within experimental error.

EXPERIMENT 2: The Curie Law

Equipment

Earth's-Field NMR instrument

Polarization power supply (floating outputs, 40 volts maximum)

Oscilloscope

125-ml sample bottle

Theory

According to the Curie law, the equilibrium magnetization of a sample containing magnetic moments μ is

$$M_\infty = \frac{n\mu^2}{3kT} B , \quad (1)$$

where μ is the magnetic moment of each spin, n is the number of magnetic moments per unit volume, B is the magnetic field, k is Boltzmann's constant, and T is the temperature on the Kelvin scale. According to the Curie law, for a given sample at constant temperature, the equilibrium magnetization M_∞ should be proportional to B . Because of the small size of the earth's magnetic field, the net field B is approximately equal to the polarizing field B_p of the coil. (See Fig. 5.5 in the section on *The Earth's-Field Free Precession Technique*.) Furthermore, B_p is proportional to the coil current I_p . Thus, we expect the equilibrium Curie magnetization M_∞ to be proportional to the polarizing current I_p in the Sample Coil.

The magnetization of the sample does not assume the equilibrium value instantaneously, but, rather, rises exponentially toward the Curie value with time constant T_1 , the spin-lattice relaxation time. The growth of $M(t)$ toward M_∞ is described by the equation

$$M(t) = M_\infty \left(1 - e^{-\frac{t}{T_1}} \right) , \quad (2)$$

where M_∞ is the equilibrium Curie magnetization, and $M(t)$ is the magnetization at time t . For polarizing times equal to 5 times the T_1 or longer, the exponential term in Eq. (2) is less than 0.01, and $M(t)$ is approximately equal to M_∞ , to within an error of less than 1%. When the polarizing current is reduced suddenly to zero at the end of the polarizing time t_p , the ensuing free-precession signal dies away with time constant T_2 (actually, T_2^* since the earth's field is not

perfectly homogeneous). In any case, the amplitude of the free precession signal is proportional to M_∞ . (Refer to Fig. 5.7(b) in the section on *The Earth's-Field Free Precession Technique*.) Thus, we expect the amplitude of the precession signal to be proportional to the polarizing current I_p . That is, a graph of initial amplitude of the free precession signal versus I_p should be a straight line.

Procedure

1. Fill a 125-ml plastic sample bottle with tap water, and place it in the center of the Sample Coil.
2. Connect the NMR SIGNAL OUTPUT and NMR AMPLITUDE DETECTOR OUTPUT to oscilloscope channels 1 and 2 (or A and B), respectively. Adjust the oscilloscope controls so you can view both channels simultaneously. Set the vertical sensitivities of both channels to 1 V/div and the COUPLING to DC. Set the horizontal sweep speed to 2 ms/div.
3. Connect the OSCILLOSCOPE TRIGGER OUTPUT on the front panel of the instrument to the EXTERNAL TRIGger input on the oscilloscope. Set the oscilloscope to trigger on EXTERNAL, DC COUPLING with HF REJECT, -SLOPE, and LEVEL \approx -1 V. These settings will cause the oscilloscope to delay its sweep 80 ms, which is sufficiently long to allow switching transients to die away before start of the sweep.
4. If the power supply is a variable voltage supply, set it at about 36 volts. If the power supply has variable voltage and current limiting, set the voltage on 36 volts, and set the current limit knob at maximum.
5. Set the polarizing time to 13.0 s, which is about five times the spin-lattice relaxation time in water at room temperature.
6. Press the MANUAL START button. When the current switches on, make the following adjustments depending on your type of power supply:

Variable Voltage but No Current Limiting

If the polarization power supply has variable voltage, but not current limiting, reduce the power supply voltage to give a polarizing current of about 3.0 A. Note the voltage that is required. At 3.0 A the power dissipated in the Sample Coil is roughly 100 watts. As time

goes by, the coil will get warm; its resistance will increase, and it will be necessary to increase the voltage slightly in order to maintain the polarizing current constant.

Variable Voltage With Current Limiting

If the polarization power supply has both variable voltage and current limiting, wait until the current switches on. Then turn the current limit knob counterclockwise until the polarizing current drops to 3.0 A. Note the power supply voltage. You will find that the current-limiting power supply has automatically reduced the output voltage in order to provide the desired current of 3.0 A. At 3.0 A the power dissipated in the Sample Coil is roughly 100 watts. As time goes by, the Sample Coil will get warm, and its resistance will increase. But the power supply will automatically increase the voltage as necessary in order to maintain the current fixed at 3.0 A. Ideally, the initial power supply voltage, which was set before the current was switched on, should be about 2 to 3 volts greater than the voltage actually required to provide the desired current. A difference of 2 to 3 volts is sufficient to allow the power supply to compensate for the coil's rise in temperature. If the voltage difference is too large, there may be problems associated with voltage transients that are invariably produced when the power supply current is suddenly switched from zero to 3.0 A.

7. Once the power supply has been properly adjusted to deliver 3.0 A, you are ready to measure the amplitude of the free precession signal. The amplified free precession signal is available at the NMR SIGNAL OUTPUT. The output of the NMR AMPLITUDE DETECTOR is the NMR SIGNAL after it has been full-wave rectified and filtered. It has the same shape as the envelope of the free precession signal, but its amplitude is $2/\pi$, or about 2/3, as large.
8. Pick a convenient reference point on the oscilloscope screen, say 1.0 division (which corresponds to 2.0 ms) after start of the sweep. With the polarizing time kept fixed at 13.0 s, measure the zero-to-peak amplitude of the free precession signal. Also measure the amplitude of the signal at the NMR AMPLITUDE DETECTOR OUTPUT.
9. Repeat Procedures 4-8 for polarizing currents of 2.5, 2.0, 1.5, 1.0, and 0.5 A. The dc resistance of the Sample Coil and connecting cable is on the order of 10-11 ohms. Therefore, reducing the current in 0.5-A steps will require reducing the power supply voltage in steps on

the order of 5.0-5.5 volts. **If you are using a current-limiting power supply, be sure to heed the warning given in the next paragraph.** As the polarizing current is reduced, the amplitude of the free precession signal drops as well. As a general rule, for maximum accuracy in measuring signal amplitudes, the oscilloscope vertical sensitivity should always be adjusted so that waveforms fill as much of the screen as possible. For low-level signals, you will need to increase the vertical sensitivity of both channels to 500 or 200 mV/div.

CAUTION: When using a variable voltage supply with current limiting, don't reduce the current limit without simultaneously reducing the power supply voltage limit as well. Ideally, the voltage limit should be set no more than 2-3 volts higher than that required to deliver the desired current.

Otherwise, unacceptably large power supply voltage transients may result. If, for example, the current limit is reduced to 0.5 A while the voltage limit is left at or near the maximum of 36 V, when the current is switched on, the output voltage from the current-limiting power supply will drop suddenly from 36 V toward a steady-state value of 6 V or less, depending on the resistance of the Sample Coil and cable. During switching, the output voltage of a typical current-limiting power supply is an under-damped transient that oscillates as it decays with a time constant on the order of 20 ms or even longer. During large amplitude transients, the power supply output voltage can undershoot so far that it reverses polarity. If that occurs, the switching circuit will turn the current off in the coil until the power supply voltage assumes its normal polarity.

10. Plot the amplitude of the free precession signal versus polarizing current. On the same graph, plot the amplitude of the signal from the NMR AMPLITUDE DETECTOR versus polarizing current. Both graphs should be straight lines having the same slope. This experiment serves as a sensitive test of both the Curie law and for proper operation of the instrument.

6. Experiments in Polarization

The claim that the hydrogen nuclei in water can be magnetized would require a delicate experiment in magnetometry to verify directly, but it gives rise to dramatic manifestations when the polarized nuclei are allowed to rotate in the local magnetic field. Success in Chapter 3 has let you hear, and see, the signals induced in a pick-up coil by precessing nuclear magnetic moments. This chapter now makes some quantitative experiments out of that audible and visible phenomenon. The experiments mostly do not require optimization of the magnetic-field gradients, and many of them can be done using just the EF-NMR head and controller alone (*without* the use of the field/gradient coils and their separate controller).

These experiments take for granted the fact that the precession frequency depends on the local magnetic field, but not on the conditions of original polarization. Confirmation of this independence is postponed to Chapter 7. Here we consider the strength of the oscillating signals induced in the pick-up coil, and investigate what that *does* depend on.

6.1. Magnetization

We assume that you have gotten some kind of free-induction-decay signal, such as those corresponding to the audible ‘pings’ described in Chapter 3, Section 1. In such traces, you can have on one channel a record of the $t = -80$ ms and $t = 0$ triggering instants. (See Fig. 3.2.) During the same time, in another channel of the ‘scope you can have a record of the signal from precessing nuclear moments, taken from the bandpass-amplifier’s NMR Signal output. In the time just after the $t = -80$ ms triggering pulse, the signal from the coil is still made up mostly of leftover transients from the polarizing current formerly in the coil. But in the text below, we will assume that by the time of the second triggering pulse, which we label as $t = 0$, the signal from the coil is almost wholly due to the nuclei in the sample. (You can always test this claim by acquiring a fresh signal, but with the sample bottle removed from the NMR head.) So this time is late enough that the coil transient has died out, but still early enough that the nuclear free-induction-decay signal is still at or near full strength.

(If you can see the nuclear signal dying away already by this $t = 0$ instant, the gradients in your local field are excessive. If you have the field/gradient coil accessory, now is the time to optimize the gradients.)

The point is that the amplitude of the FID signals in the neighborhood of $t = 0$ is a dependent variable, and this section deals with how to measure that dependent variable, and then how to investigate its dependence on two obvious *independent* variables: the size of the polarizing current, and the duration of the polarizing interval.

Here is one suggestion for measurement of the dependent variable. Arrange to trigger on the negative-going pulse we use to label $t = 0$, and use a horizontal scale of 1 or 2 ms/div to acquire data. Arrange for the $t = 0$ trigger instant to lie in the middle of the 10- or 20-ms time window that results. With FID signals appearing at a frequency near 2 kHz, and having a period of about

0.5 ms, you will see about 20 or 40 cycles of the FID signal appear in a time record. Now you can use a variety of methods for estimating the size of these signals:

- If you have ‘vertical cursors’ at your disposal, you can by eyeball line one cursor level at the level of the average of the maxima of all those oscillations, and the other at the level of the average of the minima. Then the difference in the two cursors’ levels gives the peak-to-peak excursion of the FID signal.
- If you have a ‘scope utility for rms value, you might have an automated way to have the ‘scope compute the root-mean-square measure of that oscillating signal. If your ‘scope gives you a choice, ask for a full-screen, rather than a one-cycle, rms measure.
- If you care to capture and download your FID signal to a computer, you can perform the least-squares best-fit of a sinusoid to your data. Model it with a vertical offset, and amplitude, a frequency, and an initial phase, and check that the results make sense.

Any of these methods gives a number, in Volts, which is a *relative* measure of the strength of the signal, and hence of the original magnetization of the nuclear-spin sample. Any of them will give a single number for each single execution of the Start-Polarize-Precess cycle of operation of the EF-NMR controller. That cycle of operation can be repeated, to check for repeatability.

That cycle can also be repeated with an empty sample bottle in place, to check what level of apparent signal you get as a ‘control group’ in the absence of a sample.

Now with some such protocol in place to measure the dependent variable, you can investigate its dependence on two independent variables. You have at your disposal the polarizing current I_p , and the duration of magnetization t_p , to vary. The latter is easily set, in 0.1-s increments, by the thumbwheel switches on the controller’s front panel. The former can be set, and read, on the meter of the constant-current power supply you are using to excite the polarizing coil. If you’d like a more precise way to read a surrogate for this current, see Appendix A9 to learn how to use the rear-panel COIL CURRENT MONITOR. This will give a voltage proportional to the coil current, which lasts for the duration of the polarizing current; it can be read by ‘scope or (for long enough values of t_p) by a digital multimeter.

We suggest you start with a fixed t_p -value of perhaps 4.0 seconds, and explore the strength of the FID signal as a function of I_p as you vary that over the 0-3 Ampere range. You are directly controlling the strength of the polarizing field, and indirectly changing the amount of magnetization that the sample experiences. If you had access to polarizing fields about a million-fold larger than this apparatus permits, you might see evidence of ‘saturation’, ie. of magnetization that cannot be made to increase, since all the nuclei were fully lined up already. The methods of Appendix A1 can be extended to predict where saturation would occur. But in its absence, you expect a linear increase in sample magnetization (and hence of FID signal strength) on the polarizing field (and hence on the polarizing current that you use).

Once you have made such an investigation, you can revert to a fixed (and maximal) value of the polarizing current, and investigate the dependence on the duration of the polarization. Here too you will see (for small values of t_p) an initial linear rise in your dependent variable, but that variation will not continue. Instead, you will see the degree of initial magnetization increase toward a vertical asymptote, and fail to increase with larger values of t_p . This is evidence that sample magnetization takes time to occur, and further that the magnetizing influence of the polarizing field is in competition with de-polarizing influences, with which it eventually comes

into equilibrium. The standard model for sample magnetization as a function of the polarizing time t_p you choose is

$$M(t_p) = M_\infty [1 - \exp(-t_p/T_1)] ,$$

where M_∞ is the asymptotic magnetization that would apply for indefinitely long polarizing time, and where T_1 is a time-constant called the ‘spin-lattice relaxation time’.

The value of M_∞ to be expected is discussed in Appendix A1. The value $M(t_p)$ is the magnetization achieved by the end of the polarizing time, and it of course serves as the *initial* value (labeled M_0 below) for the magnetization at the start of the precession time.

The value of T_1 is an insight into the interactions of the nuclei with their environment. An isolated nucleus would merely precess around a magnetic field B , never changing its angle of mis-alignment with respect to that field direction. It requires a mechanism of dissipation, and transfer of angular momentum, to get a nucleus to align with the field. The value of T_1 is not easy to predict a priori, but it can be changed by changing those interactions. Some experiments to prove that it can be changed are found in Section 6c.

A practical consequence of the T_1 phenomenon is that sample magnetization can never be made entirely complete. But waiting a time of $3 \cdot T_1$ will suffice to get to 95% of the asymptotic level of full magnetization.

6.2. De-magnetization

Still using the timing vocabulary of the section above, we have a time $t = -80$ ms marking the end of the polarization time, and the start of signals from the sample coil. We also have a time $t = 0$ at which nearly all the ‘coil transient’ signal has died away, so that signals for $t > 0$ are due almost entirely to the sample itself. (You can always confirm this by repeating an experiment with an empty sample bottle in place.)

Now the sample’s magnetization at $t = 0$ is just about the value it was given during the 0.1 – 4 or more seconds of polarization time, and your view of the relative size of this ‘initial magnetization’ is the strength of oscillating signal you see either at the pre-amp or bandpass-amplifier output. The new question is, how does this magnetization die away? To check on that is to look in the $t > 0$ interval for diminishing amplitude of oscillations.

If there were only one species of NMR-active nuclei present, and if all such nuclei were in identical environments (including identical values of the static magnetic field), the magnetization, and hence the electronic signals you see, would decay away in time according to a model

$$M(t) = M_0 \exp(-t/T_2) ,$$

where T_2 is a new ‘time constant’ characterizing the disappearance of magnetization in the xy -plane of precession. This intrinsic demagnetization, ascribed to ‘spin-spin relaxation’, is discussed in Appendix A5, and it is maximal in rigid solids, and minimized in liquids, for reasons you can understand qualitatively. There are also ‘radiation damping’ effects,

representing energy transfer from the spins to the LCR detection system, which contribute to the demagnetization of the sample; these are discussed in Appendix A17.

The problem is that this sort of intrinsic demagnetization is typically overwhelmed by an *apparent* decrease in magnetization due to non-uniformity of the magnetic field. It is certainly easy for you to see that changing the settings of the gradient-coil adjustment markedly changes the character of the free-induction-decay signal. That signal is always characterized on the short term (ie. on a millisecond time scale) by oscillations, due to underlying precession of magnetic moments. But the amplitude of those oscillations decays away toward zero, on a time scale of 50 ms to a few seconds, with an envelope which is not, in general, exponential at all. Even if the decay envelope looks exponential, the time constant characterizing it is usually written as T_2^* , a shorter time scale for demagnetization. In fact the reciprocals give the rate of demagnetization, and we may write

$$\frac{1}{T_2^*} = \frac{1}{T_2} + (\text{rate due to gradients}) + (\text{rate due to radiation damping}) .$$

Only if all field gradients were known to be zero, and the radiation damping were negligible, would the value of T_2^* from the data correspond to the actual T_2 of the nuclei under study.

On the other hand, if rates of depolarization can be made low enough (ie. if you have done your best with the gradient adjustments in getting long-lasting free-induction-decay signals), and if physical mechanisms under your control give a *short* T_2 timescale, then what you see as T_2^* is close to what you care about, T_2 itself. Some experiments in which you deliberately change the T_1 and T_2 timescales of a sample are in section 6.3 below.

6.3. T_1 and T_2 studies

The values of the time-constants T_1 and T_2 are the outcome of some remarkable microscopic physics, and they give information that would be hard to acquire in any other way. For example, T_1 gives a measure of how difficult it is for protons to change their angular momentum, as they orient themselves to point preferentially along a static magnetic field. The mechanism must involve torque, since that gives the time rate of change of angular momentum; and torque on a magnetic dipole in turn can come from magnetic fields. So T_1 studies can reveal what time-dependent magnetic fields a proton ‘sees’ at its location, and in particular they can tell something about how the time-dependent (and rapidly fluctuating) microscopic magnetic field (its value right at the location of a proton) might differ from the volume- and time-averaged magnetic field you’d measure with a gaussmeter.

As an illustration of this, you can try to measure T_1 and T_2^* for a pure-water sample as a ‘control group’, and then repeat these measurements for ‘doped’ water as an experimental group. The choice, and concentration, of ‘dopant’ are up to you.

For these investigations, we suggest using DI or de-ionized water as a control group. (A still-finer point would be to de-gas the water, by one of several techniques, to try to remove dissolved molecular oxygen.) For ‘dopants’, we suggest dissolving into the water a known concentration of some soluble chemical species. Clearly, the identity of the chemical, and its concentration, are the relevant variables.

It's easy to try common table salt, or ordinary sugar, as things to dissolve in the water. Notice that salt dissolves into the charged, but closed-electron-shell, species Na^+ and Cl^- , while sugar dissolves as individual but neutral sucrose molecules. More interesting dopants are those which dissolve to leave paramagnetic ions, such as the salts of transition metals. You might think of copper, and its salt copper sulfate, as non-magnetic materials, but NMR can reveal the contrary. If you want a control group against which to try copper sulfate, you can use sodium sulfate. The claim is that while Na^+ in solution is a closed-shell system, an ion such as Cu^{2+} has unpaired d -shell electrons, an ion with both an electric charge and (crucially) a magnetic moment (and a moment of the scale of a Bohr magneton, about three orders of magnitude *larger* than a nuclear magneton).

Here's one way to think about the relevant concentrations. A liter of water has a mass near 1000 g, which is about 55 moles of water molecules. So the 'background concentration' of water is near 55 moles per liter. If you have another species such as Na^+ at one one-thousandth of this concentration, ie. at "0.055 M or 0.055-molar" concentration, you have a concentration of one Na^+ ion (and also one Cl^- ion) per thousand water molecules. In a mythical 'lattice' of molecular locations, you have one Na^+ impurity in a volume whose dimensions span about $10 \times 10 \times 10$ water molecules. So the typical water molecule might be about 5 molecular diameters away from the nearest impurity molecule, atom, or ion.

You will be able to see the effects of some dopants, in changing T_1 and/or T_2^* values, at concentrations of 0.055-molar or even lower. But you can use this concentration as a starting point to segregate dopants that matter from others that matter scarcely at all. Once you've picked a dopant of interest, you can prepare solutions of various concentration, perhaps in a list of 0.1 M, 0.03 M, 0.01 M, 0.003 M, and so on. Then you can plot the measured values of T_1 and/or T_2^* , your dependent variables, against concentration (in moles/liter units) as an independent variable. The use of log-log plots is appropriate to show the large variations you will encounter.

7. Experiments in Frequency: NMR Spectroscopy

Thus far you have used the Gradient/ Field Coil System's geometric and gradient capabilities to get a long-lasting free-precession signals, but you've not made any use of their largest feature, the Helmholtz-coil pair. Their function is to create a field, adequately uniform in space over the sample volume, which can add to (or subtract from) the local value of the earth's field.

Similarly, in looking at the free-precession signals, you have been recording their initial *amplitude* as a dependent variable, but you have not yet made use of their most dramatic feature, which is their *frequency* content.

That's the motivation for using the Helmholtz coils – the field changes they generate ought to move the NMR precession frequency around in frequency space, and various forms of valuable information can be extracted from making this precession frequency a dependent variable. The connection between the total field's magnitude, and the Larmor precession frequency you can measure, is discussed in Appendix A2.

One of the glamorous outcomes is a way to measure the proton's gyromagnetic ratio in absolute units, one not depending on looking up any textbook values.

7.1. Use of the Helmholtz Coil

These coils are intended to be used with an external stable adjustable direct-current supply (to be connected to the rear-panel connectors on the Gradient/Field Coils controller box). The two coils, each of 30 turns, are connected electrically in series, and they are designed for use with continuous currents of up to ± 3 A. Appendix A14 discusses the 'coil constant' k that can be deduced from their geometry and the Biot-Savart Law; you can use its methods to improve on an approximate value, $k \approx 90 \mu\text{T/A}$.

The goal of this section is to measure the effects of the Helmholtz coil on the free-precession frequency. To see that such effects are expected, note that even a mere 1 mA current in the Helmholtz coils is predicted to create a field of $\Delta B \approx (90 \mu\text{T/A}) (0.001 \text{ A}) = 0.09 \mu\text{T}$, and that field change ought to create a frequency shift of $\Delta f = c_p \Delta B = (42.58 \text{ Hz}/\mu\text{T}) (0.09 \mu\text{T}) \approx 4 \text{ Hz}$. This in turn suggests that you will want a way to measure, and to stabilize, the Helmholtz-coil current to 1 mA accuracy or better. The stability will depend on the type of power supply you use. The measurement can use the 'field coil current-monitor' outputs available on the front panel of the Gradient/Field Coils controller box; these give access to the potential difference created by the Helmholtz-coil current across an internal $0.100 \Omega (\pm 1\%)$ series resistor.

With the total field at the sample subject to precisely known changes, you will get changes in the precession frequency that deserve to be measured to similar precision. There are several methods available for measuring the frequency of your slowly-decaying, nearly-sinusoidal free-precession signals:

- A frequency meter can count cycles directly, provided it is properly used. To use this method, you might have to use the output of the tuned amplifier to provide adequate amplitude during the whole duration of (say) 1 second. You will also want to understand

the triggering of the frequency meter; you'll want to set a triggering level at the zero-crossings of the signal. If you can count cycles reliably for a properly chosen 'gate time' of 1 whole second, you'll get frequency resolution to ± 1 Hz.

- Some digital oscilloscopes will display the frequency of a signal they acquire. To use this method, you'll need a 'scope which will acquire voltage samples at a rate of at least 5 kSa/s (to prevent aliasing) and which will acquire data for an adequate duration. The 'scope's algorithm will in effect count cycles-per-second and give a result. Best precision will come from a time record that includes the maximum possible number of cycles. Note that under certain conditions of sampling, a digital oscilloscope can give grossly fallacious depictions of the oscillatory waveform you are acquiring. This is called 'aliasing', and Appendix A6 gives the cause, and the cure.
- Fourier-transform techniques are extraordinarily convenient, since they give a frequency-domain view of the signal with a high information content. Here you'll want a way to acquire a time record for about 1 or 2 seconds, and you'll want to use a 'uniform window' optimized for a one-time signal like your free-precession signal. You'll get a 'Fourier power spectrum', perhaps on a decibel (logarithmic) vertical scale, and you'll see how superbly the signal peak stands above the noise floor. You'll want a way to locate the center of this peak on the frequency scale, perhaps to 1 Hz accuracy. Appendix A15 discusses the lineshape and linewidth you can expect in the frequency domain. But again, aliasing can result in grossly discrepant results of such a measurement, and Appendix A7 describes the issues involved.
- Numerical fitting techniques offer the highest precision, but perhaps the slowest turn-around time, for frequency measurements. Here you'll again want to acquire a time record of the free-precession signal, for a duration of order 1 s, and then perform a least-squares fit to a function of the form

$$V(t) = A + B \exp(-t/T) \cos(2\pi F t + P) ,$$

where A represents an offset, B an amplitude, T a time-scale for exponential decay, F the frequency you're trying to extract, and P a phase shift. With the proper least-squares technique, you can even extract an experimental uncertainty ∂F for your measured frequency, and this can be very small indeed.

Whatever technique you use for measurement of the precession frequency, it's convenient if it works using the pre-amplifier output signal (so there's one less tuning knob that you need to keep set), and if it works in near-real-time (so you have a result before you take the next data point).

7.2 Small variations of coil current, and linear models

What data can you acquire? You can start by measuring the proton precession frequency for zero current in the Helmholtz coils, and then for a small (< 10 mA) current in them, to establish that you can make a difference, and to find what is the *sign* of the frequency change you can create. (Below, we call a current positive if it *raises* the precession frequency.) You will want to be able to use currents of both signs, so you might build a reversing switch for the current connections to the Helmholtz coils. *Especially* if you are using a constant-current power supply for the coils, you should remember to flip the current-direction switch **only** when the current has been dialed down to zero. (Why?)

If you plot precession frequency as a function of coil current, you will start to see a linear variation emerge, but just as it becomes interesting, your signal will start to disappear. Why? Because you'll have moved the signal out of the *tuning range* to which you've adjusted the sample coil. So as you change the precession frequency of the spins, you'll need to follow it with tuning adjustments to keep it up to familiar strength. Rather than do this by tedious guesswork-tuning at each new coil current, you can invest some effort in understanding the sample-coil tuning so that you can predict what tuning settings will be required for planned coil-current settings. Appendix A11 discusses this simple model.

Coil currents in the range ± 100 mA will give field changes of order $\pm 9 \mu\text{T}$, and frequency changes of order ± 400 Hz, which is about what is needed to cover the 1.6 - 2.5 kHz tuning range of the sample coil. If you model the net magnetic field's magnitude, as a function of current, by

$$B(I) = B_0 + k I ,$$

and if you model the precession frequency as

$$f(I) = c_p B(I) = c_p (B_0 + k I) = (c_p B_0) + (c_p k)I ,$$

then you are ready to deduce from your plot the combinations $(c_p B_0)$ and $(c_p k)$. Given your work in getting a first-principles value for k , the latter will give you a measured value of c_p , the gyromagnetic constant for protons. It may fail to agree with the 'book value' of 42.58 Hz/ μT for reasons you are about to learn, but it does represent the sort of measurement which is the *source* of such 'book values'; you have measured quite directly a fundamental property of the proton, and in real SI units too. As a follow-up, your value for c_p , and the value of $(c_p B_0)$ from your fit, will give you a measured value of the local field value B_0 , also in SI units. Note that your technique certainly measures frequencies to order 1 Hz out of 2000 Hz, so absolute measurements of B_0 to precision of 1 part in 2000 are also potentially available. Such techniques of 'proton precession magnetometry' are widely used in geophysical surveying, with important and valuable applications.

7.2 Larger variations, and quadratic models

You may have found that the fit to the above linear model is imperfect, or you may have found a value for the gyromagnetic constant with a systematic error. You may also have found that even with locally optimized tuning, the signal strength, and the signal *duration*, drop off as you create larger fields with the Helmholtz coil. This is *not* because the Helmholtz coils create magnetic-field inhomogeneities of their own; rather, it can be a symptom of misalignment of the Helmholtz coil's axis relative to the local magnetic field. Because the local and Helmholtz-coils' fields might fail to be collinear, they do not add as scalars. The resultant field will change in both magnitude and *direction* in space as you vary the current. Then the gradient corrections may fail to be optimal for the field as it varies in direction. Happily, the frequency data themselves contain the diagnostic you need, as a slightly more complicated model will now reveal.

Suppose that the local field and the Helmholtz-coil field axis are separated in angle by θ , so that the local field has component $(B_0 \cos \theta)$ along the Helmholtz-coil axis, and another component $(B_0 \sin \theta)$ perpendicular to that axis. Then according to vector addition, the magnitude of the

total field, B , has a square given by

$$B^2 = (B_0 \cos \theta + kI)^2 + (B_0 \sin \theta)^2 = B_0^2 + 2B_0 kI \cos \theta + k^2 I^2 ,$$

and the free-precession frequency, assumed to depend only on the magnitude of the total field (and not its direction), ought to have a *square* obeying

$$f^2 = (c_p B)^2 = (c_p B_0)^2 + 2(c_p B_0)(c_p k)I \cos \theta + (c_p k)^2 I^2 .$$

This motivates plotting data on frequency-*squared* as a function of current, and making a *quadratic* fit to the data thus plotted. The three coefficients will give three independent values: one will be the combination $(c_p k)$ again; another will be $(c_p B_0)$; and the third will be the product $2(c_p B_0)(c_p k) \cos \theta$. From the first of these, your efforts at modelling k will give a new value of c_p itself, but now *free* of a systematic error due to misalignment. Then from the second of these, you will be able to deduce a similarly improved value of B_0 . Finally, from the third of these, you will be able to deduce a value for $\cos \theta$ and hence the misalignment-angle θ itself. Unfortunately you won't know the sign of θ , nor whether the misalignment is in azimuth or altitude, but you could try changes by $\pm\theta$, in altitude and azimuth, and see what improves the alignment.

If you can measure frequencies to 1 part in 2000, you could hope to determine all three coefficients to this order of precision. If you can deduce $\cos \theta$ to similar accuracy, you can detect misalignments of less than 2° by this method, and potentially correct them. More importantly, by this more careful modelling you can *segregate away* the misalignment error into a term separate from the $(c_p k)$ and $(c_p B_0)$ coefficients. Also you should be able to deduce, from your best estimate of k and its uncertainty, a value for the proton's gyromagnetic constant c_p with its implied uncertainty, all *without* reference to 'book values'. Your uncertainty in c_p might arise chiefly from your ability to model the Helmholtz-coil constant k .

There's yet more that you can do with your parabolic model for frequency-squared vs. coil current. Once you've determined the coefficients of the parabola, try plotting the parabola over the full range of ± 3 A, and you'll see that there are *two* regions in which it passes through the range of $f^2 = (1600 - 2500 \text{ Hz})^2$. Let your parabola predict that (non-zero) current at which the precession frequency ought to have the same value that it has at zero current. Since you've tuned up the sample coil, and the gradients, to see the optimal signal at zero current, you should be able to get a new data point, at or near the original frequency, for this predicted (sign and) value of coil current. What you're looking for is the case of the Helmholtz coils providing a field of magnitude *double*, and direction *opposed to*, the local field; if all is well, you should see a free-precession signal and thereby get another data point on your parabola.

Taking data elsewhere along this second branch of the parabola is a searching test of the alignment and gradient corrections, and it's possible that the duration of the free precession signal will not be ideal. But if you can get even a few points along this side of the parabola, then your augmented set of data points will much more tightly constrain the parameters of the parabola, and hence the coefficients you deduce from it.

The quality of your data, and the parabolic fit to it, can be so high that a special technique is needed to see if there are any imperfections. You have a list of *measured* frequency values as a function of current, and a model whose square-root will give *modelled* frequency values as a function of current. The differences between data and model are called *residuals*, and you

should form the list of residuals, and plot them as a function of current. This is a good place to look for any systematic (unmodelled) deviations between data and model. It is also a great place to learn empirically about the scatter in the data: the root-mean-square (rms) average of the residuals is a good measure of the typical degree of misfit between data and model.

7.3 Reversing the earth's field

If you have taken data at the appropriate two points on the 'tuning parabola' discussed above, you may reflect about this use of the Helmholtz coils to 'turn the field around', ie. to reverse the direction of \mathbf{B} compared to the original local field. The prediction is that protons will then be precessing at the original frequency, but in the opposite direction or sense, compared to your original data set. There is no *direct* way to detect this opposite direction of precession (why not?), but you might think creatively about how you would go about determining the *sense* of rotation for a given species of nucleus. This will teach you how the *signs*, as well as the magnitudes, of nuclear moments are measured.

7.4 The proton magnetic moment

Using the methods of section 7.1 or 7.2 above, you have determined a numerical value for c_p , the 'gyromagnetic constant' as we have named it in this manual. It gives the rate of precession (in full cycles per second) per unit magnetic field. Standard references instead quote γ_p , the gyromagnetic ratio, which gives the rate of precession (in radians per second) per unit magnetic field. You can accordingly show that $\gamma_p = 2\pi c_p$.

At one level, this is just an interesting 'natural constant', and it can be supremely useful in applications. It can translate a hard-to-measure absolute strength of magnetic field into an easy-to-measure proton precession frequency, and is thus the basis of 'proton precession magnetometry'. Notice that such a proton-based magnetometer depends *only* on the ability to measure a frequency (ie., on access to the SI time scale) and the stability of protons in time; it does not depend on any 'factory calibration constant'.

But there's a deeper reason that makes γ_p worth knowing. We allude to it in Ch. 1 and in Appendix A13; the claim is that a particle's gyromagnetic ratio ought to be related, simply, to its charge-to-mass ratio. You may recall that any classical object, whose charge and mass are distributed in the same way, has its magnetic moment and its angular momentum *both* arise due to its rigid rotation. In fact that leads to the prediction that

$$\gamma(\text{classical}) = \frac{q}{2M}$$

for a particle of total charge Q and total mass M . You have by now independently acquired data for protons which contradict this model!

The early days of quantum mechanics celebrated the successes of Dirac's relativistic theory of particles, which had some notable successes. From this theory emerge the prediction that 'Dirac particles' ought to have just double the classical value of the gyromagnetic ratio, so

$$\gamma(\text{Dirac}) = g \frac{q}{2M} \quad \text{with} \quad g = 2 \quad .$$

Lo and behold, electrons were found to have just this value of magnetic moment (to about 0.1% accuracy), indicating that Dirac theory succeeded in describing them. But your result for the proton shows that even this Dirac g-factor of 2 *still* fails to account for the proton magnetic moment you have measured. In fact, your measured gyromagnetic ratio ought to be nearly triple the Dirac prediction, almost six-fold greater than the classical model predicts.

This formed part of the evidence, unwelcome in the 1930s, that protons are not in fact 'fundamental particles'. You've been told that protons are in fact the combinations of three quarks, and that the quarks (if anything) are Dirac particles. Part of the evidence for the complexity, the inner constitution, of protons, is the very gyromagnetic-ratio data that you have now acquired.

8. Experiments on Isotopes

This section of the manual assumes that you have understood how to acquire EF-NMR signals, to align the Coil System, to set the gradient adjustments, and to use the Helmholtz coils, so as to be able to follow proton free-precession signals over some part of the 1600-2500 Hz tuning range of the EF-NMR apparatus. With this capability in hand, we now take up the possibility of detecting the free-precession signals of nuclei *other than protons*; the use of the Helmholtz coils will help extend this capability to some other nuclear species.

8.1. Issues and methods for other isotopes

Not all nuclear species are “NMR-active” in the sense of being detectable by NMR techniques; the fundamental requirement is that the nucleus in question have a non-zero, and preferably large, nuclear magnetic moment. But many stable nuclei have an even number of both protons and neutrons (think of ^{12}C and ^{16}O), and such nuclei have *zero* nuclear spin and hence no magnetic moment at all. So the candidates for NMR need to have an odd number of either protons or neutrons. They need to be stable nuclei, and have a large isotopic abundance, and be available at adequate density in a liquid environment. This list of stipulations narrows the field markedly, and the further ‘customer requirement’ of nuclei of chemical interest or biological abundance cuts the list down to a rather small list of nuclei. We’ll discuss the cases of ^{19}F , ^{31}P , and $^2\text{H}=\text{D}$ below.

8.2. Fluorine experiments

Fluorine may or may not be of any great chemical or biological interest to you, but it is certainly the next-easiest nucleus to detect (after protons), and a good introduction to the experimental issues involved in detecting other nuclei by NMR methods. You might first use as samples some perfluorinated liquids (available from TeachSpin) to provide adequate numbers of fluorine nuclei within the available sample volume. The polyether compounds in the liquid have the approximate empirical chemical formula $(\text{C}_3\text{F}_6\text{O})_n$ and an approximate density of 1.65 g/cm^3 , which is enough to show you that (happily mono-isotopic) ^{19}F is the only NMR-active nucleus present to any extent. This information also allows you to compute the number of fluorine nuclei present. Finally ^{19}F has a nucleus approximately describable as a ‘closed shell plus valence proton’, so its spin is $\frac{1}{2}$ and its magnetic moment is similar to that of a proton – just about 6% smaller.

So if you are getting good proton free-precession signals in the earth’s field, you can merely tune the sample coil to resonate with an expected frequency 6% smaller than that for protons, and you should be able to capture fluorine free-precession signals straightaway. [See Appendix A11 for a discussion of a systematic way to accomplish sample-coil tuning.] You should not expect that the magnetization timescale T_1 , or the decay timescale T_2 , will be the same as for protons in water. You might want to measure T_1 very approximately, so as to know what polarization time to use hereafter.

Once you have seen any fluorine signal at all, you should be able to obtain, from the precession frequency and the gyromagnetic constant c_p for protons, a new gyromagnetic constant c_F for fluorine. You should also be able to predict where a lot more fluorine data could be taken, since you can now exercise the Helmholtz coils and arrange to see, in fact to move, fluorine signals over the full tuning range of frequencies. Given your approximate value of c_F , you can predict where in frequency fluorine signals should appear for any given value of Helmholtz-coil current; and given your tuning model for the sample coil, you can predict ahead of time how you'll have to tune up the coil for optimal signals. Hence you should systematically and rapidly be able to acquire data over a large part, or over two branches, of the frequency-squared vs. coil-current parabola for fluorine. (See section 7.3.) Such data will very tightly constrain the combination of parameters ($c_F k$), as proton data will constrain ($c_p k$). Taking the ratio of these can give (c_F / c_p) with *very* high precision, *not* limited by the absolute accuracy with which you can estimate the Helmholtz-coil constant k .

8.3. Harder isotopes

If you are inclined to try out EF-NMR studies in other nuclei, you might look over the appropriate nuclear tables systematically to find species of large isotopic abundance, non-zero nuclear spin, and adequately large nuclear magnetic moment, just to see how your choices are limited.

8.3a) ^{31}P in phosphorus

A sample definitely worth trying is ^{31}P (in the form of phosphorus in 85% H_3PO_4 , which is orthophosphoric acid in water – corrosive, and not to be spilled!). This sample incidentally contains plenty of hydrogen nuclei, so you will see proton signals at the expected frequencies (though with T_2 times quite different than for pure water), but the sample ought also to give free-precession signals of the new (spin- $\frac{1}{2}$) nucleus under the appropriate conditions. You may circumvent a major search effort by taking as given the phosphorus-to-proton ratio $c_p/c_F \approx 0.40 \pm 0.01$. So if you see proton precession signals at $f = 2000$ Hz in your local field, you might expect phosphorus signals near 800 Hz in the same field. But you can't tune your sample coil to this low a frequency. The cure is to supplement the local field with some field from the Helmholtz coils, and while you're at it, you might as well raise the total field to a point where phosphorous signals ought *also* to appear at 2000 Hz.

Once you've planned this experiment, you will probably want to search for signals in the frequency domain, ie. by taking the Fourier transform of the free-induction-decay signals you expect. You can rehearse this technique on your proton signals, using hints from Section 7.1., and then apply it to a search for phosphorus signals. There are at least two criteria that a peak in a frequency-domain spectrum must satisfy to constitute a genuine detection of a phosphorus sample:

- a candidate peak has to go away when using a dummy sample, and return with the use of a phosphorus sample, and
- a candidate peak has to ‘move’ in the right sense, and by the right amount, for small changes in the Helmholtz-coil current.

You will have noticed that even fluorine samples gave precession signals of smaller amplitude than you got from protons in water, and now it's time to be a bit quantitative about the expected signal size for new species. Rather than try to predict absolute signal amplitudes (which would require all sorts of details about sample-coil geometry and tuning, amplifier gains and the like) we will concentrate only on *relative* signal sizes, since proton signal sizes are easily measured empirically. The calculation is done in Appendix A12, and depends on a combination of chemical, physical, and nuclear properties.

The calculation (like the experiment) is easiest if we compare two species, investigated in back-to-back experiments, that are made to precess at the same frequency, as with (protons in the local field) and (phosphorus in a Helmholtz-coil-assisted field chosen to produce that same precession frequency). Then there are no new factors involving precession frequency, coil quality factor, or amplifier response, and the calculation in Appendix A12 ought to give predictions for the relative amplitude of (initial) free-precession decay signals. Test out this model against the signal amplitudes you observe for protons and fluorine, and then see if you can make it predict the signal sizes expected for phosphorus nuclei. You will learn how rapidly the apparently enormous signal-to-noise ratio for protons gets eaten up by less favorable experimental circumstances for other nuclei.

8.3b) ^2H or D, deuterons in heavy water

If you are familiar with chemist's use of NMR, you will have heard about the widespread use of ^{13}C -NMR, especially in organic chemistry. This would be a hard enough target nucleus for an earth's-field NMR study, and is made harder still by the mere 1.1% natural abundance of ^{13}C in terrestrial carbon. Isotopically-enriched carbon is certainly available, but the prospect of filling a 125-cm³ sample bottle with such material sounds very expensive. Nevertheless, the idea of isotopically-enriched samples need not be entirely abandoned, since there is one isotope available in isotopically-enriched form in huge quantities and (relatively) modest cost. This is ^2H , deuterium, or heavy hydrogen, whose natural abundance is a pitiful 0.016%, but which is available in 99% (or even 99.9%) isotopic purity as heavy water, D₂O. It'll take about 150 g of heavy water to fill a standard sample container, and since the material is both expensive and hygroscopic, you'll want to keep the container sealed (and labelled and stored!) properly. But you will be able to see ^2H free-precession signals, even though the deuteron-to-proton ratio $c_{\text{D}}/c_{\text{p}}$ \approx 0.15; you might first confirm that (at fields chosen to give equal precession frequencies) the ^2H signals are predicted to be about 16-fold smaller for heavy (as compared to light) water. Then you'll need to create a model for expected frequency as a function of Helmholtz-coil current, and also set your sample-coil tuning appropriately, before you can search for these small signals. The use of Fourier-transform detection techniques is certainly a prerequisite for finding small signals at imperfectly known frequencies, but the payoff is considerable. The measurement of the gyromagnetic constant for deuterons in heavy water is enough to fix the magnetic moment of the deuteron, and you should be able to measure this with sufficient precision to show that it is *not* equal to the sum of the proton and the neutron magnetic moments. See Appendix A13 for the details of this calculation.

8.3c) Other nuclei

What other nuclei might you detect? Remember you're looking for chemical elements that have a spin-nonzero nucleus, preferably spin- $\frac{1}{2}$, in an isotope of large, preferably 100% abundance. You'd like the gyromagnetic ratio to be large. You need the sample bottle to contain lots of those nuclei, so you want a high-density compound containing a large fraction of your element as atoms. You want the sample to be a liquid, too. And the sample needs to be affordable and convenient – isotopically-separated and liquefied ^{129}Xe fails dramatically at these last two criteria. What's the next-easiest nucleus to try beyond the ones on which you've succeeded?

9. Experiments on Spin Echoes

The celebrated phenomenon of the ‘spin echo’ can be detected using the EFNMR Gradient/Field Coil System. Your first studies will require only a protons-in-water sample, in the ambient field, but with gradient cancellation completed after the fashion of Chapter 3. A spin echo is a phenomenon best detected in the time (not the frequency) domain, but in this apparatus it can also be detected directly by ear, in real time, so the echo is not just figurative but highly literal.

9.1. Mechanism of the spin-echo phenomenon

What is a spin echo, in any case? It’s a mechanism that reveals dephasing, by reversing it. And what is dephasing? It’s the issue of protons at different locations in the sample volume failing all to precess in unison, because they are in different local magnetic-field environments. The mechanism of initial polarization at a $t = 0$ instant lines up a sample of proton magnetic moments, or spins, all along the $+x$ -axis. Then the $t > 0$ behavior of those spins is to precess in circles in the x - y plane. In the simplest model, of identical environments for all the protons, they all precess in unison, and the sample’s magnetic moment precesses while retaining its full magnitude.

But in the more typical case of a static magnetic field whose magnitude varies from place to place within the sample, the protons do *not* all precess in unison: protons in the higher-field regions of the sample will precess faster than those elsewhere. Once protons in the highest-field part of the sample have precessed a full 180° (half of a rotation) more than protons elsewhere, their magnetic moments will start to cancel, rather than reinforce, each other. Since the pick-up coil detects a signal resulting from the *net* magnetic moment of the whole sample, that signal will drop toward zero just because of this cancellation mechanism, even though individual protons might retain their full magnetic moment.

What characterizes a spin echo is some external intervention on this proton sample, conducted at a chosen time $t = T$, which *reverses* the rate of spin-precession differences. The expectation of a successful intervention is that by time $t = 2 \cdot T$, the protons will have differentially-precessed *back into unison*, recreating the full magnetic moment of the sample as a whole.

In the TeachSpin EF-NMR system, there are two ways to conduct this intervention. One method uses deliberate gradients $\partial B_z / \partial x$ to create differential amounts of precession, and then reverses these gradients at a time $t = T$. A second method, available to those who have the Spin-Flip Coils accessory, works in the presence of unchanging gradients, but uses the deliberate perturbation of the sample, at a time near $t = T$, by imposing a brief presence of an extra magnetic field, oscillating in time and directed along the y -axis. Each method is described in its own section below.

9.2. Pulsed-gradient spin echoes

Here’s how you can imagine setting up one kind of ‘spin echo’. Suppose you have optimized all

three gradient cancellations, so that a sample of polarized protons produces a free-precession signal detectable (and audible) for a few seconds of time. Now if one of the gradients, say the x -gradient of field strength, is deliberately mis-adjusted, say by $1 \mu\text{T}/\text{m}$, then you have seen that the free-precession signal dies away in a much shorter time – about 0.2 s, according to the model of Chapter 10.2 or Appendix A16. The question is, why has the signal decayed away? Is it because the magnetic moments are lost? No, says the existence of the spin-echo phenomenon: the loss of signal is in part *reversible*, and the decayed signal can be *resuscitated*, by the variation of a gradient adjustment in time.

To consider the example above, suppose that (via the gradient adjustments) the net x -gradient is $+1 \mu\text{T}/\text{m}$ at and after $t = 0$, the start of free precession. The signal rapidly dies away, and has practically vanished by $t \approx 0.3$ s. Now suppose that later still, at $t = 0.5$ s, the net x -gradient is suddenly re-adjusted, not to the ideal value, but to *another* wrong value, this time $(-1) \mu\text{T}/\text{m}$. The signal will not magically re-appear right at $t = 0.5$ s; but if this new gradient is maintained for $t \geq 0.5$ s, then the signal will re-appear(!) around $t = 1.0$ s.

This remarkable prediction is worth testing out experimentally before you work out the details of the mechanism. You'll need to have worked out the gradient adjustments, so that you can get a long-lasting free-precession signal. Now for the first time you are about to exercise the capabilities of the X-GRADIENT STEP CHANGE part of the EF-NMR Gradient/Field Coils controller box. Arrange to measure the x -gradient coil current by monitoring the x -gradient shunt voltage at the appropriate current-monitor outputs on the controller's front panel. You will see a voltage appropriate to the current required to cancel the x -gradient in the ambient field; record that voltage. Now find the 3-position step-change toggle switch, and move it from its uppermost OFF position to the middle - STEP (say that as “minus step”) position. Note that the switch will stay in that position, and that the current-monitor output will read a lower voltage; record this voltage too. Finally, push down and hold the toggle switch to its lowest + STEP (say “plus step”) position, and note that you get a third reading of the voltage at the x -gradient-coil current monitor. Note that the toggle switch allows you to generate displacements of equal size, negative and positive, relative to that x -gradient setting which cancels the ambient x -gradient.

- First get an optimized free-precession signal with the toggle switch in its ordinary uppermost (= OFF) position.
- Next, for comparison, see what a difference you get if you put the toggle switch to its middle (= - STEP) position, and then initiate a polarization time and the subsequent free-precession time. You should see on a ‘scope, and hear on the speaker, the signal dying away in a much shorter time. (And no surprise: you're deliberately operating with an incorrectly-adjusted x -gradient.)
- Now repeat that signal acquisition, but this time with your fingers on the toggle switch. Have the toggle switch, as before, in the middle (ie. - STEP) position, but for this test, wait for the audible end of the free-precession signal, and then push down and hold the toggle switch to its bottom (ie. +STEP) position. You should hear by ear, and see on the ‘scope, the effect of this change in the gradient.

What you've heard and seen is called a 'pulsed gradient spin echo', since you achieved it by suddenly changing the gradient from one value to another.

It is well worth trying a few more attempts at this hands-on switching, to understand the time relationships involved. You can hear the beginning of the free-precession signal, and you can *choose* how long to wait before switching to the opposite sign of gradient offset. You can see what happens if you only hold the toggle switch down momentarily (as opposed to holding it down for the full duration of the echo). You can even try getting the 'echo of an echo' by releasing the toggle switch after the first echo, and letting it return to the middle (ie. the original, - STEP) position.

After you've enjoyed this hands-on, ear-detected introduction to the spin-echo phenomenon, you may want to automate and regularize the process. Here you'll want to send the TRIGGER OUT signal of the EF-NMR controller, not only to the 'scope that you've been using, but also to the TRIGGER IN connector on the EF-NMR Gradient/Field Coils controller. Set the 3-position toggle switch to its central (ie. AUTO, -STEP) position. Now the trigger pulse which arrives at the beginning of the free-precession signal will execute the start of the STEP DELAY function (adjustable on the front panel over the 0 - 3 second range), and at the end of this set interval, will execute the switch to the + STEP condition automatically (and reproducibly).

To see the time relationships involved, you might use your 'scope to display the free-precession signal, and a DMM to read out the voltage from the x -gradient coil-current monitor. You can acquire one trace with the gradient-step capability off, and a subsequent one with the x -gradient set to the - STEP, but automatically switching to the + STEP after your chosen delay time. Make a sketch of the x -gradient coil current vs. time, and the net x -gradient vs. time, appropriate to these signal acquisitions, and you'll have the timing diagram needed for understanding the theory below.

What is going on with the protons? Assume that you start with all the gradients exactly canceled, so all the protons experience the same field, and all precess at the same frequency, staying in phase for the whole duration (several T_2 's) of the free-precession signal. Now consider what happens in the - STEP condition, which applies from $t = 0$ to $t = T_{\text{delay}}$. There is now a (negative) gradient present, so protons at larger x -values experience a smaller field, and those at smaller x -values experience a larger field. The result is *differing* proton precession frequencies for differing locations in the sample; protons at negative x -values get *ahead* of the others in their precession. When phase differences between protons at opposite ends of the sample reach 180° , the signal is diminished by dephasing; not much later, the signal is virtually gone, due to more complete dephasing. But the protons and their individual magnetic moments are not gone, and the signal can be resuscitated by arranging for the 're-phasing' of the protons. A step reversal of the gradient error is all that's required to do this; if for $t \geq T_{\text{delay}}$, the x -gradient error is *opposite* to what it was before, we now have the case that protons at larger x -values experience a larger field, and those at smaller x -values experience a smaller field. Once again the protons will precess at different rates; but now those protons at larger x -values, which were *behind* in phase at $t = T_{\text{delay}}$, will precess at a faster rate, and catch up with those protons at smaller x -values, which were ahead in phase at $t = T_{\text{delay}}$. When $t = 2 \cdot T_{\text{delay}}$, this catching-up process should be complete, and *all* the protons will (temporarily) be in phase again. At this

time, the full sample will be precessing in phase, giving as large a signal as if all the protons had been in phase for the full duration of the experiment.

This model explains why the echo is delayed, and by how much the echo is delayed, after the step-change in the gradient. It also explains what would happen if the size of the ‘minus step’ and ‘plus step’ gradients were changed – there’s a rear-panel adjustment for this step size, and again the front-panel x -gradient current-monitor output will tell you what step size you’re selecting. This model also explains how you can get the ‘echo of an echo’, and even can tell you what would happen if, right at time $t = 2 \cdot T_{\text{delay}}$ (at the peak of the echo), you were to switch the gradient errors off altogether.

There are plenty of applications for these pulsed-gradient spin echoes. The first of these is a highly sensitive method for the optimal settings of the y - and z -gradients: arrange to see a triggered spin echo at (say) $t = 1$ s, and now watch the strength of the echo as a function of the y - or z -gradient setting. Only if the y - and z -gradients are set perfectly will the echo be at maximal strength. The prediction is that the echo will (temporarily) reach the full strength of the ideal free-precession signal, limited only by intrinsic $\exp(-t / T_2)$ relaxation, and no longer limited by field gradients.

Another more important application has to do with an implicit assumption in the explanation above. For the re-phasing to work out perfectly, it is crucial that a given proton be located at, and *stay* located at, the same x -location for both the - STEP and the + STEP parts of the time evolution. If a given proton is *moving* during the precession time, then it can acquire a phase gain during the interval $0 < t < T_{\text{delay}}$ which is *not* compensated by the phase loss acquired for $t > T_{\text{delay}}$. You can actually observe this effect; you might want to set to a rather large value of gradient-step size, confirm that you can get a spin echo, and then try again with a not quite full, freshly shaken-up(!) bottle of water in which the protons will be in motion during the whole free-precession time. (Less mundane proton motions can be detected in a high-field NMR apparatus, including the motion of protons due to convection or even to mere passive molecular diffusion.)

You’ll note the requirement that all three gradients need to be rather carefully optimized ahead of time for this sort of spin echo to be observed. It takes one more set of coils, and some external electronics, to create “r.f.-induced spin echoes” which can be made to work in the presence of any gradients, optimized or otherwise. These are described in section 9.3 below.

9.3. The ‘radio-frequency’ spin echo

First, a word on nomenclature. The main magnetic field of the earth, and the gradient corrections to it, are all very nearly constant in time. In this section, for the first time, you will contemplate magnetic fields which vary rapidly in time. In fact, to be maximally effective, they need to oscillate in time with just about the same frequency at which protons precess in time. Since original NMR experiments used field strength of order 1 Tesla, in which precession frequencies were of order 40 MHz, the deliberately-added oscillating fields needed similar frequencies, which fall into the radio region of the electromagnetic spectrum.

In the TeachSpin apparatus, precession frequencies are nearer 2 kHz than 20 MHz, so they might properly be called audio frequencies. But it's still the case that we want to create, uniformly in space over the sample bottle, a field *not* constant in time, but oscillating at an externally-chosen frequency. The added field is chosen to be in the *y*-direction, perpendicular both to the main static field $B_0 z$, and to the sensitive *x*-axis of the pick-up coil.

It takes new coils to generate these new fields. At TeachSpin we call them the ‘Spin-Flip Coil Accessory’, and they need to be added to the EF-NMR ‘head’ or central polarization/pick-up coil unit at the heart of your EF-NMR system. Those coils come with their own instruction Manual, which contains full details of how they work. To use them, you will suppress the X-GRADIENT STEP CHANGE function by setting its three-position toggle switch to the topmost OFF position. You will set the gradient-adjust knobs either to give (for starters) the most spatially-uniform field possible, or to create deliberate known gradients. Finally, you will need an external audio-frequency function generator with a ‘burst mode’, and a bit of timing electronics, to active the desired intervention at the desired time.

All the rest of the details are in the Manual for the ‘Spin-Flip Coil Accessory’. The result is the form of spin echo that is most commonly used in many forms of NMR, including NMR-based imaging technologies.

10. Experiments on Gradients: NMR Imaging

This Chapter of the Manual deals with the issue of *gradients*: the likelihood that the static ambient magnetic field is not spatially uniform in magnitude over the full volume of the NMR sample. By a previous geometrical alignment, you have assured that the field \mathbf{B} has only a z -component at the center of the sample, so you could write $\mathbf{B}(x,y,z)$ as having $\mathbf{B}(0,0,0) = B_0 z$. But away from the center of the sample, \mathbf{B} varies in magnitude and direction, and this inhomogeneity is the direct cause of the short duration of the free-precession signals you get from the sample in the absence of ‘gradient corrections’. Gradients like these are very small in the terrestrial magnetic field at outdoor locations, but are a serious impediment to EF-NMR work at a typical indoor location. This section tells you how to use the gradient coils of the EF-NMR Gradient/Field Coil System to cancel out the three relevant gradients of the ambient field, thereby creating a field much more uniform in magnitude over the volume of the sample, and yielding free-precession signals of markedly longer duration. (Why *three* gradients, and not five, or nine? See Appendix A16.)

You will be using the NMR signals themselves to accomplish these adjustments, so you will need to turn both Controllers on. In addition to the familiar settings on the familiar EF-NMR controller, you will be making some new settings on the Gradient/Field Coils controller:

- set the three ten-turn GRADIENT ADJUSTMENT knobs to **mid**-range (at **5** turns on their 0-10 scales), and
- set the X-GRADIENT STEP CHANGE toggle switch to its uppermost OFF position.

Now confirm that you can still get a precession signal out of the EF-NMR pre-amplifier output, and note its duration (defined, operationally, as how long it takes for the oscillating signal to decay to half its initial amplitude). This duration tells you about how large the field gradients are, and that in turn tells you about how large an adjustment you’ll need to make on the gradient-adjustment knobs.

Here’s a brief foray into the quantitative consequences of a field gradient; more details can be found in Appendix A16. Suppose that the field \mathbf{B} had at the sample’s center a magnitude of $50.00 \mu\text{T}$, so that protons at this location would precess at 2128.5 Hz . But suppose that the field’s magnitude had a rate of variation in space of even $3 \mu\text{T/m}$ (along some direction); then at another point just $2 \text{ cm} = 0.02 \text{ m}$ away from the center, protons in the sample bottle would experience a field of magnitude $50 \mu\text{T} + (3 \mu\text{T/m})(0.02 \text{ m}) = 50.06 \mu\text{T}$. Protons at this location would thus precess instead at frequency 2131.1 Hz . This difference of 2.6 cycles of precession per second entails that protons 2 cm apart, which start their precession in phase, would be 180° (one-half cycle) out of phase in just 0.19 seconds of time. So the consequences of gradients are that protons in different regions of the sample get out of phase with each other in their free precession, and thus that they cease to cooperate in inducing emfs in the sample coil. Appendix A16 shows that a gradient of strength G will cause this dephasing to become serious in a time T , where T is given by

$$T \approx \frac{1}{c_p G S} ,$$

for a sample of extension $\pm S/2$ with respect to the center. Here $c_p = 42.58 \text{ Hz}/\mu\text{T}$ is the gyromagnetic constant ($= \gamma_p/2\pi$) for protons. Thus an observation of the dephasing time T is a semi-quantitative indication of the size of the gradient you’ll want to cancel out.

The gradient coils are located in grooves cut into the wooden Helmholtz-coil forms, and they make possible the three independent and orthogonal adjustments needed. In the notation of Appendix A16, they adjust the three first-order spatial derivatives $\partial B_z/\partial x$, $\partial B_z/\partial y$, and $\partial B_z/\partial z$. That is to say, each of three sets of coils generates a field which has zero value at the origin, but whose z -component varies linearly, in one of three coordinates, across the volume of the sample. The strength of the gradients is very nearly $1 \mu\text{T}/\text{m}$ for each 4 mA of current sent through the particular coil set, and the ten-turn knobs of the gradient adjustments control three constant-current bipolar power supplies through the range of $\pm 20 \text{ mA}$ output. Since ten turns changes the current by 40 mA , each turn gives a 4-mA change, sufficient to change the gradient by $1 \mu\text{T}/\text{m}$.

Now here's the procedure: knowing (from the observed dephasing time) the approximate scale of the gradient change you need, make a change of perhaps half that size to one of the three gradient adjustments. Acquire another free-precession signal, and note its *duration* (rather than its initial amplitude, which may not have changed). The duration might be longer, in which case you've made an improvement; or it might be shorter, in which case you can try a gradient change of the *opposite sign*; or it might not have made much difference, in which case you're being limited by the gradient in one of the other two dimensions – so try an adjustment of another knob.

You're going to take repeated free-precession signals, and you'll be improving the signal's duration iteratively. You might make a first pass trying out changes of a full turn ($1 \mu\text{T}/\text{m}$'s worth) in each of the three axes in turn, at this stage not trying for perfect optimization of any one gradient adjustment, but looking for, and curing, the worst of the three gradients. Any improvement of any of the gradients makes the other two gradients even easier to adjust, since you have a longer-lasting signal and hence one sensitive to ever-smaller errors in the gradient adjustment.

[As you improve the signal's duration, you might want once or twice to fine-tune the sample coil; this will affect the amplitude (not the duration) of the free-precession signal. As the signal improves in duration and magnitude, you might try adjusting the ten-turn tuning dial of the main-amplifier section in the EFNMR controller, since this will reward you with the lovely long-lasting *audible* version of the free-precession signal.]

It is not crucial at this point to make perfect adjustments; if all three gradients are correct to $0.1 \mu\text{T}/\text{m}$ (one-tenth of a full turn on the dials), then the decay time will be of order 2 seconds. At this level you will be sensitive to imperfect geometrical alignment, if any, and the methods of Chapter 7.3 give you an alternative way to detect such misalignments. Also at the level of $0.1 \mu\text{T}/\text{m}$, you will be sensitive to slow *changes* in the gradients. Typically both the field values, and field *gradient* values, display changes on a time scale of hours, perhaps due to temperature changes in the steel frames of typical buildings. But it is worth recording what settings you have found for the gradient adjustments, as this will markedly reduce the effort required for gradient optimizations in the future. You can record either the nominal settings on the ten-turn dials for the three axes, or the potential difference at the gradient-coil current-monitor outputs of the controller. Here a voltmeter will register the voltage drop across one of three $100 \Omega (\pm 1\%)$ shunt resistors; the 'monitor selector' switch will allow you to record the three settings in turn. From

the voltage drops across the shunt resistor, you can deduce the actual coil currents; from the coil currents and the gradient-coil constants of $(1 \mu\text{T}/\text{m})/(4 \text{ mA})$, you can deduce the size of the gradients you have created, and thereby deduce the size of the pre-existing gradients in the ambient field you have canceled out.

In a location of sufficiently poor magnetic-field homogeneity, you may find that you reach the extremes of a gradient adjustment knob (nominally $\pm 5 \mu\text{T}/\text{m}$) with the free-precession signal's duration still improving but not yet optimized. A pre-existing gradient so large as this will correspond to an original signal-decay time of only 35 ms, so it's unlikely you would ever have found the signal to begin with at so poor a location. If this is your situation, one solution is to pick a better location, but it's not always obvious where you should move. Another solution is to use a small permanent magnet, artfully placed to create (at the sample's location) a field in the z -direction but also giving a corrective gradient along the axis you have identified.

10.1. The reality of magnetic-field gradients

If you have a free-precession signal of duration about 1 s at frequency 2 kHz, then about 2000 full cycles of signal of useable size are available for you to measure. This should enable you to determine that frequency to about 0.5 Hz precision; Chapter 7 discusses some of the methods you might use to accomplish this. Here's a way to use that measured frequency to assure yourself that magnetic field gradients really are present in the ambient field.

Suppose that the $\partial B_z/\partial x$ adjustment you have made in your optimization corresponds to the addition of $2.3 \mu\text{T}/\text{m}$ of gradient; since that gives a long-lasting free-precession signal, you can infer that you have canceled out a pre-existing gradient in the ambient field, along the x -direction, of magnitude $2.3 \mu\text{T}/\text{m}$. The implication is that if you translate, move in space, the whole EF-NMR Gradient/Field Coil System by (say) 0.1 m along the x -direction, you will be putting the sample in an ambient field of magnitude differing by $(2.3 \mu\text{T}/\text{m})(0.1 \text{ m}) = 0.23 \mu\text{T}$. Given the gyromagnetic constant $c_p = 42.58 \text{ Hz}/\mu\text{T}$ for protons, this implies that the free-precession frequency should change by 9.8 Hz, a readily detectable change.

So arrange to translate the whole frame of the apparatus on the tabletop along the x -dimension, preserving its azimuthal alignment. You might want to take data at displaced by $\pm 10 \text{ cm}$ and $\pm 20 \text{ cm}$ relative to its original location; this choice of position is your independent variable. You should *not* need to change anything else about the apparatus; in particular, you can leave the three gradient adjustments right where they were originally optimized. But you should see precession frequencies that vary linearly with your translated x -position; this is your dependent variable. Their variation with x -position should give you an indication of the gradient $\partial B_z/\partial x$. What's more, the *sign* of the gradient should now be clear, since you can tell unambiguously in which direction the field's magnitude increases.

It's not quite so easy to translate the whole apparatus along the y - or z -directions you have found, since these will in general not be convenient horizontal or vertical directions. But if you can create even approximate translations in y or z , you can by this same method verify that these gradients really exist, and you can also find their signs unambiguously.

10.2. Gradients along one dimension – the signal envelope

Suppose you have ‘optimized the gradients’, ie. you have found those three gradient settings which give a nice long-lasting free-precession signal. Now what happens if you deliberately offset *one* of the gradients from its best value? We’ll answer that question here “in the time domain”, showing quantitatively the effect of a gradient offset on the free-precession signal.

Appendix A16 shows that if the sample is modelled as a cylinder of length L and diameter $2R$, then the effect of a single gradient is to change the otherwise sinusoidal free-precession signal to the product of a sinusoid times an ‘envelope function’. For a gradient of strength g along the x-direction, the envelope function is predicted to have form

$$\frac{\sin(\pi c_p G L t)}{\pi c_p G L t},$$

while for a gradient along the y- or z-direction, the envelope is predicted to have form

$$\frac{J_1(\pi c_p G \cdot 2R \cdot t)}{\pi c_p G \cdot 2R \cdot t}.$$

Here $J_1(x)$ is the Bessel function of order one, and c_p is the gyromagnetic constant 42.58 Hz/ μ T for protons.

Your goal is to create a gradient offset of a size that yields envelope functions which drop off quickly compared to the (approximately exponential) decay of free-precession signal you see in optimized fields, but not too quickly to see; you might aim for the envelope to decrease to half its original value in 0.1 - 0.6 s. So record some free-precession signals under conditions in which (only) one of the three gradients is offset by a known amount from its optimum value, and see if the signals’ envelopes resemble those predicted by theory.

Note in particular that these envelope functions ‘pinch off to zero’ in a finite time, at $(\pi c_p G L t) = \pi$ for an x-gradient, or at $(\pi c_p G \cdot 2R \cdot t) = 3.8317$ for y- or z-gradients. A plot of the reciprocal of the pinch-off time vs. gradient setting ought therefore to be linear, and might even help you find to optimal gradient settings.

Note also that the signal is *not* identically zero after the pinch-off time. The model predicts, and your signals ought to display, a *revival* of the free-precession signal. What is the cause of this revival, physically speaking? You should be encouraged to think about different regions of the sample doing different things, and to think about the phase relationships of the emfs that they induce in the sample coil.

10.3. Gradients and one-dimensional imaging

This section of the manual describes the use of the EF-NMR Gradient/Field Coil System to demonstrate the glamorous technique of (one-dimensional) magnetic resonance imaging, and thereby to illustrate the physical basis of all MRI technologies. In this section, we’ll assume a proton sample, operated in the ambient field, with the gradients corrected according to the algorithm above. You will want the X-GRADIENT STEP ADJUST turned OFF, and you will finally have a chance to use the TeachSpin ‘segmented sample container’. Finally, this section definitely requires that you be able to detect free-precession signals and view them in the

frequency domain; it is very useful to have a shot-by-shot view of the Fourier transform of each free-precession signal, in addition to the oscilloscope view of the time-domain signal you've used thus far.

The basis of all magnetic imaging is the use of deliberate, tailored, non-zero gradients of magnetic field across a sample. In your TeachSpin apparatus, we'll suppose that you know how to cancel out all gradients in the ambient field, and that you now deliberately depart from a net x -gradient of zero to (say) an x -gradient of $4 \mu\text{T}/\text{m}$. (That means turning the x -gradient adjusting dial by 4 full turns relative to the position at which it best cancels the gradient in the ambient field.) Remember that this has physical significance: under these conditions, a proton located at $x = +3 \text{ cm}$ experiences a field differing from that at the origin by amount $\Delta B = (\partial B_z / \partial x) \Delta x = (4 \mu\text{T}/\text{m}) (0.03 \text{ m}) = 0.12 \mu\text{T}$, and that proton will therefore precess at a frequency differing from that at the origin by amount $\Delta f = c_p \Delta B = (42.58 \text{ Hz}/\mu\text{T}) (0.12 \mu\text{T}) = 5.1 \text{ Hz}$. The implication is that protons' spatial departure from the origin in x -position-space has been *mapped* into the signal's frequency- f -space departure from the ordinary frequency.

Now suppose there are thin 'slabs' of proton-containing water, one centered at $x = 0$ and another at $x = 3 \text{ cm}$. Both slabs' worth of protons can be polarized by the same polarizing current, and both will then precess in their own local fields. But in the presence of a deliberate gradient, protons in the two slabs will precess at distinct frequencies (differing by 5.1 Hz in the example above). Both slabs of protons will induce emfs in the sample coil, so the signal emerging will be a superposition of two distinct frequencies. This makes for a complicated waveform in the time domain, but a beautifully simple result in the frequency domain: there should be one peak at f_0 , for protons at $x = 0$, and another peak at $f_0 + 5.1 \text{ Hz}$, generated by the protons in the slab at $x = 3 \text{ cm}$. *In fact, the distribution of protons in x -space has been mapped into a distribution of signal strength in f -space.*

This calculation illustrates a few technical requirements as well. The tuned sample coil has a Q of order 70 near $f = 2000 \text{ Hz}$, so its pick-up efficiency drops to half-strength at locations $f = [1 \pm 1/(2Q)] 2000 \text{ Hz}$, or at $2000 \text{ Hz} \pm 15 \text{ Hz}$. Hence we would like protons at the ends of the sample container to be mapped to frequency-space locations no more than about $\pm 10 \text{ Hz}$ away from protons at the origin. This puts an upper limit on the size of the gradient that can be used. There's a lower limit as well, if proton signals from different slabs are to be resolved in frequency. If free-precession signals decay with $T_2^* \approx 1 \text{ s}$, then even protons at one single x -value will show up in a signal peak with width of order 0.5 Hz (and to attain this resolution will require a signal-acquisition time of 1-2 s minimum duration); so a gradient has to be chosen which will map a chosen separation in space to a separation in frequency of $\geq 1 \text{ Hz}$. But between these two limits, the size of the gradient chosen is arbitrary, so the 'scale factor' of the x -to- f mapping is under your control.

The reality of all this theory is very easily illustrated using the TeachSpin segmented sample container. This consists of seven compartments, each of x -extent about 7.8 mm, separated by partitions of x -extent about 3.2 mm (and a total length of container of 79.8 mm). You may compute that each 'cell' of the container accommodates about 11 cm^3 of water sample. Water is best added to a cell by injecting it using the syringe-needle device accompanying the cell; water is best removed from a cell by inverting the container (access holes down) and blowing air into

the cell with the syringe (thereby displacing the water out through the access hole – so execute this operation over a sink).

Now you might want to start by filling cells #1 and 2 with water, and leaving the others empty. If you place the sample container symmetrically inside the sample volume of the EFNMR apparatus, you have a sample of water roughly filling the x -interval { - 36.6 to -17.9 mm}. Practice acquiring a free-precession signal from this sample of water, first with the gradients optimized; be sure you can view this signal in the frequency domain, with resolution of order 1 Hz. Now if you change the x -gradient from optimal by amount $\pm 4 \mu\text{T/m}$ (that's 4 turns on the ten-turn dial), you should see this signal get displaced in frequency space, by about 4 Hz (why 4 Hz?). To confirm that you're really sensitive to the water-sample's position, you can remove the sample container and re-install it turned end-for-end, so that the water is now in the place where formerly empty cells #6 and 7 were located. Now the signal should be displaced in frequency by 4 Hz, but in the *other direction*. This will give you a way to understand the sign of the gradient you have added, and the sign of the linear mapping between x -space and f -space.

With this all understood, you may fill any cells you wish, with whatever volume of water you wish (the syringe will let you deliver a metered amount of water), and thus create a chosen distribution of protons in x -space. Find the conditions that give you the best view of the resulting free-precession signal in frequency space; you may also want to display the Fourier spectrum on a *linear* rather than logarithmic scale. You should be able to see an *image* of your chosen proton distribution, obtained by one-dimensional MRI technology!

To get another look at the power of Fourier transformations, look instead at the time-domain view of the precession signal on your ‘scope. You’ll see what looks like a weak signal, lasting only a short time, followed by mere noise. But that signal is the superposition of the emfs induced by the protons in the separate cells, and it contains (in encoded form) *all* the information that goes into the Fourier transform. Then the transformation into frequency space *decodes* that information, and what comes out is recognizable as a depiction of proton distribution in space.

There are lots of other ‘images’ you can get out of this form of MRI. Your image, thus far, depicts proton abundance, so image contrast depicts differing densities of protons. But you can imagine medical contexts in which proton density in space is boringly uniform, and there’s the need instead to depict some *other* property of protons. How about an image which depicts not proton abundance, but proton T_1 time? You could *fill* all seven cells of your sample container, but using water with differing concentrations of some paramagnetic ion, so that they varied from short to long T_1 times. Then the use of long polarization times would fully polarize protons in all the cells, and give an ‘image’ without contrast, whereas the use of an intermediate polarization time would differentially polarize the protons, so now the resulting image should display contrast.

Or, you could use a peeled banana as a sample. Confirm, first with x -gradients cancelled, that you can get a signal from the banana. (What do you suppose is the source of this signal?). Now, with a deliberate setting for a non-zero gradient, you can ‘spread out’ that signal in frequency space, and get a 1-dimensional image of the banana. It’s a boring image, since the banana is pretty nearly uniform along the x -dimension. Finally, take out the banana, and put a bite into it

(from the side, not the end), re-install it in the sample space, and take another 1-d NMR image of it. Can you see that bite, in frequency space? Does this make a believer out of you?

The data acquisition rate of this MRI device is rather low, and the signal-to-noise ratio is only adequate, but in principle this device could give the data required for obtaining three-dimensional images. The technique used in high-field MRI devices for 3-d image acquisition is the repetitive acquisition of multiple 1-d images, each one projected along another, out of a whole set, of different axes. Since one has full control of the three gradients, one can readily acquire an image mapping y -location to f -location, and subsequently an image mapping z -location to f -location. In fact, the general use of non-zero settings of all three gradients defines a series of slabs in the form of parallel planes, all perpendicular to a gradient vector, each such slab contributing signals at one unique frequency. From enough of these images projected along the directions of gradient vectors, the magic of tomographic reconstruction can yield the fully-resolved three-dimensional distribution of NMR-active nuclei throughout the sample volume.

The Spin-Flip Coil accessory to TeachSpin's Earth's-Field NMR apparatus

Table of Contents

0. What's a 'spin flip', and why would I want one?
1. Accessories needed for using TeachSpin's spin-flip coils
2. Spin flips, as applied to creating spin echoes
3. How a 'spin flip' can revive a free-induction-decay signal
4. What your spin-flip coils produce, and what effect it has
5. Executing the simplest spin-flip experiments
6. What you can investigate systematically on spin flips
7. What you can investigate systematically *with* spin flips
8. The properties of the spin-flip coils
9. Appendix: methods for creating the delay, and the tone burst

0. What's a 'spin flip', and why would I want one?

Earth's-field NMR is one of those experiments in physics that depends on spins -- here, the spins of protons, the nuclei of hydrogen atoms in molecules in the liquid state.

Everything you can do with EF-NMR depends on what you can do with those spins, using their associated magnetic moments as 'handles'. Thus far, you've polarized the proton spins, and then you've let them precess; but *spin flips* are an example of a new kind of manipulation of spins. Here are some motivations for you:

- Spin flips will allow you to make up for the spatial inhomogeneity that remains in the nearly uniform magnetic field in which your protons precess.
- Spin flips are the tools by which ever more intricate spin manipulations are achieved with nuclei in all sorts of applied NMR techniques.
- Spin flips are illustrations of 'driven quantum transitions', and are thus a model for understanding quantum transitions in many other areas of physics.
- Spin flips are used in NMR imaging (MRI), and even in NMR techniques in quantum computing.
- Spin flips will make available to you the lovely phenomenon of a 'spin echo', and in your EF-NMR case it'll occur at an audible frequency, and on a human time scale.

1. Accessories needed for using TeachSpin's spin-flip coils

- a) The TeachSpin EF-NMR (basic) system, including the EF-NMR controller unit and the EF-NMR 'head', plus a dc power supply for the spin polarization.
- b) The ability to use these items to produce to produce a proton 'free induction decay' signal, lasting for at least 100 ms.
- c) A digital oscilloscope by which to capture such signals.
- d) A sine-wave generator of some sort, which can be triggered to produce, on command, a 'burst' of sine waves of chosen frequency, amplitude, and duration. You'll need to be able to cover 1-3 kHz in frequency, 0-5 or 10 V in amplitude, and 1-100 cycles in duration of oscillation.
- e) A time-delay generator of some sort, homemade or otherwise, capable of being triggered by a positive rising edge, and of generating (after a chosen delay of 0.5 to 5 s) another edge for triggering your tone-burst generator.

Suggestions for meeting requirements d) and e) are in Section 9.

What you **won't** need to have is

- f) The TeachSpin EF-NMR Gradient/Field Coil system and its separate controller unit. If you *do* have this system, and have your NMR 'Sample Head' mounted inside these coils, there is no need to remove it for spin-flip experiments. But you'll be able to do spin-flip experiments with or without this Gradient/Field coil system.

2. Spin flips, as applied to creating spin echoes.

There is some three-dimensional geometry associated with spin flips in the TeachSpin EF-NMR system. It's best understood if you have at hand the TeachSpin EF-NMR 'head' (containing the 125-ml sample bottle), a compass and/or dip needle, and a set of spin-flip coils already mounted on the 'head'.

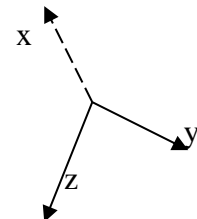
You'll want to use your compass and dip needle to establish the direction, in 3-dimensional space, along which the local (ambient, earth's) magnetic field lies. Call that direction the z -axis. Next, find a horizontal line perpendicular to that, and call it the x -axis. Then there's a unique y -axis perpendicular to both of these.

Now set up your TeachSpin 'Sample Head' so that the axis of symmetry of the NMR pick-up coil, and of the sample bottle, lie along the x -axis. But tilt the base of your NMR head so that the axis of symmetry of the new, white-framed, spin-flip coils (ie. the axis passing through the center of both square coil forms) lies along the y -axis.



Sample Head with Spin-Flip Coils Mounted

The photograph shows the Sample Head with the white-framed spin-flip coils mounted around the solenoid. The sample bottle is inside the solenoid and the dip needle shows the direction of the local Earth's magnetic field.



The z -axis is along the Earth's magnetic field and is parallel to both the plane of the white coil forms and the wooden base of the 'Head'. The x -axis goes through the center of the sample and the y -axis points into the tilted base.

Why all this fuss? It's to get all your magnetic fields pointing in the necessary directions. Recall that your NMR pick-up coil plays its first role in conducting a sizeable current (1-3 A) for some time (1-6 s), in polarizing your sample. The process leaves the sample with a magnetic moment μ , lying along the x -axis. Once the polarizing current is cut off, that magnetic moment μ precesses around the static earth's field $B = B_z z$, so $\mu = \mu(t)$ precesses in the xy -plane, staying perpendicular to z . It's the variation in time of μ_x , the component of μ along the sample-coil axis, which induces the emf in the pick-up coil to generate your NMR signals.

The role of the spin-flip coils is to create *another* magnetic field; this one

- lies along the y -axis, not the z -direction;
- is oscillating in time, rather than static; and
- has a frequency, an amplitude, and a duration which are all under your control.

You'll see that under certain conditions, even a brief (≈ 10 ms) and weak excitation of these coils can have dramatic effects on your proton spins, with the result of taking each spin and rotating it in 3-d space, by 180° around the y -axis.

And why would you want to do that? For a first experiment, because that intervention can create, apparently out of nothing, the phenomenon of a spin echo. In particular, by this intervention, you can eliminate some of the effects of the spatial non-uniformities in the static magnetic field $\mathbf{B} = B_z \mathbf{z}$.

3. How a 'spin flip' can revive a free-induction-decay signal

This section shows you why proton free-induction-decay signals (FID signals) die away, and what field-inhomogeneity means, quantitatively. It then explains how a spin-flip procedure can counteract these effects.

To make the calculations easier, let's think about an environment in which the static value of the ambient field happens to be exactly $46.98 \mu\text{T}$, which is in the right order of magnitude for the earth's magnetic field in some latitudes. That particular value was picked because it translates into a very convenient proton precession frequency.

$$f_{\text{precession}} = (\gamma_p B_z / 2\pi) = (42.57 \text{ Hz}/\mu\text{T})(46.98 \mu\text{T}) = 2000.0 \text{ Hz}.$$

This means the protons will perform a total of 200.0 turns in space within the first 100 ms of precession.

But inside buildings, or in proximity to iron objects, the ambient magnetic field is not uniform in space, and spatial *gradients* exist in its value. It's routine to find gradients of size (1-5) $\mu\text{T}/\text{m}$ in typical indoor environments, and that has consequences even over the volume of an NMR sample bottle. Typical protons in the 125-ml sample bottle in your Earth's-Field NMR experiment are at a distance of order 2 cm away from the center of the bottle, so a typical gradient of $2 \mu\text{T}/\text{m}$ translates into a difference of $(2 \mu\text{T}/\text{m})(0.02 \text{ m}) = 0.04 \mu\text{T}$ relative to the center of the sample. This gradient means there are protons in the sample experiencing field strength not just of $46.98 \mu\text{T}$, but also of $(46.98 \pm 0.04) \mu\text{T}$. Thus protons at various locations experience precession frequencies of not just 2000 Hz, but also $(2000. \pm 1.7)$ Hz. In a precession time even as short as 100 ms, various protons precess through not just 200.0, but also (200.0 ± 0.17) , turns in space.

While this barely 0.1% variation in the precession frequencies may seem trivial, the spread in amounts of rotation has dramatic consequences. If some protons precess through only 199.75 turns, while others rotate through 200.25 turns, then there will be groups of protons that have gotten fully *half a turn out of phase* with other groups. To put it geometrically, if all the protons were polarized in the x -direction at time $t = 0$, now at time $t = 100$ ms, there is no unique direction in which all the protons are pointing. Instead, the spins are spread out in a 'fan' of directions, all still in the xy -plane, but spread out throughout a wide angle. In our example, it won't be much longer until the proton spins have fanned out to fill a whole circle, at which point the sample's *net magnetic moment* will average to a near-zero value just because of this spread over a range of angles.

So even if individual protons continues to precess for many seconds (and they do!), the sample as a whole loses its magnetic moment in a much shorter time, given the presence of field inhomogeneities. The larger the sample, and the larger the field gradients, the sooner this happens; and once the average magnetic moment is gone, the average emf induced by the precessing protons drops to zero too.

This is the 'dephasing' process that accounts, in typical cases, for the bulk of the decay of the proton free-induction-decay signal. It is, of course, the motivation for the use of the 'gradient coils' in the EF-NMR Gradient/Field Coil part of this apparatus. But with or without such coils, there is always some non-uniformity in the field, and some dephasing of protons, to contend with.

Here's how to understand the role of a spin-flip pulse to counteract the effects of gradient-induced dephasing. We suppose that via some 'magic wand', we can intervene instantaneously, say at time $t = 100$ ms in the example above, and that our intervention is to rotate each proton's spin direction, by a rotation of 180° in space, about the y -axis. It helps for you to draw a diagram of a collection of vectors, originally all along the $+x$ -axis, but now spread out in a fan in the xy -plane, having turned through 199.83, or 200.00, or 200.17 turns at time $t = 100$ ms. If that flip-around- y operation could be conducted instantaneously,

the protons formerly pointing at the 200.0-turns direction would instead be pointing at the 200.5-turns direction,

the protons formerly pointing at the 199.83-turns direction would instead be pointing at the 200.67-turns direction, and

the protons formerly pointing at the 200.17-turns direction would instead be pointing at the 200.34-turns direction.

The point of this 'flip' operation is that protons formerly 'in the lead', 0.17 turns ahead of the pack, will now be 'behind the pack'; and similarly protons that were formerly 'trailing the pack' are now in the lead.

At the end of the 'flip' operation, the precession resumes (in actual fact, it was going on all along, even during a spin-flip operation of finite duration). One important thing has *not* changed: those protons which were in higher-than-average B -field locations will still be in those locations, and will still precess faster than average. And the same will be true for protons in the lower-than-average B -locations. Now, however, the former 'leaders' and 'trailers' have changed places. For a time interval which, in this case, lasts 100 ms, the fast-precessers play a sort of catch-up with the slow precessors which were vaulted into the lead by the spin-flip operation. In this example, at a time just 100 ms after the intervention, all the deficits (or excesses) of rotation have been made up for, and at $t = 200$ ms, all the protons will have turned through 400.5 turns in total.

At, and in the neighborhood, of that time, all the effects of 'dephasing' will have disappeared, and all the protons will be precessing in unison, and the sample as a whole will then be inducing in the pick-up coil a signal as big as it was at the beginning of the spin precession. Because of the location in time of this re-phasing, the signal that emerges is called a 'spin echo'.

The same 'rephasing' argument still works even if the dephasing due to different rates of precession has gone on much longer. If, in the example above, we had waited not 100 ms, but 500 ms, to intervene, we'd find dephasing by not ± 0.17 turns, but ± 0.85 turns, and we'd find a proton sample with spins pointing every which way. Right after the proper

spin-flip pulse, the spins would *still* be pointing every which way; but their directions would be such that, another 500 ms into the future, the spins would all have rejoined into a single pack, pointing in a single direction.

It's quite remarkable that this spin-flip intervention can seem to 'reverse time' in its dephasing effects. It's an example in real life of the thought-experiment called a 'Loschmidt reversal' in kinetic theory, and in this case it succeeds in reversing the effects of non-uniform field strength. There's a lovely tabletop demonstration of the effects of this sort of time-reversal in fluid mechanics, called an 'unmixing' demonstration, in Am. J. Phys. **28**, 348-353 (1960) and nowadays visible on YouTube videos.

This picture of the effects of a spin flip makes some assumptions, which can now be addressed.

- a) In the argument above, it assumes that protons at high-field location before the spin flip *stayed* at high-field locations in space after the spin flip. Any mechanism that causes protons to *move* within the volume of non-uniform field can defeat this assumption, and will lessen the effectiveness of the spin flip. One such mechanism is the diffusion of molecules of the sample in their fluid environment. An easier one to study is mere mechanical motion of the liquids in the sample bottle -- you can imagine the effects of a continual stirring of the sample in defeating the effectiveness of a spin-flip operation.
- b) In the argument above, there's the additional assumption that each proton moment stay fixed in magnitude, and that the sample's total moment decays in time due only to dephasing. But in practice, even in a totally uniform (external) field, there is dephasing due to internal interactions. These are called 'spin-spin relaxation' effects, and they effectively cause the spin-precession signals to decay exponentially with a time constant traditionally labelled T_2 . So even in an ideal environment, the signals would decay as $\exp(-t/T_2)$. In practice, samples might have a T_2 -timescale of whole *seconds*, so a non-uniform magnetic field will cause signals to decay much faster than they would have, intrinsically.

One of the main attractions of spin-echo methods is that they make it possible to see what part of the spin dynamics are due to intrinsic dephasing, by allowing a reversal and elimination of the effects due to extrinsic causes like field non-uniformity.

4. What your spin-flip coils produce, and what effect it has

This section shows you how to understand how you can use the spin-flip coils to create a fully-known magnetic field on the sample. It's all done by keeping track of the current flowing in the coils.

Electrical access to the spin-flip coils is via the little plastic box at the end of their black cable. You'll see a BNC connector labelled DRIVE, and another labelled MONITOR.

(There is also a pair of banana plugs allowing direct access to the coil windings, which you won't need to use.) The little schematic diagram on the box shows that if you connect an ac (or dc) generator to DRIVE, you'll drive a current $i = i(t)$, through the coils. (There are two coils, one on each of the two white plastic coil forms, and they are connected to be electrically in series, and so as to be magnetically additive at the sample's location.) That current $i(t)$ will also pass through a $50\text{-}\Omega$ resistor in the box, making available a MONITOR signal $V_{\text{mon}}(t) = i(t) \cdot 50\text{ }\Omega$.

Now the coils are arranged in space so as to create a magnetic field which is spatially rather uniform over the sample-bottle's volume, and which lies chiefly along the y -direction. If the coils produce a field $\mathbf{B}(t) = \mathbf{y} B_{\text{osc}}(t) = \mathbf{y} k i(t)$, where k is a 'coil constant', then an oscillating current

$i(t) = i_0 \sin \omega t$
will give a spin-flip field

$\mathbf{B}(t) = \mathbf{y} B_{\text{osc}}(t) = \mathbf{y} k i_0 \sin \omega t$.
That oscillating-along- y field can be written as the superposition of two fields, each of which is *rotating* in the xy -plane:

$$\mathbf{B}(t) = (k i_0/2)[\mathbf{x} \cos \omega t + \mathbf{y} \sin \omega t] + (k i_0/2)[-\mathbf{x} \cos \omega t + \mathbf{y} \sin \omega t].$$

The value of this decomposition is that one of these fields, rotating in the xy -plane at angular frequency ω , and with fixed magnitude ($k i_0/2$), will have a strong effect on precessing spins in the sample. The other of these fields will be rotating in the *opposite* sense in the xy -plane, and will have a negligible effect on the precessing spins. The part of the field that has a big effect is called the 'rotating field', and its effect is largest if its angular speed of rotation nearly matches the precession rate of the spins. The other part of the field is called the 'counter-rotating term', and has a negligible effect under these circumstances -- so we'll neglect it hereafter.

One of the attractions of the TeachSpin spin-flip coils is that you can reliably calculate the size of the magnetic field they produce. Suppose you have a generator with a $50\text{-}\Omega$ output impedance, set to give a sine-wave output of amplitude 2 V into an open circuit. Hooked to the DRIVE input of your coils, it'll drive a current through its own internal impedance of $50\text{ }\Omega$, through the coils' resistance of about $3\text{ }\Omega$, and through the monitor resistor of $50\text{ }\Omega$. You'd get an ac current of amplitude about $(2\text{ V})/(103\text{ }\Omega) = 19\text{ mA}$ passing through the coils. There will also be some inductive reactance in the coils, perhaps decreasing the current a bit from this computed value; but *whatever* the current waveform is, the MONITOR output will allow you a measure of it. If you see a sine wave of 800-mV amplitude at the monitor output, you can infer that a current of amplitude

$i = V/R = 800 \text{ mV}/50 \Omega = 16 \text{ mA}$
is passing through the monitor resistor, and also through the windings of the spin-flip coils.

Here's how to get from there to the spin-flip field you want to compute:

If there's a current $i(t) = (16 \text{ mA}) \sin \omega t$ in the coil, and if the coil has a coil constant of $k = 95 \mu\text{T/A}$, then the amplitude of the oscillating field created by the spin-flip coils is
 $B_{\text{osc}} = (95 \mu\text{T/A}) (0.016 \text{ A}) = 1.52 \mu\text{T}$.

What's relevant to NMR spin flips is that you have created a rotating field, of magnitude *half* this, $B_{\text{rot}} = 0.76 \mu\text{T}$, rotating in the xy -plane. (The counter-rotating field, also of $0.76 \mu\text{T}$ magnitude, has negligible effect.)

A necessary (though not sufficient) condition for creating the desired 180° (or π -radian) spin flip is that this field exist for a time T , given by

$$\gamma_p B_{\text{rot}} T = \pi,$$

where $\gamma_p = 267.5 \text{ (rad s}^{-1}\text{)/ }\mu\text{T}$ is the gyromagnetic ratio for protons. Using $\gamma_p = 2\pi c_p$ with $c_p = 42.57 \text{ Hz}/\mu\text{T}$, this gives the requirement as

$$c_p B_{\text{rot}} T = 1/2,$$

and for the numbers above, requires

$$(42.57 \text{ Hz}/\mu\text{T}) (0.76 \mu\text{T}) T = 1/2,$$

or $T = 0.5/(0.76 \cdot 42.57 \text{ Hz}) = 15.4 \text{ ms}$.

The point is that there's a firm line of evidence which connects all the way from the observable MONITOR signal the coils' connector box, to a quantitative prediction of what effect the spin-flip coils ought to have on the nuclei in a hydrogen-containing sample.

5. Executing the simplest spin-flip experiments

This experiment will provide you with an audible spin echo from a proton sample.

For starters, you'll need to be able to get a free induction decay (FID) signal from a proton sample (independent of any use of the spin-flip coils). For that, you might want a 125-ml sample bottle filled with tap water, mounted inside the pickup coil in the NMR head. You might want to use ≈ 3 A of polarizing current (provided by an external dc power supply), for ≈ 4 s of polarizing time, to polarize your proton sample. You'll want the tuning-capacitor switches on your EF-NMR controller set so that the LC-resonant frequency of the coil-capacitor combination matches the precession frequency of protons in your ambient value of static magnetic field. You'll want to connect the pre-amplifier output of your EF-NMR controller to a 'scope, set to perhaps 50 mV/div vertically, and perhaps 50 ms/div horizontally. And you'll want to trigger that 'scope using the TRIGGER OUTPUT of the EF-NMR controller; set the 'scope to trigger on a positive slope and a positive level of about 1 V.

Then a single push of the START button will give you about 4 seconds of polarization time, followed by a trigger event which you may label as $t = 0$. Starting at $t = 0$, your 'scope ought to show some signal emerging from the pre-amplifier. Part of this signal, from $t = 0$ until $t \approx 50$ ms, is the 'coil transient' -- it'll be there whether you have a sample installed or not. But another part of this signal, the part dominant from $t \approx 50$ ms onwards, should be due only to the presence of the sample.

This signal-from-sample is the FID signal attributable to the protons in the sample. You can try to peak up its strength by fine-tuning the capacitor setting in your LC circuit. The duration of this FID signal is unpredictable, since it's controlled by the size of the magnetic-field non-uniformities over your sample bottle's volume. If there is even 100 ms of decent FID signal, you'll now be able to get a spin echo.

Before going on to do so, it's important to find a way to measure the *frequency* of oscillations in your FID signal to modest precision (≈ 10 Hz). The result will of course depend on the strength of the ambient field, B_z , at your location.

[If you have the Field/Gradient part of the TeachSpin EF-NMR system, you can use the gradient-coil adjustments to improve the homogeneity of your static field, and thus improve the duration of your FID signal. But for spin-echo measurements, you *don't* actually want an optimally long-lasting FID signal, but instead an FID signal that basically died away to the baseline noise level by $t \approx 0.5$ s or sooner.]

Now you're finally ready to use the spin-flip coils to create a spin flip, and thereby a spin echo. What you want to do is to create a 'burst' of sine-wave excitation in your spin-flip coil, at a time like $t \approx 0.5$ s (when the FID has died away). If everything is adjusted optimally, you'll see the FID *revive*, reappearing *not* at $t = 0.5$ s, but *later* in time, in fact centered around the point $t \approx 1.0$ s. If everything is right, the effect is not small -- the

revived signal will be nearly as large in size, and of *double* the duration, as your original FID signal. That's the spin echo.

So you'll need a way to derive, from the pulse that's triggering your 'scope at $t = 0$, another pulse occurring at (say) $t = 0.5$ s. This later pulse needs to be of a size and duration suitable for triggering your sine-burst generator. [The Appendix suggests some ways to do this.]

The generator needs to be set correctly, too. The chief requirement is for its frequency nearly to match the protons' ongoing precession frequency, to a modest precision of perhaps $\pm 1\%$. The second requirement is jointly on its amplitude and its duration; try starting with a generator set to deliver a burst of about 2 V amplitude, and a burst of 20 cycles' duration of sine wave.

If you see evidence of a spin echo on the 'scope, you'll be able to *hear* it too. Use the right setting of the TUNING of the main-amplifier section of the EF-NMR controller to optimize its gain at the frequency of your FID signal, and it'll thus be able to send onward both the original FID, and the revived spin-echo signal, from the pre-amplifier, through the (tuned) main amplifier, to the speaker. Now you should hear, after the polarization interval, the sequence in time of the FID signal, a click at the occurrence of the sine-wave burst, and then, later still, the spin echo itself.

Notice that the brief (≈ 10 ms duration) tone-burst signal sent into the spin-flip coils will also couple (capacitively) to the NMR pick-up coils around the sample, so that you'll be able to see, right on your 'scope record, an indication of when in time the tone-burst occurs. The spin-echo signal will come at a predictable *delay* after this marker of the tone burst. If you can vary, from shot to shot, the time delay (0.5 s in the discussion above) at which you apply the tone burst, you'll be able to see the effect that has on the location in time of the spin echo. And you'll see why the poetic term 'spin echo' was invented for this process.

Once you've seen a spin-echo signal, adjust the amplitude of your tone-burst generator, up or down, to optimize the strength of the spin echo signal. You'll know you have a genuine spin-echo phenomenon if, upon *doubling* the generator amplitude compared to this optimal setting, you get just about no spin echo at all! The reason is that a double-strength intervention will give you a ' 2π pulse' in place of the desired ' π pulse', and the result is a no net spin flip, and so no revival of the signal.

There are other experimental tests that a genuine spin-echo signal has to fulfill, some of them of amazing subtlety. The model above clearly claims that the precessing spins in the sample bottle are literally the spinning generator which creates the spin-echo signal by Faraday's Law of Induction. It follows that if the sample bottle is removed from the sample space, after the initial FID (whether before or after the spin-flip intervention), then there can be no spin-echo signal. (Try it!) Less obviously, if the water in the sample bottle is moving, due to the bottle having recently been vigorous swirled, then the spin-

echo effect will be decreased, since you can no longer count on protons being in the same location in space for their dephasing and rephasing intervals of time.

To investigate this latter effect more systematically, it's fun to build a sample bottle in which protons are locally in a liquid environment, but in which they are mechanically nearly tied to the bottle. One way to do so is to stuff an empty sample bottle with glass wool, and then to fill it with water; the glass wool partly 'immobilizes' the water. Even more effective is to fill a sample bottle with (liquid-state) gelatin (ordinary, even flavored, Jello™ works fine) and then let it set to a 'solid'. Either way, you can confirm that you can get an ordinary FID, and then a normal spin-echo effect, from your new samples. The truly subtle experiment now consists in causing a one-time rotational displacement of the sample bottle, by perhaps a quarter-turn, about its own symmetry axis (the x -axis) during the spin experiment. (You're moving, but not *removing*, the sample bottle during the experiment.) The prediction of the modeling above is that such a rotation, conducted either just before or just after the spin flip, will defeat the rephasing mechanism (why?), and thus abolish or diminish the spin-echo signal. Quite apart from forming a detailed confirmation of all the theoretical modeling above, the relevance of this demonstration to flow studies in hydrodynamics ought to be obvious.

6. What you can investigate systematically on spin flips

If you're set up to create,

at a fixed time delay T_{delay} after $t = 0$,
a tone-burst into the spin-flip coils,

and if you're seeing,

in the vicinity of $t = 2 T_{\text{delay}}$,
a spin-echo signal from your pre-amplifier or amplifier output,

then you're ready to investigate the detailed predictions of theory for the effectiveness of the spin-flip intervention.

The claim is that the probability of a spin flip, and therefore the relative strength of the spin-echo signal, is given by

$$P_{\text{flip}} = \frac{(\gamma_p B_{\text{rot}})^2}{(\omega_{\text{osc}} - \gamma_p B_z)^2 + (\gamma_p B_{\text{rot}})^2} \sin^2 \left[\frac{T}{2} \sqrt{(\omega_{\text{osc}} - \gamma_p B_z)^2 + (\gamma_p B_{\text{rot}})^2} \right] .$$

where B_z is the strength of the static field in the z -direction, B_{rot} is the magnitude of the rotating field, which rotates at angular frequency ω_{osc} in the xy -plane, where γ_p is the nuclear gyromagnetic ratio, and where T is the duration of the intervention. This can be more usefully translated into the language of ordinary (rather than angular) frequencies by defining $f_{\text{prec}} = (\gamma_p B_z)/2\pi$ as the precession frequency of the protons, and f_{osc} as the frequency of the oscillating current sent by the generator into the spin-flip coils. It's also useful to introduce $c_p = \gamma_p/(2\pi)$ as a version of the gyromagnetic ratio, but in units of Hz/T [rather than (rad/s)/T]. We find

$$P_{\text{flip}} = \frac{(c_p B_{\text{rot}})^2}{(f_{\text{osc}} - f_{\text{prec}})^2 + (c_p B_{\text{rot}})^2} \sin^2 \left[\pi T \sqrt{(f_{\text{osc}} - f_{\text{prec}})^2 + (c_p B_{\text{rot}})^2} \right] .$$

This allows an investigation of the separate roles of the

frequency f_{osc}

duration T

and strength B_{rot}

of your tone-burst intervention.

It is probably best to start with the tone-burst generator's frequency f_{osc} set to lie at your best estimate of the proton precession frequency, and to make B_{osc} or T your first independent variable.

If you fixed T , the duration of the tone burst, to be 20 cycles' duration, you'll find that you can vary your generator's amplitude over a wide range, perhaps 0-10 V, and find a complicated variation of size of spin echo. Concentrate first on the 0-2 V range (in which the spin-echo signal strength should rise toward a maximum), then in the 2-4 V range (where the signal should peak and then drop again). The reason for this behavior is that the $f_{\text{osc}} = f_{\text{prec}}$ limiting case of the formula above is

$$P_{\text{flip}}(f_{\text{osc}} = f_{\text{prec}}) = \sin^2 [\pi c_p B_{\text{rot}} T] ,$$

which reaches a maximum (of 1) at the ' π -pulse' setting

$$c_p B_{\text{rot}} T = 1/2 ,$$

but which falls again to a minimum (of 0) at

$$c_p B_{\text{rot}} T = 1.$$

(Remember that each new observation of spin-echo strength is a wholly new experiment, starting with a few seconds' polarization time, a brief occurrence of the FID signal, a wait until you intervene with a spin-flip pulse, and another wait until the spin-echo signal reaches a maximum. So you'll get a new data point on your curves only every 10 s or so.)

Once you've explored this (or a larger) range, set the generator's amplitude to that value which gave a peak (ie. a π -pulse), and now explore the effects of varying duration T , say from 10, through 20, to 40 cycles' duration. Again you should see evidence of sine-squared oscillations in spin-echo strength.

Once you have a combination of B_{rot} and T which you're sure is giving you a π -pulse, fix these two values, and try the effects of varying f_{osc} (the frequency of your tone burst). Try varying f_{osc} over a range of $\pm 1\%$, then $\pm 2\%$, then $\pm 5\%$, relative to your previous center. In practice, it might be easier to keep constant the *number of cycles* of oscillation, N , in the spin-flip pulse. If you have a combination of field strength B_{rot} and duration T , namely N cycles of oscillation at f_{osc} , which gives an optimal π -pulse at $f_{\text{osc}} = f_{\text{prec}}$, and then you keep N constant while you vary f_{osc} , the prediction for spin-flip probability becomes

$$P_{\text{flip}} = \frac{1}{1 + (\frac{2N}{f})^2 (f_{\text{osc}} - f_{\text{prec}})^2} \sin^2 \left[\frac{\pi}{2} \sqrt{1 + (\frac{2N}{f})^2 (f_{\text{osc}} - f_{\text{prec}})^2} \right] ,$$

which again displays a maximum (of value 1) at $f_{\text{osc}} = f_{\text{prec}}$.

Collecting enough data points, you should see the 'resonant peak' predicted by the appropriate limit of P_{flip} , reaching a maximum when $f_{\text{osc}} = f_{\text{prec}}$, and dropping down to zero at locations to either side of f_{prec} . The width-in-frequency of this peak is fixed chiefly by your choice of T , the duration of the intervention you're using; if you stick with $N=20$ cycles' duration, the full width at half maximum of your 'resonant peak' will be about 4.0% of the precession frequency. The *larger* your choice of T (or number of cycles N), the *narrower* this peak will be. This may fairly be called an illustration of the 'energy-time uncertainty principle'.

The location in frequency of this peak is thus a measure of f_{prec} , the precession frequency of the protons in your ambient field. What you've done is to find what frequency of rotation-in-space of the rotating component of the 'intervention field' best matches the frequency of the precession-in-space of the proton spins themselves -- that's the condition for the most effective spin flip.

There's another viewpoint on this result, even more directly tied to quantum mechanics. You may view the static magnetic field B_z as creating a splitting in energy between the spin-up, and the spin-down, orientations of the nuclear spin. It's easy to show that the energy difference between these (now non-degenerate) energy eigenstates is

$$\Delta E = \gamma_p B_z \hbar .$$

Now you may view your added, time-dependent, oscillating field in the y -direction as *driving quantum transitions* between these two states, and driving them resonantly when the energy of its photons, given by

$$E_{\text{photon}} = \hbar\omega_{\text{osc}} ,$$

matches the energy difference between the two spin states. This use of the ordinary 'Bohr condition' reproduces the prediction that spin flips will be most effective when $\omega_{\text{osc}} = \gamma_p B_z$, or when $f_{\text{osc}} = c_p B_z = f_{\text{prec}}$.

[However interesting your result, this is probably not the most *efficient* way to measure f_{prec} ; you can get a better estimate of its value, in a lot less time, by taking a record of a single occurrence of the FID signal, and forming its Fourier transform. The peak of that Fourier transform will tell you f_{prec} for a 'single shot' observation. The effectiveness of this procedure is the basis for Fourier methods so widely used in NMR nowadays.]

Back to your data: notice that your frequency scan over f_{osc} reveals the zeroes of either side of f_{prec} predicted by the equations above. By artful choice of T , you can make these 'nulls' fall where you wish in frequency space. By this means, you could arrange to spin-flip all the protons in your sample (precessing perhaps at 1900 Hz), but to leave *unflipped* all the fluorine nuclei in your sample (precessing as they would at ≈ 1790 Hz). This is one example of the many artful, and *selective*, spin manipulations that are used by NMR practitioners.

Note finally that out beyond these zeroes, the spin-flip probability is predicted to have some subsidiary maxima. You can compute where these should occur, then confirm that they exist, and (hardest of all) try to come to some sort of mental picture of why they occur.

7. What you can investigate systematically *with* spin flips

This section assumes that you've seen a spin echo (section 5), and that you've assured yourself that you're optimally generating an on-resonance π -pulse (section 6). What does that make possible?

The first thing you can check is the strength of the spin-echo signal, as measured perhaps by the rms size of the oscillations it shows in the vicinity of its center. Here's a way to persuade yourself that the spin-flip mechanism really works to revive the original FID signal -- the method depends on comparing

- a) the biggest signal you can get (given the presence of field gradients) at the center of the spin echo, versus
- b) the biggest signal you can get, at that same time after $t = 0$, *without* using any spin-flip pulse, by trying instead to cancel out all the effects of gradients.

This comparison depends on the availability and use of the EF-NMR Gradient/Field Coils. The point of the comparison is this: method b) gives a long-lasting FID signal, which might have as an envelope an exponential decay curve. We'd write it as $\exp(-t/T_2^*)$, where the decay time T_2^* is attributable both to intrinsic relaxation of the size of spin magnetic moments, and to residual dephasing effects due to leftover field inhomogeneity. But typically the decay time T_2^* is still shorter than the true, ie. the intrinsic, spin-spin dephasing time T_2 .

To prove that is the task of method a). The goal is to show that a) can give, for the fixed location in time at the center of the spin echo, a larger signal than b) can deliver (at this same point in time). The claim is that, under conditions of a perfect π -pulse for the whole of the sample, the strength of the revived FID signal will be governed by $\exp(-t/T_2)$, where t is the time-location of the center of the spin echo. That is to say, method a) ought to reveal the effects of spin-spin relaxation only, *uncomplicated* by the additional effects of field inhomogeneity.

So, concretely, if you intervene with a π -pulse at time $t = 0.5$ s after the start of an FID, you'll get a spin -echo signal peaking around $t = 1.0$ s. And the claim is that at the peak of the echo you'll be getting a *bigger* signal than you can get in the vicinity of $t = 1.0$ s, even by your best efforts at method b).

Here's another application of spin echoes, one *not* requiring the use of gradient coils. The payoff is getting the 'echo of an echo', and the effect is the most enjoyable if you can trigger a π -pulse at will, via fingertip push-button command.

The procedure might be to get a usual FID signal, decaying rapidly, and to intervene with a π -pulse at around $t = 1$ s. You expect, and should hear, a spin echo around $t = 2$ s.

Now what happens if you create *another* π -pulse intervention, this one at $t = 2.6$ s? It's been 0.6 s since the spins were optimally re-phased; they should therefore re-phase again, and give another echo, this one centered at $t = 3.2$ s.

The pleasure of this method is that it's entirely up to you to decide, *in real time*, when to intervene with a first, and then with a second, π -pulse. A single oscilloscope record can be arranged to show the original FID, both interventions, and both echoes, all laid out in time.

Once you've seen the 'echo of an echo', and understood how it arises, you're ready to create a series of multiple echoes by using a series of π -pulses. You stand ready to harvest a T_2 -value from a single (long) record of the relative strength of multiple echoes. To make this sort of investigation repeatable, you'll want to devise some sort of 'pulse timer', to initiate π -pulse interventions at a chosen and repeatable set of times, all fixed relative to the original $t = 0$ start pulse.

Suppose you get an FID signal of brief duration starting at $t = 0$, and that it's decayed basically to baseline noise at $t = 0.3$ s. Then clearly your timer can intervene with a π -pulse at $t = 0.3$ s, and you'll get a first spin echo signal centered around $t = 0.6$ s. Then a second intervention at $t = 0.9$ s will give a second spin echo centered at $t = 1.2$ s. A third intervention may come at $t = 1.5$ s, giving a third echo centered at $t = 1.8$ s, and so on. (Note the requirement of a series of delays of $T, 2T, 2T, 2T \dots$) The peak sizes of each spin echo will give you a series of samples, taken at $t = 0.6, 1.2, 1.8$ s and so on, of what should be the function $\exp(-t/T_2)$. So the appropriate graph of echo strengths -- all obtained in one long 'scope recording of the signals following a single START -- plotted as a function of time, can give you the (true) T_2 value for your sample.

The method does assume that each π -pulse is giving a perfect 180° spin flip for the whole of your sample; so in practice, this method requires that you've optimized your π -pulse parameters quite carefully. For a check on that, you can try doubling N , the number of cycles of sinusoid in each intervention pulse -- that is to say, you can test the effects of a series of what you think are all 2π -pulses. Only if you've gotten a negligible echo after each of these interventions can you be sure that you're delivering a series of accurate 2π -pulses, and in fact you will have proven

- a) each is a pulse of the right size, and uniform enough over your whole sample volume, and
- b) that there aren't any cumulative errors, even in a series of many 2π -pulses.

Once you've demonstrated such a 'null result' with a series of 2π -pulses, you can be well assured that a succession of pulses, each of half as many cycles of oscillation, will faithfully represent a series of π -pulses. When you've used echoes from a series of π -pulses to extract a T_2 -value, you'll have re-created the Carr-Purcell pulse sequence first used in high-field NMR. You'll also have developed a technique capable of precise measurement of T_2 for a given sample, and could then go on to ask the physics question: what *determines* T_2 , and how can I change it?

[In these experiments, note that there is no 'r.f.' pulse used at $t = 0$ to initiate the original FID signal, and further, that there is no continually-operating oscillator running at frequency f_{osc} , gated into play successively at each intervention. Hence there is no way to achieve the clever Meiboom-Gill pulse sequence also used in high-field NMR. But in

this apparatus, you can create π -pulses so nearly perfect as to render the M-G pulse sequence unnecessary.]

8. The properties of the spin-flip coils

The design of the TeachSpin spin-flip coils is to create a 'square Helmholtz' geometry, using two square coils, each of 10 turns, designed to have, as dimensions, a side $S = 172.2$ mm, and a plane-to-plane separation of $H = 93.8$ mm.

The coils are electrically in series, and are connected so that their fields reinforce (rather than cancel) at the center of the coil system. The separation H is chosen to give optimal homogeneity of the field created in the vicinity of the center. The size S is chosen to be about as big as possible, and still let the coil system be mounted inside the bucking coil of the NMR 'head'.

What follows is some discussion of the 'coil constant' k , which gives the field strength B_y due to these coils, per unit current in (each of the turns of) their windings. The short form of the answer is that $k \approx 95 \mu\text{T/A}$. Because the coils are wound on non-conductive forms, and used in an iron-free and conductor-free environment, this value ought also to apply for alternating currents in the coils.

Here are some methods for computing that k -value:

Start with a single square in the xz -plane, centered around the y -axis and lying at $y = 0$. Let the square extend from $-s/2$ to $+s/2$ in x and z , and let there be a test point at $(0, h, 0)$ on the y -axis. Then each side of the square contributes equally to the field B_y at the test point, and the Biot-Savart Law makes it easy to compute the field component B_y at the test point. One single element of wire, at location $(x, 0, 0)$ on one side of one square, carrying current i , gives

$$dB_y = \frac{\mu_0 i}{4\pi} \frac{s/2}{[x^2 + h^2 + (s/2)^2]^{3/2}} ,$$

and to take into account the whole of one side, this needs to be integrated over the interval $-s/2 < x < +s/2$. For the whole of a single square 1-turn coil, this method gives

$$B_y = 8 \frac{\mu_0 i}{4\pi} \left(\frac{s}{2}\right)^2 \frac{1}{h^2 + (s/2)^2} \frac{1}{\sqrt{h^2 + s^2/2}} .$$

That gives a resource sufficient to solve the problem of interest, in which two such square coils, of side length S , are located in the $y = -H/2$ and $y = +H/2$ planes, and the test point is at $(0, y, 0)$, ie. is at a distance $|H/2 - y|$ from one coil plane, and $|y + H/2|$ from the other. The result is a complicated function for $B_y(0, y, 0)$, but it is an even function of y . The 'Helmholtz condition' for uniformity is achieved by picking H such that $B_y(y)$ has a vanishing second derivative at $y = 0$. This optimal-flatness condition is achieved for $H = 0.5445 S$, and that spacing has been built into the TeachSpin coils.

With that choice for H , the field at the geometrical center of the coil combination is given, for a 10-turn winding of each of the two coils, by

$$B_y(\text{center}) = 10 \frac{\mu_0 i}{S} (1.2961) ,$$

and for $S = 0.1722$ m, that gives $k = (B_y/i) = 94.6 \mu\text{T/A}$. The uncertainty in this value is of order 1%.

One of the attractions of the Biot-Savart method used above is that it can be repeated for an arbitrary test point (x, y, z) near the origin, in an arena in which the two square coils are located in the $y = -H/2$ and $y = +H/2$ planes. The calculation for square-form coils is rendered easier than the traditional circular forms by the fact that the current elements in the coil are everywhere only in either the x - or the z -directions. So any Cartesian component of the Biot-Savart expression ($i \mathbf{dl} \times \mathbf{r}$) can be written down analytically. For a generic test point, the integrations over the eight sides of the two squares need to be conducted numerically, but the result is that B_y (or, if desired, another component of \mathbf{B}) can be computed for any location of test point.

The results can be used to confirm the k -value derived above, and also to check the homogeneity of the spin-flip field for points not so close to the origin. This will give a way to see how nearly uniform the k -value is for generic points within the sample volume. It will also give a way to see why spin-flip pulses meeting the '11- π ' condition would likely be less effective than ' π -pulses': it's hard to achieve so uniform a B_y -field that the '11- π ' condition is adequately met for all the spins in the sample.

There's a separate, and NMR-based, method for checking directly the coil constant, the k -value, computed above. It depends on the availability of the gradient coils in the EF-NMR G/FC unit, and their having been adjusted for optimal field homogeneity. This will give proton FID signals of some seconds' duration. The method also depends on a way (perhaps using FFT methods on those FID signals) for extracting the proton precession frequency with high precision. But given those tools, the idea of the method is simple: putting a *dc* current of i into the spin flip coils will generate a field $B_y = k i$, and this will change the total field from B_z to $[B_z^2 + (k i)^2]^{1/2}$. This motivates a plot, as a function of the chosen current i , of the *squares* of the observed f_{prec} values, to permit the extraction of k .

In practice, it might be enough to vary i over the range -50 mA to + 50 mA, giving a B_y -contribution of about 5 μT . This adds, in quadrature, to a typical B_z -field of 50 μT , to give a total field whose magnitude can be raised by about 0.25 μT . That's only about 0.5% of the typical B_z -value, but this NMR-based method is easily able to detect with some precision these small changes in the precession frequency.

[There are further complications, however; the gradient-cancellation procedure on which this method depends is ideal for correcting the gradients in a field along the $+z$ -direction. But the addition of the B_y -contribution of up to one-tenth of the main B_z -field also achieves the rotation of direction in space of the total \mathbf{B} -field by up to 0.1 radians. And the gradient cancellation will now be imperfect for a field that's been rotated. So there's merit, in this method, of working outdoors (where gradients are smallest), or with a sample container of reduced size (to lessen the effects of gradients over the sample volume).]

Back to coil design parameters: the two coils are each wound with ten turns of #28 AWG copper wire. With one side of one turn of one square having a length S , the complete coil

contains length $(4)(10)(2)S \approx 13.8$ m of wire. The resistance of the windings, at room temperature, is thus about computed to be about 2.9Ω . There is additional resistance in the connections and the cabling, but it is clear that in regular operation, the current in the coils is limited almost wholly by the resistance of the monitor resistor, and the internal impedance of the generator driving the coils.

For excitation of the coils by an ac source, there is an additional consideration of the inductance of the coils. It's easy to do a very approximate calculation of the inductance L , if we approximate that the coils create a field of $B = k i$ everywhere throughout a volume of size $S \times S \times H$ (and if we ignore entirely the fringing fields outside the coils' volume). Then we find the volume-integrated magnetic energy of the system is

$$U_{mag} = \int \frac{B^2}{2\mu_0} dV \approx \frac{(ki)^2}{2\mu_0} S^2 H .$$

If we equate this to the magnetic energy of an inductor, $(1/2) L i^2$, we get $L \approx (k^2/\mu_0) S^2 H$, and evaluating, we find this to be about $20 \mu\text{H}$. Clearly, an actual value for the coils could be measured empirically, *in situ*. The relevance of this approximate inductance is to use it to compute the spin-flip coils' inductive reactance at a typical operating frequency of $f = 2$ kHz; the result is $Z_L \approx 0.25 \Omega$, smaller even than the dc resistance.

Independent of coil resistance and impedance, in any case, all the current passing through them also passes through the $50\text{-}\Omega$ monitor resistor. So the potential difference at the MONITOR output of the coils' connector box is always a faithful surrogate for the actual (time-dependent) current waveform in the coils.

9. Appendix: methods for creating the delay, and the tone burst

The 'tone burst'

Perhaps the simplest way to generate a tone burst on command is to use one of the rather low-priced 'direct digital synthesis' signal generators now available. For example, a Protek B8003FD will generate several kinds of waveforms, including sinusoids, at user-chosen frequencies and amplitudes, and easily covers the range of frequencies and amplitudes needed for earth's-field NMR. It also has a 'burst mode', allowing the generation, on command, of a fixed number of cycles of a sinusoid. The command can be exercised using a front-panel hand-pushed 'trigger' button, or by the arrival of a brief positive-going pulse at a back-panel BNC input.

Of course there are alternative methods. Users enjoying a computer-interfaced environment can easily create a 'virtual oscillator' to create the necessary sine waves via a look-up table and a digital-to-analog computer. Since the waveforms needed in these experiments are sinewaves at audio frequencies, and since a computer might contain a sound card suitable for generating audio frequencies, the necessary hardware might already be present. Since the frequency-precision requirements of the spin-flip experiments are very modest, it won't matter that there is no direct control over the computer's actual time base.

Nor is the use of sinewaves crucial. Even a square-wave waveform at a given frequency contain plenty of the fundamental waveform (which is sinusoidal, and which will drive a spin flip); of course it contains some harmonics too (but they are far off resonance, and will affect a spin flip negligibly). The use of a square wave will make it harder to understand the absolute strength of the rotating spin-flip magnetic fields, however.

Nor does the square wave even need to be symmetrical about zero! A suitably scaled TTL waveform will alternate between voltages near 0 and V , and it is thus the superposition of a dc offset of $V/2$ plus a symmetrical square wave. The dc offset will create, via the spin-flip coils, a small dc field component in the y -direction; this will contribute to the total value of the dc field, but only quadratically since it'll typically be much smaller than the ambient field B_z . Meanwhile the ac component will serve to drive a spin flip.

The time delay

The user's environment will dictate what is the easiest way to arrange the tone burst to be delivered at a desired time. Users with a computer-based solution to the tone burst can of course generate the time delay in software, based on the registration, by the computer, of the same input trigger pulse which triggers the 'scope in the usual data-acquisition scheme.

Those using a separate hardware function-generator for producing the tone burst will probably want a hardware time-delay generator. There are commercial devices expressly

designed to create such time delays, but in this case the timing demands are so simple and so modest that there is an easy breadboard solution, involving a single chip.

We've used a 7400-series dual multivibrator chip, the 74HC221A, to address the timing needs in two stages:

- a) the positive-going trigger pulse emerging from the EF-NMR controller box will trigger a one-shot multivibrator, resulting in a TTL level of HIGH that lasts as long as an external resistor and capacitor dictate. It's easy to achieve a time delay of 0.5 s, and not quite as easy to make this delay time readily variable.
- b) the negative-going edge at the end of this 'wide pulse' can be used to trigger the other one-shot multivibrator in the chip, this one arranged to create a brief ($\approx 25 \mu\text{s}$) positive-going pulse. The descending edge of that 'narrow pulse' pulse will trigger the Protek generator to create its tone burst, as described above.

This makes a fine project in 'laboratory electronics', easy to achieve if a powered digital breadboard is on hand. The design and verification of correct operation of the time-delay generator, and confirmation that the tone-burst is emerging at the right time, make for a real-life proficiency exercise in electronics, and a good test of a student's facility is using an oscilloscope artfully.

SPECIFICATIONS

TeachSpin EF-NMR Sample Coil and Controller,
EFNMR1-A
www.teachspin.com

Sample coil:

1 Coil, of 1340 turns of copper litz wire
Coil Constant: near 15 mT/A
Inductance \approx 73 mH; d.c. Resistance \approx 10.5 Ω
Coil *Q*-factor (at 2.0 kHz): \approx 70
Current Limit: 0.5 to 3.0 Amperes; 0.1 to 99.9 s duration

Notice that an *external* current-regulated power supply is needed for the sample coil used in its polarizing-coil mode.

Sample holders:

Both fit into the sample coil's tunnel of inside diameter 2.00"
Standard holder: 125 ml Nalgene bottle
Segmented holder: 7 compartments, 11 ml each

Accessible frequencies:

1.6 to 2.6 kHz

Controller:

Pre-amplifier gain: \approx 1000
Band-pass amplifier gain: \approx 15

TeachSpin EF-NMR Gradient/Field Coils and Controller, EFNMR G/FC1-A

Helmholtz coils:

- 2 Coils, each of 30 turns of #20 AWG copper wire, connected in series
 - Nominal Diameter of coils: 604 mm
 - Nominal Separation of coils: 303 mm
 - Coil Constant: near 89 ($\pm 1\%$) $\mu\text{T/A}$
 - Current Limit: 3.0 Amperes continuous current
 - Field Uniformity: 0.01 %, for volume within 3 cm of center of coils
 - Frame, permitting altitude/azimuth adjustment of coils' z -axis

Notice that an *external* current-regulated power supply is needed for the Helmholtz coils.

Gradient coils:

- 3 Coil Systems, for creating gradients $\partial B_z / \partial x$, $\partial B_z / \partial y$, $\partial B_z / \partial z$
 - Gradient coil systems are embedded in the planes of the Helmholtz-coil forms.
 - Coil Constants: near 250 $\mu\text{T/m}$ per Ampere of coil current
 - Current Supply: 3 supplies, each ± 20 mA, with 10-turn manual controls
 - Gradient Capability: $\pm 5 \mu\text{T/m}$, for ± 5 turns from center position

Notice that the EF-NMR G/FC Controller *contains* the current-regulated power supplies for these coils.

Current-Monitor points:

- Monitor Resistor in series with Helmholtz coil: 0.1 Ω , 1% tolerance, 25 W
- Monitor Resistors in series with each gradient coil: 100 Ω , 1% tolerance, $\frac{1}{4}$ W

Appendices

- A0. Notation, and values of the proton gyromagnetic ratio
- A1. Magnetizing protons in water
- A2. Deriving the Larmor precession frequency
- A3. The expected size of EF-NMR signals
- A4. Noise expected from the pick-up coil and LCR circuit
- A5. Proton-proton depolarization effects
- A6. Aliasing, its cause and cure
- A7. Aliasing in FFTs and best fits
- A8. Modulating the main field
- A9. Monitoring the polarizing coil
- A10. Signal-averaging at the Amplitude output
- A11. A tuning model for the pick-up coil's LC-circuit
- A12. Comparative signals for differing isotopes
- A13. Understanding the deuteron magnetic moment
- A14. The Helmholtz coils' geometry
- A15. The Fourier transform of a decaying sinusoid
- A16. Counting gradients, and their consequences
- A17. Radiation damping and the FID decay timescale
- A18. Checking the sensitivity of the detection system
- A19. The 'bucking coil', and how it works
- A20: The nuclear spin isomers -- ortho- vs. para-water

Specifications and Safety Data Sheets

Specifications
HT-70
HT-110
PFS-2

Appendix A0: Notation, and values of the proton gyromagnetic ratio

This appendix establishes some notation, and gives some ‘best values’, for proton precession frequencies.

We introduce first the gyromagnetic ratio γ , defined classically as the ratio between a system’s magnetic moment μ and its angular momentum L :

$$\gamma \equiv \frac{\mu}{L} .$$

The definition is extended into quantum mechanics by taking (for both μ and L) their maximum projections along any axis, and applied to nuclei whose angular momentum is given in terms of their spin operator I by

$$L = I \hbar .$$

Now the precession of an angular momentum vector is described by

$$\frac{d\mathbf{L}}{dt} = \boldsymbol{\tau} = \boldsymbol{\mu} \times \mathbf{B} = \gamma \mathbf{L} \times \mathbf{B} ,$$

which is an equation of motion for \mathbf{L} which conserves both the magnitude of \mathbf{L} and its projection on the axis defined by \mathbf{B} . (See Appendix A2.) But \mathbf{L} does change with time, by precessing about \mathbf{B} at (angular) frequency

$$\omega = \gamma B .$$

According to the latest (2010) results at <http://physics.nist.gov/cuu/Constants/index.html>, the gyromagnetic ratio for free and isolated protons is given by

$$\gamma_p = 2.675\,222\,005(63) \times 10^8 \text{ s}^{-1}\text{T}^{-1} ,$$

where the (63) expresses the uncertainty in the preceding two digits, which amounts to 0.024 parts per million (ppm) uncertainty in the value. But NMR users do *not* work with free and isolated protons, instead using protons inside atoms or molecules. Such protons experience *less* than the full external field B , and hence they precess at a slightly *lower* rate, on account of the ‘diamagnetic shielding’ created by the molecular environment. The gyromagnetic ratio for protons, inside water molecules, in a spherical sample, at 25 °C is called the ‘shielded gyromagnetic ratio’ and is given at the same source by

$$\gamma'_p = 2.675\,153\,268(66) \times 10^8 \text{ s}^{-1}\text{T}^{-1} ,$$

Note that there’s a difference of nearly 26 ppm between the two values, a difference vastly exceeding the uncertainties of the numbers. Furthermore, the ‘shielding correction’ provided by the molecular environment *differs* from molecule to molecule, which accounts for the usefulness of the ‘chemical shift’ to NMR users in chemistry. For example, the NMR frequencies, measured in the same field, for protons in water and protons in benzene (C_6H_6), differ by about 5.8 parts per million.

In this experimental manual, we will use only ordinary (not angular) frequencies, and because $f = \omega/2\pi$, we will find most useful the combination

$$c_p \equiv \frac{\gamma_p'}{2\pi} = 42.576\,3866(10) \times 10^8 \text{ Hz T}^{-1} \text{ or } 42.576\,3866(10) \text{ Hz}/\mu\text{T} ,$$

and in this manual we choose to call this the ‘gyromagnetic constant, labelling it c_p for explicit reference to protons.

Appendix A1: Magnetizing protons in water

This section calculates the degree of magnetization expected for a sample of protons in a magnetic field. The magnetization is the result of a competition between two factors: the orienting, or aligning, effect of the magnetic field on the protons' magnetic moment, vs. the disorienting, or randomizing, effect of interactions of the protons with their thermal environment.

We'll use a quantum-mechanical approach, and we'll assume protons are spin- $\frac{1}{2}$ objects. So there's a magnetic quantum number m_I , with allowed values $m_I = \pm\frac{1}{2}$, which arises from the $I = \frac{1}{2}$ angular momentum of the protons.

The magnetic interaction of the protons with the field is described by the Hamiltonian operator

$$\hat{H} = -\boldsymbol{\mu} \cdot \mathbf{B} ,$$

which assigns a lowest energy to protons whose $\boldsymbol{\mu}$ lies *along* the magnetic field \mathbf{B} . Now since the gyromagnetic ratio γ is defined here by $\boldsymbol{\mu} = \gamma \mathbf{I}$, we have

$$\hat{H} = -\gamma \mathbf{I} \cdot \mathbf{B} ,$$

And if \mathbf{B} is a constant, and taken to lie along the z -axis, we have

$$\hat{H} = -\gamma I_z B .$$

But the $m_I = \pm\frac{1}{2}$ states of the proton are eigenstates of I_z , and thus give us two energy eigenvalues,

$$E\left(m_I = \pm\frac{1}{2}\right) = -\gamma\left(\pm\frac{\hbar}{2}\right)B .$$

So the two eigenstates are separated in energy by an energy difference

$$\Delta E = E\left(m_I = -\frac{1}{2}\right) - E\left(m_I = +\frac{1}{2}\right) = \gamma\hbar B .$$

An energy transition between these two states will be resonant with an external field of frequency f (and angular frequency ω) only if

$$hf = (h/2\pi)(2\pi f) = \hbar\omega = \Delta E = \gamma\hbar B , \text{ ie. if } \omega = \gamma B .$$

This is the quantum-mechanical analog of the classically-derived condition for a ‘spin flip’: the applied frequency has to match the Larmor precession frequency of the protons.

Now here's the quantum-statistical way to compute the aligning effect of the magnetic field.

When the field is zero, there is a 50% probability for a given proton to be in either of the $m_I = \pm\frac{1}{2}$ states, and thus the expected value of μ_z is zero. The presence of a non-zero B field *lowers* the energy of the $m_I = +\frac{1}{2}$ state, and *raises* its probability of occupation above 50%. The expected value of μ_z , in competition with thermal interactions, is given by a Boltzmann ratio, in the form

$$\langle \mu_z \rangle = \frac{\sum_m \mu_z(m) \exp[-E(m)/k_B T]}{\sum_m \exp[-E(m)/k_B T]} .$$

The sums extend only over two terms, as m_I takes on only two values. We also have $\mu_z(m_I) = (\gamma I_z) = \gamma(\pm\hbar/2)$ in these two states. We thus can write

$$\langle \mu_z \rangle = \frac{\left(+\gamma \frac{\hbar}{2}\right) \exp\left[-E(m=+\frac{1}{2})/k_B T\right] + \left(-\gamma \frac{\hbar}{2}\right) \exp\left[-E(m=-\frac{1}{2})/k_B T\right]}{\exp\left[-E(m=+\frac{1}{2})/k_B T\right] + \exp\left[-E(m=-\frac{1}{2})/k_B T\right]} .$$

The sums could be performed exactly, but in our case of low-field, room-temperature NMR, the values of $E(m_l) / (k_B T)$ are so excessively small as to motivate the use of the expansion $\exp(-x) \approx 1 - x$ for $x \ll 1$.

Then we get

$$\langle \mu_z \rangle = \frac{\left(+\gamma \frac{\hbar}{2}\right) \left[1 - \frac{-\gamma(\hbar/2)B}{k_B T}\right] + \left(-\gamma \frac{\hbar}{2}\right) \left[1 - \frac{+\gamma(\hbar/2)B}{k_B T}\right]}{\left[1 - \frac{-\gamma(\hbar/2)B}{k_B T}\right] + \left[1 - \frac{+\gamma(\hbar/2)B}{k_B T}\right]} = \left(+\gamma \frac{\hbar}{2}\right) \frac{0+2\left(\frac{+\gamma(\hbar/2)B}{k_B T}\right)}{2+0} .$$

Since there are N protons in our sample, the total magnetic moment of the sample is larger than this by a factor of N . And the magnetization, the total magnetic moment per unit volume, thus has the value

$$M = (N/V)[\gamma \hbar/2]^2 B / (k_B T) .$$

This is the nuclear version of Curie paramagnetism: the magnetization is predicted to be proportional to the field B , but inversely proportional to the (absolute) temperature T .

It is worth working out the numerical value of this magnetization for conditions appropriate to EF-NMR. In the TeachSpin apparatus, the largest B encountered is the polarizing field, of size $B \approx 50$ mT at a full 3-A polarizing current. (Note this gives a magnetization fully 10^3 times larger than would the ambient field, of about 50 μ T.) For room-temperature operation, $T \approx 300$ K, we find $k_B T \approx 4 \times 10^{-21}$ J. We'll take $\gamma = 267 \times 10^6$ (rad/s)/T, so

$$\gamma \hbar/2 = (267 \times 10^6 \text{ s}^{-1} \text{ T}^{-1})(1.055 \times 10^{-34} \text{ J} \cdot \text{s})/2 = 1.41 \times 10^{-26} \text{ J/T} .$$

For a sample of liquid water, it's easy to compute the number density N/V for an imaginary sample of volume $V = 1 \text{ m}^3$. That volume will contain 1000 kg of water, at 18 grams/mole, or $\approx 56,000$ moles of water molecules. Each contributes two hydrogen nuclei to act as NMR-active protons, giving the number density for any sample of water:

$$N/V \approx (111 \times 10^3 \text{ moles}) (6.02 \times 10^{23} / \text{mole}) / 1 \text{ m}^3 = 6.7 \times 10^{28} \text{ protons/m}^3 .$$

So we put these factors together and get

$$\begin{aligned} M &= (6.7 \times 10^{28} / \text{m}^3) (1.41 \times 10^{-26} \text{ J/T})^2 (50 \times 10^{-3} \text{ T}) / (4 \times 10^{-21} \text{ J}) \\ &\approx 167 \times 10^{-6} \text{ m}^{-3} (\text{J}^2/\text{T}^2) (\text{T}/\text{J}) \approx 1.7 \times 10^{-4} \text{ A/m} . \end{aligned}$$

For comparison, the magnetization inside a NdFeB permanent magnet is about $1. \times 10^{+6}$ A/m, showing that our water sample is very weakly magnetized indeed. What's more, our sample's magnetization is not permanent ferromagnetism, but instead temporary paramagnetism, and so it will disappear when the polarizing field is removed.

But it will not disappear immediately! In fact the interactions between the thermal environment and the polarized protons are weak enough that this magnetization, which takes several seconds to develop, also can last for *several seconds*. This rather long-lasting polarization is what makes all of the phenomena of NMR feasible.

This computed value of magnetization will be used, in Appendix A3, to compute the size of the electrical signals that a sample of precessing protons ought to induce in the pick-up coil. Since those electrical signals can be quantified, the level of magnetization computed above is subject to an actual experimental check.

Appendix A2: Deriving the Larmor precession frequency

If you've never heard the word 'precession', you should read about the 'axial precession' of the earth's rotational axis. While the earth preserves a 23° inclination of its rotational axis (relative to the normal to its orbital plane), the direction in space of the earth's rotational axis changes very slowly, taking 26,000 years to trace out a circle in the sky. It follows that the 'pole star' for Northern Hemisphere viewers will not always be Polaris.

Nuclei which have angular momentum can be made to undergo precession as well. As with the earth, so with nuclei: it takes an external torque to change the direction of their angular-momentum vector. In the case of the earth, the torque is gravitational, but in our case of nuclear precession, the torque is due to an external magnetic field interacting with the magnetic moment of the nucleus.

So if a nuclear moment μ is related to its angular momentum \mathbf{I} by $\mu = \gamma \mathbf{I}$, we have two equations:

- the torque exerted on μ is $\tau = \mu \times \mathbf{B}$, where \mathbf{B} is the magnetic-field vector;
- and the effect of the torque is to change \mathbf{I} , according to $d\mathbf{I}/dt = \tau$.

The result is

$$\frac{d\mathbf{I}}{dt} = \tau = \mu \times \mathbf{B} = \gamma \mathbf{I} \times \mathbf{B} .$$

We'll now show, by two independent methods, that this equation of motion for \mathbf{I} will entail the phenomenon of precession, in the important case of a constant magnetic field \mathbf{B} .

Algebraic method

Here we write $\mathbf{I} = (I_x, I_y, I_z)$ and $\mathbf{B} = (0, 0, B)$, and we work out the cross product to get

$$\frac{d\mathbf{I}}{dt} = \gamma \mathbf{I} \times \mathbf{B} = \gamma (+I_y B, -I_x B, 0) .$$

This vector equation of motion gives three component equations:

$$\frac{dI_x}{dt} = \gamma B I_y(t) ; \quad \frac{dI_y}{dt} = -\gamma B I_x(t) ; \quad \frac{dI_z}{dt} = 0 .$$

The third equation immediately tells us that $I_z(t) = I_z(0)$, ie. that the z -component of angular momentum does not change. The other two equations, for I_x and I_y , are coupled first-order differential equations. We differentiate the first to get an uncoupled equation:

$$\frac{d^2 I_x}{dt^2} = \frac{d}{dt} \left(\frac{dI_x}{dt} \right) = \frac{d}{dt} [\gamma B I_y(t)] = \gamma B [-\gamma B I_x(t)] = -(\gamma B)^2 I_x(t) .$$

Similar methods show that $I_y(t)$ obeys this differential equation too; both equations are now second-order but uncoupled. So both I_x and I_y obey the same differential equation; both are proportional to their own second derivatives. This is the basic equation of simple harmonic motion. Because the proportionality constants are also the same, the frequency of sinusoidal variation must be the same for both I_x and I_y .

Now there is some choice of the $t = 0$ origin of time which gives $I_x(t)$ a purely-cosine behavior, so

$$I_x(t) = I_x(0) \cos \omega t ,$$

and for this to work requires $-\omega^2 = -(\gamma B)^2$, ie. it requires that the frequency ω equals γB .

With this form of $I_x(t)$, we find $I_y(t)$ using the first equation of motion:

$$I_y(t) = (\gamma B)^{-1} \frac{dI_x}{dt} = (\gamma B)^{-1} I_x(0) \cdot -\omega \sin \omega t = -I_x(0) \sin \omega t .$$

This completes the solution, which can now be written in terms of two initial conditions:

$$\mathbf{I}(t) = (I_x(0) \cos(\omega t), -I_x(0) \sin(\omega t), I_z(0)) .$$

Notice that in this solution, the magnitude of \mathbf{I} stays fixed, since $\mathbf{I}^2(t) = \mathbf{I}(t) \cdot \mathbf{I}(t)$ gives the fixed value $I_x(0)^2 + I_z(0)^2$. So the vector \mathbf{I} maintains a fixed length, and a fixed z -component, with its tip describing uniform circular motion in x and y , while staying fixed in z -coordinate.

Notice the precession frequency $\omega = \gamma B$ is independent of either initial condition. So for any length of the \mathbf{I} -vector, and for any initial tilt of the \mathbf{I} -vector relative to the \mathbf{B} axis, the precession is at the same angular frequency ω , fixed only by the gyromagnetic ratio γ and the magnetic-field strength B .

Geometric method

We return to the equation of motion

$$\frac{d\mathbf{I}}{dt} = \gamma \mathbf{I} \times \mathbf{B}$$

and now solve this equation without need for a coordinate system, but with maximal use of geometrical insight. We first form the square of \mathbf{I} 's length, $\mathbf{I}^2(t)$, and compute

$$\frac{d}{dt} [\mathbf{I}^2(t)] = \frac{d}{dt} [\mathbf{I}(t) \cdot \mathbf{I}(t)] = \frac{d\mathbf{I}}{dt} \cdot \mathbf{I}(t) + \mathbf{I}(t) \cdot \frac{d\mathbf{I}}{dt} = (\gamma \mathbf{I} \times \mathbf{B}) \cdot \mathbf{I}(t) + \mathbf{I}(t) \cdot (\gamma \mathbf{I} \times \mathbf{B}) .$$

But both vector triple-products are zero, since \mathbf{I} and $\mathbf{I} \times \mathbf{B}$ are necessarily perpendicular. So the time derivative vanishes, and $\mathbf{I}^2(t)$ is thus a constant; we conclude that \mathbf{I} is a vector of constant length.

Next we form the dot product $\mathbf{I}(t) \cdot \mathbf{B} = |\mathbf{I}(t)| \mathbf{B} \cos \theta$, where θ is the angle between $\mathbf{I}(t)$ and \mathbf{B} ; we'll soon prove that this dot product is a constant. Since we've assumed \mathbf{B} is a constant, and have just shown that $|\mathbf{I}(t)|$ is also constant, this will prove that $\cos \theta$, and therefore θ itself, must be constant. So relative to a \mathbf{B} -vector fixed in space, \mathbf{I} must be a vector which preserves a constant length, and a constant tilt θ relative to the \mathbf{B} axis.

The proof we need is easy:

$$\frac{d}{dt} [\mathbf{I}(t) \cdot \mathbf{B}] = \frac{d\mathbf{I}}{dt} \cdot \mathbf{B} + \mathbf{I}(t) \cdot 0 = (\gamma \mathbf{I} \times \mathbf{B}) \cdot \mathbf{B} ,$$

but again this vector triple product is zero, because $\mathbf{I} \times \mathbf{B}$ is perpendicular to \mathbf{B} .

Now since \mathbf{I} is a vector of fixed length and of fixed angle with respect to \mathbf{B} , we can picture \mathbf{I} 's ‘tail’ at the origin, and its ‘tip’ floating in space. The ‘arrow’ of \mathbf{I} needs to lie along a cone, and its tip along a circle, as shown in a diagram:

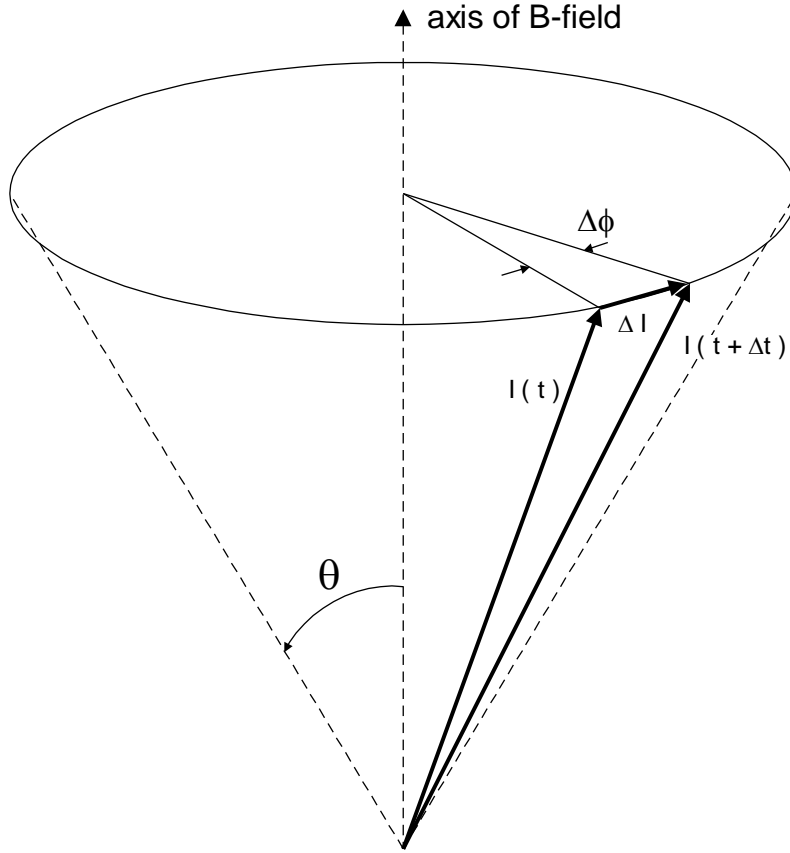


Fig. A2.1: The cone which is the locus of possible values of the vector $\mathbf{I}(t)$.

We have shown vector \mathbf{I} lying in the cone at time t , and another vector $\mathbf{I} + \Delta\mathbf{I}$ applicable to later time $t + \Delta t$, where the difference vector must be

$$\Delta\mathbf{I} = (\gamma \mathbf{I} \times \mathbf{B}) \Delta t$$

from the finite-difference form of the differential equation. Notice that $\Delta\mathbf{I}$ is correctly shown as lying perpendicular both to \mathbf{I} and to \mathbf{B} , which is predicted by this $\Delta\mathbf{I}$ equation.

Notice too that \mathbf{I} and $\mathbf{I} + \Delta\mathbf{I}$ make, as they must, equal projections $I \cos \theta$ on the \mathbf{B} -axis, and also projections of equal length $I \sin \theta$ into the plane of the circular base of the cone. Next, the size of $\Delta\mathbf{I}$ is $|\Delta\mathbf{I}| = |(\gamma \mathbf{I} \times \mathbf{B}) \Delta t| = |\gamma \Delta t| I B \sin \theta$ from the geometrical definition of the cross product.

Now lying inside the circle shown at the cone’s top, we have an isosceles triangle with equal legs $I \sin \theta$, and an opening angle $\Delta\phi$ lying opposite the third (short) side, whose length is given by $|\Delta\mathbf{I}| = \gamma \Delta t I B \sin \theta$. In the limit that Δt goes to zero, we get for this pie-wedge triangle, from the definition of radian measure,

$$\Delta\phi = \frac{\text{arc}}{\text{radius}} = \frac{|\Delta\mathbf{I}|}{I \sin \theta} = \frac{\gamma \Delta t I B \sin \theta}{I \sin \theta} .$$

Notice that the magnitude of I and the value of $(\sin \theta)$ both cancel out, leaving

$$\frac{\Delta\phi}{\Delta t} = \gamma B .$$

But in the limit that Δt goes to zero, this becomes $d\phi/dt$, which is the rate of change of ϕ , and that gives ω , the angular velocity of the precessional motion. Notice that in this method too, we've seen that the size and opening-angle of the cone don't matter, and the precession rate is still fixed only by γ and B .

(The instantaneous proportionality between precession rate and strength of B -field even applies when the magnitude of B itself is time-dependent. Experiments related to this can be found in Appendix A8.)

Finally, the *sense* of precession is also fixed; both the algebraic and the geometric method agree that (for $\gamma > 0$) the precession is in the *counter-clockwise* direction, as seen looking down the positive \mathbf{B} -axis.

Non-precessional motions

Under our assumptions of a constant (or at least a constant-direction) magnetic field \mathbf{B} , and purely magnetic interactions, we see that the only motion possible for \mathbf{I} (and hence for the magnetic moment μ) is precession. There are two important departures from this ideal case, which ought to be mentioned here for completeness.

First of all, if there are dissipative interactions, or interactions with things *other* than the constant magnetic field \mathbf{B} , we can get a motion of μ which matches our intuition. We expect 'in the long term' that μ will line up parallel with \mathbf{B} . Indeed this parallel-alignment does eventually occur, but it is a change which is not described by the Larmor precession above. In the purely precessional motion we have described, the angle θ between \mathbf{I} and \mathbf{B} stays fixed at its initial value. In particular, it does not decay to zero, which is what would be required for \mathbf{I} (and μ) to line up with the magnetic field \mathbf{B} .

The neglect of this effect is appropriate in the case of NMR, because the precessional motion is so fast compared to the dissipative change. Even in weak magnetic fields like the earth's, we'll see the precession time is under 1 millisecond, whereas the time required for 'relaxation' of the sample's collective magnetic moment to lie along the static field is of order 1 second.

The second departure from pure Larmor precession comes when the magnetic field is not static. There is a very important case in which \mathbf{B} is made up of a strong but constant field, but with a small, perpendicular, and rotating or oscillating field component also present. Under these conditions, the precessional motion can itself change with time. In particular, even a weak oscillating transverse component of \mathbf{B} can eventually change the cone angle θ , provided the frequency of oscillation of the component of external field matches the Larmor frequency appropriate to the static component of the field.

This effect is exploited in creating ‘spin flips’, and is very widely used in all sorts of earth’s-field and high-field NMR investigations. But even in this case, the algebraic and geometric vocabulary of Larmor precession is the indispensable starting point for understanding what’s going on.

There’s a third case of Larmor precession which occurs when \mathbf{B} stays fixed in direction, but becomes time-variable in its magnitude. In this case, the motion continues to be precessional in character, and the procession rate continues to be $\omega = \gamma B$; but now B itself varies with time, and hence this result gives the *instantaneous* value of the precession rate. The consequences of this result are tested in Appendix A8.

Appendix A3: The expected size of EF-NMR signals

This section calculates the size of signals that can be induced in a pick-up coil by a sample of precessing protons. This physics of this section is Faraday's Law of Induction, and the surprise is that magnetic moments as tiny as those of protons can (collectively) induce a macroscopic and observable voltage in a pick-up coil.

To simplify the calculations as much as possible, we'll assume a 125-ml spherical sample of water, initially magnetized to the previously-computed $M = 1.7 \times 10^{-4}$ A/m, and then precessing at 2 kHz. We'll further simplify from the actual pick-up coil of solenoidal form to a coil of the same number of turns, but all tightly wound around the equator of a spherical sample.

Now a sphere of volume 125 ml has a radius of $r = 0.031$ m, so each turn of the pick-up coil has area $A = \pi r^2 = 3.0 \times 10^{-3}$ m². We now need to know the time rate of change of the magnetic flux through that coil turn, in order to use Faraday's Law. For that we need the size of the internal field B_{int} which arises inside the uniformly magnetized sphere of water. By the solution of a standard boundary-value problem in electromagnetism, we find that such a sphere creates an external field which is purely dipole in character, but an internal field which is spatially uniform:

$$B_{int} = \frac{2}{3} \mu_0 M .$$

[This result follows from an internal demagnetizing field $H = - (1/3) M$ and the general result $B = \mu_0 (H + M)$. You can compute B_{int} 's numerical value, and see why 'direct detection' of the B -field is difficult.]

Since this field is uniform over the turn's area A , the maximum value of the magnetic flux is

$$\begin{aligned} \Phi_{max} &= B A = \frac{2}{3} \mu_0 M \cdot \pi r^2 \\ &= \frac{2}{3} (4\pi \times 10^{-7} \text{ T} \cdot \text{m/A}) (1.7 \times 10^{-4} \text{ A/m}) (3.0 \times 10^{-3} \text{ m}^2) = 43 \times 10^{-14} \text{ T} \cdot \text{m}^2 . \end{aligned}$$

But if the magnetization is precessing in space (and if the pick-up coil's axis is perpendicular to the direction of the B -field which is causing the precession), then the flux changes in time, according to

$$\Phi(t) = \Phi_{max} \cos(2\pi f t) ,$$

where f is the precession frequency. This gives

$$-\frac{d\Phi}{dt} = -\Phi_{max} \cdot -2\pi f \sin(2\pi f t) ,$$

and the emf induced in one turn of pick-up coil is thus

$$\varepsilon(t) = -\frac{d\Phi}{dt} = \Phi_{max} (2\pi f) \sin(2\pi f t) .$$

So the sinusoidal emf induced in an N -turn coil has amplitude

$$\begin{aligned} N(\Phi_{max})(2\pi f) &= N(4.3 \times 10^{-13} \text{ T} \cdot \text{m}^2)(2\pi \times 2.0 \times 10^3 \text{ Hz}) \\ &= N(27 \times 10 \text{ T} \cdot \text{m}^2/\text{s}) = N(2.7 \text{ nV}) \end{aligned}$$

The actual solenoidal coil in the TeachSpin system has $N = 1340$ turns, which if used in our mythical equatorial coil would give

$$\varepsilon(t) = (3.6 \text{ }\mu\text{V}) \sin(2\pi f t) ,$$

which is a signal of detectable amplitude.

In practice, a solenoidal coil will give a smaller amplitude, since not every turn is ‘filled’ with flux, as in our equatorial-coil model. To see this in another way, we can compute the expected emf by a second method. In this calculation we regard the interaction of the coil, and a magnetized sample of water, in two situations that are related by a reciprocity theorem:

- a) we put current through the polarizing coil, and compute the torque per unit current that would be exerted on a magnetic moment within the coil;
- b) we remove the current supply, and instead attach a voltmeter to the coil, and then consider that *same* magnetic moment rotating within the *same* coil, and inducing an emf in it.

The reciprocity theorem say that (torque/unit current) in situation a) is exactly equal to the (emf/unit angular velocity) in situation b). Of these equal numbers, b) is the one we want for a signal calculation, but a) is much easier to compute.

So we imagine $1 \text{ cm}^3 = 10^{-6} \text{ m}^3$ of water at the center of a fully-magnetized sample, and recall that it will have a magnetic moment

$$\mu = M V = (1.7 \times 10^{-4} \text{ A/m})(10^{-6} \text{ m}^3) = 1.7 \times 10^{-10} \text{ A} \cdot \text{m}^2 .$$

In a field \mathbf{B} , this would experience a torque $\tau = \mu \times \mathbf{B}$, of maximal size μB . The field B produced by the coil in situation a) can be written at $B = k i$, where $k \approx 15 \text{ mT/A}$ is the ‘coil constant’ for the coil. Then $\tau = \mu B = \mu k i$, so the torque per unit current is

$$\tau/i = \mu k = (1.7 \times 10^{-10} \text{ A} \cdot \text{m}^2)(1.5 \times 10^{-2} \text{ T/A}) = 2.6 \times 10^{-12} \text{ T} \cdot \text{m}^2 .$$

By the reciprocity theorem, this also gives the emf per unit angular velocity,

$$\varepsilon/\omega = 2.6 \times 10^{-12} \text{ T} \cdot \text{m}^2 = 2.6 \times 10^{-12} \text{ V} \cdot \text{s} .$$

But the 1-cm³ sample’s magnetic moment is presumed to be precessing at angular velocity

$$\omega = 2\pi f = 2\pi \times 2 \text{ kHz} = 12.6 \times 10^3 \text{ rad/s} .$$

So the predicted emf attributable to 1 cm³ of sample has an amplitude of

$$\varepsilon = (2.6 \times 10^{-12} \text{ V} \cdot \text{s})(12.6 \times 10^3 \text{ rad/s}) = 33 \times 10^{-9} \text{ V} .$$

If all of the 125 cm³ of sample were to be located at the optimal central location in the coil, the total signal would have amplitude

$$\varepsilon = 125(33 \text{ nV}) = 4.1 \mu\text{V} .$$

Again, the actual emf will be smaller, by a ‘filling factor’ due to the location of parts of the sample in sub-optimal locations within the coil. But it is encouraging that this independent calculation gives a result so similar to that derived above.

In any case, the central lesson is clear: under conditions appropriate to the use of the EF-NMR apparatus, an emf of amplitude few microVolts can be expected to be induced in the pick-up coil by precessing protons. This is a weak signal, but it is easily amplified up to milliVolt and Volt levels; the more vital question is how this emf due to precession competes with emfs due to *noise*. An approximate calculation of the noise level to be expected is found in Appendix A4.

The amplification can be briefly summarized here. We have computed the Faraday emf that appears in the pick-up coil, but that get immediately amplified by a factor of Q , the ‘quality factor’ of the LC-circuit of which the coil forms the inductor. For the audio frequencies involved, the Q -value is about 70, so the signal level to be expected emerging from the LC-circuit is near $3 \mu\text{V} \times 70 = 200 \mu\text{V}$ amplitude.

The pre-amplifier to which this signal is sent has a gain near 1000, so out of the pre-amp should emerge a signal with amplitude of order 200 mV. There is a further amplification by a gain near 15 in the main, or band-pass, amplifier, so final signals with amplitudes near 3 Volts can be expected. These macroscopic signals originate wholly from the precession of a collection of nuclei, the ‘magnetized protons’ in water.

Relating such externally-observed signals to the magnetization of the sample offers a route to *checking* these calculations. The method is to take out the bottle of (temporarily) precessing protons, and to substitute for it a small coil generating a (continuously) oscillating magnetic moment. That is to say, the whole pick-up coil/LC system/pre-amplifier chain of electronics can be calibrated for sensitivity, by using a signal generator to drive a small coil of known (area·turns) product with an a.c. current of known amplitude. That coil, installed into the sensitive volume of the pick-up coil, then generates an a.c. magnetic moment of known size, and its value of μ_x can be arranged to substitute for the sample’s value of $\mu_x = M_x V$. The method is described in Appendix A18, and the results can be a check on the absolute size of the magnetization that was computed in Appendix A1.

Appendix A4: Noise expected from the pick-up coil and LCR circuit

We've seen that the pick-up coil is the source of an oscillating emf of amplitude a few μV , and frequency about 2 kHz. Now we compute what *noise level* can be expected to emerge from the EF-NMR detection system.

The emf produced in the coil drives an LC-resonant system, in which the coil provides the inductance L , and the tuning capacitors in the Controller unit provide the (adjustable) capacitance C . Such a system has a ‘quality factor’ or Q given by $\omega L / R$, where R is the resistance of the coil. For operation at $f = 2 \text{ kHz}$, the observed Q is about 70. The d.c. resistance of the coil is $R = 9.5 \Omega$. Assuming this value is also applicable at 2 kHz, we deduce

$$70 = (2\pi \times 2 \text{ kHz}) L / (9.5 \Omega) ,$$

which gives $L = 53 \text{ mH}$. (A more accurate value can be derived from measurements via the methods of Appendix A11.)

Now the Q has a very real effect, in multiplying by a factor of Q the driving emf of amplitude (say) 3 μV , to an amplitude of about 200 μV expected to appear across the LC circuit.

This signal is then enlarged by a gain near 1000 in the pre-amplifier, to a predicted amplitude of about 200 mV. There is further amplification, by a factor near 15, in the band-pass amplifier, so this predicts a final output signal which is sinusoidal and of amplitude near 3 Volts. These predictions match the observed signal strengths to remarkable accuracy, considering that they are derived wholly from the theory of protons' magnetization, and factors appropriate to the apparatus.

But the real question is not just how large are the signals, but what is the level of electrical *noise* which with they have to compete. We divide ‘noise’ in two categories:

- a) interference, in principle deterministic, as in signals induced in the pick-up coil by flux from other sources, and
- b) noise proper, in principle random, as in signals generated in the pick-up coil by fundamental mechanisms.

Here we'll ignore type-a) interference, as these effects (at least for distant sources) can be (almost) entirely cancelled by the bucking coil wound outside the pick-up coil. Instead, we'll focus on type-b) genuine noise, a lower limit on which is provided by the Johnson noise generated by the resistance of the wire of the pick-up coil.

For a coil of $R = 9.5 \Omega$ at $T = 300 \text{ K}$, the predicted mean-square measure of the Johnson noise is $\langle V^2 \rangle = 4 k_B T R \Delta f = (0.157 \times 10^{-18} \text{ V}^2/\text{Hz}) \Delta f$.

We could call that a noise continuum with a ‘power spectral density’ $0.157 \times 10^{-18} \text{ V}^2/\text{Hz}$, or (taking the square root) with a ‘voltage spectral density’ $0.396 \times 10^{-9} \text{ V}/\sqrt{\text{Hz}}$, or about 0.4 nV/ $\sqrt{\text{Hz}}$.

That noise emf is just as real as the signal, so it too is amplified by a factor of Q , at least for frequency components near the resonant frequency of the LC-system. That raises the Johnson noise level (in the vicinity of the signal frequency) to $70 \times 0.4 \text{ nV}/\sqrt{\text{Hz}}$ or 28 nV/ $\sqrt{\text{Hz}}$.

Thus we expect, across the LC-resonant circuit, a signal of about 200 μV amplitude, and a lower limit to noise of about 30 $\text{nV}/\sqrt{\text{Hz}}$. These numbers are literally incommensurate, having different *units* as they do. That's because the effects of noise will depend on the bandwidth over which they are effective, and this bandwidth Δf has thus far been left unspecified. In practice, the bandwidth of the system is limited by two effects:

- the LC-resonant circuit has a half-power bandwidth of $f_{\text{res}} / Q = 2 \text{ kHz} / 70 = 30 \text{ Hz}$;
- the band-pass amplifier also has half-power points about 100 Hz apart.

If we want the signal-to-noise ratio at the pre-amp output, we are ‘upstream’ of this latter effect, so we can take for bandwidth an estimate $\Delta f = 30 \text{ Hz}$. Then the Johnson noise is predicted to give, as a mean-square voltage across the LC-resonant system,

$$\langle V^2 \rangle = (28 \text{ nV}/\sqrt{\text{Hz}})^2 (30 \text{ Hz}) = 23,520 \times 10^{-18} \text{ V}^2 .$$

which says that the rms measure (the square root of the mean of the square) of the noise is predicted to be $153 \times 10^{-9} \text{ V}$ or 153 nV . This noise signal will also experience the 1000-fold gain of the pre-amp, and appear at its output as a noise signal of rms measure 153 μV or 0.15 mV .

Now we can finally compare two commensurate numbers: at the pre-amp output, we have computed a (sinusoidal) EF-NMR signal of amplitude 200 mV , and a (random) noise of rms measure 0.15 mV . If we use rms measure for the signal as well, we can compute an estimate for the rms-signal-to-rms-noise ratio,

$$S/N = (200 \text{ mV}/\sqrt{2})/(0.15 \text{ mV}) = 950 .$$

Before comparing this prediction to observation, we'll do an alternative calculation of the expected effects of Johnson noise. This new method is free of the curious $\text{V}/\sqrt{\text{Hz}}$ unit, and free of calculations of bandwidth. Instead, it uses a result of the equipartition theorem to compute directly the expected rms measure of the noise that will be observed across the LC-circuit. The net effect of dissipation in the resistor is to give a fluctuating voltage across the capacitor, of mean-square size obeying

$$\frac{1}{2}C\langle V^2 \rangle = \frac{1}{2}k_B T ,$$

which is (oddly enough) independent of the value of the resistance R in the LC-circuit.

(The reason is that larger R -values give larger Johnson noise voltages, but also cause a lower Q by which they are amplified, as well as a larger bandwidth over which they are important. The three factors together give an R^0 dependence to the result computed.)

With this simple calculation, we get for the mean-square noise voltage the prediction

$$\langle V^2 \rangle = k_B T/C .$$

Now using the previously-assumed $f = 2 \text{ kHz}$, and the previously-computed $L = 53 \text{ mH}$, we can compute the value of C required to put the LC-system at resonance with the EF-NMR signal.

We get

$$2\pi f = \frac{1}{\sqrt{LC}} , \text{ so } C = [L(2\pi f)^2]^{-1} = 120 \text{ nF} .$$

This then gives

$$\langle V^2 \rangle = (1.38 \times 10^{-23} \text{ J/K})(300 \text{ K})/(120 \times 10^{-9} \text{ F}) = 3.45 \times 10^{-14} \text{ V}^2 ,$$

and gives a square root of the mean-square, ie. an rms measure, of 186 nV for the noise measured across the LC circuit. (This replaces the approximate value 153 nV computed by bandwidth-based methods above.) The predicted signal-to-noise ratio of voltages observed across the LC-system is re-computed to be

$$S/N = (200 \mu\text{V}/\sqrt{2})/(186 \text{ nV}) = 750 ,$$

and this value is just about what can be observed in interference-free locations. One may conclude that Johnson noise is the main source of noise in this experiment, and that other sources of noise have been neglected without falsifying the comparison with observations.

The astute reader will note that precession signals, and the relevant noise components with frequencies near 2 kHz, are *both* equally amplified by the Q of the LC-system, and are *both* equally amplified by the pre-amp and the band-pass amplifier. This brings up the question of what the LC-system is *for*, given that it amplifies Johnson noise by the same factor as the signal. There are two good answers to this question.

- 1) Both the resonance of the LC-system, and the gain of the band-pass amplifier, render them frequency-selective. By tuning, both are made to exhibit their full gain for the signal frequency. This also ensures that they also exhibit their full gain for noise components in the immediate vicinity of the signal frequency. But the noise is broadband, so most of the noise power will fall *outside* the region over which the Q of the LC-system, or the gain of the band-pass amplifier, apply at their full values. So all of the signal, but only a small part of the noise, will pass this frequency-selectivity test.
- 2) We have seen that the LC-system elevates the signal amplitude from 3 to 200 μV , but also elevates the noise level from 0.4 nV/ $\sqrt{\text{Hz}}$ to 28 nV/ $\sqrt{\text{Hz}}$ (for frequencies in the immediate vicinity of the signal frequency). In this local-in-frequency sense, the high Q of the LC system increases the signal-to-noise *ratio* not at all. Why then do we take the trouble to get a high Q ? Why not use a Q of 1, and just amplify the signal (and the nearby noise) by a factor of 70 in a pre-preamplifier?

The explanation has to do with the previously-unconsidered *amplifier noise*. The amplification by $Q = 70$ in the LC-system introduces no extra noise, but it does succeed in elevating the signal (and the Johnson noise) to a level, compared to which the equivalent input noise of the pre-amp is negligible.

In practice, the pre-amp has an equivalent input voltage-noise-density of about 15 nV/ $\sqrt{\text{Hz}}$. This is huge compared to the raw Johnson noise level due to the coil resistance R (of about 0.4 nV/ $\sqrt{\text{Hz}}$), but rather small compared to the Q -fold amplified Johnson noise (of about 28 nV/ $\sqrt{\text{Hz}}$). So the purpose of the high- Q front end of the system is to elevate signal (and Johnson noise) to a level large enough that (in comparison) the pre-amp's input noise can be neglected.

This method of ‘noise-free amplification’ is very widely used in physics, precisely because it can render much less important the effects of imperfections of subsequent electronic amplifiers. Similar resonant methods are used in high- Q mechanical systems, microwave cavities, and laser resonators, for precisely the same reasons.

Appendix A5: Proton-proton interactions

We're used to thinking of proton magnetic moments μ as responding passively to an external field B_{ext} . But each proton moment μ is also the active source of a magnetic field. This dipole field has a complicated angular dependence, but the size of the field is of order

$$B_{\text{dipole}} = \frac{\mu_0 \mu}{4\pi r^3}$$

at a site that is distance r away from the source proton.

Now we want to know what field a 'source proton' creates at the site of another 'victim proton'. For a relevant distance r , we'll compute the proton-to-proton distance we'd get for liquid water if all the $N/V = 67 \times 10^{27}$ protons/m³ were in separate cubical cells. We'd have volume-per-cell of $V/N = 0.015 \times 10^{-27}$ m³, and its cube root,

$$r = (V/N)^{1/3} \approx 0.25 \times 10^{-9} \text{ m} ,$$

as the cell dimension and therefore also the typical proton-to-proton distance. (The distance between the two protons within a single H₂O molecule is about 0.15×10^{-9} m, but this smaller distance between 'NMR-equivalent' protons turns out not to be relevant.)

Now if we take for the proton moment

$$\mu = \gamma L = (267 \times 10^6 \text{ s}^{-1} \text{ T}^{-1})(\hbar/2) = 1.41 \times 10^{-26} \text{ J/T} ,$$

we get (at the calculated distance r) a field strength of

$$B_{\text{dipole}} = (1.00 \times 10^{-7} \text{ T m/A}) (1.41 \times 10^{-26} \text{ J/T})/r^3 \approx 90 \times 10^{-6} \text{ T} .$$

This 90- μ T field is *not at all* small compared to the earth's field of size $\approx 50 \mu$ T in which EF-NMR free precession might be occurring. And that fact is part of the explanation of why EF-NMR gives such very different results in ice and in liquid water.

The picture appropriate to liquid water is that any given proton precesses (with one full cycle taking about half a millisecond) in a field which is the sum of the earth's field B_{ext} and other protons' fields B_{dipole} . Of these two terms, the first is constant, while the other varies very rapidly in time. Because of the dipole character of the field from other molecules of random orientation, the field B_{dipole} 'averages down', from a characteristic instantaneous scale of 100 μ T, to an effective value which is zero. This argument works because in a liquid, a source proton passes by a given victim proton in a time scale of just pico- or nano-seconds appropriate to molecular rotation, vibration, or translation. So in liquid water, the net effect of B_{dipole} on the average precession rate is zero, for any and all protons involved in the NMR precession. (The rapid fluctuations in the field B_{dipole} do have a role to play in the explanation of spin-spin relaxation, however.)

The picture appropriate to ice, or to protons in an even more rigid crystal lattice, is much different. Here we can imagine the opposite limiting case, in which each victim proton is *fixed* into a lattice of source protons, and (for a millisecond or even a whole second) experiences a *constant* value of B_{dipole} . Different protons in the sample then experience a total field in the range $B_{\text{ext}} \pm B_{\text{dipole}}$, ie. in a range $(50 \pm 90) \mu$ T in our estimate. In this limit, NMR free-precession signals would be spread out over a large range of frequencies, experiencing a total field's

magnitude somewhere in the range 0 to 140 μT . In a time-domain view, various protons which started out all polarized in the same direction would have precession rates spread out over a range of proportions 0:140. After a time (about half a millisecond) accommodating just one full cycle of precession in the ‘average’ field, other protons would have precessed anywhere from zero to three cycles. Clearly, the μ -vectors of variously-precessing protons would almost immediately be pointing into a set of effectively-randomized directions, destroying any net magnetic moment of the sample. So the induced-emf signal in the coil would have vanished too. We conclude that solid samples will give EF-NMR signals, if any, of undetectably short duration.

It is a very interesting question to discover just what constitutes a ‘solid sample’ by this criterion. You can check to see if ice is a solid for NMR purposes. And what about the water of hydration in a crystal? What about the water content in a fresh banana, in a live white mouse, or in a batch of gelatin dessert? What about the protons in hydrogen atoms in a highly viscous liquid such as glycerine, or in various water/glycerin mixtures? What about protons in a batch of mixed epoxy, while it is curing? Or after it has cured? You can begin to see that the spin-spin interactions, described by the T_2 time-scale, are indeed a diagnostic of microscopic behavior in a material. Furthermore, you’ll find that it’s faster just to *execute* some of these experiments than it is either to argue about the theory or to look up standard references.

Appendix A6: Aliasing in oscilloscope captures

The primary data that you'll record in earth's-field NMR experiments are time records of 'free induction decay' signals. These occur as one-time transients, lasting a few seconds, and exhibiting oscillations are frequencies near 2 kHz. Digital oscilloscopes make it easy to capture these transients for storage, steady display, and subsequent numerical modeling. But digital 'scopes can capture data in a way that gives a *grossly deceptive* view of the transient. The problem is generic to any kind of waveform digitization: it's called *aliasing*, and this Appendix will teach you how to avoid or surmount it.

Aliasing arises from the way that digital 'scopes capture data. They do *not* record the continuous-in-time waveform $V(t)$. Instead, they capture a finite list of voltage samples, $\{V(t_1), V(t_2), \dots, V(t_N)\}$, where t_1, t_2, \dots, t_N are the sampling instants. They are separated by a (uniform) sampling interval. The reciprocal of the sampling interval is the *sampling rate*, given in Samples/second, or Sa/s.

Oscilloscope users have direct control of the horizontal (time) axis via a 'sweep speed' control, typically given in units of time/division. If you want to record 2 seconds' worth of data, you might choose a sweep-speed setting of 200 ms/div, so the 'scope's ten divisions cover the 2.0 s of time you wish to record. But you generally do *not* directly control the sampling rate; and on some 'scopes, you do not even see this number displayed. That's a problem, because

inadequate sampling rate is the cause of aliasing.

The actual sampling rate is set by the 'scope, and it is limited by the *memory depth*, the number of voltage samples the 'scope can store. You need to know this number! If you have a way to save an acquired waveform to a memory device, and examine it later on a computer, then you can find the memory depth from the number of lines of data in the file. Back when the cost of memory was a limiting factor, memory depth might have been only 500 or 1000 samples; nowadays, even budget 'scopes will store 2500 samples. Even so, this is not always enough!

Memory depth N , total time duration recorded T , and the sampling rate f_{sa} are interconnected by

$$f_{\text{sa}} \cdot T = N , \text{ so } f_{\text{sa}} = N / T .$$

If you can store 2500 samples, and you want to record over a time duration $T = 5.0$ s, then the sampling rate is limited to $f_{\text{sa}} = 2500 \text{ Sa} / 5.0 \text{ s} = 500 \text{ Sa/s}$. And this is *not* enough to prevent aliasing of EF-NMR signals.

Here's the EF-NMR user's form of Shannon's sampling theorem. Your signals are 'narrow-band' in frequency space, and centered at precession frequencies in the 1.6 – 2.5 kHz region. It is a safe assumption that they contain negligible spectral content above 5 kHz. Then the sampling theorem says:

if your sampling rate f_{sa} is 10 kSa/s or above, you will avoid aliasing.

In fact, in this case, you will also get so faithful a capture of the waveform $V(t)$ that you could reconstruct the waveform, not only at the sampled points $\{V(t_i)\}$, but *also* at (un-sampled) times interpolated between the sampling points(!).

But you can't always achieve a sampling rate of 10 kSa/s, given the memory-depth limit. To capture 5.0 s of data at this sampling rate would require memory depth $N = f_{\text{Sa}} \cdot T = (10 \text{ kSa/s}) (5.0 \text{ s}) = 50,000$ samples. If your 'scope lacks that much memory, it will default to a lower sampling rate. An example above gave a case in which the sampling rate was 500 Sa/s, *below* the Shannon requirement. That sampling rate will lead to aliasing, as is best seen in a set of concrete examples.

Here's a plausible EF-NMR waveform $V(t)$, taken to be a cosine wave (at precession frequency 2088 Hz), with a damped-exponential envelope (of e^{-1} decay timescale $\tau = 0.8$ s). Then the true waveform is

$$V(t) = \cos(2\pi \cdot 2088 \text{ Hz} \cdot t) \exp(-t/0.8 \text{ s}) .$$

If such a waveform is sampled at 500 Sa/s, then there is a sampling interval of 0.002 s, or 2 ms, per sample. It's easy to generate, and plot, a list of samples

$$\{V(t = 0), V(t = 2 \text{ ms}), V(t = 4 \text{ ms}), \dots\}$$

from the function above. A view of the first 2.0 seconds of such data gives a first hint of the presence of aliasing:

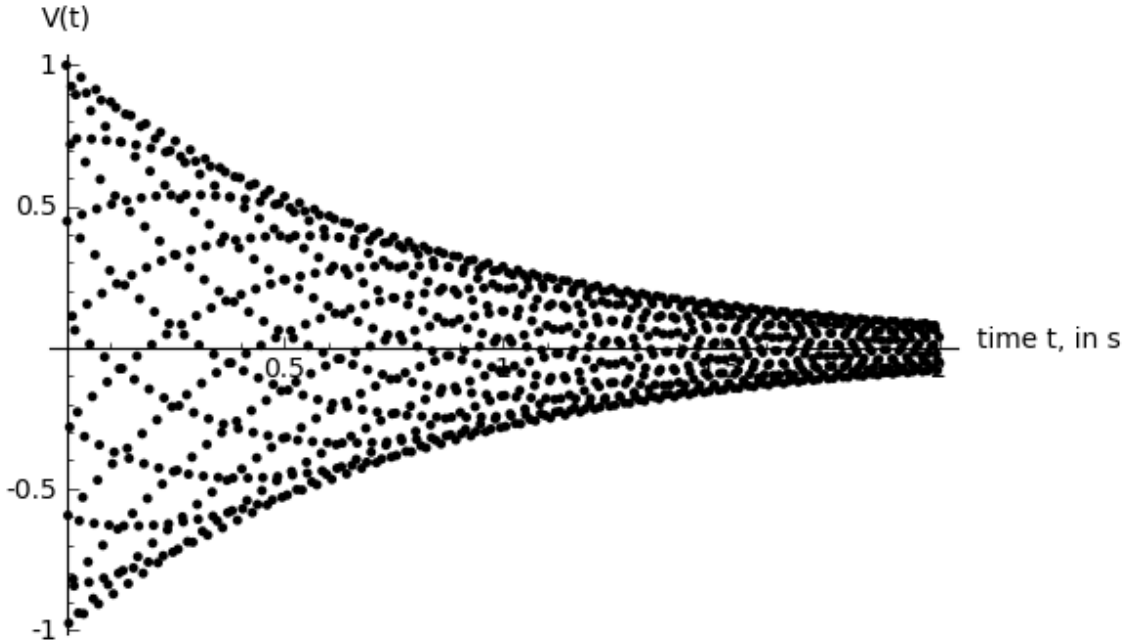


Fig. A6.1: 1000 sampled points, taken from the $V(t)$ model, at 2.0 ms spacing for 2.0 seconds, and plotted as a function of time.

The graph looks as if it's the overlay of seventeen separate traces, instead of a continuous waveform. To see what's going on, just as you can on a 'scope, so in the plot above, you can 'expand the time axis' after the fact. Here's another view of the sampled data over the first 0.1 s or 100 ms of data. The fifty sampled points are shown as dots, with line segments added to join successive samples:

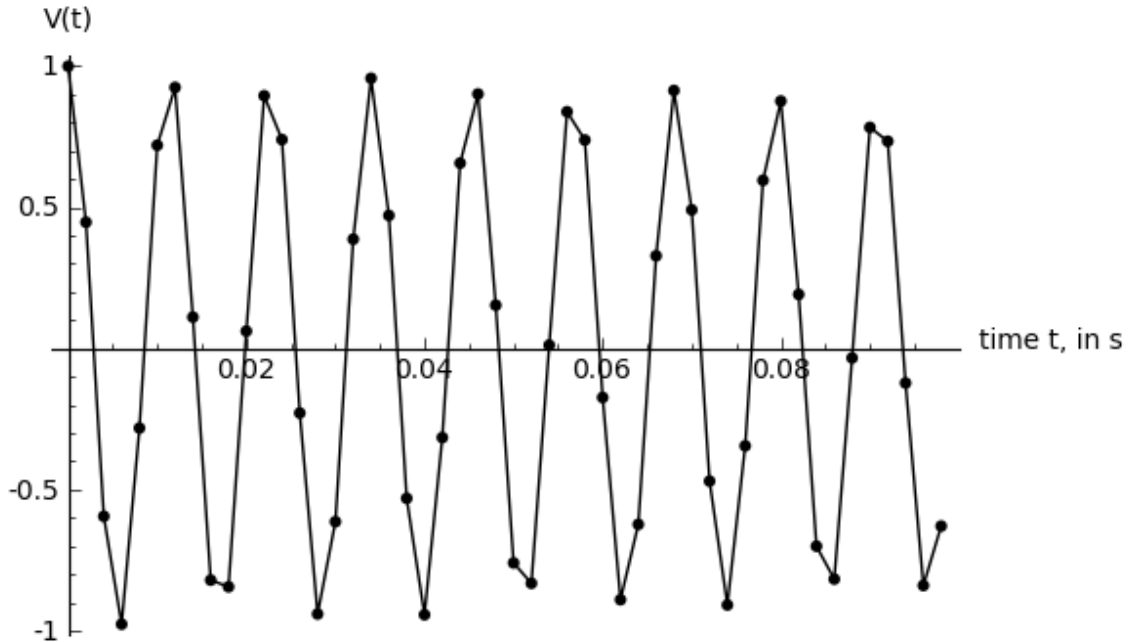


Fig. A6.2: 50 sampled points, taken from the $V(t)$ model, at 2.0 ms spacing for 100 ms, and plotted as a function of time. The line segments join successive points.

The dots are all true samples, but the lines (as we will see) are *fallacious and deceptive*. This plot *seems* to show 8 full cycles occurring in ≈ 0.091 s or 91 ms, for an indicated period of ≈ 11.4 ms, or an indicated frequency of 88 Hz. This is *not* the true frequency of 2088 Hz; it is an *alias* of that true frequency.

This is not merely an artifact of the lines connecting the dots. Suppose I write a *false* waveform, not of 2088-, but of 88- Hz frequency, but otherwise like the true waveform:

$$V_{\text{false}}(t) = \cos(2\pi \cdot 88 \text{ Hz} \cdot t) \exp(-t/0.8 \text{ s}) .$$

and plot its curve (Fig. A6.3) atop the previously sampled points, again covering 100 ms of time. Notice the aliased waveform is now free of the jagged corners of the line-segment plot; but notice also that the false waveform nevertheless *hits* all the sampled points, ‘fitting’ them perfectly! You can see that, because the data comes from an under-sampling of the original waveform, an aliased frequency of 88 Hz is appearing as just-as-perfect a fit to a set of data of true frequency 2088 Hz.

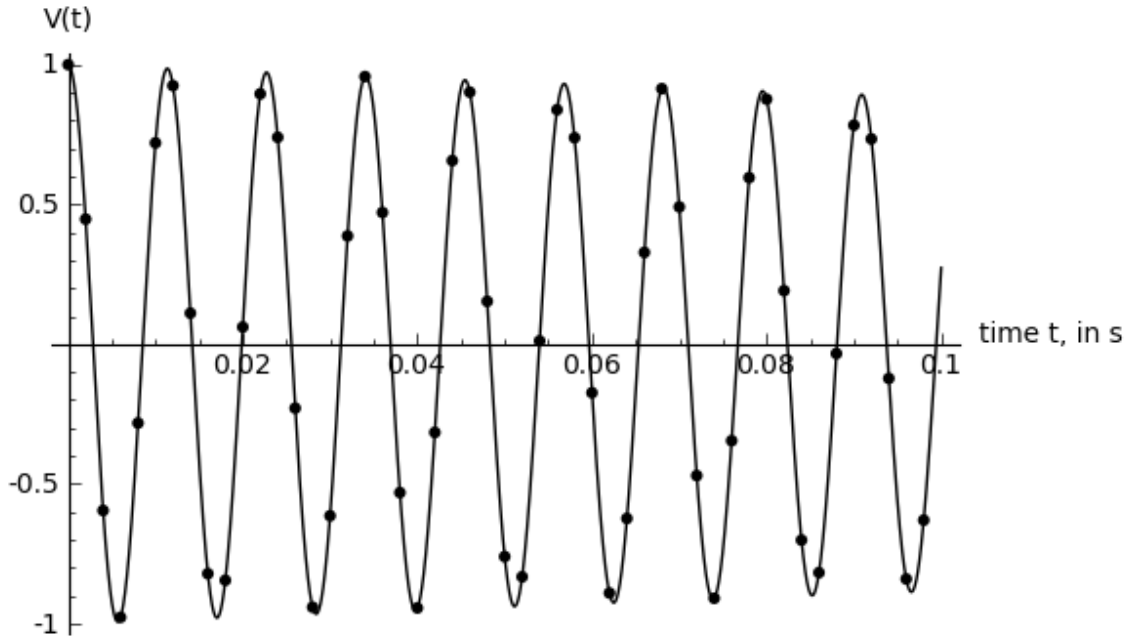


Fig. A6.3: 50 sampled points, taken from the 2088-Hz $V(t)$ model, and overlaid by a plot of the $V_{\text{false}}(t)$ function having 88-Hz periodicity.

Another view (Fig. A6.4), expanded even further in time, shows the true waveform (shown solid), and the aliased waveform (shown dashed), *both* passing through all the sampled points in the first 8.0 ms of time. To put it another way: if all you had was the list of sampled voltages, you *could not tell* (after the fact) whether the actual waveform's frequency was 2088 Hz or 88 Hz.

You can now see how aliasing can happen, in the case of insufficiently dense sampling – the voltage samples captured as points have ‘lost track’ of some number of whole cycles that might have intervened between sampling times.

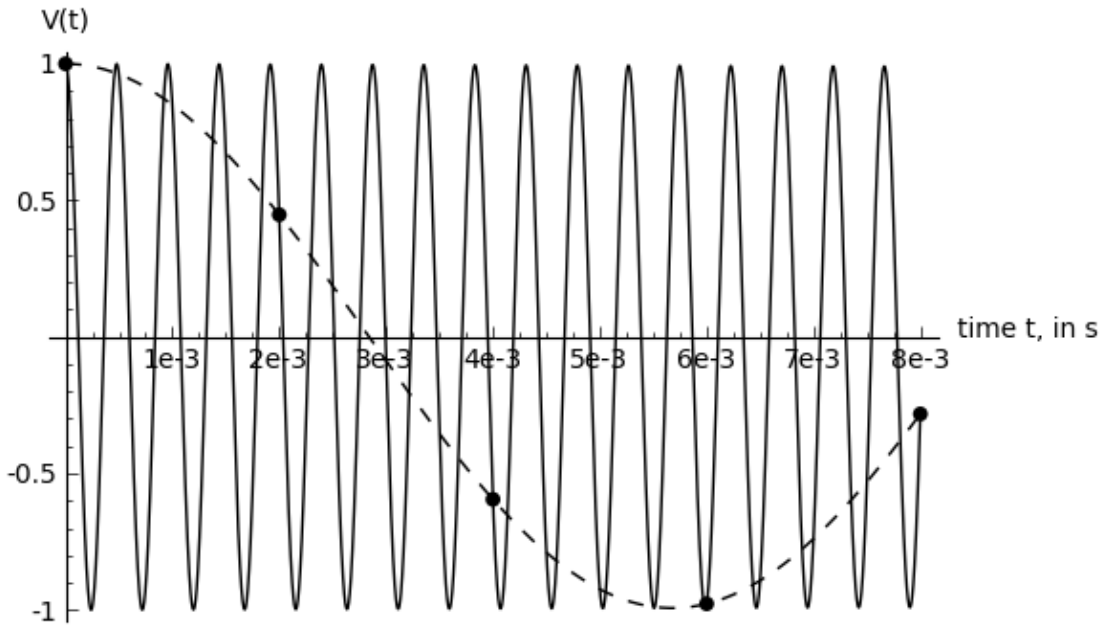


Fig. A6.4: Five sampled points, taken from the $V(t)$ model, at 2.0 ms spacing for 8.0 ms, and overlaid with plots of both models, $V(t)$ and $V_{\text{false}}(t)$.

Exercise: Replicate these plots, in your favorite computing environment. Now go on to show that 8.0 ms of sampled points are ‘fit’ perfectly, not only by the true 2088-Hz waveform, and by an 88-Hz alias, but also by *another* alias, this one at 1912 Hz(!). Lesson: when aliasing occurs, there can be *multiple aliases*.

Now that you are awakened to the seriousness of the problem, here’s how to avoid or surmount it:

0. Learn your ‘scope’s memory depth; or find a way to display, for every acquisition of data, the sampling rate you’re using.
1. For best results, ensure the sampling rate is *at least double* the highest frequency component present in the true waveform.
2. You may have to *give up duration* of acquisition, given a fixed and finite memory depth, and the requirement of this minimum sample rate.
3. If you need a longer duration, consider using the ‘peak detect mode’ of acquisition on your ‘scope. In this mode, you give up getting actual samples, in favor of seeing the true envelope of the waveform.

Here’s how that latter mode would work in covering 5.0 s of time using a memory depth of only 2500 points. The ‘scope will end up displaying something every $5.0 \text{ s}/2500 = 2.0 \text{ ms}$, but it’ll use a new and different kind of display. Rather than sample $V(t)$ only at discrete times 2.0 ms apart, it’ll sample $V(t)$ at its maximal rate (which might be hundreds of *millions* of times per second). Since there isn’t enough memory to store such a firehose of data, the scope will only keep track of the maximum, and the minimum, value of $V(t)$ found in each 2.0-ms interval of time. Then it’ll display this min-to-max range, as a shaded or filled-in band, in each of 2500 places 2.0 ms apart, to give coverage of 5.0 s of time.

An example of this mode, applied to an actual EF-NMR transient, is shown in two ‘scope captures below. Both were obtained with sweep speed 100 ms/div (and thus cover 1.0 s of total time), and with a memory depth of 2500 samples (hence a sampling rate of 2500 kSa/s, or a sampling interval of 0.4 ms). The *apparent* precession frequency is about 4.5 cycles of waveform per single 100-ms division, or 45 cycles/s = 45 Hz; but the *true* precession frequency was about 2545 Hz. The waveform captured in the ordinary (sampling) mode shows aliasing due to under-sampling.

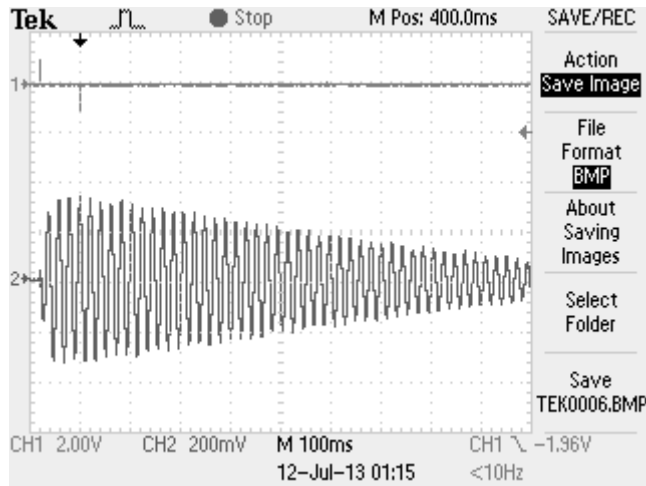


Fig. A6.5: Data obtained in the sampling mode. Upper trace, the trigger events at $t = -80$ ms and $t = 0$ ms; lower trace, the pre-amplifier output for a free-induction-decay transient.

The waveform obtained in the peak-detect mode shows the true heights of the (very brief) trigger events, and also the true envelope of the free-induction-decay signal, free of apparent cycles of a 45-Hz alias – but it also loses all the actual frequency information about the waveform.

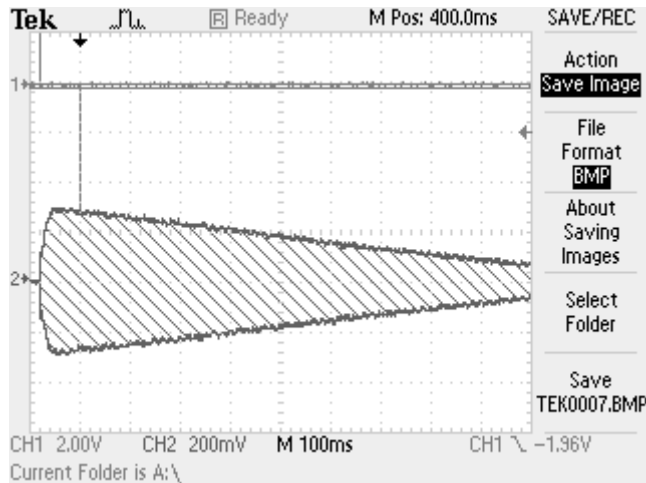


Fig. A6.6: Data obtained in the peak-detect mode. Upper trace, the same trigger events; lower trace, the same pre-amplifier output.

Appendix A7: Aliasing in Fourier Transforms and Best Fits

Modern digital ‘scopes can not only acquire and store a time-domain record of a voltage waveform $V(t)$, they can also transform that data, by computation, into a frequency-domain representation $V(f)$. This section describes how aliasing can yield a *fallacious* view of $V(f)$.

As in Appendix A6, we’ll use the vocabulary of EF-NMR signals, of rather narrow-band frequency content, at a central frequency somewhere between 1.6 and 2.5 kHz. Again, we’ll need to know the actual sampling frequency used by the ‘scope during the actual capture of data. The reason is another consequence of Shannon’s sampling theorem:

**the frequency-domain view of $V(f)$ can only be naively trusted
up to *half* the sampling frequency,
and only if there is no spectral content at higher frequencies than this.**

So if you use a sampling frequency of 10 kSa/s, then any signal in the 0-5 kHz range will show up, in frequency space, at its true and correct location. But if you use a sampling frequency of 500 Sa/s, then only signals in the 0-250 Hz band will show up in the right place in frequency space; all other signal frequencies will *not* be neglected or rendered invisible, they will (much worse) be *aliased* to false, and initially mysterious, locations in frequency.

Another way to say this: the after-the-fact use of the FFT or fast-Fourier-transform mode of a ‘scope will *not* cure a problem built in during data acquisition due to under-sampling.

A ‘scope user will typically lack direct control of the sampling rate, so here’s a smart strategy:

- 0) Learn the ‘memory depth’ of your ‘scope, and learn how a direct choice of sweep speed will *indirectly* enforce a value of sampling rate.
- 1) For a first view of EF-NMR precession frequencies, use a fast enough sweep speed (ie. acquire data for a *short* enough duration in time) that the sampling rate is at least 5.0 kSa/s.

Example: If your memory depth is $N = 2500$, these storage location will be filled in just 0.5 s of time, at this sampling rate ($5.0 \text{ kSa/s} \times 0.5 \text{ s} = 2.5 \text{ kSa} = 2500 \text{ samples}$). So you need a sweep rate of 50 ms/div, for ten divisions to cover only 500 ms of time. (The transient you’d like to record might last well beyond 500 ms, but you have to give up on recording that data.)

- 2) Then an FFT of the captured data will put each frequency component of the input waveform, in the 0-2.5 kHz band, into its proper place in the FFT’s depiction of the frequency-domain content of the data.
- 3) If you want a longer time record, you’ll get better time coverage of a transient, and better frequency resolution in your FFT spectrum. But you might also get aliasing!

Example: If you slow down from 50 ms/div in the previous example to 100 ms/div, you’ll capture 1.0 s of data in ten divisions. But your sampling rate will be down to 2500 Sa/1.0 s = 2.5 kSa/s. In this case, only frequencies in the 0-1250 kHz range will appear at the right place in frequency space. Frequencies in the band 1250-2500 Hz, *including all the EF-NMR frequencies you seek*, will show up in very strange places: A true frequency of 1251 Hz will appear at 1249 Hz; a true frequency of 1260 Hz will appear at 1240 Hz; a true frequency of 1300 Hz will appear at 1200 Hz; and so on.

You should confirm that this actually happens, using a continuous-wave sine-wave input from a signal generator to send to your ‘scope. As you dial up the generator frequency from zero, the frequency indicated by FFT on the ‘scope will at first rise, all the way up to half the sampling frequency, and then *fall*, all the way down to zero indicated frequency(!). Further increases of the generator frequency will then again cause rises in the indicated frequency, but still not at the correct location in frequency space.

Here’s a graph of indicated-by-FFT frequency as a function of true frequency, under the assumption of a 2.5 kSa/s sampling rate.

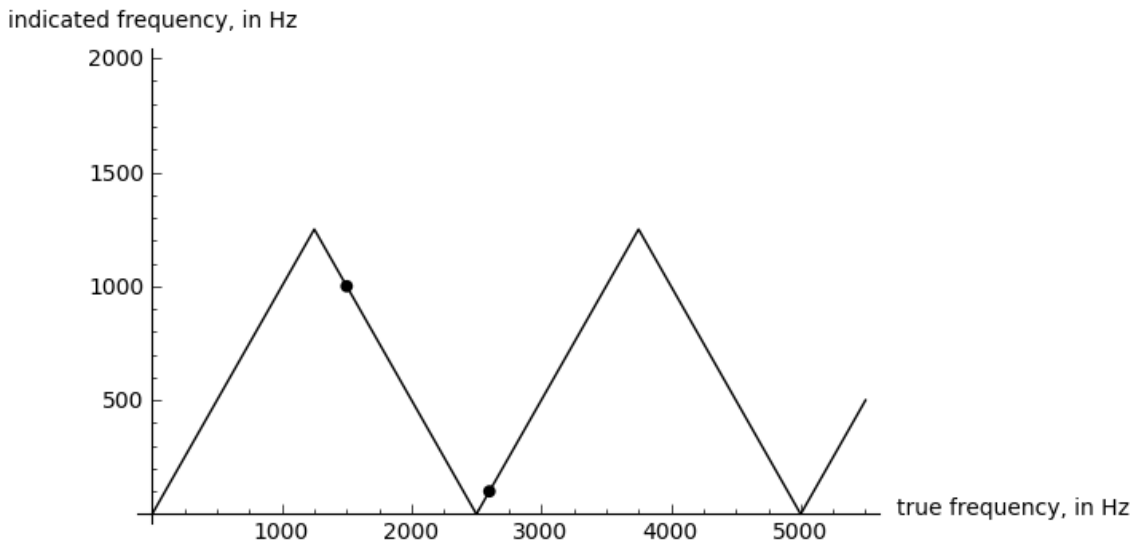


Fig. A7.1: Plotting the consequences of aliasing, in the case of a sampling rate of 2500 Samples/second. Only the true-frequency range of 0-1250 Hz is mapped correctly to apparent frequency; all other true frequencies are mapped to *differing* apparent frequencies.

The dots show a true frequency of 1500 Hz appearing at 1000 Hz, and a true frequency of 2600 Hz appearing at 100 Hz. The details of the diagram above apply only to a 2.5 kSa/s sampling rate, but the character of it can be extended to any sampling rate. In particular, the first ‘turn-around’ occurs at *half the sampling frequency*.

- 4) *If you know, on the basis of previous un-aliased and properly-sampled data, the actual frequency of a (narrow-band) waveform, and you’re willing to live a little dangerously, then you can dare to use under-sampling.*

Example: if a true frequency is 2088 Hz, and you sample at 500 Sa/s, then only frequencies in the 0-250 Hz band will be represented correctly. A version of the diagram above shows that frequencies in the range 250-500 Hz get mapped (backwards!) into the 250-0 Hz range. But continuing, you’ll see that frequencies in the 2000-2250 Hz range get mapped (frontwards) into the 0-250 Hz band. So if you were to *see* 88-Hz content in the FFT depiction of the spectrum, and *if* you knew (by previous measurement, under conditions of higher sampling rate but shorter duration) that the true frequency was near 2100 Hz, then you could dare to infer that the true frequency was 2088 Hz.

Notice that a true frequency of 1912 Hz will *also* alias to 88 Hz under these conditions. So your earlier, lower-resolution measurement has to be good enough to *exclude* a possible frequency value near 1900 Hz.

- 5) Similarly for least-squares fitting of under-sampled data. Appendix A6 on Aliasing shows that, for sampling at 500 Sa/s, a true waveform at 2088 Hz, and an aliased waveform at 88 Hz, pass through the same set of data points (and so would an aliased waveform at 1912 Hz!). Thus if all you have is the list of sampled data points, you can achieve a perfectly good fit to the data using 88 Hz, 1912 Hz, 2088 Hz (and a list of other frequencies). Again, you need prior knowledge, obtained from a different data set, to exclude the good fits to the aliased frequencies, and to give you confidence in the just-as-good fit to the true frequency.

Appendix A8: Field modulation and its effects

Users of the Earth's-Field apparatus ought to be well aware of the effects of magnetic field gradients. Undesired gradients can reduce the free-precession time of a polarized sample; alternatively, deliberate gradients can be used for spatial encoding, as in magnetic resonance imaging. But here we'll introduce another kind of field disturbance which has counter-intuitive effects on free precession.

Magnetic field gradients are fields that are inhomogeneous in space, but constant in time. By contrast, we now take up fields that are uniform in space, but *varying in time*. The usual culprit is 60- (or 50-)Hz modulation of the field B_z , due to magnetic fields generated by alternating currents in a building's power wires. (Time-varying fields in the x - or y -direction have only a second-order effect on the field's magnitude, or on the precession rate.) For simplicity, we'll consider sinusoidal modulation. In this case, the field's magnitude can be written as

$$B(t) = B_0 + B_1 \cos(\omega t) .$$

Here B_0 is the static value of the average local field, and B_1 is the amplitude of the (inadvertent or deliberate) sinusoidal modulation lying atop that field. For the typical perturbations, the angular frequency ω is given by 2π times the local value of the a.c. line frequency, and so is typically 377 (or 314) rad/s. Now to be concrete, imagine that the steady field is given by $B_0 = 54.32 \mu\text{T}$, and the oscillating field amplitude is $B_1 = 0.1 \mu\text{T}$. The result is that in each time interval of 16.67 (or 20.00) ms, the total field makes an excursion between extreme values of 54.22 and 54.42 μT . The question is, what does that do to the FID (free-induction-decay) signal?

One intuitive answer comes from thinking in the frequency domain, and from understanding the gyromagnetic ratio ($\gamma_p \approx 267.5 \text{ rad/s per } \mu\text{T}$ for protons) as the factor which maps magnetic field to precession frequency. So we expect a precession rate Ω which varies in angular frequency between the extremes

$$(54.22 \text{ to } 54.42 \mu\text{T})(267.5 \text{ rad s}^{-1}/\mu\text{T}) = (14,504 \text{ to } 14,557) \text{ rad/s}$$

In more familiar experimental units, the instantaneous precession frequency varies between the extremes (2308 to 2317) Hz. Now consider the timescales involved – we have protons precessing, through one full circle in less than 0.5 ms; we have the net field varying, over a cycle lasting 16.7 (or 20.0) ms; and we have a free-induction-decay process, lasting several hundred milliseconds (ie. many cycles of the modulation). The question is, what will the frequency spectrum of the FID signal look like?

In the absence of the modulating field B_1 , the answer is simple – pure free precession at 2312 Hz, and a Fourier spectrum which is a peak centered at 2312 Hz, with a width of order 1 Hz due to the finite duration of the decaying FID signal. In the *presence* of the modulating field, one might suspect this narrow line spectrum would be broadened, so as to spread out over the 2308- to 2317-Hz region. But that intuition is *incorrect*!

We'll now show that the actual spectrum still includes the original 2312-Hz line, but ***unbroadened***, and that the effects of the field modulation are confined to *sidebands*, located at (multiples of) 60 (or 50) Hz to either side of the narrow spectral peak (at 2312 Hz in our

example). This is an illustration of a frequency-modulation effect, and it has applications far beyond earth's-field NMR.

Theory of the frequency-modulation effect

Frequency modulation is a topic covered in many contexts, but it is particularly simple to understand in the case of EF-NMR, because the experienced user can so easily visualize a sample's magnetic moment precessing in the x - y plane. We will adopt a precession angle of radian measure ϕ in that plane, where ϕ starts at value zero when the sample is initially polarized along the $+x$ -axis. Then we will assume that the instantaneous rate of precession, $d\phi/dt$, is proportional to the instantaneous value of the field, $B(t)$. (That result can be derived, without approximation, from the Bloch equations in the limit of long relaxation times.) Then we have

$$\frac{d\phi}{dt} = \gamma B(t) = \gamma [B_0 + B_1 \cos(\omega t)] .$$

Integrating this with respect to time gives the total precession angle accumulated up to time t ,

$$\phi(t) = \gamma B_0 t + \frac{\gamma B_1}{\omega} \sin(\omega t) .$$

Then the x -component of magnetization, the component lying along the axis of the pick-up coil, is given by

$$M_x(t) = M_0 \cos \phi(t) = M_0 \cos[\gamma B_0 t + \frac{\gamma B_1}{\omega} \sin(\omega t)]$$

where M_0 is an assumed initial value of the magnetization. It's the time derivative of this magnetization function which gives the emf generated in the coil. (This model has not included spin-spin relaxation, which causes a slow exponential decay with time-constant T_2 .)

Now in the absence of the modulating field B_1 , this gives the time dependence $M_0 \cos(\gamma B_0 t)$, a pure sinusoid, whose Fourier spectrum is a single peak at (angular) frequency γB_0 ; that's the ordinary FID signal. The question is, what is the spectrum when B_1 is present? The answer depends on the 'modulation index' $\beta \equiv (\gamma B_1 / \omega)$, and it takes on a simple form only in the $\beta \ll 1$ limiting case of weak modulation. In that case, we have by an angle-addition formula

$$\begin{aligned} M_x(t) &= M_0 \cos[\gamma B_0 t + \beta \sin(\omega t)] \\ &= M_0 [\cos(\gamma B_0 t) \cos(\beta \sin \omega t) - \sin(\gamma B_0 t) \sin(\beta \sin \omega t)] . \end{aligned}$$

But since in our limiting case the argument $\beta \sin(\omega t)$ stays $\ll 1$ at any and all times, we can use the approximations $\cos(\theta) \approx 1$, $\sin(\theta) \approx \theta$ to get

$$\begin{aligned} M_x(t) &\approx M_0 [\cos(\gamma B_0 t) \cdot 1 - \sin(\gamma B_0 t) \cdot \beta \sin \omega t] \\ &= M_0 \cos(\gamma B_0 t) - M_0 \left(\frac{\beta}{2}\right) [\cos(\gamma B_0 - \omega)t - \cos(\gamma B_0 + \omega)t] , \end{aligned}$$

which reveals that the magnetization oscillates as a superposition of *three* frequencies. The first is the usual precession (angular) frequency, γB_0 . The other two terms have amplitudes smaller than the first term by the factor ($\beta/2$), and they occur at two new and distinctive frequencies: they are two 'sidebands', displaced in frequency from the 'carrier frequency' to new angular frequencies $(\gamma B_0 - \omega)$ and $(\gamma B_0 + \omega)$.

So the first-order effect of the modulation in the field is *not* to broaden, or to shift, the central frequency γB_0 , at all. It is, instead, to create (relatively weak) sidebands displaced by $\pm\omega$ in angular frequency, which means displaced by ± 60 (or 50) Hz in ordinary frequency. So in our example with $B_1 = 0.1 \mu\text{T}$, in which case the instantaneous frequency seemed to vary by ± 8 Hz relative to the average frequency of 2312 Hz, the actual Fourier spectrum of the FID waveform shows *not* a broadening, nor a shift, by 8 or by 16 Hz, but instead, the appearance of sidebands at frequencies (2312 ± 60) Hz. The strength of B_1 does indeed control the *amplitude* of these sidebands, but the *location* of the sidebands in frequency space is set by the *frequency*, not by the amplitude, of the modulating field.

Now we'll see that the modulating field can easily be made large enough that the modulation index, $\beta = (\gamma B_1 / \omega)$, can be made to equal or exceed 1. In this case, it is profitable to use a beautiful expansion in Bessel functions, given by

$$\exp[i(\Omega t + \beta \sin \omega t)] = \sum_{n=-\infty}^{\infty} J_n(\beta) \exp[i(\Omega + n\omega)t] .$$

Here we have a modulating frequency ω , with a modulation index β , affecting a 'carrier' of frequency Ω , to create a sum of terms with frequencies $\Omega + n\omega$, where n runs over all the integers (negative, positive, and zero). In the limit of small β , we have the $n=0$ term with $J_0(\beta) \approx 1$ giving an un-affected carrier, while the $n=\pm 1$ terms, which have $J_1(\beta) \approx \beta/2$, $J_{-1}(\beta) \approx -\beta/2$, reproduce the calculation above for the strength of the order-(± 1) sidebands. But the value of this expression is that its real part,

$$\cos[\Omega t + \beta \sin \omega t] = \sum_{n=-\infty}^{\infty} J_n(\beta) \cos(\Omega + n\omega)t ,$$

has exactly the form needed to describe the function $M_x(t)$ above. So now we see that the magnetization oscillates at many frequencies, but all of them described by the form $(\gamma B_0 \pm n\omega)$, which are sidebands displaced, by integer multiples of ω , from the original or central frequency γB_0 . The relative strength of any sideband is given by $J_n(\beta)$, which varies with sideband order n and with modulating-field strength B_1 through the parameter $\beta = (\gamma B_1 / \omega)$.

The strength of the component at the central or carrier frequency is given by $J_0(\beta)$, and in the limit $\beta \ll 1$, this is the main term in the sum. But J_0 is an oscillating function of its argument, and as β increases to and beyond 1, the J_0 -function drops below 1, and in fact reaches a first *zero* when its argument reaches $\beta \approx 2.4048$. So this tells us that there is a strength of modulating field B_1 where the modulation index first reaches this magic value, at which point the magnetization $M_x(t)$ (and hence also the FID signal) is 'all sidebands', with *no* spectral power left in the original carrier. This requires

$$\frac{\gamma B_1}{\omega} \approx 2.4048 , \quad \text{or} \quad B_1 \approx 2.4048 \frac{\omega}{\gamma} ,$$

which we will see is an easily attained condition on the strength of (say) a modulating field at frequency 60 Hz.

It is quite striking to make a time-domain plot of such a frequency-modulated function of this modulation index, to see how the time-domain waveform seems little affected, but the frequency-domain view shows so drastic a change in the spectrum.

Experiments in frequency modulation

To investigate frequency-modulation effects, all that is needed is a way to get reasonably long-lasting free-induction-decay signals from the EF-NMR apparatus. That will typically involve a water sample, a polarization time of about 5 s and maximal 3-A polarizing current, and free precession in an ambient field that has been corrected for spatial gradients. The result should be an FID signal with a ‘half-life’ of better than 500 ms. Finally, it is very important to have access to real-time or subsequent Fourier transformation of the FID waveform, since the effects of modulation are best seen in the frequency domain. For reasons laid out in Appendix A6, it is important to acquire the FID signal with a sampling rate of at least 5000 Samples/second, and it is ideal if acquisition can last at least 1 second. This will give Fourier transforms with a 1-Hz spectral resolution. (Most features of the phenomena can be seen with a shorter acquisition time, but it is crucial to keep the sampling rate at 5 kSa/s or higher to avoid aliasing.)

It is important to distinguish frequency-modulation effects from another sort of signal easily seen in the frequency domain. It is perhaps best for investigators first to acquire a ‘dummy FID’, with everything identical to real experiments, except for the absence of a sample in the apparatus. The FID signal might contain a bit of the coil transient (depending on what trigger is used to start the data acquisition), but will consist mostly the external interference picked up by the sample coil. The Fourier spectrum of that interference will show three features in the frequency domain:

- an underlying noise floor, given by Johnson noise;
- a ‘peaking’ above that floor, to create a bulge or peak around the sample-coil’s LC-tuning frequency;
- and also a line spectrum, showing lines at integer multiples of 60 (or 50) Hz, due to changes in magnetic flux, periodic in time with the line frequency, with harmonic content that extends well into the kHz regime. (It is often the case that odd harmonics are stronger than even harmonics.) This is a multiple-line spectrum; in our example, with an NMR precession frequency near 2312 Hz, and the coil therefore tuned to this frequency, the most prominent spectral peaks will be 2280 Hz and 2340 Hz, with other integer multiples not as prominent.

It’s important to take notice of these ‘interference lines’, because the ‘sideband lines’ that will be produced by frequency modulation are *distinct* from them. We will see sidebands at spacings of (say) 60 Hz, but they are spaced 60 Hz from the main FID peak. So the nearest sidebands we expect should be located at $2312 \text{ Hz} \pm 60 \text{ Hz}$, so at 2252 and 2372 Hz, which are *not* at integer multiples of 60 Hz.

So, with a ‘dummy run’ to show the spectrum of the interference, and a ‘sample run’ to get the best possible FID spectrum, it is now possible to look for sidebands, 60 Hz to either side of the main FID peak, as evidence of line-frequency modulation in the ambient field. It is not possible to predict how much line-frequency modulation will be present, as that depends on the details of the electrical wiring in the vicinity of the apparatus. So here’s a way to create *deliberate* modulation effects instead.

The idea is to inject a sinusoidal, a.c. current waveform into the Helmholtz coils. These coils map current to field with a coil constant of about $90 \mu\text{T/A}$, and because of their construction, that mapping ought also to apply for a.c. currents. Thus a sinusoidal current of amplitude just 1.1

mA ought to give a sinusoidal field modulation of amplitude $(0.0011 \text{ A})(90 \mu\text{T}/\text{A}) = 0.10 \mu\text{T}$. But the frequency of this modulation can be deliberately set to 60, or 50, or 37 or 57 Hz, whatever the experimenter wishes to use.

Quantitative control of the current amplitude is not difficult. The Helmholtz coils present a d.c. resistance of order 10Ω , and an inductive reactance (near 60 Hz) of order 1Ω , so if they are driven by a signal generator of output impedance 50Ω , the current achieved will be approximately given by (generator amplitude)/ 60Ω . A more precise result can be measured using a multimeter in series to measure the a.c. current (note that this will give an rms measure!), or by adding a series resistor of 1- or 10Ω value, and an oscilloscope to measure the amplitude of the voltage-drop resulting.

[If you want or need to retain the use of some d.c. current in the Helmholtz coils, then you should connect the Helmholtz coils, their power supply, and the secondary winding of a suitable transformer, all in series. Now you can drive the primary of that transformer with your a.c. generator. In this case, a multimeter in series with the coils will display the time-average of the d.c. current (if used in its d.c. mode), and it is not as easy to measure the size of the a.c. current.]

So now the amplitude, and the frequency, of the a.c. field component B_1 are independent variables. The goal of these investigations is to look for sidebands, on either side of the FID frequency, with locations that match expectations, and amplitudes that are directly visible in the frequency-domain view of the spectrum of the FID.

Look first at modest amplitudes of the modulation, for which the ± 1 -sidebands ought to be small, and all others invisible. For example, for $B_1 = 0.1 \mu\text{T}$ (at 60-Hz frequency) as computed above, the sidebands of order ± 1 are predicted to have amplitude 0.071 relative to the carrier, so they should contain power 0.0050 relative to the carrier. That would be

$$20 \log_{10}(0.071) = 10 \log_{10}(0.0050) = -23 \text{ dB}$$

below the carrier in the usual decibel display of typical FFT presentations. In principle, viewing these sidebands, and measuring their intensity relative to the carrier, can be used to give a quantitative indication of the strength of the a.c. component of the magnetic field.

In practice, the sidebands will appear at a level *lower* than in the example above, since the LC-tuning of the coil is resonant for the carrier, but off-resonant for the sidebands. Recall that the Q of the LC-system is about 70, so its FWHM is about 30 Hz, so sidebands even 15 Hz from the carrier would be seen at half-power, 3 dB down. So sidebands 60 Hz away from the carrier will be even more suppressed by the coil's LC-resonance. (If you are viewing the signal at the band-pass amplifier output, there is yet more suppression of the sidebands, since the band-pass function has a width of about 100 Hz. So sidebands beyond ± 50 Hz begin to be suppressed relative to the carrier.)

Rather than model this effect quantitatively, there are other things to experience qualitatively. One of them is to raise the amplitude of the modulation until the sidebands of order ± 2 or ± 3 come into view. Even more dramatic is the prediction that, as spectral power is shifted into the sidebands, the power in the carrier diminishes. The prediction of the theory above is that when

the ‘modulation index’ reaches 2.4048, the power in the carrier has been reduced to *zero*, and the main spectral peak in the FID ought to disappear entirely.

For 60-Hz modulation, the prediction above is that this first occurs when

$$\frac{\gamma B_1}{\omega} = 2.4048, \text{ whence } B_1 = 2.4048 \frac{\omega}{\gamma} \approx \\ \approx 2.4048 (377 \text{ rad/s}) / (267.5 \text{ rad s}^{-1}/\mu\text{T}) = 3.39 \mu\text{T},$$

and a field of this amplitude can be produced by sending through the Helmholtz coil an easily-produced 60-Hz current of amplitude near 38 mA. Though the main carrier peak in the spectrum is predicted to *vanish* at this magic amplitude, the FID in the *time domain* is certainly not invisible. So this combination of time- and frequency-domain views is an instructive exercise in Fourier methods and frequency modulation.

Other implications

This exercise in frequency modulation may have given you some intuition that is *transferable* into other areas of physics. Consider transferring your new-formed intuition into the spectroscopic interrogation of moving sources. We might think of an excited atom (or nucleus) which emits radiation upon decaying to a lower-energy state. The expected frequency of emission is

$$f = (E_2 - E_1)/h,$$

but if the source is in motion relative to the detector, the observed frequency of the radiation will be Doppler-shifted from this value. For emission from a gas of atoms in thermal motion, this gives the usual ‘Doppler broadening’ of the emission, replacing a delta-function spectral line with a (continuous) Gaussian distribution of frequencies.

But sources that are *captive*, such as atoms or ions in a trap, or nuclei in atoms in a crystal lattice, are in a different kind of motion. In fact their motion is *periodic in time*, and this means the Doppler effect has different consequences. If the duration of the emission (ie. the lifetime of the higher-energy state) is long compared to period of that periodic-in-time motion, then we are in the same limiting case as above in EF-NMR. In particular, the emission will be frequency-modulated, as the instantaneously-received frequency varies above and below the expected frequency due to the Doppler effect.

But the spectrum of the received radiation does *not* consist of a broadened or Gaussian spectrum; rather, it forms a multi-line spectrum, with a central or carrier frequency, and sidebands displaced by integer multiples of the modulation frequency. That sideband spacing would be equal to a trap oscillation frequency, or a lattice vibration frequency, in the cases considered above. What is exciting is that (for low enough modulation index) most of the spectral power stays in an *unshifted*, and *unbroadened*, central frequency.

One example of this is provided by the Mössbauer effect, most easily seen in the emission of 14.4-MeV gamma rays from an excited state in the Fe⁵⁷ nucleus. Such a gamma-ray has a frequency near 3.5×10^{21} Hz. For an atom in a solid, the kinetic energy of vibration is expected to give

$$\frac{1}{2}mv^2 = \frac{1}{2}k_B T ,$$

which can be used to show that typical speeds of vibrational motion have speeds v with $v/c \approx 0.7 \times 10^{-6}$. Intuitively, we might think this would give fractional frequency shifts of parts-per-million in the observed gamma-ray frequencies, creating a spectral spread with width of order $(1.4 \text{ ppm})(3.5 \times 10^{21} \text{ Hz}) \approx 5 \times 10^{15} \text{ Hz}$ around the central frequency. But in fact, the effects of vibration leave most of the spectral power in an unshifted, and unbroadened, spectral line, with a fractional linewidth which is of order parts-in- 10^{12} , or *a million-fold smaller* than the parts-per-million naively expected. This permits the spectacular spectral resolution for which the Mössbauer effect is famous.

There do exist residual effects of the lattice vibrations, since they cause some of the spectral power to appear in sidebands, displaced by vibrational frequencies of the lattice. Since such frequencies are in the THz or 10^{12} -Hz regime, the actual emission spectrum in the Mössbauer effect will contain spectral features away from the carrier. But the usual resonance-absorption method of detection is *blind* to these sidebands, and yet fully sensitive to the recoil-free, and thus unbroadened, central or carrier frequency. And that emission line has exactly the frequency which would be expected for a nucleus held exactly at rest – even though all the actual nuclei involved are vibrating vigorously. So despite vibrational motions of characteristic speeds of order 200 m/s, the Doppler shifts due to macroscopic motion of an entire lattice, at speeds of only *millimeters per second*, are readily observed.

Appendix A9: Monitoring the Polarizing Coil

This appendix is devoted to some *back-panel* capabilities of the EF-NMR Controller, in monitoring the coil current and potential difference during, and just after, the polarizing interval. The information given here is *not* needed in normal operation, but it is of interest in case of trouble-shooting, verification, or certain theoretical studies of the polarization process.

We can draw a sort of ‘timing diagram’, which lays out the sequence of events associated with the polarization process. This sequence occurs for a thumbwheel-set duration *in advance of* any of the free-precession signals normally observed. Your mental model of this process has been a quiescent coil, in which a polarizing current I_p (perhaps 3.0 Amperes) is turned on, and then turned off (say) 4.0 seconds later. But in fact the current cannot be turned on (or turned off) instantaneously, and there is some interesting physics associated with the beginning and the end of polarizing process.

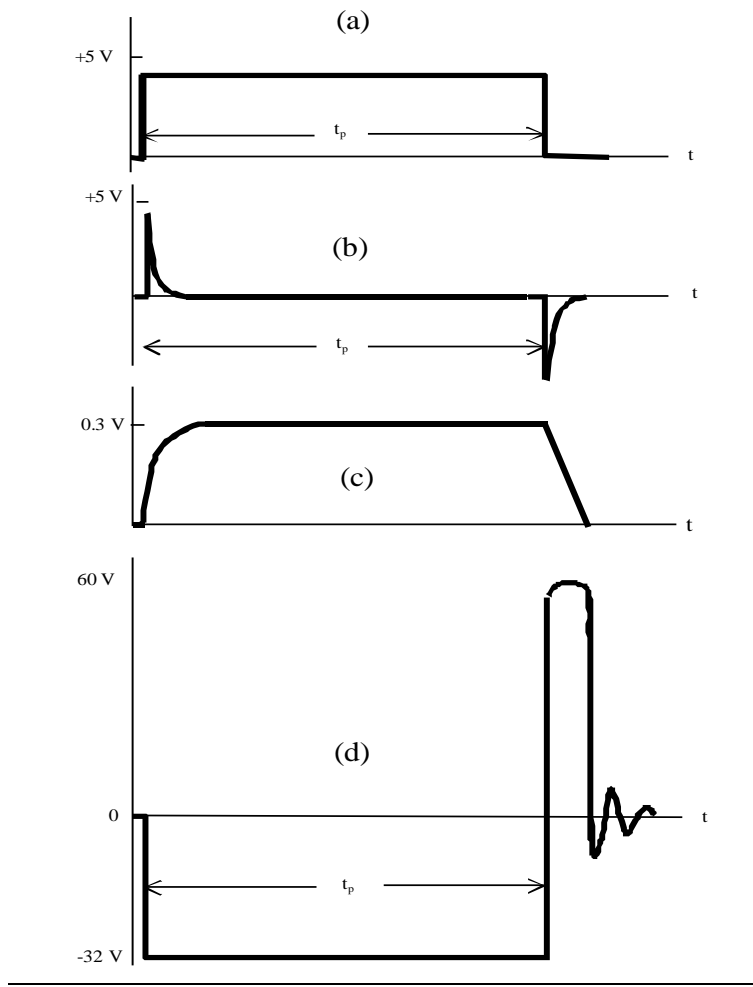


Fig. A9.1: (not to scale) A timing diagram of several waveforms associated with the current in the sample coil, during the polarizing interval. a) An internal TTL waveform, at logic-HIGH during the polarization time. b) The back-panel trigger-output waveform. c) The back-panel coil current monitor voltage output, shown inverted. d) The back-panel coil voltage monitor test-point signal.

The a) line in the diagram shows an *internal* TTL waveform, which is at the logic-HIGH level for the full duration of the polarizing time. The waveform's rising edge is initiated by the START button, and it falls back to logic-LOW at the end of the preset polarization time. The b) line below that shows a waveform that *is* visible to the user, at the OSCILLOSCOPE TRIGGER OUTPUT connector on the Controller's *back* panel. It is a differentiated version of that TTL waveform, and it shows a fast positive pulse at the start, and a fast negative pulse at the end, of the polarizing interval. These pulses, just milliseconds in duration, occur with (say) 4.0 seconds of separation in time, and they are provided as a convenience to the user, to trigger a 'scope and thereby permit a close-up view of short-duration phenomena around either the start or the end of the polarizing interval.

Also on the back panel is a COIL CURRENT MONITOR BNC output, which gives access to the voltage drop across an $r = 0.10\text{-}\Omega$ resistor, through which the coil current I_p is flowing. When the coil current is flowing, the potential (relative to ground) at this point is negative, and given by $V = -I_p r$. We instead plot, in line c) of Fig. A9.1, what a 'scope's 'invert' function would display, the voltage $V = +I_p r$.

In the time just after the start of the polarizing interval, this monitor of the coil current shows a current rising toward an asymptotic value, with an L/R time constant of about 6 ms. Once that asymptotic value is reached, the coil-current monitor voltage will display the value $V = -I_p r$, which is -0.3 V for a coil current of 3.0 A. Finally, in the time just after the *end* of the polarizing interval, this monitor of the coil current shows a current falling, *linearly*, toward a zero value.

The reason for that linear decrease is that the current in the coil cannot be changed to zero instantaneously (as would be optimal for NMR purposes), and it is not changed toward zero by connecting the coil to a resistor (which would give an exponential decay). Rather, the coil's stored energy is 'discharged' by connecting the coil to a Zener diode, such that the emf arising during the current's change is held at the reverse-breakdown voltage (about 60 Volts) of the Zener. In fact the coil current $I_p(t)$ obeys

$$-L \frac{di}{dt} = +60 \text{ V}$$

during the 'discharge' process, which accounts for a linear-in-time decrease in the current.

In addition to this COIL CURRENT MONITOR, there is also on the back panel a COIL VOLTAGE MONITOR testpoint. (This is the point marked with a WARNING, because of the rather large voltages that can appear here.) We plot (again, not to scale), in line d) of Fig. A9.1, the expected waveform visible at this test point. The voltage during the bulk of the polarizing time is negative, and is the voltage drop across the coil, given by the product of the current used and the coil's resistance. (The sign is negative because the external polarizing power supply is used with its positive terminal grounded inside the Controller.) Because the coil's resistance increases with time as it warms up, this is not the best way to measure that coil current.

The most interesting part of this monitor of the coil voltage is the waveform at the end of the polarizing time. During the time while the coil current is dropping (from a few Amperes to a few milliAmperes) the Zener is conducting at a nearly-fixed potential difference, and the current therefore drops linearly, taking about 4 ms to get quite small. During the whole of that linear discharge, the COIL VOLTAGE MONITOR testpoint shows a potential of about +60 V (best

observed using a ‘scope’s 10 \times probe). Once the current gets small enough, the Zener diode can no longer remain conducting, and it reverts to a high-impedance state. But it is still a requirement of the NMR polarization process that the current drop quickly, and smoothly, the rest of the way to zero, and this last stage of ‘discharge’ occurs through a 5.6-k Ω resistor that’s put in parallel with the coil. The combination of this resistance with the coil’s inductance, and stray capacitance, gives a damped oscillatory decay of the remaining current, and this oscillatory signal is also visible at the COIL VOLTAGE MONITOR test-point.

For the resistor supplied, these decaying oscillations should be slightly underdamped, and it should not be necessary for users to change this. But the damping can be increased, if desired, by connecting another resistor between the EXTERNAL DAMPING RESISTOR banana-plug sockets on the rear panel. The block diagram of Fig. 5.8 shows that this R_{ext} is put in series with an internal 0.47-k Ω resistor, and then that series combination is put in parallel with the internal 5.6-k Ω damping resistor. This makes it possible to change the damping from below-critical, to critical, or to over-critical damping.

If you choose to try this, note that potential differences as large as 60 Volts can occur across this resistor during the ‘discharge’, and that powers as large as 1 Watt can be dissipated by this resistor for the duration of the polarizing interval.

It is quite interesting that the magnitude of the magnetic polarization of the sample depends on the fine details of the way in which the coil current drops through the last few milli-Amperes on its way to zero. The reason has to do with nuclear spins. Let’s suppose that the polarizing time has been very long, several multiples of the nuclear T_1 time, so that the sample has become maximally polarized along the x -direction. The field (at a current of 3 A) is about 50 mT, so the Larmor frequency of the protons is high – about 2 MHz. Notice that during this time, the earth’s field, in the z -direction and of size about 50 μ T, is wholly negligible. But when the coil current has dropped from 3 A to 3 mA, the coil’s field is down from 50 mT to 50 μ T, so it does not any longer dominate over the earth’s field.

So if the coil current were to be reduced the rest of the way to zero *slowly*, the net field, which is in the x -direction during the polarizing process, would slowly and smoothly rotate from the x -direction toward the z -direction, settling along the z -axis once the coil current reached zero. But if the protons’ spins were to follow that changing direction (and they *would* do so, for slow enough changes in the field strength), then the proton spins would end up all pointing along the z -direction. The sample might still be magnetized, but its magnetization would have no x -component to precess around the z -directed field and generate an emf in the coil.

The art of the linear, and then the underdamped-oscillatory decay, is to leave the sample with the greatest possible magnetization in the xy -plane. The calculation is not simple, as can be seen from the fact that the Larmor precession time in the late stages of the process is about 0.5 ms, but the timescale for the current ramping down to zero is several milliseconds. The details of the process, and its optimization, are found in two articles by Melton and Pollak:

1. B. F. Melton and V. L. Pollak, “Optimizing Sudden Passage in the Earth’s-Field NMR Technique”, Journal of Magnetic Resonance, **A122**, 42-49 (1996)

2. B. F. Melton and V. L. Pollak, "Condition for Adiabatic Passage in the Earth's-Field NMR Technique", Journal of Magnetic Resonance, **158**, 15-22 (2002)

Appendix A10: The Amplitude Detector and Signal Averaging

The (main) Controller for the EF-NMR head has, in addition to the band-pass amplifier output, another output marked as NMR AMPLITUDE DETECTOR. This section explains the motivation for, and the use of, this output.

The band-pass amplifier output will display, in ordinary operation, a free-induction-decay signal, typically an oscillating waveform of frequency 1.5 to 2.6 kHz, and an amplitude a few Volts, decaying within about a second. This is the waveform, appearing at the NMR SIGNAL OUTPUT, which is also sent to the speaker for live audio output. This output is a detailed view of the actual precession of nuclei in the apparatus. But there are occasions on which it is worth giving up this cycle-by-cycle view, in favor of viewing only the ‘envelope’ of the waveform.

The way this is done in the Controller is to make a full-wave-rectified version of the bandpass-amp’s output, and then average that result over a timescale of about five milliseconds. Such a rectify-and-time-average operation applied to a uniform sinusoid yields a d.c. level equal to $(2/\pi)$ times the amplitude of the sinusoid. So applied to the decaying sinusoidal free-precession waveform, this output will display a value which is about 2/3 the height of all the peaks of the sinusoid, and sharing the shape of those peaks’ time development.

The best way to understand this waveform is to acquire an FID transient on a two-channel ‘scope, with triggering from the Trigger output, while using ch.1 to view the SIGNAL output (from the band-pass amplifier), and ch.2 to view the AMPLITUDE output. If you deliberately change the field gradients, so that the time development of the FID changes, you will also see those changes reflected in the AMPLITUDE output.

Now clearly there is *less* information in the AMPLITUDE output compared to the SIGNAL output – you have lost all the phase information (when does each cycle arrive?) and also the frequency information (how many cycles occur per unit time?). What then is the point of the AMPLITUDE output?

Check against aliasing

If you do not understand aliasing, you can be badly deceived by the SIGNAL output. There is no difficulty if you are viewing only 10 millisecond’s worth of Signal output; that will contain about 20 cycles of sinusoid, and be correctly displayed on any digital ‘scope. But when you slow the time base, so as to view a longer duration of the FID waveform, you will necessarily get more cycles of SIGNAL on the screen. Eventually the finite number of sampling points at which the ‘scope reads the waveform will ‘undersample’ the many cycles of the actual SIGNAL waveform, with consequences that can lead to grossly deceptive presentations.

The AMPLITUDE output is free from this difficulty. Its typical appearance is a rapid rise to a few-Volt, positive, value at the start of an FID, followed by a slow decay over the next several tenths of a second. There are no rapid cyclic variations to be undersampled, and you will always get a true view of its time development. The two-channel view of AMPLITUDE and SIGNAL outputs

will enable you to understand when the SIGNAL output is giving you a faithful view, and when it is deceiving you because of aliasing.

Signal Averaging

Each FID transient gives you a one-time view of a single case of free precession, and each such transient is subject to its own version of electronic noise and interference. The idea of signal averaging is to acquire several copies of the FID and average them together, allowing the true signal to reinforce, while the particular noise of each run averages toward zero, combined as it will be with the unrelated noise other runs.

For signal averaging to work, you need to acquire multiple FIDs; each will be initiated by Manual (or External) START, and each will provide a TRIGGER OUT pulse so as to synchronize the ‘scope to the time marking the start of the FID waveform. Such FID waveforms will be acquired about 10 seconds apart in time, since the polarizing and the waiting intervals will intervene between successive episodes of precession. But averaging the bandpass-amplifier’s SIGNAL output on such recurring waveforms will certainly fail to give the desired results. The reason is that ‘coherent addition’ of multiple waveforms around 2 kHz would require the maxima, and the minima, of time-separated FID transients to line up in time, to a precision of well under the duration of half a cycle.

But if you acquire a transient lasting (say) one full second, that will contain about 2000 full cycles of precession, so to get successive such transients to line up to half a cycle’s precision requires extreme reproducibility of successive acquisitions. The problem is not with the electronics, but with the physics: if the ambient magnetic field were to change by one part in 4000 during the 10 or so seconds that separate the acquisition of two successive transients, this would spoil the co-addition of the (late) cycles of the FID waveforms. Inside most buildings, the field is not sufficiently stable in time to ensure this matching of cycles.

So if signal-averaging of the SIGNAL output won’t work right, this leaves the possibility of averaging multiple copies of the AMPLITUDE output. That *will* work, since this output lacks the detailed timing of individual cycles that are present in the SIGNAL output. If you wish to study the decay rate of an FID, or wish to see its disappearance and then re-appearance in spin-echo studies, then the signal-averaging of multiple runs of the AMPLITUDE output can raise the signal-to-noise ratio. If you invest the time required to acquire N successive FIDs, then the average of them ought to show an improvement by \sqrt{N} in the signal-to-noise ratio in the envelope’s waveform.

Appendix A11: A tuning model for the pick-up coil's LC-circuit

Using the EFNMR Gradient/Field Coil System, you might want to be ‘frequency-agile’, since you’ll be able to change the current in your Helmholtz coils and thereby move your NMR signals around in frequency space. For NMR signals at any one fixed frequency, it’s easy enough to tune the resonance of the sample coil to match the NMR frequency, but for data-taking over a range of frequencies, it’s a good idea to be able to tune the coil systematically rather than by trial and error. This appendix describes how that systematic tuning might be achieved.

For purposes of tuning, the sample coil may be thought of as a fixed inductance L . The emf induced in this coil is magnified by placing a capacitance C_{total} in parallel with L ; here C_{total} is all contained in the controller box, but it’s made up of three parts:

$$C_{\text{total}} = C_{\text{fixed}} + N \cdot 5.0 \text{ nF} + n \cdot 0.50 \text{ nF} ,$$

where C_{fixed} is a fixed capacitance, and where N and n are integers in the range 0-15, corresponding to the settings of the coarse, and the fine, tuning switches. Each clockwise ‘click’ of either switch adds another increment of capacitance to the total, and those increments are (nominally) 5.0 nF and 0.50 nF for the coarse and fine adjustments respectively. Finally, the complete LC -system resonates at (angular) frequency

$$\omega_{\text{res}} = \frac{1}{\sqrt{LC_{\text{total}}}} ,$$

which can be converted to ordinary frequency $f_{\text{res}} = \omega_{\text{res}} / 2\pi$ and rearranged to give

$$\frac{1}{f_{\text{res}}^2} = 4\pi^2 L [C_{\text{fixed}} + (10N + n) \cdot 0.50 \text{ nF}] .$$

This result motivates a plot, in which the settings N and n form an independent variable $10N + n$, and in which the resonant frequencies f_{res} form a dependent variable $1/f_{\text{res}}^2$; the plot is predicted to display a linear variation, from which can be extracted empirical values for L and C_{fixed} . With those values once known, the whole tuning system will be so well modelled that tuning to a desired frequency can be done from the *model* (rather than by trial-and-error tuning).

Here’s a method for determining the resonant frequencies f_{res} ; it can be used *without* the need to generate actual NMR signals. Instead, it uses as a source a signal generator, capable of giving a (steady) sine-wave output in the 1-3 kHz range. It’s best if the generator has a ‘sync’ output, since that can be used to trigger an oscilloscope and also to run a digital frequency meter. The only device that you need to build is a small circular coil, of perhaps 10 turns and 1-cm radius, hand-wound with copper wire. The idea is to tape that coil into place, perhaps onto one of the wooden beams supporting the Helmholtz coils in the EFNMR Field Coil apparatus, in such a position that ac signals in the little coil will couple some flux, and therefore induce some emf, in the sample coil. When you have such a coil in place, send an attenuated sine-wave from the generator to the coil, and use the ‘scope to look at the output of the pre-amp in the EF-NMR controller; the signal generator is going to be producing a (steady-state) surrogate for the signal which would otherwise be generated by precessing nuclear moments.

Once you can detect such a signal at the pre-amp output, set the generator to a fixed frequency of (say) 2000 Hz, and tune up the LC system (ie. vary the coarse- and fine-adjust switch settings) to maximize the output of the preamp. [To simulate the proper *scale* of the signals, adjust the amplitude of the generator output until the pre-amp output is about 200 mV peak-to-peak.] Now

you can record N and n , the settings (in the 0-15 ‘clicks’ range) of the switches which make the LC-circuit resonant at this frequency value.

To take data systematically, it’s easiest to set N and n to fixed values, and then vary the generator frequency f until resonance is achieved; once a resonant value f_{res} is thereby found, you have another datum in the form of a combination of $\{N \& n, f_{\text{res}}\}$ which can contribute to the data set. It is not required that you try all $16^2 = 256$ combinations of N and n , since the model above can fix all the unknowns using only a subset of these possibilities.

Given a suitable data set, you can form independent variable $10N + n$, and dependent variable $1/f_{\text{res}}^2$, and look for a linear dependence. From the coefficients of a best-fit line, you can determine the values of L and C_{fixed} . (You should find values on the order of $L \approx 70 \text{ mH}$ and $C_{\text{fixed}} \approx 50 \text{ nF}$.) That fully determines the model, which can then be turned around to give

$$10N + n = \frac{1}{4\pi^2 L(0.50 \text{ nF})f_{\text{res}}^2} - \frac{C_{\text{fixed}}}{0.50 \text{ nF}} .$$

You might use this expression as follows: suppose that you are back to doing NMR, and you are varying the Helmholtz coil current; and that you are graphing, as you go along, the NMR precession frequency f as a function of this current. Suppose your plot suggests that the next point you want to take is near $f = 1700 \text{ Hz}$; the plot will tell you about what current will be needed, and the equation above, given best-fit values of L and C_{fixed} , and a chosen value of $f = 1700 \text{ Hz}$, will tell you what number is needed for the integer $10N + n$. That will tell you how to set the tuning switches. For example, if the formula tells you that $10N + n$ needs to be 132, you could set $N = 13$ and $n = 2$ (or $N = 12$ and $n = 12$) and you’d have the sample-coil system all set to be resonant near the 1700-Hz signal you expect to get from your next NMR datum.

A model like this can materially speed the process of data-taking, since it avoids the tedious tuning-by-guess that is otherwise required at each new value of Helmholtz-coil current. It also illustrates the important lesson that not only natural phenomena, but also scientific apparatus, can and should be modelled mathematically by the proficient physicist.

Finally, while you have a signal generator in place to excite emf in the sample coil, you might also monitor the output of the main or ‘tuned’ amplifier of the EF-NMR controller, to determine the setting required on its ten-turn tuning knob to get its gain to peak at any particular target frequency. There may not be a simple model relating this setting to the tuned-amplifier passband frequency, but a plot of your data will give you a graphical version of a ‘look-up table’, so that you can set this tuning knob to the proper value for data-taking at some target frequency.

Appendix A12: Comparative Signals for differing isotopes

This Appendix takes up the question of what signal strengths can be expected for the NMR detection of nuclei other than protons. The purpose of this section is to make a comparison between ‘easy’ signals, such as those from free-induction decay signals from protons in water, with ‘harder’ signals, those arising from another nuclear species. In particular, this section is the basis of feasibility predictions for the detection of NMR in other elements.

The calculations that follow are somewhat different than the ‘responsivity’ computed by high-field NMR users for various nuclei. That’s because in high-field NMR, both the initial polarization of the nuclei, and their subsequent precession, occur in one and the same field, a single value B_0 . The calculations we’ll do for EF-NMR are somewhat different:

First of all, the nuclei are polarized in a modest field B_{pol} , the polarizing field, which is provided by (say) a 3-A current in the polarizing coil. This field value might be 50 mT, and we’ll assume it has the *same* value in both cases.

Secondly, the nuclei once polarized will precess in a smaller field B_{prec} . This might be as small as the earth’s field of about 50 μT , but via the use of the Helmholtz coils, it is in fact up to the user what value B_{prec} has.

We’ll do the simplest comparisons of all, assuming that we use the Helmholtz coils such that protons (on the one hand) and other nuclear species X (on the other hand) are tested in paired experiments, with the Helmholtz-coil currents adjusted so that the precession frequencies are the *same* in the two experiments. So we can imagine free precession of protons at 2.143 kHz in just the earth’s field, and then free precession of nuclear species X *also* at 2.143 kHz in the field provided jointly by the earth and the Helmholtz coils.

The advantage of this calculation is that factors of precession frequency f will be the same in the ‘p’ and the ‘X’ experiments. Also, the same tuning of the pickup-coil LC circuit can be used in the two cases, and this makes it unnecessary to wonder if the Q of that LC-circuit differs at two distinct frequencies.

Finally, we will restrict our calculation to spin- $1/2$ nuclei for convenience. So the question is, if the FID signals from protons appear with a given amplitude, what amplitude should we expect for signals from nuclear species X? The results are computable, given our previous computations.

We introduce the gyromagnetic ratios γ_p and γ_X for protons and another species respectively. We introduce N_p and N_X as the number of protons and X-nuclei present in the sample bottles in the two cases. Then we use a result from Appendix A2, for the magnetization of the sample that can be expected for long enough exposure to a polarizing field B_{pol} . The result is

$$M = (N/V)[\gamma\hbar/2]^2 B_{\text{pol}}/(k_B T) \quad ,$$

so we can get the relative magnetizations as

$$\frac{M_X}{M_p} = \frac{N_X}{N_p} \left(\frac{\gamma_X}{\gamma_p} \right)^2 \quad .$$

Now we imagine the two magnetized samples precessing, in two distinct fields that have been arranged to make the precession frequencies equal. Results from Appendix A3 allow us to predict the emf that will appear in the pick-up coil as

$$\varepsilon(t) = (2\pi f) \sin(2\pi f t) \cdot \frac{2\mu_0}{3} M \cdot \pi r^2 ,$$

and since by arrangement all other factors have been made to be equal, we get a prediction for the ratio of amplitudes of FID signals as

$$\frac{\varepsilon_X}{\varepsilon_p} = \frac{N_X}{N_p} \left(\frac{\gamma_X}{\gamma_p} \right)^2 .$$

This calculation assumes that both nuclei have been polarized for several times their respective T_1 -values, so that they've reached asymptotic full polarization. It also predicts only the initial amplitudes of the FID signals, which may then decay with distinct T_2 -values. But it gives the basis for real predictions.

Here's an example: We fill two 125 ml sample bottles with water and a fluorinated compound such as Galden HT-70. We need the density of each to compute the mass of the samples; those are 1.00 and about 1.65 g/cm³ respectively, so we have 125 g of water and 206 g of the fluorine sample. Next, we need molecular formulae for both; these are H₂O and (approximately) C₃F₆O. The proportions of NMR-active nuclei are therefore {2 moles of protons per 18 g} in the one case, and {6 moles of fluorine per 166 g} in the other case. The results are 13.9 moles of protons, and 7.45 moles of fluorine nuclei. So the desired ratio (N_X/N_p) is (7.45/13.9) = 0.54.

Next, we need the ratio of the gyromagnetic ratios, and this has to be computed from the results of a different experiment (such as measuring the FID precession frequencies of protons and fluorines in the *same* magnetic field). Or one can look up a result, and find (γ_F/γ_p) = 0.941.

Combining the pieces, we predict

$$\frac{\varepsilon_X}{\varepsilon_p} = \frac{N_X}{N_p} \left(\frac{\gamma_X}{\gamma_p} \right)^2 = (0.54)(0.941)^2 \approx 0.48 .$$

This rather favorable ratio means fluorine NMR experiments are relatively easy; that is to say, the signal-to-noise ratio for a first fluorine-NMR experiment is fully *half* that of the easiest proton experiments. The results for other nuclear species are much more discouraging, and for two independent reasons.

The first is that the ratio of gyromagnetic ratios (γ_X/γ_p) is rarely so high as the case just computed; and this ratio appears as a *square* in the prediction.

The second is that few samples allow, as with water, as many as 13.9 moles of NMR-active nuclei to fit within a sample bottle. The results in a general case depend on the density of the sample chosen, and the degree to which the target nucleus makes up its mass.

As a result, the detection of other nuclei takes more care. A biologist might care, a lot, about the NMR detection of ³¹P, phosphorus. As with protons and ¹⁹F, here too we have the advantage that the target NMR nucleus has basically 100% of the isotopic abundance of the chemical element. A favorite sample for NMR detection of phosphorus is phosphoric acid (properly, an 85%

solution of orthophosphoric acid in water). You should be able to work out the discouraging prediction that

$$\frac{\epsilon_p}{\epsilon_p} \approx 0.028$$

for this particular choice of sample. So if you can detect an FID for protons-in-water with a signal-to-noise ratio of 500, you can expect a signal-to-noise ratio of only 14 for this (optimal) case with phosphorus. And that still presupposes that you know ‘where to look’, since the calculations above assume foreknowledge of the gyromagnetic ratios to allow the proper setting of the Helmholtz-coil currents.

If you are inclined to do computations for the NMR detection of other nuclei, you will see why experimenters are so greedy for high signal-to-noise ratios to start with, and how rapidly they can be ‘eaten up’ by unfavorable isotopic ratios, lower densities or chemical fractions, and small gyromagnetic ratios. And you may also see the difference between a ‘confirmatory’ experiment (detecting ^{31}P when you know where to look) with a ‘discovery’ experiment – someone had to be the first to detect NMR in ^{31}P to *find* the value of the gyromagnetic ratio when it was as yet unknown!

Appendix A13: Understanding the deuteron magnetic moment

This appendix touches on a bit of nuclear physics, as it illustrates the conversion between gyromagnetic constants and nuclear magnetic moments, introduces the ‘nuclear magneton’ as a scale for nuclear magnetic moments, and addresses the glamorous question of predicting the deuteron magnetic moment by ‘additivity’. The purpose is to show you why the deuteron magnetic moment is worth measuring, say by the technique of EF-NMR in heavy water.

Recall that the classical calculation of the angular momentum and magnetic moment expected to exist for any rotating rigid body in which charge and mass are spatially distributed in the same way. If the total charge is Q and the total mass is M , then the result is

$$\gamma = \frac{\mu}{L} = \frac{Q}{2M} .$$

If such a model is applied to a spin-1/2 proton, with magnetic moment μ_p and mass m_p , we get the expectation

$$\mu_p = \frac{e}{2m_p} L = \frac{e}{2m_p} \frac{\hbar}{2} = \frac{e\hbar}{4m_p} .$$

If the proton were a “Dirac particle”, we’d expect a proton magnetic moment larger than this by a famous factor of 2, allowing the prediction

$$\mu_p \cong \frac{e\hbar}{2m_p} .$$

This combination of fundamental constants is in fact called the ‘nuclear magneton’ μ_N , and it gives a natural unit in terms of which to measure generic nuclear magnetic moments. Imagine the surprise when the proton magnetic moment was in fact measured, and found to have a value, in units of nuclear magnetons, more like *three* than one!

Your NMR data already give a value for the proton magnetic moment, since we’ve written the gyromagnetic ratio as

$$\gamma = \frac{\mu_p}{L} = 2\pi c_p ;$$

accepting that the angular momentum for protons is $L = \hbar/2$, we get

$$\mu_p = \gamma L = 2\pi c_p L = 2\pi c_p \hbar/2 = \pi \hbar c_p .$$

You can now evaluate μ_p from your data, and $\mu_N \equiv e \hbar / (2m_p)$ from accepted values, and see for yourself that μ_p/μ_N is emphatically not one. The ratio that you do get is called “the proton magnetic moment in nuclear magnetons”.

Now if you have obtained any free-precession signals at all from heavy water, you have the data to determine the gyromagnetic constant c_D for deuterons. Accepting that deuterons are spin-1 nuclei, you can by a similar procedure compute μ_D from your data, and then the ratio μ_D/μ_N , which is called “the deuteron magnetic moment in nuclear magnetons”.

Finally you can look up (though alas, not easily measure) the neutron magnetic moment, also in units of nuclear magnetons. Here the first surprise is that a neutral particle like a neutron should have any magnetic moment *at all*. The next surprise comes from adding up the proton and

neutron magnetic moments, both in units of nuclear magnetons: compare the result to your measurement of the deuteron magnetic moment, also in nuclear magnetons. Here you'll need to pay attention to your uncertainty estimates to decide whether you too are entitled to be surprised.

In fact there are at least three mysteries in a nucleus as simple as a deuteron: the first is why the two spin-1/2 constituents pair up to form a spin-1, rather than a spin-0, aggregate; the second is why the magnetic moments of the constituents fail to add up to give the magnetic moment of the aggregate; the third is why the aggregate also exhibits an electric quadrupole moment, characteristic of a departure from spherical symmetry. Much more detailed models of the deuteron are invoked to explain these mysteries.

Appendix A14: The Helmholtz coils' geometry

The Helmholtz coil pair in the EFNMR Gradient/Field Coil System is designed and manufactured in terms of an archaic but perfectly well-defined length unit, the inch: 1 inch \equiv 25.4 mm. The design data given here will enable you to compute your best estimate of the ‘coil constant’ k , which gives the field generated at the center of the coils per unit current in the wires. Recall that there are 30 turns in each of the two coils, and that the same current I flows in each and every turn, because of a series connection of the coils.

The coils are wound on wooden forms designed to have a center-to-center separation along the z -axis of 11.95 inches; you may measure the actual separation yourself, and check to see if it’s uniform around the circumference.

The coils are wound in three layers, each of ten turns, starting at the bottom of a groove in the wooden frame having nominal diameter 23.69 inches. The #20 AWG copper wire used has a diameter of 0.035 inches, and the successive layers are separated by a layer of Kapton tape of nominal thickness 0.002 inches. Thus the outer sides of the outermost turns are expected to define a diameter of 23.91 inches; this number you may also check by direct measurement (on both coils, and at several places around the circumference).

With these measurements completed, you have all that’s needed to locate each of the 30 turns on each coil both in radius away from the z -axis and in position along the z -axis. Now find or derive a result, depending on the Biot-Savart Law, for the field generated on the axis of a co-axial pair of coils, each of radius a , located at $z = +b$ and $-b$. This field will be a function of z , and you’ll first want to evaluate it at $z = 0$.

A first model of the coils assumes that all 30 turns in each coil may be conflated to a single turn, carrying a current of $30I$, taken to have the ‘average position’ of the separate turns. Evaluate the coil constant in this model, and see if you get $k \approx 90 \mu\text{T/A}$. You might also evaluate the predicted on-axis field as a function of z , to see the degree of uniformity that can be expected in the relevant range of $|z| \leq 2.5 \text{ cm}$. (The variation in field strength for points *off* the z -axis is much harder to compute, but you may be assured that variations off-axis are no worse than the ones you’ve just seen for on-axis locations.)

A more complicated model of the coils locates all 30 turns, in each coil, at their actual locations, and assigns separate a_j and b_j values to each of 30 superimposed coil pairs. Then the field at the center, or the field as a function of z , is also the superposition of the results for the 30 two-turn coil pairs. You should get a result very similar to, but perhaps more reliable than, your result above.

The hardest part of your modelling task might be to estimate, or justify, an uncertainty ∂k for your coil constant k ; the uncertainty will depend mostly on the degree to which you can be sure where the coils’ turns are located in space. The payoff of an honest calculation of $k \pm \partial k$ is a first-principles measurement of the proton’s gyromagnetic constant, together with its uncertainty. Of course (after paying your dues) you can always retrospectively calibrate your coils by using the results of proton precession frequencies, but this method depends on *someone else* having

done the honest calculation, and it deprives you of obtaining your own self-measured value for protons' magnetic moments.

Appendix A15: The Fourier Transform of a decaying sinusoid

This appendix works out the detailed analytic form of the Fourier transform to be expected for the *ideal* free-precession signal, and extracts from it a relationship between the T_2 decay time of the signal and the linewidth of the computed transform.

We suppose that the real voltage signal emerging from the EFNMR controller box can be written as

$$V(t) = V_0 \exp(-q t) \cos(\omega_0 t) .$$

where q describes the rate of exponential decay: it might also be written as $q = 1/T_2$. Here $\omega_0 = 2\pi f_0$ gives the central frequency of the signal. Since the signal's duration is only of order a few times T_2 , we might expect (from an ‘uncertainty principle’ sort of argument) a frequency ‘uncertainty’ of order $\Delta f \approx 1/T_2$. The calculation below is intended to make this argument both clear and precise.

To perform the Fourier transform mathematically (as data-processing equipment might perform it in the experiment) we first realize that this signal exists only for $t \geq 0$, and then generalize it to the complex wave,

$$V_{\text{complex}}(t) = V_0 \exp(-q t) \exp(-i \omega_0 t) \quad \text{for } t \geq 0 .$$

Then the Fourier transform,

$$\tilde{V}(\omega) = \frac{1}{\sqrt{2\pi}} \int_{t=-\infty}^{+\infty} V(t) e^{+i\omega t} dt ,$$

can be computed analytically, with the result

$$\tilde{V}(\omega) = \frac{V_0}{\sqrt{2\pi}} \frac{q-i(\omega_0-\omega)}{q^2+(\omega_0-\omega)^2} .$$

This complex function is likely to be displayed via its magnitude and phase; alternatively, its absolute square gives the Fourier power spectrum,

$$|\tilde{V}(\omega)|^2 = \frac{V_0^2}{2\pi} \frac{1}{q^2+(\omega_0-\omega)^2} .$$

This is a Lorentzian function, centered at frequency $\omega = \omega_0$, and falling to half its peak value at $\omega = \omega_0 \pm q$. Hence its full width (in angular frequency) at half maximum is $\Delta\omega = 2q$, so its FWHM in ordinary frequency is $\Delta f = 2q/(2\pi)$. In instrumental practice, this width is best found by locating two points on the sides of the Lorentzian peak which are lower than the peak by 3 dB (a factor of two) in power, or equivalently two points lower than the peak by a factor of $1/\sqrt{2} \approx 0.707$ in indicated voltage.

If this Δf gives the width in frequency, we can choose a variety of measures for the duration-in-time of the time-domain signal. Our decay rate q is connected to the standard T_2 time-scale via $q = 1/T_2$; in turn T_2 is operationally available as the time during which the signal $V(t)$ decays to $1/e$ of its initial amplitude. Even easier to read off a ‘scope is $t_{1/2}$, the time during which the signal $V(t)$ decays exponentially to half of its initial amplitude; this is given by $t_{1/2} = (\ln 2)/q$.

So we now have both factors for a “frequency-time uncertainty product”, giving

$$\Delta f \cdot t_{1/2} = \frac{2q}{2\pi} \cdot \frac{\ln 2}{q} = \frac{\ln 2}{\pi} \approx 0.2206 \quad .$$

Sure enough, the product is independent of the decay rate, and shows the correlation between long decay times and narrow spectral lines. The product is also of order 1, but is now precisely specified, provided that the two ‘uncertainties’ are also precisely defined as they were above.

It follows that if a free-precession signal with a decay time of $T_2 = 1.0$ s is observed, this will have $t_{1/2} = 0.69$ s and the Fourier transform of this signal ought to have a full width (at half-maximum-power points) of

$$\Delta f = \frac{0.2206}{t_{1/2}} = \frac{0.2206}{0.69 \text{ s}} = 0.32 \text{ Hz} \quad .$$

But it is actually important *not* to call this Δf the ‘uncertainty in frequency’; what this Δf really gives is the linewidth of the Lorentzian peak observed. The actual experimental uncertainty for the frequency location of the *center* of this peak is likely to be *smaller* than Δf ; an experimentally-derived spectral line can have its center location estimated to a small fraction of its line width. If there are no other sources of frequency uncertainty, the uncertainty in the estimated location of line center, δf_0 , might be as small as the above Δf divided by the signal-to-noise ratio of the data.

Appendix A16: Counting gradients, and their consequences

This appendix works out the *number* of relevant magnetic-field gradients for earth's-field NMR, and then derives (at two levels of detail) some *consequences* of magnetic-field gradients in NMR.

First, a discussion of just what, and how many, gradients a magnetic field can have. The generic vector field $\mathbf{V}(x,y,z)$ in three dimensions has *nine* first-order gradients, from the list $\partial V_x/\partial x$, $\partial V_x/\partial y, \dots, \partial V_z/\partial z$. But the magnetic field \mathbf{B} satisfies Maxwell's equations, which impose (one) divergence and (three) curl conditions on the first-order spatial derivatives, and this leaves only *five* independent gradients.

If the z -axis is aligned with \mathbf{B} at the origin, and the gradients are small enough over the region of interest, we can define the field as

$$\mathbf{B}(x, y, z) = B_0 \hat{\mathbf{z}} + \mathbf{B}_1(x, y, z) ,$$

where the constant B_0 gives the field's magnitude at the origin, and where the function \mathbf{B}_1 vanishes at the origin and can be taken to be of first-order smallness near the origin. Since NMR precession frequencies depend only on the *magnitude* of \mathbf{B} , we desire only that the magnitude, or equivalently the magnitude-squared, of the field be independent of position to first order. That magnitude-squared is given by

$$B^2(x, y, z) = \mathbf{B} \cdot \mathbf{B} = B_0^2 + 2B_0 \hat{\mathbf{z}} \cdot \mathbf{B}_1(x, y, z) + \text{smaller terms} ,$$

and because of the dot product, we now see that only the z -component of the \mathbf{B}_1 function matters. Making a Taylor expansion of the B_{1z} function about the origin, and taking the square root to first order, we get for the magnitude B the result

$$B(\delta x, \delta y, \delta z) = B_0 + \delta B = B_0 + \frac{\partial B_{1z}}{\partial x} \delta x + \frac{\partial B_{1z}}{\partial y} \delta y + \frac{\partial B_{1z}}{\partial z} \delta z ,$$

which shows that only *three* first-order gradients, gradients of the field B_{1z} , need to be corrected to make the magnitude of the field spatially uniform.

Note that the x - and y -components of the \mathbf{B}_1 function do not enter (to first order). One might say that rather than correcting all five (independent) gradients by NMR diagnostics, we are achieving two corrections geometrically (by alignment of the gradient-coil system in azimuth and altitude), and leaving only three corrections to be performed using NMR as a diagnostic. This accounts for the number, the labeling, and the function of the gradient-adjust knobs on the EF-NMR Gradient/Field controller unit.

Next, we work out a very approximate *consequence* of gradients. In the presence of a gradient of strength G , two points separated in space by distance S will have field differing in magnitude by

$$\Delta B = G S ,$$

and protons at these two sites will precess at different frequencies, differing in fact by

$$\Delta f = c_p \Delta B = c_p G S .$$

$$\Delta f = c_p \Delta B = C .$$

In a time T for which $\Delta f \cdot T = 1$, protons at two such sites will be a full cycle out of phase, so surely there will be observable consequences at a time

$$T \approx \frac{1}{c_p G S} .$$

For typical values with $c_p = 43 \text{ Hz}/\mu\text{T}$, $g = 3 \mu\text{T}/\text{m}$, and $S = 4 \text{ cm} = 0.04 \text{ m}$, this gives a dephasing timescale of $T \approx 0.19 \text{ s}$, or 190 ms. Of course this timescale varies inversely as the size of the magnetic-field gradient.

Finally, a more detailed treatment of gradients' consequences. We might model the sample in the TeachSpin apparatus as a circular cylinder of length $L = 7 \text{ cm}$ and diameter $2R = 5 \text{ cm}$, and then compute the detailed consequences of having protons distributed through a range of field strengths, and having precession frequencies distributed through a range of frequency values.

For a field whose magnitude has only an x -gradient, we can write

$$B = B(x) = B_0 + G x , \text{ so } f = f(x) + c_p B(x) = f_0 + c_p G x .$$

Now if we form phasors $\exp[-i 2\pi f(x) t]$, and include the whole sample by integrating over x from $-L/2$ to $+L/2$, we get the resultant phasor at time t , and find that its real part can be written

$$V(t) \approx \cos(2\pi f_0 t) \frac{\sin(\pi c_p G L t)}{\pi c_p G L t} ,$$

which displays oscillations at the central frequency f_0 , but multiplied by a time-dependent envelope function of the form $\sin(q)/q$. This envelope function falls to half its initial value at $q = 1.895$, and to zero at $q = 3.142$; it allows us to define a half-amplitude point at time

$$t_{1/2} = \frac{1.895}{\pi} \frac{1}{c_p G L} .$$

For a field whose magnitude has only an y - or z -gradient, we can write (say)

$$B = B(y) = B_0 + G y , \text{ so } f = f(y) + c_p B(y) = f_0 + c_p G y ,$$

Again we form phasors $\exp[-i 2\pi f(y) t]$ and integrate over y from $-R$ to $+R$, but this time weighting the phasors according to $(R^2 - y^2)^{1/2}$ to describe a circular cross section, thereby getting a much less familiar integral. Nevertheless, the resultant phasor at time t has a real part that can be written

$$V(t) \approx \cos(2\pi f_0 t) \frac{J J_1(2\pi c_p G R t)}{2\pi c_p G R t} ,$$

where $J_1(q)$ is the first-order Bessel function of the first kind. In this case $J_1(q)/q$ forms the envelope function; it falls to half its initial value at $q = 2.215$, and to zero at $q = 3.832$. This allows us to define a half-amplitude point at

$$t_{1/2} = \frac{2.215}{\pi} \frac{1}{c_p G \cdot 2R} .$$

Both detailed results support the approximate form first introduced above. Either can also be used to account for the 'pinch-off time' predicted by the first zero of the envelope function.

Appendix A17: Radiation damping and the FID decay timescale

Once you've learned how to use the gradient coils in the EF-NMR apparatus, you can strive to get long-lasting free-induction-decay signals from protons precessing in water in the earth's field. You might wonder just how well you can do towards this goal, and what *limits* the duration of these free-precession signals. This Appendix mentions the requirements for getting the longest decay times, and the limiting mechanism in the EF-NMR apparatus as it is configured.

There are requirements for getting long decay times. The prime requirement is careful adjustments of the gradients. There are five adjustments, in fact: two of them are alignment of the field/gradient coils along the direction of the ambient field. (This alignment is best checked using the methods of Chapter 7.3.) The other three adjustments are the gradient corrections' values, and the process of optimization is discussed in Chapters 3 or 10. The methods of Appendix A16 show that gradients need to be corrected to better than $0.2 \mu\text{T}/\text{m}$ to get 'half-lives' of 1 second or more for free-induction-decay signals. So that means the three gradient dials need to be optimized to about one-tenth turn precision.

A second requirement for getting long decay times is 'real water'. Here it is worth using de-ionized (instead of tap) water, to ensure that paramagnetic ions are in low enough concentration. To achieve the book-value T_2 -timescale of 2.5 s for EF-NMR in water, it is also necessary that (paramagnetic) dissolved molecular oxygen (O_2) be removed from the water. There are various physical or chemical 'de-gassing' methods which you can use to achieve this.

But after all these precautions are taken, you will still observe decay times *worse* than the claimed T_2 -value for pure water, and there's a physical reason for this. It is called 'radiation damping', and it amounts to loss of energy from the system of precessing protons, into the LCR system that surrounds the protons. (There is *not* 'radiation' into free space, however.) To put it another way, it is the back-action of the induced currents in the pick-up coil on the protons that shorten the duration of the FID signal. So for the first time we need to consider that the pick-up coil is not just a passive observer, but also a perturber, of the proton sample.

In our EF-NMR experiments, we have a magnetic moment precessing about the z -axis, which is inducing, via Faraday's Law, a time-varying emf ε in the pick-up coil. One could imagine detecting that emf in an open-circuit way, but in actual practice, the emf drives a resonant LCR circuit. As a result, non-zero currents flow in the pick-up coil. If the LC-system is properly tuned, the size of those currents is $i = \varepsilon/R$, where R is the resistance of the coil (since at optimal tuning, the coil's inductive reactance has been cancelled by the capacitor's reactance, leaving only the coil resistance to limit the current).

So now there is a new magnetic field $B_x = k i(t)$ present inside the pick-up coil, where k gives the field-per-unit-current generated by the pick-up coil. Since that's an a.c. field, and since it's resonant with the precession frequency, and since it is transverse to B_z , it acts like the spin-flip coil mentioned in Chapter 9.3, and it starts to rotate the sample's magnetization out of the xy -plane, back up toward the z -axis. As usual, we resolve this oscillating field of amplitude B_x into

two fields, each of magnitude $B_x/2$, which are respectively rotating and counter-rotating about the z -axis in the xy -plane.

A timescale on which such a spin-flipping process would be complete is given by

$$\gamma \frac{B_x}{2} T = \frac{\pi}{2} ,$$

which says that the effect of the rotating field $B_x/2$, if continued, would rotate the magnetic moment right up to the $+z$ -axis within time T . (This is the ‘ $\pi/2$ pulse’ of pulsed-NMR parlance.) But rotating the magnetization up to the $+z$ -axis would ensure that none of it lies in the xy -plane, and that would mean the disappearance of the free-induction-decay signal.

In a more complete calculation, the effect of this back-action of the coil on the protons is to decrease the magnetization in the xy -plane, and to make the FID signal decay with a time-scale of the order of T above, even if there were no intrinsic T_1 or T_2 damping effect on the protons. So the T computed above is an approximate measure of the radiation damping time, a timescale on which the precession signal would die away even if there were no spin-spin relaxation.

This timescale can be evaluated quantitatively. A standard use of the EF-NMR system gives an emf induced in the pick-up coil of size $\varepsilon \approx 3 \mu\text{V}$ (as computed in Appendix A3). The coil’s resistance is about $R \approx 9 \Omega$, so $i = \varepsilon/R \approx 0.3 \mu\text{A}$ gives the amplitude of the a.c. current flowing the in the LCR circuit.

The pick-up coil generates fields with coil constant $k \approx 0.015 \text{ T/A}$, so the size of the oscillating B_x -field is $k i \approx (0.015 \text{ T/A})(0.3 \mu\text{A}) = 0.005 \mu\text{T}$. This is a very small field compared to the $\approx 50 \mu\text{T}$ static field, but because it is an oscillating field, transverse in direction and resonant in frequency, it can have big effects.

If fact it gives a radiation-damping timescale of order

$$T = \frac{\pi/2}{\gamma B_x/2} \approx \frac{\pi}{2\pi(43 \text{ Hz}/\mu\text{T})(0.005 \mu\text{T})} = \frac{1/2}{0.22 \text{ Hz}} = 2.3 \text{ s} .$$

The implication is that even for a sample without intrinsic dephasing ($T_2 = \infty$), and even for the case of fully-corrected gradients, FID signals should be expected to decay with a time-constant of about 2 seconds. This, together with the actual T_2 spin-spin relaxation time for water, accounts for what is observed in practice: the net dephasing rate implies a $1/e$ time-constant of about 1 second, which corresponds to a ‘half-life’ of ≈ 0.7 s, just about matching the best that can be achieved by gradient adjustments.

It is therefore tempting to suppose that after all other improvements, radiation damping is the strongest remaining relaxation mechanism. It is not easy to test this hypothesis, or to remove this limitation, without hardware changes in the EF-NMR system. The use of a lower Q of the LCR system is predicted to reduce the effect of back-action, but it would also cut down the size of the signals, so in practice the Q has been engineered to be as high as copper-coil technology permits.

One feasible test for radiation damping is to operate the system with a deliberately mis-tuned sample coil. This (of course) lowers the signal level, but in consequence is also lowers the a.c. current in the sample coil, and reduces the coil's back-action on the sample.

To test for this effect, you can acquire FID transients at the band-pass amplifier output, where the signal-to-noise ratio is highest. The ‘control group’ experiment is to capture an FID transient with everything optimized, including the tuning of the LC circuit to the protons’ Larmor precession frequency. Then the comparison experiment is to *mis*-tune the LC circuit by one click of the COARSE adjust. This will (of course) lower the signal level by a factor of order 5 (just how big a factor depends on what FID frequency your local field gives), but tracking that effect backwards will persuade you that the a.c. current in the coil is now smaller by the same factor. Leaving everything else exactly the same, but raising the sensitivity of your oscilloscope by a compensating factor, the acquisition of another FID transient will give you the comparison data you need to test the radiation-damping hypothesis. In particular, you might be able to observe a *longer time constant* for the exponential decay of this new transient.

Again, a more complete treatment would show that such a mistuned coil exerts not only a reduced damping effect, but also a ‘frequency-pulling’ effect, on the precession of the protons. The protons ‘want’ to precess at the Larmor frequency, and the LC circuit now ‘wants’ to oscillate at a different frequency. The coupled system in fact oscillates at a compromise frequency, pulled slightly away from the Larmor frequency. Such a frequency-shifting effect is a consequence of the fact that the tuned LC-system has both absorptive (lifetime-reducing) and dispersive (frequency-pulling) back-action effects on the precessing protons. Effects like this are well known and important in the design of masers.

Appendix A18: Checking the sensitivity of the detection system

This Appendix describes a ‘sensitivity check’ on the EF-NMR apparatus which tests the estimates made earlier about the size of the precessing magnetic moment of the NMR sample, and also tests the sensitivity of the entire detection system: the pick-up coil, the LC resonant system, and the pre-amplifier and main amplifier gains. So it can serve as a quantitative reality check for the claim that protons, precessing in water, are the cause of the signals you can see and hear emerging from this apparatus.

Recall that Appendix A1 claimed to compute the saturation magnetization that could be achieved in a room-temperature sample of water, and gave $M = 1.7 \times 10^{-4} \text{ A/m}$ for its value. If this magnetization were to be uniform over the full volume ($125 \text{ ml} = 125 \text{ cm}^3 = 125 \times 10^{-6} \text{ m}^3$) of the sample container, we would predict a magnetic moment, due to the partially-polarized protons in the sample, of

$$\mu = M V = (1.7 \times 10^{-4} \text{ A/m})(125 \times 10^{-6} \text{ m}^3) \approx 210 \times 10^{-10} \text{ A m}^2 .$$

So a magnetic moment, with direction along the axis of the polarizing coil, builds up to this size and is held there statically as the polarizing current continues. Then upon the (sudden) removal of the polarizing current, this magnetic moment begins precessing about the earth’s field. The component of magnetic moment along the axis of the coil is thereafter given by the oscillating function

$$\mu(t) \approx 2.1 \times 10^{-8} \text{ A m}^2 \cdot \cos(2\pi f t) ,$$

where f is the precession frequency in the local static magnetic field (and where the slow exponential decay of the polarization has been neglected).

The idea of this Appendix is that an artificial, non-NMR, oscillating magnetic moment of this size can easily be set up to *mimic* the oscillating moment attributable to precessing protons – and that the entire electronic detection system (from pick-up coil, to LC resonant system, to pre-amplifier, through band-pass or main amplifier) ought to respond identically to these two sorts of magnetic-moment source.

Here’s one method for setting up an oscillating magnetic moment of about this size. You can use (for example) a wooden dowel or plastic rod of $\frac{1}{4}$ " diameter as a ‘coil form’, and you can wind onto it a coil of 10 full turns to make a small one-layer close-packed solenoid. You might want to use fairly thin copper wire to do this winding, and you will want to bring out the two leads from your coil as a twisted pair (so that the magnetic fields generated by the two leads cancel each other out). Each turn of that coil has an area of $\pi r^2 = (\pi/4)d^2$, so the net ‘area product’ of the whole coil is

$$A = 10(\pi/4)d^2 ,$$

which you can show is about $3.2 \times 10^{-4} \text{ m}^2$ for this coil.

Now suppose you have previously found the precession frequency f for protons-in-water under your conditions of ambient static magnetic field, and that you now set up an electronic sine-wave generator to give a voltage waveform with this same frequency f , and with an amplitude 0.66 V. If you connect this generator, through a $10\text{-k}\Omega$ resistor, to the coil you have wound, there will be a sinusoidally-oscillating current of amplitude $(0.66 \text{ V})/(10 \text{ k}\Omega) = 66 \mu\text{A}$ flowing in your coil.

So the coil will create an oscillating magnetic moment of

$$\mu(t) = i(t) \cdot A = (66 \times 10^{-6} \text{ A})(3.2 \times 10^{-4} \text{ m}^2) = 2.1 \times 10^{-8} \text{ A m}^2$$

whose value has clearly been contrived so as to *match* the predicted size of the oscillating, along-the-coil-axis, magnetic moment we've claimed is set up by the precessing protons. That is to say, you have made a 'surrogate source' of time-varying magnetic moment (out of a coil and an external generator) which ought to mimic the precessing proton sample, for purposes of downstream electronic pick-up and processing.

In particular, the coil and the drive which you have contrived ought to give a (continuous) a.c. signal which matches the (initial) a.c. signals you get from precessing protons (at the beginning of their free induction decay). So you can remove the sample bottle, ignore the polarizing current, and yet test all the rest of the electronics of the EF-NMR detection system.

There are two ways to view the results of such a test:

First, you can view them as a check on the claimed magnetization of the protons, the *M*-value mentioned above. The only distinction between the real, and the surrogate, sample is that the precessing protons are distributed in space over the full volume of the sample bottle, while the surrogate magnetic moment is developed in a small coil, point-like by comparison.

Second, you can use your surrogate coil to measure empirically the sensitivity of the entire electronic detection chain. Provided your generator frequency has been set to match the local proton precession frequency, then all four factors (the emf induced in the coil, the voltage gain of the LC-circuit, the gain of the pre-amplifier, and the gain of the band-pass amplifier) are the same for the NMR, and for the surrogate, source of oscillating moment. Since you can compute the size of the surrogate moment from electrical and geometrical measurements, you can measure this sensitivity empirically.

There is yet another use for the small 'surrogate-moment' coil you have made, and that is to check the geometric variation of the pick-up/detection system's sensitivity. That is to say, with everything else held constant, you can vary the *position* of your little source coil, say from the center of the sample volume, to off-axis, or off-center, locations. Your intuition ought to suggest that moving the source coil from side to side within the pick-up coil should make little difference (we'd expect no change at all, if the pick-up coil were infinitely long), but that moving your source coil on-axis from end to end of the sample volume should make a reasonably large difference in the signal picked up (dropping to half-size signal when the source coil is at the end of the pick-up coil).

So the pick-up coil is *not* uniformly sensitive to all the protons in the sample bottle; relative to a 1-cm³ sample of water at the geometric center of the bottle, protons in a 1-cm³ sample near the ends of the bottle experience signal pickup at sensitivity of about 0.6, while protons in a 1-cm³ sample near the sides of the bottle experience signal pickup at sensitivity of about 0.9. You may survey this variation and estimate a 'volume average' of this sensitivity.

The same variation-over-volume exists during the polarization of the protons, as well, since the same pick-up coil is used as the polarizing coil. So a sensitivity-for-reception of 0.6 (at the

bottle's ends) is accompanied by another factor of 0.6 for size-of-magnetization, giving each 1-cm³ sample of water near the bottle's ends an overall effectiveness near 0.36.

The average of this squared (polarizing and pickup) relative sensitivity over the whole of the bottle is called the 'filling factor' of the apparatus, and it is clearly less than 1. But now you have a method for measuring it, and therefore giving an even better estimate for just how large the NMR signals you observe ought to be.

Appendix A19: The ‘bucking coil’ and how it works

You know that the sample bottle in the TeachSpin EF-NMR apparatus gets inserted into the bore of a coil. This ‘sample coil’ serves, sequentially in time, first as a solenoid (carrying a high current, to polarize the sample), and then as a pick-up coil (in which precessing nuclei induce a Faraday’s-Law emf as signal). But this sample coil, with inner diameter about 5 cm, is part of an EF-NMR ‘head’ which includes a much larger coil, one wound on a form of diameter near 30 cm. What’s that bigger coil, what is it for, and how does it work?

It’s called a ‘bucking coil’, which is only a name, until you think through all the *other* magnetic fields that could be inducing an emf in the sample coil. Every turn (out of $N_{\text{sample}} \approx 1340$ of them) of the sample coil presents a considerable area A to external magnetic fields B_{ext} , and the rate of change of external fields creates an induced emf having nothing to do with nuclear precession. The sample coil will give a non-NMR signal of size

$$\mathcal{E} = -N \frac{d\Phi_B}{dt} = -N_{\text{sample}} \cdot A \cdot \frac{dB}{dt}$$

The electrified world in a typical laboratory is full of time-varying magnetic fields, varying not just at the line frequency of 50 or 60 Hz, but also at high harmonics of these frequencies. We find that odd-numbered harmonics typically dominate over even harmonics; you should appreciate that harmonics with frequencies near 2 kHz will interfere the worst with the actual NMR signals that fall into the same frequency range.

If such a field has an amplitude of even $B_{31} = 0.1 \mu\text{T}$, and a frequency (say) of $31 \times 60 \text{ Hz} = 1860 \text{ Hz}$, then it generates, by Faraday’s law, an emf of amplitude

$$\mathcal{E} = N_{\text{sample}} \cdot \pi R^2 \cdot 2\pi f \cdot B_{31} \approx (1340)(50 \times 10^{-4} \text{ m}^2)(2\pi \times 1860/\text{s})(0.1 \mu\text{T}),$$

which comes to 8 mV, *huge* compared to the few- μV signal induced in the same coil by precessing nuclei (see Appendix A3).

This problem can be solved because time-dependent external fields are chiefly produced by rather distant sources. Thus to a good approximation, these fields are spatially uniform in the vicinity of the sample coil. So we add another coil, the bucking coil, co-axial with the sample coil, and having the same (area \times turns) product as the sample coil itself. Then remote sources of time-dependent fields will induce identical emfs in the bucking, and the sample, coils. Finally, we wire the sample coil, and the bucking coil, in anti-series, so that the effects of distant sources ought to cancel out entirely.

In practice, the cancellation is not perfect, in part because the external sources are not quite infinitely distant, and in part because some of the interference from distant sources comes from capacitive pick-up, rather than from induced emfs. But the cancellation is good enough that these extraneous emfs cease to dominate over the signal of interest.

That brings up another question – if the bucking coil just cancels out the sample coil’s pick-up of distant sources, why doesn’t it also cancel out the pick-up of nearby sources – like those from the precessing nuclei themselves? To investigate this, it’s helpful to think of the most-easily modelled of all situations: consider as a sample a sphere of radius R , wrapped with a pick-up

coil having m^2 turns, each also of radius R , wound around it in a great circle. (Here m is a multiplier, some convenient integer.) Then think of a bucking coil, with just one turn, but with radius mR , lying concentric and co-planar with the sample coil. [Note the (area \times turns) product of the sample coil is $\pi R^2 \cdot m^2$, and that of the pick-up coil is $\pi(mR)^2 \cdot 1$, so we have the perfect matching we intend.]

Now if that spherical sample is uniformly magnetized, to magnetization M , its magnetic moment is

$$\mu = MV = M \cdot \frac{4\pi}{3} R^3 ,$$

and because the sample is spherical, its external magnetic fields are given by the point-dipole result,

$$\mathbf{B}(\mathbf{r}) = \frac{\mu_0}{4\pi} \left[3 \frac{\mu \cdot \mathbf{r}}{r^5} \mathbf{r} - \frac{\mu}{r^3} \right] .$$

In the ‘equatorial plane’ which contains the sample coil and the bucking coil, this gives, at a test point distant by r from the center of the sample, a field

$$\mathbf{B}_{out}(\mathbf{r}) = - \frac{\mu_0 \mu}{4\pi r^3} .$$

Inside the sample itself, where $r < R$, the B -field is spatially uniform, with size

$$\mathbf{B}_{in}(\mathbf{r}) = \frac{2}{3} \mu_0 M .$$

These results enable us to compute the flux through both coils. For a single turn of the pick-up coil, the flux is just a field \times area product,

$$\Phi_{sample} = B_{in} \cdot \pi R^2 = \frac{2\pi}{3} \mu_0 M R^2 .$$

For the bucking coil, we divide the total area into the $r < R$ and the $R < r < mR$ regions, and get the total flux through the whole of the area:

$$\Phi_{bucking} = B_{in} \cdot \pi R^2 + \int_R^{mR} 2\pi r dr B(r) = \frac{2\pi}{3} \mu_0 M R^2 - \left(1 - \frac{1}{m}\right) \frac{2\pi}{3} \mu_0 M R^2 .$$

Notice that in the $m \rightarrow \infty$ limit, this flux goes to zero: each line of \mathbf{B} runs one way through the sample, and returns in the outer region outside the sample, and if the bucking coil is big enough, the net flux it intercepts drops toward zero.

Now the sample coil contains m^2 turns, and the bucking coil only one, so the net flux for the anti-series combination of the two coils is

$$\Phi_{net} = m^2 \cdot \frac{2\pi}{3} \mu_0 M R^2 - 1 \cdot \frac{1}{m} \frac{2\pi}{3} \mu_0 M R^2 = m^2 \left(1 - \frac{1}{m^3}\right) \frac{2\pi}{3} \mu_0 M R^2 .$$

Here the parenthesis gives the reduction, due to the bucking coil, of the net flux seen by the anti-series combination of both coils.

In the TeachSpin set-up, the ‘multiplier’ m is a ratio of diameters of coils, with value about 3.6, and the quantity

$$\left(1 - \frac{1}{m^3}\right) \approx (1 - 0.02) .$$

Since the flux is diminished only by about 2% by the addition of the bucking coil in anti-series, the rate-of-change of flux is diminished in the same proportion. Thus we see that while the ‘cost’ of the bucking coil is a loss of a few percent of the signal generated by the precessing protons, the ‘benefit’ of the bucking coil is a near-100% cancellation of Faraday’s-Law interference from distant sources.

Appendix A20: The nuclear spin isomers -- ortho- vs. para-water

The magnetization calculations of Appendix A1 assume that in a volume V , there are N protons, all of them treated as independent spin-1/2 nuclei, each of them responding (only) to the external field B and thereby getting collectively magnetized.

But actual protons in water occur in molecules; there are $N/2$ of those molecules in the volume V , and in each molecule, there are 2 protons which interact with each other very weakly indeed. Yet just as in H_2 molecules, so in H_2O molecules, there is a spin-statistics theorem, connecting the two-nucleus spin state with the allowed rotational state of the molecule, and the result is similar: at very low temperatures, and suitably catalyzed, water molecules will settle into their rotational ground states and necessarily turn entirely into para-water, with a total nuclear spin $I = 0$. By contrast, above about 100 K, and in statistical equilibrium, water molecules will be $\frac{3}{4}$ ortho-water with nuclear spin $I = 1$, and $\frac{1}{4}$ para-water with nuclear spin $I = 0$.

Now para-water will be ‘NMR silent’, having as it does only the $m_I=0$ spin projection. So the question is – does the prediction of Appendix A1 have to be modified, to a magnetization only $3/4$ of what we computed there? The answer turns out to be *no* – as we’ll now confirm by redoing the calculation from scratch, assuming two-proton states from the beginning.

We start with the new two-proton Hamiltonian

$$\hat{H} = -\gamma(\mathbf{I}_1 + \mathbf{I}_2) \cdot \mathbf{B} ,$$

and we work in a field so low that magnetic splittings are small compared to any proton spin-spin interaction. In such a field, the eigenstates of the two-spin system are a triplet of spin-1 states, plus a singlet of a spin-0 state. [These states are *not* just a ‘hyperfine splitting’ apart in energy, since the spin-0 state occurs in the lowest rotational state of the molecule, while the spin-1 state can only occur with the first excited rotational state.]

The magnetic energies of the three triplet states are easily found to be

$$E = -\gamma\hbar B, 0, +\gamma\hbar B ,$$

arising from the three states which have values of $\mu_z = \gamma I_z = \gamma(I_{1z} + I_{2z})$ of size

$$\mu_z = +\gamma\hbar, 0, -\gamma\hbar .$$

Note that energy differences between adjacent magnetic sub-states are still given by $\Delta E = \gamma \hbar B$, so in this model the precession frequency of the sample’s magnetization still has the familiar Larmor value $\omega = \gamma B$.

Now we compute $\langle \mu_z \rangle$ for the triplet state using the Boltzmann formula, using a sum over the *three* sub-states, and making a suitable series expansion:

$$\langle \mu_z \rangle = \frac{\sum_m \mu_z(m) \exp[-E(m)/k_B T]}{\sum_m \exp[-E(m)/k_B T]} \approx \frac{\sum_m \mu_z(m)[1 - E(m)/k_B T]}{\sum_m [1 - E(m)/k_B T]} .$$

The denominator comes to

$$\left[1 - \frac{-\gamma\hbar B}{k_B T}\right] + [1 - 0] + \left[1 - \frac{+\gamma\hbar B}{k_B T}\right] = 3 + 0 .$$

The numerator has the form

$$(+\gamma\hbar)\left[1 - \frac{-\gamma\hbar B}{k_B T}\right] + (0)[1 - 0] + (-\gamma\hbar)\left[1 - \frac{+\gamma\hbar B}{k_B T}\right] = 0 + 2(\gamma\hbar)^2 \frac{B}{k_B T} .$$

Hence we get, for one ortho-molecule's worth of spins,

$$\langle \mu_z \rangle = \frac{2(\gamma\hbar)^2 B / k_B T}{3} .$$

In a volume in which there are N protons, there are $N/2$ molecules; but of these, only $\frac{3}{4}$ will be in the ortho-water state, so the magnetization comes out as that of the $(3/8)N$ ortho-water molecules:

$$M = \frac{\Sigma \mu}{V} = \frac{3N/8}{V} \cdot \frac{2(\gamma\hbar)^2 B / k_B T}{3} = \frac{2 N}{8 V} (\gamma\hbar)^2 \frac{B}{k_B T} .$$

For comparison, the calculation of Appendix A1 treated N protons as entirely independent, and got a magnetization of

$$(N/V)[\gamma\hbar/2]^2 B / (k_B T) = \frac{1 N}{4 V} (\gamma\hbar)^2 \frac{B}{k_B T} .$$

So these two results agree! This shows that there was a conceptual omission, but no numerical error, in treating the protons-in-water as entirely independent spins.

This result also demonstrates that EF-NMR could indeed reveal whether a sample was a statistical mixture ($\frac{3}{4}$ ortho, $\frac{1}{4}$ para) as opposed to a separated sample. For example, a sample full of 100% ortho-water would give a signal $4/3$ as large as the usual ‘statistical water’. More amazingly still, a sample bottle full of para-water would give no EF-NMR signal at all. [You can look up the current research on the use of rather easily-prepared para-hydrogen in NMR – para-water is harder to come by.]

Notice finally that this calculation of magnetization shows that M is proportional to the field B , and hence also to the auxiliary field H . Since we’ve shown $M \propto H$, the constant of proportionality will give the magnetic susceptibility χ due to nuclear moments. That susceptibility is positive, and predicted to vary as $1/T$. In practice, it is dwarfed by a negative (diamagnetic) susceptibility due to the electron distribution in the molecule. Yet the nuclear part of the susceptibility predicts the sample’s magnetic moment due to the nuclei; and this, uniquely, is the moment which precesses in an ambient B field to produce the signals detected in NMR.



Instruments Designed for Teaching

**Specifications
and
Safety Data Sheets
for liquid Samples
for
EFNMR**

www.teachspin.com

SPECIFICATIONS

TeachSpin EF-NMR Sample Coil and Controller,
EFNMR1-A
www.teachspin.com

Sample coil:

1 Coil, of 1340 turns of copper litz wire
Coil Constant: near 15 mT/A
Inductance \approx 73 mH; d.c. Resistance \approx 10.5 Ω
Coil *Q*-factor (at 2.0 kHz): \approx 70
Current Limit: 0.5 to 3.0 Amperes; 0.1 to 99.9 s duration

Notice that an *external* current-regulated power supply is needed for the sample coil used in its polarizing-coil mode.

Sample holders:

Both fit into the sample coil's tunnel of inside diameter 2.00"
Standard holder: 125 ml Nalgene bottle
Segmented holder: 7 compartments, 11 ml each

Accessible frequencies:

1.6 to 2.6 kHz

Controller:

Pre-amplifier gain: \approx 1000
Band-pass amplifier gain: \approx 15

TeachSpin EF-NMR Gradient/Field Coils and Controller, EFNMR G/FC1-A

Helmholtz coils:

- 2 Coils, each of 30 turns of #20 AWG copper wire, connected in series
 - Nominal Diameter of coils: 604 mm
 - Nominal Separation of coils: 303 mm
 - Coil Constant: near 89 ($\pm 1\%$) $\mu\text{T/A}$
 - Current Limit: 3.0 Amperes continuous current
 - Field Uniformity: 0.01 %, for volume within 3 cm of center of coils
 - Frame, permitting altitude/azimuth adjustment of coils' z -axis

Notice that an *external* current-regulated power supply is needed for the Helmholtz coils.

Gradient coils:

- 3 Coil Systems, for creating gradients $\partial B_z / \partial x$, $\partial B_z / \partial y$, $\partial B_z / \partial z$
 - Gradient coil systems are embedded in the planes of the Helmholtz-coil forms.
 - Coil Constants: near 250 $\mu\text{T/m}$ per Ampere of coil current
 - Current Supply: 3 supplies, each ± 20 mA, with 10-turn manual controls
 - Gradient Capability: $\pm 5 \mu\text{T/m}$, for ± 5 turns from center position

Notice that the EF-NMR G/FC Controller *contains* the current-regulated power supplies for these coils.

Current-Monitor points:

- Monitor Resistor in series with Helmholtz coil: 0.1 Ω , 1% tolerance, 25 W
- Monitor Resistors in series with each gradient coil: 100 Ω , 1% tolerance, $\frac{1}{4}$ W



Instruments Designed for Teaching

**Specifications
and
Safety Data Sheets
for liquid Samples
for
EFNMR**

www.teachspin.com

SPECIFICATIONS

TeachSpin EF-NMR Sample Coil and Controller,
EFNMR1-A
www.teachspin.com

Sample coil:

1 Coil, of 1340 turns of copper litz wire
Coil Constant: near 15 mT/A
Inductance \approx 73 mH; d.c. Resistance \approx 10.5 Ω
Coil *Q*-factor (at 2.0 kHz): \approx 70
Current Limit: 0.5 to 3.0 Amperes; 0.1 to 99.9 s duration

Notice that an *external* current-regulated power supply is needed for the sample coil used in its polarizing-coil mode.

Sample holders:

Both fit into the sample coil's tunnel of inside diameter 2.00"
Standard holder: 125 ml Nalgene bottle
Segmented holder: 7 compartments, 11 ml each

Accessible frequencies:

1.6 to 2.6 kHz

Controller:

Pre-amplifier gain: \approx 1000
Band-pass amplifier gain: \approx 15

TeachSpin EF-NMR Gradient/Field Coils and Controller, EFNMR G/FC1-A

Helmholtz coils:

2 Coils, each of 30 turns of #20 AWG copper wire, connected in series
Nominal Diameter of coils: 604 mm
Nominal Separation of coils: 303 mm
Coil Constant: near 89 ($\pm 1\%$) $\mu\text{T/A}$
Current Limit: 3.0 Amperes continuous current
Field Uniformity: 0.01 %, for volume within 3 cm of center of coils
Frame, permitting altitude/azimuth adjustment of coils' z-axis

Notice that an *external* current-regulated power supply is needed for the Helmholtz coils.

Gradient coils:

3 Coil Systems, for creating gradients $\partial B_z/\partial x$, $\partial B_z/\partial y$, $\partial B_z/\partial z$
Gradient coil systems are embedded in the planes of the Helmholtz-coil forms.
Coil Constants: near 250 $\mu\text{T/m}$ per Ampere of coil current
Current Supply: 3 supplies, each ± 20 mA, with 10-turn manual controls
Gradient Capability: $\pm 5 \mu\text{T/m}$, for ± 5 turns from center position

Notice that the EF-NMR G/FC Controller *contains* the current-regulated power supplies for these coils.

Current-Monitor points:

Monitor Resistor in series with Helmholtz coil: 0.1 Ω , 1% tolerance, 25 W
Monitor Resistors in series with each gradient coil: 100 Ω , 1% tolerance, $\frac{1}{4}$ W



td { text-align: left; }

KJLC Code: HT70CA

ACTIO MSDS ID: 564138

View Section: [1](#) [2](#) [3](#) [4](#) [5](#) [6](#) [7](#) [8](#) [9](#) [10](#) [11](#) [12](#) [13](#) [14](#) [15](#) [16](#)

SECTION 1: CHEMICAL PRODUCT and COMPANY IDENTIFICATION (N/A)Product Name: **Galden HT 70**

Synonyms: None

Chemical Family: Fluorocarbons,
Perfluorinated polyethers

Manufacturer Name: Solvay Solexis, Inc.

Address: 10 Leonards Lane
Thorofare, NJ 08086Emergency Telephone:
856-853-8119

Business Phone: 856-853-8119

CHEMTREC Numbers:

For emergencies in the US, call CHEMTREC: 800-424-9300

Revision Date: May 24, 2005

Physical Form: Clear, liquid

Color: Colorless

Chemical Name: Propene, 1,1,2,3,3-hexafluoro, oxidized, polymerized

Emergency Overview: Thermal decomposition will generate hydrogen fluoride (HF), which is corrosive.

NFPA Ratings (Scale of 0-4)

Product Codes:

[To Top of page](#)**SECTION 2: COMPOSITION, INFORMATION ON INGREDIENTS** (N/A)

Ingredient Name	CAS#	Ingredient Percent
Propene, 1,1,2,3,3-hexafluoro, oxidized, polymerized	69991-67-9	Approximate: 100% by Weight
EC Index Number:	1	

[To Top of page](#)**SECTION 3 : HAZARDS IDENTIFICATION** (N/A)

Emergency Overview: Thermal decomposition will generate hydrogen fluoride (HF), which is corrosive.

Physical State: Clear liquid.

Color: Colorless

Propene, 1,1,2,3,3-hexafluoro, oxidized, polymerized :

Potential Health Effects:

Eye Contact: Eye contact may cause slight irritation.

Skin Contact: Skin contact may cause slight irritation.

Inhalation: Inhalation of vapors or mists may cause respiratory tract irritation.

Ingestion: No ill effects are expected.

[To Top of page](#)

SECTION 4 : FIRST AID MEASURES

(N/A)

Eye Contact: Flush eyes for 15 minutes with copious amounts of water, retracting eyelids often. Seek medical attention if irritation persists.

Skin Contact: Wash skin thoroughly with mild soap and water. Flush with lukewarm water for 15 minutes.

Inhalation: If symptoms of irritation, discomfort or overcome by exposure, remove affected person to fresh air. Give oxygen or artificial respiration as needed.

Ingestion: If conscious, drink three to four 8 ounce glasses of water or milk. Call a physician. If unconscious, immediately take affected person to a hospital. Do not give anything by mouth to an unconscious person.

[To Top of page](#)

SECTION 5 : FIRE FIGHTING MEASURES

(N/A)

Flash Point: Not Applicable

Upper Flammable or Explosive Limit: Not Applicable

Lower Flammable or Explosive Limit: Not Applicable

Auto Ignition Temperature: Not Applicable

Extinguishing Media: Water (spray or fog), foam, dry chemical or carbon dioxide (CO₂).

Fire Fighting Instructions: Use self contained breathing apparatus (SCBA) and skin protection for acid gas exposure. Do not enter fire area without proper protection. Fight fire from safe distance. If possible, air monitoring should be performed.

Unusual Fire Hazards: Fluoropolymers will degrade upon prolonged heating or in a fire, liberating hydrogen fluoride (HF) and carbonyl fluoride (COF₂). This gas is toxic if inhaled or it comes into contact with moist skin. HF has an ACGIH PEL TLV (8hr TWA) of 0.5 ppm and a ceiling limit of 2 ppm (1.7 mg/m³). COF₂ has an ACGIH TLV of 2 ppm (5.4 mg/m³) and an OSHA PEL TWA of 2 ppm (5 mg/m³).

[To Top of page](#)

SECTION 6 : ACCIDENTAL RELEASE MEASURES

(N/A)

Spill Cleanup Measures: Releases: In case of a release or spill, absorb material onto vermiculite or similar inert absorbent. Use Perfluorosolv0 PFS-1 as an aid in cleaning. Place spilled material into covered container for disposal. Dispose of according to applicable local, state and federal regulations. Extinguish all ignition sources and evacuate the area. Exercise caution; spill area may be slippery.

[To Top of page](#)

SECTION 7 : HANDLING and STORAGE

(N/A)

Handling: Wash hands after use and before handling food or applying cosmetics. Do not use tobacco products in the immediate area.

Storage: Keep containers closed. Keep away from heat, sparks and flames. Do not store near combustible materials.

[To Top of page](#)

SECTION 8 : EXPOSURE CONTROLS, PERSONAL PROTECTION

(N/A)

Local Exhaust: Vent vapors or mists generated by processing away from operating personnel. Local exhaust ventilation at a rate of 50 feet per minute.

Skin Protection Description: Rubber or latex recommended but not necessary.

Eye/Face Protection: ANSI Z87.1 approved safety glasses with side shields or equivalent.

Respiratory Protection: No occupational exposure standards have been developed for this material. In situations where exposure to vapors or mists is likely, NIOSH/MSHA approved respirators are recommended. Respirator use limitations made by NIOSH/MSHA or the manufacturer must be observed. Respiratory protection programs must be in accordance with 29 CFR 1910.134.

Exposure Limits: ACGIH Threshold Limit Value (8 hr. time weighted average): None established

OSHA Permissible Exposure Limit Value (8 hr. time weighted average): None established

Solvay Acceptable Exposure Limit 1000 ppm

[To Top of page](#) **SECTION 9 : PHYSICAL and CHEMICAL PROPERTIES**

(N/A)

Physical State/Appearance:	Clear liquid
Color:	Colorless
Odor:	Odorless
Vapor Pressure:	141 torr
Vapor Density:	(Air=1): Not available
Boiling Point:	70 deg C
Melting Point:	Not available
Solubility:	In Water: Insoluble
Specific Gravity:	1.7-1.9
Percent Volatile:	By Volume: 0

[To Top of page](#) **SECTION 10 : STABILITY and REACTIVITY**

(N/A)

Chemical Stability:	This material is stable.
Conditions to Avoid:	Heat, sparks, flames, and other ignition sources; avoid heating above 290 deg C/554 deg F.
Incompatibilities with Other Materials:	Incompatibility (Materials to Avoid): Alkali metals and halogenated compounds.
Reactivity:	Materials to Avoid: Strong or non-aqueous alkali and Lewis acids above 100 deg C/212 deg F.
Hazardous Decomposition Products:	This material is not reactive. Thermal decomposition of this product will generate hydrogen fluoride (HF), which is corrosive, causing burns on contact with skin and other tissue.

[To Top of page](#) **SECTION 11 : TOXICOLOGICAL INFORMATION**

(N/A)

Propene, 1,1,2,3,3,3-hexafluoro, oxidized, polymerized:	
Acute Health Effects:	Rat intraperitoneal LD50: Greater than 25 g/kg
Skin Effects:	Rat dermal LD50: Greater than 2 g/kg
Ingestion Effects:	Rat oral LD50: Greater than 25.65 g/kg
Sensitization:	Guinea pig sensitization: Not a sensitizer
Irritation:	Rabbit skin irritation: Not irritating Rabbit eye irritation: Not irritating
Other Toxicological Information:	Solvay Acceptable Exposure Limit 1000 ppm

[To Top of page](#) **SECTION 12 : ECOLOGICAL INFORMATION**

(N/A)

Ecological Paragraph:	No ecotoxicological information is available for this material.
-----------------------	-----------------------------------------------------------------

[To Top of page](#) **SECTION 13 : DISPOSAL CONSIDERATIONS**

(N/A)

Waste Disposal:	Material, as supplied, is not a hazardous waste. Landfill according to current federal, state and local regulations, or incinerate in a high-temperature incinerator designed to burn fluorine-containing materials. Processing, use or contamination may make this information inaccurate or incomplete.
-----------------	-----------------------------------------------------------------------------------------------------------------------------------------------------------------------------------------------------------------------------------------------------------------------------------------------------------

[To Top of page](#) **SECTION 14 : TRANSPORT INFORMATION**

(N/A)

DOT Hazard Class:	Shipping Class: Not regulated by DOT.
-------------------	---------------------------------------

SECTION 15 : REGULATORY INFORMATION

(N/A)

Propene, 1,1,2,3,3,3-hexafluoro, oxidized, polymerized:

TSCA 8(b): Inventory Status:	All components of this product are listed on the Toxic Substances Control Act (TSCA) Section 8(b) Chemical Inventory.
Section 302:	Extremely Hazardous Substances: Not listed
Section 312 Hazard Category:	SARA 311/312:
Acute:	No
Chronic:	No
Fire:	No
Reactive:	No
Pressure:	No
Section 313 Toxic Release Form:	Not listed
OSHA 29 CFR 1200:	This product is not a "hazardous substance" as defined by OSHA Hazard Communication Standard (29 CFR 1910.1200).
Canada WHMIS:	All components of this product are listed on the Canadian Environmental Protection Act (CEPA) provisional domestic substances list (DSL). This product is not a "controlled product" as defined by the Canadian Workplace Hazardous Materials Information System (WHMIS).

SECTION 16 : ADDITIONAL INFORMATION

(N/A)

NFPA:

Health:	1
Fire Hazard:	0
Reactivity:	0
MSDS Revision Date:	May 24, 2005

Disclaimer:

Material Safety Data Sheets contain country-specific regulatory information; therefore, the MSDS's provided are for use only by customers of Solvay Solexis, Inc. in North America. If you are located in a country other than Canada, Mexico or the United States, please contact the Solvay Group company in your country for MSDS information applicable to your location.

The previous information is based upon our current knowledge and experience of our product and is not exhaustive. It applies to the product as defined by the specifications. In case of combinations or mixtures, one must confirm that no new hazards are likely to exist. In any case, the user is not exempt from observing all legal, administrative and regulatory procedures relating to the product, personal hygiene, and integrity of the work environment. (Unless noted to the contrary, the technical information applies only to pure product).

To our actual knowledge, the information contained herein is accurate as of the date of this document. However, neither Solvay Solexis, Inc. nor any of its affiliates makes any warranty, express or implied, or accepts any liability in connection with this information or its use. This information is for use by technically skilled persons at their own discretion and risk and does not relate to the use of this product in combination with any other substance or any other process. This is not a license under any patent or other proprietary right. The user alone must finally determine suitability of any information or material for any contemplated use, the manner of use and whether any patents are infringed.

Copyright:

Solvay Solexis, Inc. All rights reserved. Copyright 2004

Trademarks and/or other Solvay Solexis, Inc. products referenced herein are either trademarks or registered trademarks of Solvay Solexis, Inc. or its affiliates, unless otherwise indicated.

NFPA Ratings (Scale of 0-4)

ADDENDUM: Other Client Information**Notes:**

, HT70CA, HT70CP, HT70G2.5,

Copyright© 1996-2009 Actio Corporation. All Rights Reserved.

td { text-align: left; }

KJLC Code: HT110CA

ACTIO MSDS ID: 2587

[View Section](#)[1](#) [2](#) [3](#) [4](#) [5](#) [6](#) [7](#) [8](#) [9](#) [10](#) [11](#) [12](#) [13](#) [14](#) [15](#) [16](#)

(N/A)

SECTION 1: CHEMICAL PRODUCT and COMPANY IDENTIFICATIONProduct Name: **Galden HT 110**

Synonyms: None

Chemical Family: Fluorocarbons,
Perfluorinated polyethers

Manufacturer Name: Solvay Solexis, Inc.

Address: 10 Leonards Lane
Thorofare, NJ 08086Emergency Telephone:
856-853-8119

Business Phone: 856-853-8119

CHEMTREC Numbers:

For emergencies in the US, call CHEMTREC: 800-424-9300

Revision Date: May 24, 2005

Physical Form: Clear, liquid.

Color: Colorless.

Chemical Name: Propene, 1,1,2,3,3,3-hexafluoro, oxidized, polymerized

Emergency Overview:
Thermal decomposition will generate hydrogen fluoride (HF), which is corrosive.

NFPA Ratings (Scale of 0-4)

Product Codes:

[To Top of page](#)**SECTION 2: COMPOSITION, INFORMATION ON INGREDIENTS**

(N/A)

<i>Ingredient Name</i>	<i>CAS#</i>	<i>Ingredient Percent</i>
Propene, 1,1,2,3,3,3-hexafluoro, oxidized, polymerized	69991-67-9	Approximate: 100% by Weight
EC Index Number:	1	

[To Top of page](#)

SECTION 3 : HAZARDS IDENTIFICATION

(N/A)

Emergency Overview: Thermal decomposition will generate hydrogen fluoride (HF), which is corrosive.
 Physical State: Clear, liquid.
 Color: Colorless.

Propene, 1,1,2,3,3,3-hexafluoro, oxidized, polymerized :

Potential Health Effects:
 Eye Contact: Eye contact may cause slight irritation.
 Skin Contact: Skin contact may cause slight irritation.
 Inhalation: Inhalation of vapors or mists may cause respiratory tract irritation.
 Ingestion: No ill effects are expected.

[To Top of page](#) **SECTION 4 : FIRST AID MEASURES**

(N/A)

Eye Contact: Flush eyes for 15 minutes with copious amounts of water, retracting eyelids often. Seek medical attention if irritation persists.
 Skin Contact: Wash skin thoroughly with mild soap and water. Flush with lukewarm water for 15 minutes. If symptoms of irritation, discomfort or overcome by exposure, remove affected person to fresh air. Give oxygen or artificial respiration as needed.
 Inhalation: If conscious, drink three to four 8 ounce glasses of water or milk. Call a physician. If unconscious, immediately take affected person to a hospital. Do not give anything by mouth to an unconscious person.

[To Top of page](#) **SECTION 5 : FIRE FIGHTING MEASURES**

(N/A)

Flash Point: Not Applicable.
 Upper Flammable or Explosive Limit: Not Applicable.
 Lower Flammable or Explosive Limit: Not Applicable.
 Auto Ignition Temperature: Not Applicable.
 Extinguishing Media: Water (spray or fog), foam, dry chemical or carbon dioxide (CO₂).
 Fire Fighting Instructions: Use self contained breathing apparatus (SCBA) and skin protection for acid gas exposure. Do not enter fire area without proper protection. Fight fire from safe distance. If possible, air monitoring should be performed.
 Unusual Fire Hazards: Fluoropolymers will degrade upon prolonged heating or in a fire, liberating hydrogen fluoride (HF) and carbonyl fluoride (COF₂). This gas is toxic if inhaled or it comes into contact with moist skin. HF has an ACGIH PEL TLV (8hr TWA) of 0.5 ppm and a ceiling limit of 2 ppm (1.7 mg/m³). COF₂ has an ACGIH TLV of 2 ppm (5.4 mg/m³) and an OSHA PEL TWA of 2 ppm (5 mg/m³).

[To Top of page](#) **SECTION 6 : ACCIDENTAL RELEASE MEASURES**

(N/A)

Spill Cleanup Measures: In case of a release or spill, absorb material onto vermiculite or similar inert absorbent. Use Perfluorosolv® PFS-1 as an aid in cleaning. Place spilled material into covered container for disposal. Dispose of according to applicable local, state and federal regulations. Extinguish all ignition sources and evacuate the area. Exercise caution; spill area may be slippery.

[To Top of page](#) **SECTION 7 : HANDLING and STORAGE**

(N/A)

Handling: Wash hands after use and before handling food or applying cosmetics. Do not use tobacco products in the immediate area.
 Storage: Keep containers closed. Keep away from heat, sparks and flames. Do not store near combustible materials.

[To Top of page](#)

SECTION 8 : EXPOSURE CONTROLS, PERSONAL PROTECTION

(N/A)

Local Exhaust:	Vent vapors or mists generated by processing away from operating personnel. Local exhaust ventilation at a rate of 50 feet per minute.
Skin Protection Description:	Rubber or latex recommended but not necessary.
Eye/Face Protection:	ANSI Z87.1 approved safety glasses with side shields or equivalent.
Respiratory Protection:	No occupational exposure standards have been developed for this material. In situations where exposure to vapors or mists is likely, NIOSH/MSHA approved respirators are recommended. Respirator use limitations made by NIOSH/MSHA or the manufacturer must be observed. Respiratory protection programs must be in accordance with 29 CFR 1910.134.
Exposure Limits:	Solvay Acceptable Exposure Limit 1000 ppm

Ingredient Guidelines

Ingredient: Propene, 1,1,2,3,3-hexafluoro, oxidized, polymerized

Guideline Type:	ACGIH TLV-TWA
Guideline Information:	(8 hr. time weighted average): None established.
Guideline Type:	OSHA PEL-TWA
Guideline Information:	(8 hr. time weighted average): None established.

[To Top of page](#)**SECTION 9 : PHYSICAL and CHEMICAL PROPERTIES**

(N/A)

Physical State/Appearance:	Clear liquid
Color:	Colorless
Odor:	Odorless
Vapor Pressure:	17 torr
Vapor Density:	(Air=1): Not available.
Boiling Point:	110 deg C
Melting Point:	Not available.
Solubility:	In Water: Insoluble.
Specific Gravity:	1.7-1.9
Percent Volatile:	By Volume: 0

[To Top of page](#)**SECTION 10 : STABILITY and REACTIVITY**

(N/A)

Chemical Stability:	This material is stable.
Conditions to Avoid:	Heat, sparks, flames, and other ignition sources; avoid heating above 290 deg C/554 deg F.
Incompatibilities with Other Materials:	Materials to Avoid: Alkali metals and halogenated compounds.
	Materials to Avoid: Strong or non-aqueous alkali and Lewis acids above 100 deg C/212 deg F.
Reactivity:	This material is not reactive.
Hazardous Decomposition Products:	Thermal decomposition of this product will generate hydrogen fluoride (HF), which is corrosive, causing burns on contact with skin and other tissue.

[To Top of page](#)**SECTION 11 : TOXICOLOGICAL INFORMATION**

(N/A)

Propene, 1,1,2,3,3-hexafluoro, oxidized, polymerized :

Acute Health Effects:	Rat intraperitoneal LD50: > 25 g/kg
Skin Effects:	Rat dermal LD50: > 2 g/kg
Ingestion Effects:	Rat oral LD50: > 25.65 g/kg
Sensitization:	Guinea pig sensitization: Not a sensitizer.
Irritation:	Rabbit skin irritation: Not irritating Rabbit eye irritation: Not irritating
Other Toxicological Information:	Solvay Acceptable Exposure Limit 1000 ppm

[To Top of page](#)

SECTION 12 : ECOLOGICAL INFORMATION

(N/A)

otoxicity:

No ecotoxicological information is available for this material.

[To Top of page](#) **SECTION 13 : DISPOSAL CONSIDERATIONS**

(N/A)

Waste Disposal:

Material, as supplied, is not a hazardous waste. Landfill according to current federal, state and local regulations, or incinerate in a high-temperature incinerator designed to burn fluorine-containing materials. Processing, use or contamination may make this information inaccurate or incomplete.

[To Top of page](#) **SECTION 14 : TRANSPORT INFORMATION**

(N/A)

DOT Hazard Class:

Not regulated by DOT.

[To Top of page](#) **SECTION 15 : REGULATORY INFORMATION**

(N/A)

Propene, 1,1,2,3,3,3-hexafluoro, oxidized, polymerized:

TSCA 8(b): Inventory Status:

All components of this product are listed on the Toxic Substances Control Act (TSCA) Section 8(b) Chemical Inventory.

Section 302:

Extremely Hazardous Substances: Not listed

Section 312 Hazard Category:

SARA 311/312:

Acute:

No

Chronic:

No

Ire:

No

Reactive:

No

Pressure:

No

Section 313 Toxic Release Form:

Toxic Chemical: Not listed.

OSHA 29 CFR 1200:

This product is not a "hazardous substance" as defined by OSHA Hazard Communication Standard (29 CFR 1910.1200).

Canada WHMIS:

All components of this product are listed on the Canadian Environmental Protection Act (CEPA) provisional domestic substances list (DSL).

This product is not a "controlled product" as defined by the Canadian Workplace Hazardous Materials Information System (WHMIS).

[To Top of page](#) **SECTION 16 : ADDITIONAL INFORMATION**

(N/A)

NFPA:

Health:	1
Fire Hazard:	0
Reactivity:	0

MSDS Revision Date:

May 24, 2005

Disclaimer:

Material Safety Data Sheets contain country-specific regulatory information; therefore, the MSDS's provided are for use only by customers of Solvay Solexis, Inc. in North America. If you are located in a country other than Canada, Mexico or the United States, please contact the Solvay Group company in your country for MSDS information applicable to your location.

The previous information is based upon our current knowledge and experience of our product and is not exhaustive. It applies to the product as defined by the specifications. In case of combinations or mixtures, one must confirm that no new hazards are likely to exist. In any case, the user is not exempt from observing all legal, administrative and regulatory procedures relating to the product, personal hygiene, and integrity of the work environment. (Unless noted to the contrary, the technical information applies only to pure product).

our actual knowledge, the information contained herein is accurate as of the date of this document. However, neither Solvay Solexis, Inc. nor any of its affiliates makes any warranty, express or implied, or accepts any liability in connection with this information or its use. This information is for use by technically skilled persons at their own discretion and risk and does not relate to the use of this product in combination with any other substance or any other process. This is not a license under any patent or other proprietary right. The user alone must finally determine suitability of any information or material for any contemplated use, the manner of use and whether any patents are infringed.

Copyright:

Solvay Solexis, Inc. All rights reserved. Copyright 2004

Trademarks and/or other Solvay Solexis, Inc. products referenced herein are either trademarks or registered trademarks of Solvay Solexis, Inc. or its affiliates, unless otherwise indicated.

NFPA Ratings (Scale of 0-4)

ADDENDUM : Other Client Information

Notes:

, HT110CA, HT110CP, HT110SAMP,

Copyright© 1996–2009 Actio Corporation. All Rights Reserved.

[To Top of page](#) 

KJLC Product Code: MFYPFS-2CA

View Section:	1	2	3	4	5	6	7	8	9	10	11	12	13	14	15	16
----------------------	----------	----------	----------	----------	----------	----------	----------	----------	----------	-----------	-----------	-----------	-----------	-----------	-----------	-----------

SECTION 1: CHEMICAL PRODUCT AND COMPANY IDENTIFICATION (N/A)

Product Name: **Galden Perfluorosolv PFS-2**

Synonyms: None

Chemical Family: Fluorocarbons,
Perfluorinated polyethers

Manufacturer Name: Kurt J. Lesker Company

Address: 1925 Worthington, Ave.,
Clairton, PA 15025

Emergency Telephone:
856-853-8119

Business Phone: 412.387.9200

CHEMTREC Numbers:

For emergencies in the US, call CHEMTREC: 800-424-9300

Revision Date: May 25, 2005

Trade Names: Galden Perfluorosolv(TM) PFS-2

Physical Form: Clear liquid

Color: Colorless

Chemical Name: Propene, 1,1,2,3,3,3-hexafluoro, oxidized, polymerized

Emergency Overview: Thermal decomposition will generate hydrogen fluoride (HF), which is corrosive.

NFPA Ratings (Scale of 0-4)

[To Top of page](#)

SECTION 2: COMPOSITION/INFORMATION ON INGREDIENTS (N/A)

Ingredient Name	CAS#	Ingredient Percent
Propene, 1,1,2,3,3,3-hexafluoro, oxidized, polymerized	69991-67-9	Approximate: 100% by Weight

[To Top of page](#)

SECTION 3: HAZARDS IDENTIFICATION (N/A)

Emergency Overview: Thermal decomposition will generate hydrogen fluoride (HF), which is corrosive.

Physical State: Clear liquid.

Color: Colorless

Propene, 1,1,2,3,3,3-hexafluoro, oxidized, polymerized :

Potential Health Effects: Eye contact may cause slight irritation.

Eye Contact:

Skin Contact: Skin contact may cause slight irritation.
 Inhalation: Inhalation of vapors or mists may cause respiratory tract irritation.
 Ingestion: Not an expected exposure route. Ingestion may cause nausea and vomiting.

[To Top of page](#)**SECTION 4: FIRST-AID MEASURES**

(N/A)

Eye Contact: Flush eyes for 15 minutes with copious amounts of water, retracting eyelids often. Seek medical attention if irritation persists.
 Skin Contact: Wash skin thoroughly with mild soap and water. Flush with lukewarm water for 15 minutes. Seek medical attention if irritation persists.
 Inhalation: If symptoms of irritation, discomfort or overcome by exposure, remove affected person to fresh air. Give oxygen or artificial respiration as needed.
 Ingestion: If conscious, drink three to four 8 ounce glasses of water or milk. Call a physician. If unconscious, immediately take affected person to a hospital. Do not give anything by mouth to an unconscious person.

[To Top of page](#)**SECTION 5: FIRE FIGHTING MEASURES**

(N/A)

Flash Point: Not Applicable
 Upper Flammable or Explosive Limit: Not Applicable
 Lower Flammable or Explosive Limit: Not Applicable
 Auto Ignition Temperature: Not Applicable
 Extinguishing Media: Water (spray or fog), foam, dry chemical or carbon dioxide (CO₂).
 Fire Fighting Instructions: Use self contained breathing apparatus (SCBA) and skin protection for acid gas exposure. Do not enter fire area without proper protection. Fight fire from safe distance. If possible, air monitoring should be performed.
 Unusual Fire Hazards: Fluoropolymers will degrade upon prolonged heating or in a fire, liberating hydrogen fluoride (HF) and carbonyl fluoride (COF₂). This gas is toxic if inhaled or it comes into contact with moist skin. HF has an ACGIH PEL TLV (8hr TWA) of 0.5 ppm and a ceiling limit of 2 ppm (1.7 mg/m³). COF₂ has an ACGIH TLV of 2 ppm (5.4 mg/m³) and an OSHA PEL TWA of 2 ppm (5 mg/m³).

[To Top of page](#)**SECTION 6: ACCIDENTAL RELEASE MEASURES**

(N/A)

Spill/Release Reporting: Releases: In case of a release or spill, absorb material onto vermiculite or similar inert absorbent. Use Perfluorosolv(TM) PFS-1 as an aid in cleaning. Place spilled material into covered container for disposal. Dispose of according to applicable local, state and federal regulations. Extinguish all ignition sources and evacuate the area. Exercise caution; spill area may be slippery.

[To Top of page](#)**SECTION 7: HANDLING and STORAGE**

(N/A)

Handling: Wash hands after use and before handling food or applying cosmetics. Do not use tobacco products in the immediate area.
 Storage: Keep containers closed. Keep away from heat, sparks and flames. Do not store near combustible materials.

[To Top of page](#)**SECTION 8: EXPOSURE CONTROLS, PERSONAL PROTECTION**

(N/A)

Local Exhaust: Vent vapors or mists generated by processing away from operating personnel. Local exhaust ventilation at a rate of 50 feet per minute.
 Skin Protection Description: Rubber or latex gloves recommended but not necessary.
 Eye/Face Protection: ANSI Z87.1 approved safety glasses with side shields or equivalent.
 Respiratory Protection: No occupational exposure standards have been developed for this material. In situations where exposure to vapors or mists is likely, NIOSH/MSHA approved respirators are recommended. Respirator use limitations made by NIOSH/MSHA or the manufacturer must be observed. Respiratory protection programs must be in accordance with 29 CFR 1910.134.
 Exposure Limits: Solvay Acceptable Exposure Limit 1000 ppm
 Ingredient Guidelines

Ingredient: Propene,
1,1,2,3,3,3-hexafluoro,
oxidized, polymerized

Guideline Type:	ACGIH TLV-TWA
Guideline Information:	(8 hr. time weighted average): None established
Guideline Type:	OSHA PEL-TWA
Guideline Information:	(8 hr. time weighted average): None established

[To Top of page](#) 

SECTION 9: PHYSICAL and CHEMICAL PROPERTIES

(N/A)

Physical State/Appearance:	Clear liquid
Color:	Colorless
Odor:	Odorless
Vapor Pressure:	228 mg Hg @ 25 deg C/77 deg F
Vapor Density:	(Air=1): Not available
Boiling Point:	57 deg C/135 deg F
Melting Point:	Not available
Solubility:	In Water: Insoluble
Specific Gravity:	1.65
Percent Volatile:	By Volume: 0%

[To Top of page](#) 

SECTION 10: STABILITY and REACTIVITY

(N/A)

Chemical Stability:	This material is stable.
Conditions to Avoid:	Heat, sparks, flames, and other ignition sources; avoid heating above 290 deg C/554 deg F.
Incompatibilities with Other Materials:	Materials to Avoid: Alkali metals and halogenated compounds. Strong or non-aqueous alkali and Lewis acids above 100 deg C/212 deg F.
Reactivity:	This material is not reactive.
Hazardous Decomposition Products:	Thermal decomposition of this product will generate hydrogen fluoride (HF), which is corrosive, causing burns on contact with skin and other tissue.

[To Top of page](#) 

SECTION 11: TOXICOLOGICAL INFORMATION

(N/A)

Propene, 1,1,2,3,3,3-hexafluoro, oxidized, polymerized :

Acute Health Effects:	Rat intraperitoneal LD50: greater than 25 g/kg
Skin Effects:	Rat dermal LD50: greater than 2 g/kg
Ingestion Effects:	Rat oral LD50: greater than 25.65 g/kg
Sensitization:	Guinea pig sensitization: Not a sensitizer
Irritation:	Rabbit skin irritation: Not irritating Rabbit eye irritation: Not irritating
Other Toxicological Information:	Solvay Acceptable Exposure Limit 1000 ppm

[To Top of page](#) 

SECTION 12: ECOLOGICAL INFORMATION

(N/A)

Ecological Paragraph: No ecological information is available for this material.

[To Top of page](#) 

SECTION 13: DISPOSAL CONSIDERATIONS

(N/A)

Waste Disposal:

Material, as supplied, is not a hazardous waste. Incinerate in a high-temperature incinerator designed to burn fluorine-containing materials. Processing, use or contamination may make this information inaccurate or incomplete.

[To Top of page](#) 

SECTION 14: TRANSPORT INFORMATION

(N/A)

DOT Hazard Class: Not regulated by DOT.

[To Top of page](#)

(N/A)

SECTION 15: REGULATORY INFORMATION**Propene, 1,1,2,3,3,3-hexafluoro, oxidized, polymerized:**

TSCA 8(b): Inventory Status: All components of this product are listed on the Toxic Substances Control Act (TSCA) Section 8(b) Chemical Inventory.

Section 302: Extremely Hazardous Substances: Not listed

Section 312 Hazard Category: SARA 311/312:

Acute: No

Chronic: No

Fire: No

Reactive: No

Pressure: No

Section 313 Toxic Release Form: Toxic Chemicals: Not listed

OSHA 29 CFR 1200: This product is not a "hazardous substance" as defined by the OSHA Hazard Communication Standard (29 CFR 1910.1200).

Canada WHMIS: This product is not a "controlled product" as defined by the Canadian Workplace Hazardous Materials Information System (WHMIS).

All components of this product are listed on the Canadian Environmental Protection Act (CEPA) provisional domestic substances list (DSL).

[To Top of page](#)

(N/A)

SECTION 16: ADDITIONAL INFORMATION**NFPA:**

Health: 1

Fire Hazard: 0

Reactivity: 0

MSDS Revision Date: May 25, 2005

Disclaimer:

Material Safety Data Sheets contain country-specific regulatory information; therefore, the MSDS's provided are for use only by customers of Solvay Solexis, Inc. in North America. If you are located in a country other than Canada, Mexico or the United States, please contact the Solvay Group company in your country for MSDS information applicable to your location.

The previous information is based upon our current knowledge and experience of our product and is not exhaustive. It applies to the product as defined by the specifications. In case of combinations or mixtures, one must confirm that no new hazards are likely to exist. In any case, the user is not exempt from observing all legal, administrative and regulatory procedures relating to the product, personal hygiene, and integrity of the work environment. (Unless noted to the contrary, the technical information applies only to pure product).

To our actual knowledge, the information contained herein is accurate as of the date of this document. However, neither Solvay Solexis, Inc. nor any of its affiliates makes any warranty, express or implied, or accepts any liability in connection with this information or its use. This information is for use by technically skilled persons at their own discretion and risk and does not relate to the use of this product in combination with any other substance or by any other process. This is not a license under any patent or other proprietary right. The user alone must finally determine suitability of any information or material for any contemplated use, the manner of use and whether any patents are infringed.

Trademarks and/or other Solvay Solexis, Inc. products referenced herein are either trademarks or registered trademarks of Solvay Solexis, Inc. or its affiliates, unless otherwise indicated.

Copyright:

Solvay Solexis, Inc. All rights reserved. Copyright 2004

NFPA Ratings (Scale of 0-4)

Copyright© 1996-2006 Actio Software Corporation. All Rights Reserved.

[To Top of page](#)